Imaging of coronary atherosclerosis and vulnerable plaque
Velzen, J.E. van

Imaging of Coronary Atherosclerosis and Vulnerable Plaque:
From Mechanism to Management

Joëlla E. van Velzen

IMAGING OF CORONARY ATHEROSCLEROSIS AND VULNERABLE PLAQUE: FROM MECHANISM TO MANAGEMENT

Proefschrift

ter verkrijging van

de graad van Doctor aan de Universiteit Leiden,
op gezag van Rector Magnificus prof. mr. P.F. van der Heijden,
volgens besluit van het College voor Promoties
te verdedigen op donderdag 16 februari 2012

klokke 16.15 uur

door

Joëlla Esther van Velzen

geboren te Fullford, Groot-Brittannië
in 1982

PROMOTIE COMMISSIE

Voor mijn ouders
en voor Rolf

TABLE OF CONTENTS

General introduction and outline of the thesis

Part 2 Imaging of coronary atherosclerosis and clinical management

General introduction and
outline of the thesis

CHAPTER 1

Imaging of Atherosclerosis;
Invasive and Non-invasive
Techniques

Joëlla E. van Velzen, Joanne D. Schuijf, Fleur R. de Graaf, J. Wouter Jukema,
Albert de Roos, Lucia J. Kroft, Martin J. Schalij, Johan H.C. Reiber, Ernst E.
van der Wall, Jeroen J. Bax

INTRODUCTION

Coronary artery disease (CAD), or narrowing of the coronary arteries due to atherosclerosis, remains one of the leading causes of morbidity and mortality worldwide. However, a substantial number of patients that present with an acute coronary event due to rupture or erosion of an atherosclerotic plaque do not experience any prior symptoms. This observation emphasizes the need to improve early detection of atherosclerosis. Traditionally, imaging of the coronary arteries has focused on the assessment of luminal dimensions and the presence of severe stenosis by means of invasive coronary angiography. However, invasive coronary angiography can only assess the degree of stenosis and is less suited to evaluate the presence of atherosclerosis, including the presence of (potentially high-risk) plaques. As a result, there is an emerging need for imaging modalities that can identify atherosclerotic plaques with high-risk features indicating increased vulnerability. In this regard, particularly non-invasive techniques may be valuable as they may identify high-risk patients at a relatively early stage and may provide the opportunity for novel treatment strategies. Additionally, non-invasive imaging techniques may be used to monitor progression and/or regression of coronary atherosclerosis and thus possibly to evaluate the effectiveness of anti-atherosclerotic therapies at a larger scale. Accordingly, the present chapter will focus on invasive and non-invasive imaging modalities for the evaluation of atherosclerosis and detection of vulnerable lesions in the coronary arteries.

CHARACTERISTICS OF THE POTENTIALLY "VULNERABLE PLAQUE"

Due to the lack of prospective data and natural history studies, most details concerning the potentially vulnerable plaque have been derived from retrospective post-mortem studies.[1-3] It has been established that the majority of acute coronary events (>70%) are caused by plaque rupture followed by thrombus formation.[3] The most common substrate for superimposed thrombus formation is presumed to be the thin capped fibroatheroma; a plaque with a large necrotic core and thin fibrous cap (<65 mm thick) infiltrated by macrophages and lymphocytes (Figure 1).[4] The thin fibrous cap contains a decreased smooth muscle content which in certain circumstances can rupture and cause the thrombogenic parts of the plaque to be exposed into the lumen. This subsequently leads to the activation of the clotting cascade and the formation of a thrombus which can compromise the lumen resulting in an acute coronary syndrome (ACS). In the remaining ~30% of acute coronary events, thrombosis may be due to other causes than plaque rupture, including plaque erosion, intraplaque hemorrhage and calcified nodules.[3] The various atherosclerotic lesions and their association with thrombus are described in Table 1.

Additional characteristics of plaques prone to rupture include large plaque volume, positive remodeling, presence of microcalcifications and proximal location of the lesion. It has still not been fully elucidated which trigger actually causes the plaque to rupture, although it has been postulated that inflammation plays a critical role. Indeed, as shown
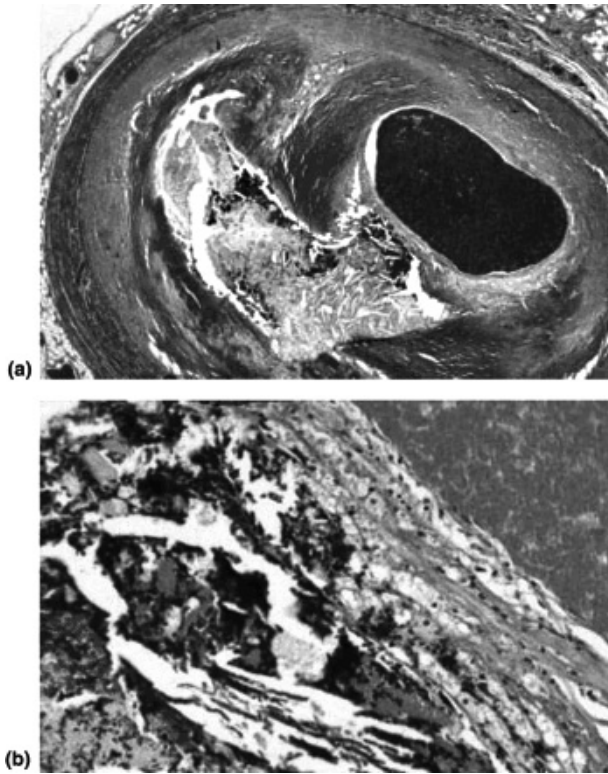
Figure 1. Histological specimen of inflamed thin capped fibroatheroma with trichrome stain, rendering lipid colorless, collagen blue and erythrocytes red. (A) Atherosclerotic coronary artery containing a large lipid core and thin fibrous cap, with post-mortem injected contrast in lumen. (B) Detail of the fibrous cap demonstrating that the cap is heavily inflamed. The fibrous cap consists of many macrophages and within the necrotic core extra-vasated erythrocytes can be seen indicating a possible plaque rupture. Reprinted with permission from Schaar et al.[4]

by studies assessing macrophage infiltration, in particular the fibrous cap is locally heavily inflamed (Figure 1).[5] Inflammation is often a result from endothelial dysfunction. Initially, endothelial dysfunction results from a disturbance in blood flow (flow reversal or oscillating shear stress) at bifurcations or tortuousness of vessels.[6] However, not only blood flow disturbances but also cardiovascular risk factors such as hypercholesterolemia, smoking and diabetes have been suggested to induce endothelial dysfunction.[7] [8] Due to endothelial cell activation, increased expression of adhesion molecules (e.g. selectins, VCAMs (vascular cell adhesion molecules) and ICAMs (intercellular adhesion molecules) promote the infiltration and homing of monocytes. Consequently, the monocytes migrate into the plaque and convert into macrophages, contributing to the process of atherogenesis.[7]

At present, there is no widely accepted diagnostic technique for the identification of vulnerable plaques. However, several invasive and non-invasive imaging modalities are currently under development that may allow to some extent detection of plaques prone to rupture.

Table 1. Morphological description of atherosclerotic lesions. Table modified from Virmani et al.[3] SMC, smooth muscle cell; TCFA, thin capped fibroatheroma.

Lesion name	Lesion description	Thrombus
Non-atherosclerotic intimal lesions		
Intimal thickening	Normal accumulation of SMCs in the intima without lipid or macrophage foam cells.	Absent
Intimal xanthoma	Subendothelial accumulation of foam cells in intima without necrotic core or fibrous cap.	Absent
Progressive atherosclerotic lesions		
Pathologic intimal thickening	SMCs in proteoglycan-rich matrix with areas of extracellular lipid accumulation without necrosis	Absent
With erosion	Luminal thrombosis, plaque same as above	Thrombus most often mural and infrequently occlusive
Fibrous cap atheroma	Well-formed necrotic core with overlying fibrous cap	Absent
With erosion	Luminal thrombosis; plaque same as above, no communication of thrombus with necrotic core	Thrombus most often mural and infrequently occlusive
TCFA	Thin fibrous cap infiltrated with macrophages and lymphocytes, rare SMCs, and an underlying necrotic core	Absent, with intraplaque hemorrhage/fibrin
With rupture	Fibroatheroma with cap disruption; luminal thrombus communicates with underlying necrotic core	Thrombus usually occlusive
Calcified nodule	Eruptive nodular calcification with underlying fibrocalcific plaque	Thrombus usually non-occlusive
Fibrocalcific plaque	Collagen-rich usually with significant stenosis; large areas of calcification with few inflammatory cells, necrotic core	Absent

INVASIVE IMAGING OF ATHEROSCLEROTIC PLAQUES

Invasive coronary angiography

Invasive coronary angiography is currently the gold standard for the diagnosis of CAD and provides an accurate and detailed overview of the anatomy of the coronary artery tree, including precise quantification of the degree of stenosis. Accordingly, the technique is extensively used to guide further treatment strategies, such as coronary angioplasty or bypass surgery.

However, evaluation of percentage diameter stenosis has limited value in predicting future cardiac events. Indeed, as demonstrated during the follow-up of patients admitted for acute myocardial infarction, almost two-thirds of plaques prone to rupture were located in non-flow limiting atherosclerotic lesions and only a minority was located in severely obstructed lesions.[9] [10] Although the likelihood of occlusion for an individual

lesion is directly related to the severity of stenosis, non-obstructive lesions are far more common and thus may frequently cause coronary occlusion due to their greater number (Figure 2). Accordingly, evaluation of the percentage diameter stenosis by means of invasive coronary angiography does not allow differentiation between stable and unstable plaques.
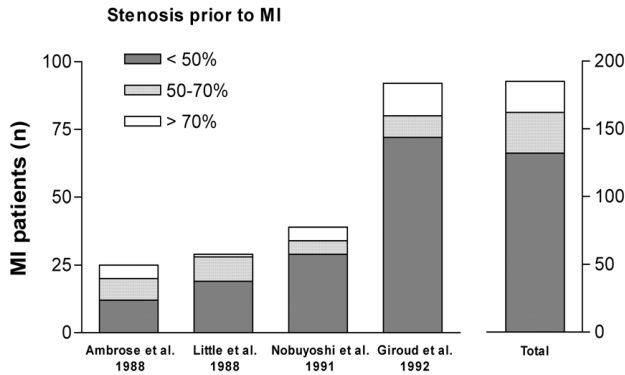
Figure 2. Bar graphs representing stenosis severity and related risk of myocardial infarction (MI) as assessed by repeated angiographic examination. As can be observed from the figure, lesions that are non-significant (< 50% stenosis) on prior angiography are frequently the underlying cause of MI. Moreover, non-significant lesions outnumber the more severely obstructive lesions and therefore account for the majority of MI. The bar graphs are constructed from data published by Ambrose et al.[9], Little et al.[96], Nobuyoshi et al.[97], and Giroud et al.[98]

Notably, novel promising angiographic acquisition approaches have been developed recently. One of these acquisition methods is rotational 3-dimensional coronary angiography, a new imaging technique in which the gantry is mechanically rotated around the patient providing a multitude of x-ray projections during a single contrast injection.[11] Using this technique, motion information of the coronary arteries can be extracted including vessel displacement and pulsation.[12] Furthermore, reconstruction of 3-dimensional images from 2-dimensional projections using specially developed dedicated software may further enhance angiographic assessment of coronary arteries (Figure 3). However, whether this novel technique will allow more accurate evaluation of atherosclerotic plaques remains to be determined more precisely.[13] Overall, it seems evident that invasive coronary angiography is an excellent modality for detecting obstructive coronary artery disease, however, detailed imaging of atherosclerosis such as determining the presence of vulnerable plaque characteristics, remodeling and inflammation, is still not feasible using this technique. Therefore other, more insightful modalities are needed for this purpose.
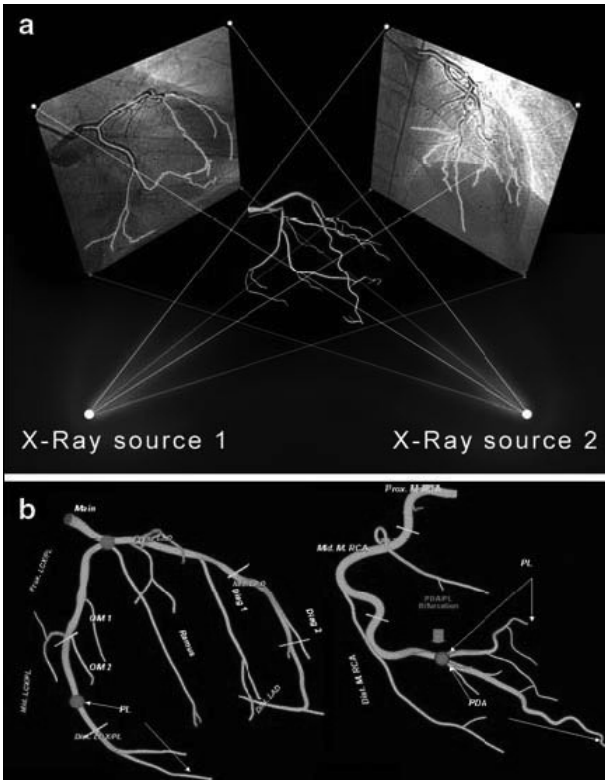
Figure 3. (A) Illustration of three-dimensional coronary modeling based on two angiograms acquired in two different projection geometries. (B) Modified American Heart Association (AHA) classification of coronary segments. Reprinted with permission from Garcia et al.[99]

Intravascular ultrasound

With respect to imaging of atherosclerosis, substantial progress has been achieved with the development of intravascular ultrasound (IVUS). IVUS is a minimally invasive imaging modality which uses miniaturized crystals incorporated at the catheter tip to provide real-time, high-resolution, cross-sectional images of the arterial wall and lumen. Axial resolution is approximately 150 μm and the lateral resolution 300 μm. As a result, the technique provides high-resolution images of the atherosclerotic process in the arterial wall.

Importantly, the technique has been extensively validated against histological autopsy specimens of human coronary arteries.[14-17] Both lumen and vessel dimensions, such as plaque and vessel area, plaque distribution, lesion length and remodeling index, can be accurately determined in vivo. In addition, semi-quantitative tissue characterization can be achieved based on plaque echogenicity. In conventional grayscale ultrasound images, calcium highly reflects ultrasound which appears as a bright and homogenous signal, resulting in acoustic shadowing.[15][18] In addition, the severity of calcifications can be quantified by measuring the angle or arc of calcium. Hypo-echoic or low reflectance in IVUS images are usually due to lipid-laden lesions (also referred to as "soft" or "sonolucent" plaques). An example is provided in Figure 4. Grayscale IVUS features of potentially vulnerable plaques have been evaluated prospectively by Yamagishi et al.[19] The investigators
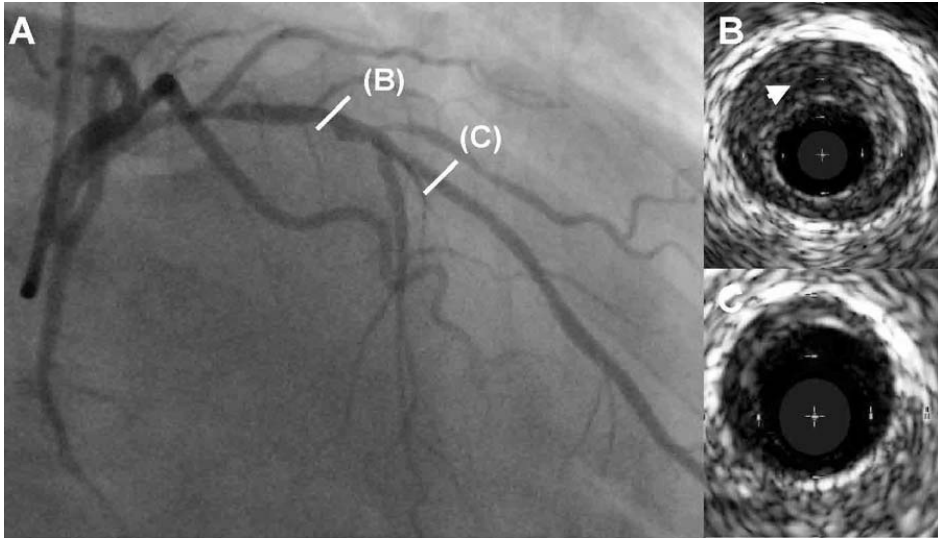
Figure 4. Coronary angiogram (A) of the left anterior descending coronary artery and corresponding intravascular ultrasound (IVUS) images (B and C) of a 55 year old patient presenting with an acute coronary syndrome. In panel B an IVUS frame is provided showing a large plaque area with an echolucent zone (arrowhead) and luminal obstruction, possibly suggesting the presence of a vulnerable plaque. Panel C shows a more distally obtained IVUS frame with minimal plaque burden.

evaluated 114 coronary plaques without luminal obstruction and assessed which plaques during a follow-up period of 21-months were related to an acute coronary event. Interestingly, it was reported that large, eccentric, positive remodeled plaques with an echolucent zone were at increased risk of instability (Figure 5). In addition, several retrospective studies confirmed that IVUS was able to identify plaques at higher risk of rupture (large echolucent area, thin fibrous cap).[20-22] Moreover, studies examining the differences between ruptured plaques and non-ruptured plaques in the same coronary artery demonstrated that the IVUS-derived lumen eccentricity index of ruptured plaques was greater.[23]

In addition, IVUS has been increasingly used as the gold standard in trials evaluating progression or regression of plaque in the coronary arteries. Indeed, unlike angiography, accurate quantification of plaque volume and area is provided by IVUS. Interestingly, Von Birgelen and co-workers performed IVUS examination of the left main coronary artery in 56 patients during initial angiography and repeated imaging after 18 months.[24] Adverse cardiovascular events occurred in 18 patients during follow-up; in patients with events, annual plaque progression was significantly greater than in the remaining asymptomatic patients. Hence, it seems feasible that IVUS-measured progression of coronary plaque may serve as a marker for future cardiovascular events.

Nevertheless, the main limitation of grayscale IVUS remains its inability to accurately differentiate plaque composition. In particular, areas with low echo reflectance such as fibrous tissue, fibro-fatty tissue and thrombus remain hard to distinguish.[14] [18] More
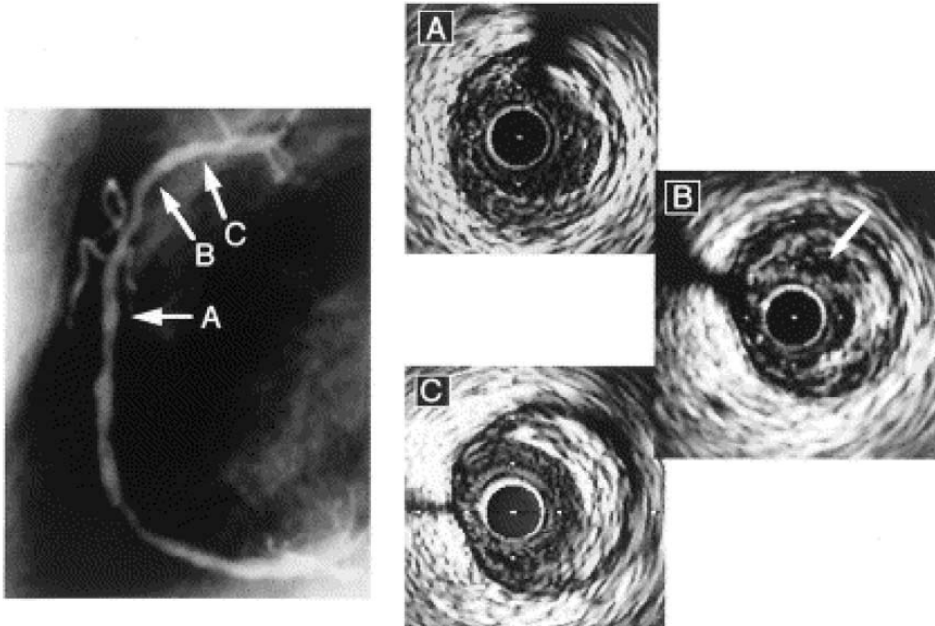
Figure 5. Coronary plaque in the right coronary artery (RCA) of a patient presenting with an acute coronary syndrome as evaluated by coronary angiography (left) and intravascular ultrasound (right). (A) A mild concentric lesion at the distal part of the RCA. (B) In the proximal portion a significant eccentric lesion with an echolucent area (arrow) and high plaque burden of 67%. (C) More proximally an eccentric lesion with high echo density. Reprinted with permission from Yamagishi et al.[19]

recently, integrated backscatter IVUS (IB-IVUS) systems have been developed to overcome this problem. Using this technique, a 2-dimensional color-coded map is constructed which reflects the tissue characteristics of the coronary arterial wall. In a prospective study by Sano et al., tissue characteristics of vulnerable plaques in patients prior to presentation with ACS were evaluated using IB-IVUS.[25] The authors demonstrated that tissue characteristics of vulnerable plaques before causing an ACS were different from those of plaques related to stable angina. However, a low positive predictive value of only 42% was reported for the identification of lipid area, indicating that further improvement is needed before application of this technique is feasible.

Virtual histology intravascular ultrasound

Virtual histology intravascular ultrasound (VH IVUS) can potentially differentiate plaque composition more accurately than conventional grayscale IVUS. The technique is based on radiofrequency analysis of intravascular ultrasound backscatter signals. A combination of spectral parameters were used to develop statistical classification schemes for analysis of in vivo IVUS data in real-time. Using these parameters, color-coded maps of plaque composition for each cross-sectional image are provided which are superimposed on the grayscale IVUS images. As illustrated in Figure 6, these tissue maps can differentiate
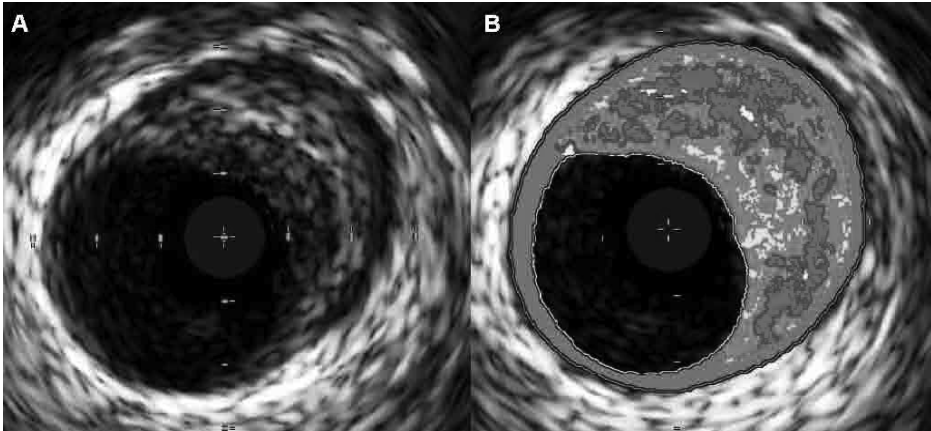
Figure 6. Plaque characterization by virtual histology intravascular ultrasound (VH IVUS). (A) Traditional grayscale intravascular ultrasound (IVUS) frame showing coronary plaque. (B) Example of VH IVUS color-coded map superimposed on grayscale IVUS frame. The colors correspond to different tissue types such as fibrous (dark green), fibro-fatty (light green), dense calcium (white) and necrotic core (red). Panel B shows a plaque with predominantly necrotic core, small dense calcium deposits and a thick fibrous cap, corresponding to a fibroatheroma.

fibrous (dark green), fibro-fatty (light green), dense calcium (white) and necrotic core (red) areas. Since its introduction, the technique has been validated with histology in several studies.[26] [27] Nair and colleagues have shown accuracies of 90.4% for fibrous, 92.8% for fibro-fatty, 90.9% for calcified and 89.5% for necrotic core regions demonstrating the potential of this imaging tool for analyzing plaque composition.[26]

The ability of VH IVUS to evaluate the presence of vulnerable plaques was first demonstrated by Rodriguez-Granillo et al.[28] The investigators observed that vulnerable plaques as determined on VH IVUS were more prevalent in patients presenting with ACS than stable angina pectoris. Similar results were recently reported by Pundziute and co-workers who demonstrated that in culprit lesions of patients with ACS, the thin capped fibroatheroma was more prevalent than in plaques of patients presenting with stable symptoms (Figure 7).[29] Interestingly, the presence of positive remodeling identified by VH IVUS was found to be similarly linked to the presence of vulnerable plaques. A retrospective study using VH IVUS demonstrated that positive remodeled plaque contained significantly more necrotic core and features of high-risk plaque, whereas negative remodeled plaques showed a more stable phenotype.[30]

Of note, in addition to remodeling, Valgimigli et al. demonstrated that plaque composition on VH IVUS was influenced by the location of the plaque in the coronary artery tree.[31] As shown by VH IVUS, proximal segments of coronary arteries had a larger necrotic core area when compared to distal coronary segments whereas the other plaque components (fibrous, fibro-fatty and dense calcium) were distributed evenly along the coronary artery tree. Accordingly, distance from the ostium was demonstrated to be inversely associ-
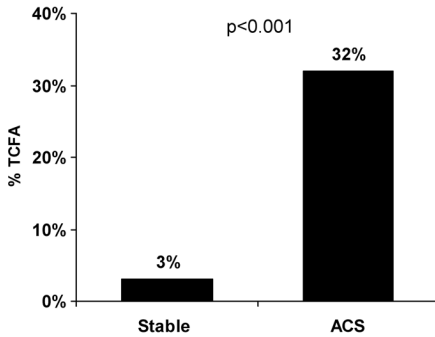
Figure 7. The prevalence of thin capped fibroatheroma (TCFA) in patients presenting with stable symptoms versus patients presenting with an acute coronary syndrome (ACS) evaluated by virtual histology intravascular ultrasound. TCFA were more frequently observed in plaques of patients with ACS (32%) as compared to patients with stable symptoms (3%). The bar graph is constructed with data from Pundziute et al.[29]

ated to plaque vulnerability, possibly explaining the higher incidence of culprit lesions in proximal parts of the coronary artery tree.

Interestingly, in addition to evaluating progression or regression in plaque burden, VH IVUS may also have the ability to monitor changes in plaque composition (and possibly even plaque vulnerability) after treatment with anti-atherosclerotic therapy. Serruys et al. assessed the effect of the direct lipoprotein-associated phospholipase A2 (Lp-PLA2) inhibitor darapladib on plaque composition by VH IVUS.[32] The investigators showed that necrotic core size increased in patients receiving placebo. In contrast, Lp-PLA2 inhibition prevented further progression of necrotic core, suggesting stabilization of atherosclerosis.

Although VH IVUS is a promising imaging modality for plaque characterization, some limitations remain. Importantly, detection of the thin fibrous cap (<65 μm) is not yet feasible as VH IVUS has limited radial resolution of only 100 μm. However, with the introduction of 40 MHz catheters imaging of the thin fibrous cap may eventually become possible.

Optical coherence tomography

Optical coherence tomography (OCT) is an unique high-resolution imaging technique which uses low coherence, near infrared light for intravascular imaging of the coronary artery wall. It has excellent spatial resolution of 10-20 μm which is ten times higher than the resolution of IVUS. Furthermore, using histological controls, it has been demonstrated that OCT is superior than IVUS in detecting important features of vulnerable plaque components including thickness of fibrous cap, thrombus and density of macrophages.[33-35]

One of the first investigations to demonstrate the feasibility of plaque characterization with OCT in vivo was performed by Jang et al.[36] Furthermore, using this technique the authors reported a higher frequency of thin capped fibroatheroma in patients with ACS as compared to patients with stable angina pectoris. In addition, Kubo et al. compared assessment of culprit plaque morphology on OCT to grayscale IVUS and coronary angioscopy.[37] The authors concluded that OCT was superior in identifying the thin capped fibroatheroma and thrombus, and that OCT was the only modality that could distinguish the thickness of fibrous cap (Figure 8).

Another interesting feature of OCT is that it enables quantification of macrophages within fibrous caps. Tearney and colleagues showed in vitro, by comparing OCT images
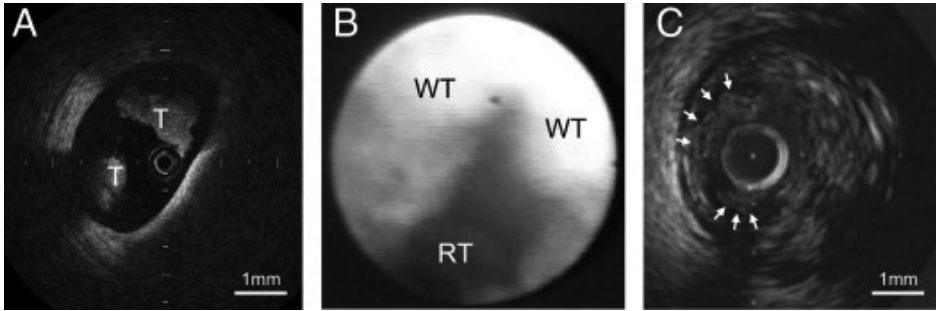
Figure 8. Intraluminal thrombi in corresponding images of optical coherence tomography (A), coronary angioscopy (B), and intravascular ultrasound (C). (A) Thrombus with optical coherence tomography signal attenuation (T). (B) Large white thrombus (WT) and small red thrombus (RT) adhering to a rough surface of yellow plaque. (C) Thrombus (arrows) identified as a mass protruding into the vessel lumen from the surface of the vessel wall. Reprinted with permission from Kubo et al.[37]

to histological specimens, that a high positive correlation exists between OCT measurements and fibrous cap macrophage density (r=0.84).[38] In vivo, Raffel and colleagues demonstrated a significant relationship between systemic inflammation (white cell blood count) and macrophage density in fibrous caps identified by OCT.[39]

At present, it is important to realize that there are some important limitations in the use of OCT. Blood leads to significant attenuation of the emitted infrared light, therefore regular saline flushes or balloon occlusion of the artery is necessary for adequate imaging. Consequently, data acquisition is time-consuming and is therefore limited to focal lesion exploration. Furthermore, the penetration depth of near infrared light is only 1-2 mm. As a result, OCT is not able to visualize the complete plaque and vessel wall and quantitative measurements of plaque and/or lipid volume are currently not possible. However, a second-generation OCT technology, namely optical frequency domain imaging (OFDI), has recently been developed, which enables imaging of the coronary arteries with a short, non-occlusive saline flush and rapid spiral pullback.[40]

OTHER INTRA-CORONARY TECHNIQUES

Intravascular Ultrasound Palpography

Intravascular palpography is a technique based on intravascular ultrasound. This imaging modality allows assessment of local mechanical tissue properties by assessing tissue deformation or strain. At a given pressure limit, fatty tissue components will show more deformation than fibrous components. Accordingly, palpography uses these differences in tissue deformation to differentiate between various plaque components. Indeed, differences of strain between fibrous, fibro-fatty and fatty components of the plaque of coronary and femoral arteries have been reported in vitro.[41] In addition, a distinctive
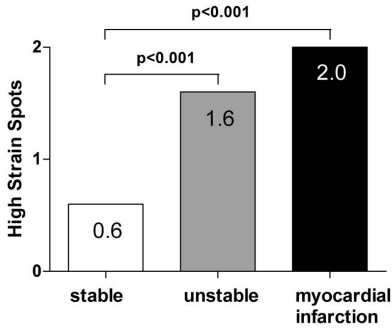
Figure 9. Bar graph representing the relation between the number of high strain spots as assessed by palpography and clinical presentation in 55 patients. High strain spots correspond to the more vulnerable plaques. More high strain spots were demonstrated by palpography in patients presenting with unstable angina pectoris and acute myocardial infarction as compared to patients presenting with stable angina pectoris. Bar graph constructed with data from Schaar et al.[42]

strain pattern was found with a high sensitivity and specificity (89%) for the detection of thin capped fibroatheroma in postmortem coronary arteries. Schaar et al. performed the first clinical study using palpography in patients to assess the incidence of vulnerable plaque.[42] In 55 patients presenting with stable symptoms, unstable symptoms and acute myocardial infarction, palpography was performed and the number of deformable plaques was assessed. The investigators reported that patients with stable angina pectoris had significantly fewer deformable plaques (high strain spots) per vessel as compared to patients presenting with unstable angina pectoris or acute myocardial infarction (Figure 9). Thus, although additional validation is required, intravascular ultrasound palpography appears to have potential for the identification of vulnerable plaque characteristics.

Intracoronary angioscopy

Intracoronary angioscopy is an imaging technique which uses optic fibers to allow direct visualization of the plaque surface, presence of thrombus and color of the luminal surface. A normal artery appears as glistening white, whereas a plaque can be categorized based on its angioscopic color such as yellow or white. Additionally, thrombus can be identified as white (platelet rich) or red (platelets and erythrocytes) (Figure 8B). Uchida and co-workers performed intracoronary angioscopy in 157 patients presenting with stable angina.[43] In a 12-month follow-up period, ACS occurred more frequently in patients with glistening yellow plaques (69%) than in those with white plaques (3%).

Of interest, intracoronary angioscopy can also be applied as a tool for monitoring changes in plaque morphology following pharmaceutical therapy. Using this technique, Takano and colleagues were able to demonstrate an effect of preventive treatment with atorvastatin.[44] Interestingly, lipid-lowering therapy with atorvastatin changed plaque color and morphology as determined by angioscopy, thereby suggesting plaque stabilization.

A major limitation of angioscopy remains that, similar to OCT, the technique requires a blood-free field while investigation is restricted to a limited part of the vessel.

NON-INVASIVE IMAGING OF ATHEROSCLEROTIC PLAQUES

Calcium score

It has been well established that the presence of coronary artery calcifications (CAC) confirms the presence of atherosclerosis. In fact, an association between visible CAC on invasive coronary angiography and the risk of cardiovascular events has been demonstrated in the early 1980s.[45] The introduction of electron beam computed tomography (EBCT) allowed non-invasive evaluation of CAC and resulted in the development of the widely established quantification method by Agatston.[46] More recently, assessment of CAC is performed by means of multislice computed tomography (MSCT) (Figure 10).

The relation between the presence and extent of CAC and presence of coronary artery stenosis has been assessed in several studies.[47-49] As expected, a high sensitivity of CAC for the presence of obstructive CAD has been reported. However, extensive calcifications can be present in the absence of luminal narrowing. As a result, specificity for obstructive CAD is low. Accordingly, the technique may be more suited to provide an estimate of total plaque burden rather than stenosis severity.
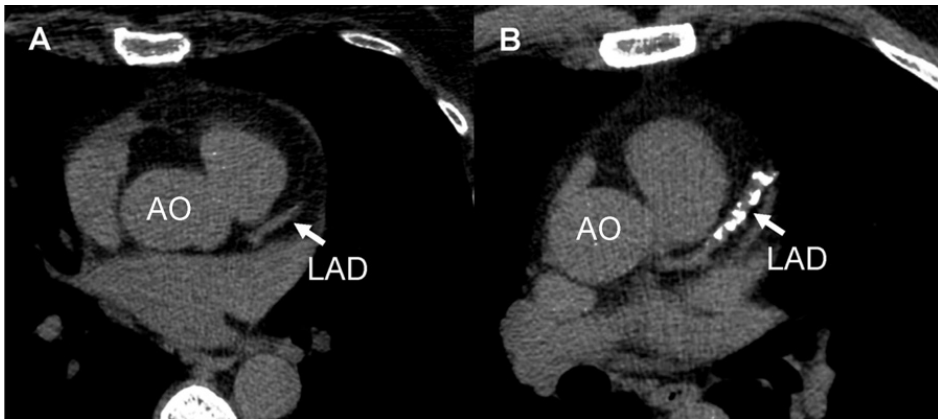
Figure 10. Example of coronary calcium on non-contrast enhanced multislice computed tomography (MSCT) axial images. Calcifications appear as bright white dense structures on MSCT. Panel A shows a 57 year old patient without evidence of coronary calcifications in the left anterior descending coronary artery (LAD). Panel B shows a 53 year old patient with calcifications in the LAD. AO - Aorta.

Importantly, the information on calcified plaque burden has been shown to translate in prognostic information. Indeed, the value of CAC scoring for risk stratification has been extensively studied. A large clinical trial by Greenland and colleagues showed the distinct incremental value of CAC scoring over the Framingham risk score in asymptomatic patients.[50] In addition, Detrano et al. demonstrated that CAC performed equally well among the four major racial and ethnical groups.[51] In a even larger cohort of 25,253 asymptomatic individuals, Budoff and colleagues confirmed that CAC was an independent
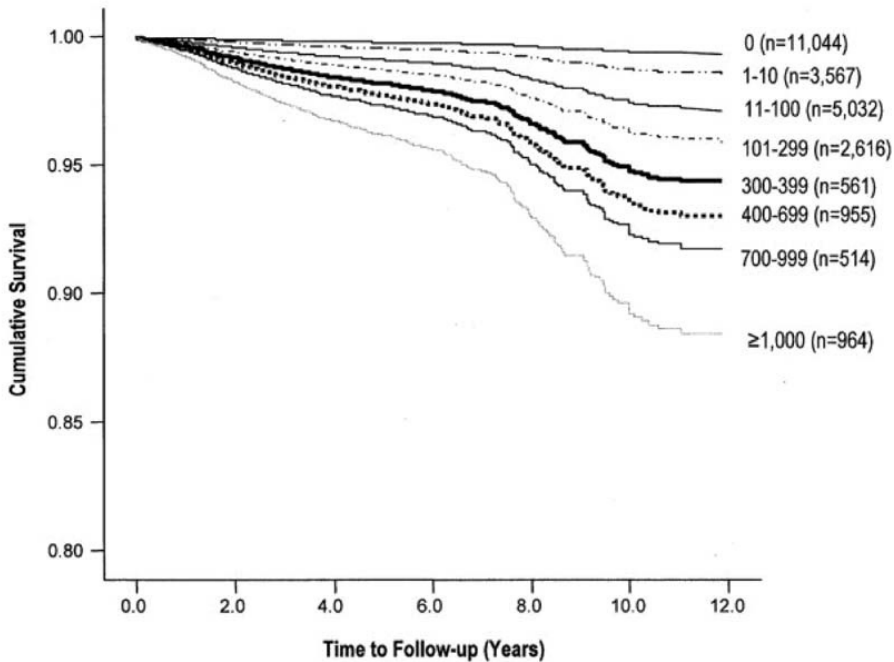
Figure 11. Cumulative survival by coronary artery calcification score adjusted for risk factors such as age, hypercholesterolemia, diabetes, smoking, hypertension, and a family history of premature coronary artery disease. Increasing calcium scores were associated with worse survival and each increment of calcium score was associated with significant increased risk of all-cause mortality. Reprinted with permission from Budoff et al.[52]

predictor of mortality and that risk scores increased proportionally with higher CAC scores (Figure 11).[52] Particularly in patients initially classified as being at intermediate risk, knowledge of the extent of CAC may be valuable to refine risk stratification and determine further management.

In addition to risk stratification, it has been suggested that CAC scoring may allow non-invasive monitoring of changes in atherosclerotic plaque burden. Several investigations have demonstrated a halt in progression or even regression of coronary calcifications as a result of reductions in serum low-density lipoprotein (LDL) cholesterol concentrations.[53] However, other investigations failed to show such effect despite effective reductions in systemic inflammation or LDL cholesterol concentrations. Possibly, changes in calcified plaque burden may not adequately reflect changes in total atherosclerotic plaque burden. Moreover, it has been suggested that plaque stabilization may even be associated with a relative increase of coronary calcifications rather than decrease. Indeed, it remains important to realize that the presence or absence of calcium itself is not a direct marker for vulnerability. Since no information is obtained on the presence of non-calcified plaques, CAC scoring does not allow for reliable distinction between potentially unstable versus stable plaques.[54]

Multislice computed tomography angiography

MSCT is a rapidly evolving imaging tool that allows non-invasive visualization of coronary atherosclerosis. Since the introduction of 4-slice scanners, the technique has developed rapidly and 64-slice and even 320-slice systems are currently available. Accordingly, the temporal and spatial resolution have improved resulting in superior image quality and diagnostic accuracy for the detection of CAD. Although the resolution of MSCT remains inferior as compared to invasive coronary angiography, high diagnostic accuracies have been demonstrated for the detection of significant CAD.[55] Additionally, the technique may be of use in the work-up of patients presenting to the emergency department with suspected ACS. Promising results were reported by Hoffmann and co-workers who demonstrated that the absence of significant coronary artery stenosis (73 of 103 patients) and non-significant coronary atherosclerotic plaque (41 of 103 patients) on MSCT accurately ruled out ACS.[56] Accordingly, a high negative predictive value was observed indicating that MSCT angiography may be a valuable gatekeeper for invasive coronary angiography.

Furthermore, MSCT is not only able to identify coronary artery stenosis but also has the potential to provide information on lesion morphology and plaque composition. As illustrated in Figure 12, the technique can distinguish non-calcified, mixed and calcified plaques. Due to the substantially higher density values, identification of calcified plaque is relatively simple on MSCT. However, identification of non-calcified plaque is more
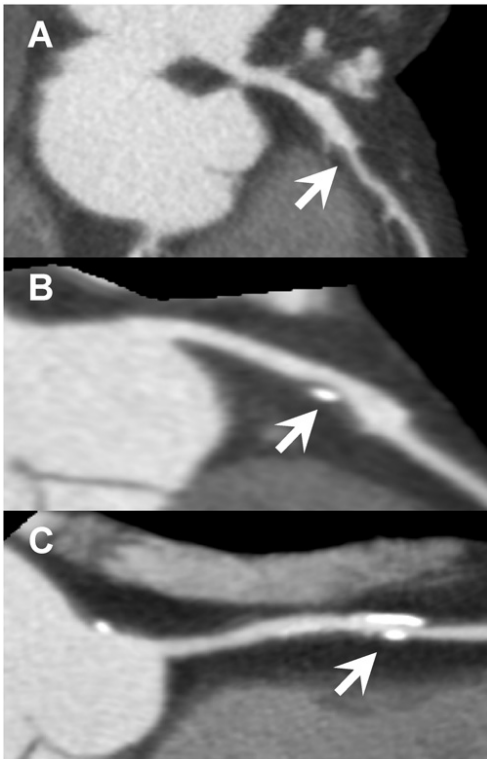
Figure 12. Example of plaque imaging performed on 320-slice multislice computed tomography coronary angiography. (A) Curved multiplanar reconstruction of the left anterior descending artery (LAD) with non-calcified plaque (arrow). (A) Curved multiplanar reconstruction of the LAD demonstrating mixed plaque (arrow). (C) Curved multiplanar reconstruction of the right coronary artery demonstrating calcified plaque (arrow).

demanding because of the more subtle difference in attenuation and relatively larger influence of body-mass index, cardiac output and amount of contrast injected. Interestingly, comparison of density measurements of non-calcified plaques on MSCT to invasive IVUS showed that the attenuation within hyper-echoic (fibrous) plaques was higher than within hypo-echoic (lipid-rich) plaques (mean attenuation values of 121 ± 34 HU versus 58 ± 43 HU).[57] However, for individual lesions a substantial overlap between hyper-echoic and hypo-echoic attenuation values was observed, indicating that, at this stage, further characterization of non-calcified plaque is not yet feasible.

Plaque composition as evaluated by MSCT has been linked to clinical presentation. Motoyama and colleagues compared plaque morphology on MSCT in 38 patients with ACS versus 33 patients with stable angina pectoris and demonstrated that plaques associated with ACS showed lower density values, positive remodeling and spotty calcification.[58] Moreover, Pundziute and colleagues compared plaque characteristics on 64-slice MSCT and VH IVUS in patients with ACS and stable angina pectoris and demonstrated that non-calcified (32%) and mixed plaques (59%) were more frequently present in ACS.[29] In line with these findings, using 64-slice MSCT, Henneman et al. demonstrated in 40 patients suspected of ACS that CAC was absent in a large proportion of patients (33%). However, as illustrated in Figure 13, in these patients non-calcified plaques were highly prevalent (39%).[59] As a result, atherosclerosis and even obstructive CAD were frequently observed, even in the absence of detectable calcium. Thus, the investigators suggested that in patients presenting with ACS, absence of CAC does not reliably exclude CAD.
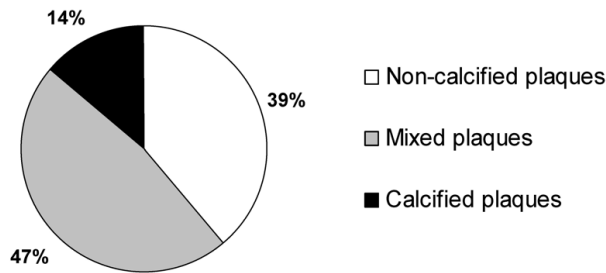
Figure 13. Prevalence of different plaque types in patients presenting with suspected acute coronary syndrome (ACS). A high prevalence of non-calcified and mixed plaques was observed in patients presenting with suspected ACS. Pie graph constructed with data from Henneman et al.[59]

Preliminary studies have suggested that information on atherosclerosis derived from MSCT angiography may also provide prognostic information.[60][61] Interestingly, van Werkhoven et al. demonstrated that the presence of substantial non-calcified plaque burden was an independent predictor of events (all-cause mortality, non-fatal myocardial infarction, and unstable angina requiring revascularization).[62] However, further investigations are required in larger patient populations to confirm these observations.

In addition, MSCT may potentially be applied to monitor progression and/or regression of coronary plaque burden. Preliminary results from an experimental animal model reported that MSCT could accurately document serial changes in aortic plaque burden which correlated well with measurements derived from magnetic resonance imaging (MRI).[63] In humans, Burgstahler and co-workers studied the effect of lipid-lowering therapy on coronary plaque burden with MSCT after one year.[64] Although no differences were found in total plaque burden and CAC, significantly lower non-calcified plaque burden was demonstrated after lipid-lowering therapy.

While MSCT angiography may have potential for non-invasive evaluation of plaque composition and subsequent identification of patients at higher risk of events, several important limitations remain. Firstly, the technique is associated with radiation exposure, although significant dose reductions have been achieved with recent advances in scanner hardware and acquisition protocols.[65-67] In addition, the resolution remains inferior as compared to invasive atherosclerosis imaging techniques and no validated algorithms are currently available for quantification of observations. Further improvement in plaque characterization however, is expected by the development of dual-energy MSCT or dedicated contrast agents.

Magnetic resonance imaging

MRI is a versatile imaging technique with a high potential to visualize vessel anatomy. The technique is able to differentiate atherosclerotic tissue without exposure to radiation using features such as chemical composition, water content, molecular motion-, or diffusion. Due to recent improvements in MR techniques such as high-resolution and multi-contrast MR (time-of-flight (TOF) imaging T1- and T2- weighted and proton density (PD) weighted imaging), plaque characterization has become possible as demonstrated in experimental models, histological specimens, human carotid arteries and the aortic wall in vivo (Table 2).[68-71] Fayad and colleagues assessed aortic wall plaque composition with MR images matched to transesophageal echocardiograms, demonstrating a strong correlation for plaque composition, thickness and extent.[68] In several studies the potential of MRI to characterize different plaque characteristics, including the fibrous cap, lipid core and even the presence of hemorrhage in human carotid atherosclerotic plaques (Figure

Table 2. Multicontrast weightings and corresponding plaque characterization on magnetic resonance imaging (MRI). Intensities are relative to that of the sternomastoid muscle. Table modified from Yuan et al.[94] TOF, time of flight; PD, proton density.

Component	TOF	T1-weighted	T2-weighted	PD-weighted
Hemorrhage	High	High - moderate	Variable	Variable
Lipid-rich necrotic core	Moderate	High	Variable	High
Calcification	Low	Low	Low	Low
Fibrous tissue	Moderate - low	Moderate	Variable	High
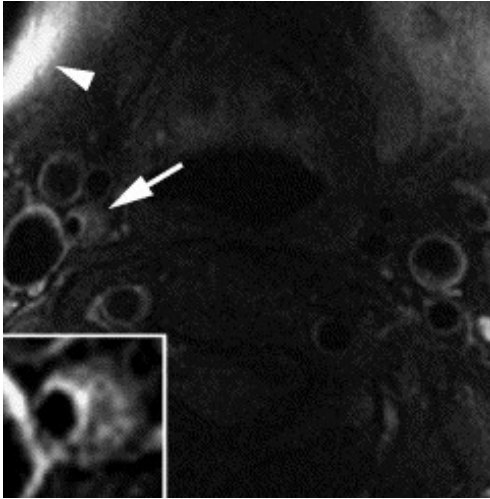
Figure 14. Example of MR image (T2-weighted) of the carotid arteries. A stenotic lesion of the right internal carotid artery can be observed just distal of the bifurcation (arrow). The arrowhead indicates a high signal artifact of the close-placed superficial phase-array coil. Finally, in the enlargement, a hypo-intense signal within the plaque corresponding to lipid accumulation can be observed. Reprinted with permission from Corti et al.[100]

14), has been demonstrated.[72] [73] In addition, a good correlation has been identified between fibrous cap integrity on MRI and histopathological specimens.[69]

Plaque imaging with MRI of the coronary arteries remains challenging as deep location, motion and respiratory artifacts and small caliber vessels remain obstacles for accurate coronary visualization and plaque differentiation. Nevertheless, several novel approaches for coronary plaque imaging are currently under development and may potentially allow accurate evaluation of atherosclerotic plaque in the coronary arteries.[74] In particular 'black-blood' techniques (an imaging approach in which the blood appears black and the arterial wall can be seen) are promising for accurately portraying plaque presence, size and morphology with sub-millimeter resolution and high reproducibility.[75] Kim et al. recently applied a novel 3D free breathing black-blood fast gradient technique with real-time motion correction developed by Botnar et al. to evaluate patients with non-significant CAD and compared these patients to a control group without CAD.[76] [77] The investigators demonstrated that MRI could identify significantly increased vessel wall thickness with preserved lumen size in patients with non-significant CAD.

High-resolution MRI in combination with molecular contrast agents targeted to specific cells or molecules offers an interesting alternative approach for more detailed plaque characterization.[78-80] In particular contrast agents dedicated to the identification of vulnerable plaque components are of considerable interest. Paramagnetic contrast agents such as gadolium (T1 shortening contrast with a high affinity for lipid-rich lesions) are able to assess the more subtle differences in plaque composition.[79] Furthermore, T2 shortening contrast agents such as ultra small superparamagnetic particles of iron oxide (USPIOs) have been studied both in vitro and in vivo. Interestingly, these particles were found to accumulate in plaques with high macrophage content and cause signal decrease in MR images.[81] Additionally, promising results have been achieved with fibrin targeted contrast agents, which have the potential to allow non-invasive molecular imaging of thrombus. Spuentrup and colleagues demonstrated in an experimental animal model that

using these agents, acute pulmonary, cardiac and coronary thrombosis could be accurately visualized by MR imaging.[82] Furthermore, continued advances in radiofrequency hardware have resulted in an increase in the operating field strength from 1.5T (tesla) to 3T and even 7T. At 3T an approximately two-fold increase in signal-to-noise-ratio can be obtained, resulting in a four-fold reduction in scanning time and significant increase in temporal resolution.

Moreover, recent studies support MRI as an effective tool to evaluate plaque regression following lipid-lowering therapy. Corti et al. demonstrated in 18 hypercholesterolemic patients that MRI could document a marked reduction in atherosclerotic lesion size induced by statin therapy in humans.[83] Accordingly MRI may become a particular attractive modality to non-invasively monitor the effect of anti-atherosclerotic interventions in vivo.

Nevertheless, detailed characterization of plaque including the identification of high-risk features remains difficult at present. Although much is expected from current developments, evidently more data are needed before plaque characterization with MRI may be clinically used for identification and management of patients at risk.

Molecular imaging with nuclear techniques

Using dedicated tracers, nuclear imaging techniques such as single photon emission tomography (SPECT) and positron emission tomography (PET) can target distinct mediators and regulators involved in the cascade of atherosclerosis. As a result of increasing knowledge regarding the pathophysiology of atherosclerosis, several radionuclide-labeled tracers that serve as markers of inflammation, angiogenesis, apoptosis and lipid metabolism have been developed for plaque imaging (Table 3).

Matrix metalloproteinases (MMP) are released by activated macrophages and are therefore used to identify proteolytic activity in atherosclerotic lesions. MMPs modulate the degrading of the extracellular matrix and the thin fibrous cap of an atherosclerotic lesion, contributing to the vulnerability of the plaque. In several animal models the feasibility of in vivo imaging of MMP activity using radionuclide-labeled MMP inhibitors has been shown.[84-86]

Additionally, it has been proposed that apoptosis is one of the features of an atherosclerotic unstable lesion and that apoptosis consequently leads to growth of the necrotic core and influences plaque stability. Annexin A5 has a high affinity for phospatidylserine (exposed on the plasma membrane of apoptotic cells) and therefore radionuclide-labeled Annexin A5 can be used as a marker of apoptotic cells in atherosclerotic lesions. In experimental models, a direct correlation was demonstrated between Annexin A5 uptake, macrophage burden and histologically demonstrated apoptosis.[87] In a small patient cohort with a history of transient ischemic attack, Annexin A5 imaging of carotid atherosclerosis was performed by Kietselaer et al.[88] Imaging was performed before carotid surgery and correlated to histopathology findings. The investigators reported that Annexin A5 uptake in carotid lesions correlated highly with plaque instability. However, only preliminary data are available and further research in humans is necessary.

Table 3 . Targets for molecular imaging of plaque vulnerability. Table modified from Narula et al.[95] FDG - fluorodeoxyglucose; HLA - human leukocyte antigen; ICAM - intercellular adhesion molecule 1; MCP-1 - monocyte chemotactic protein 1; MMP - matrix metalloproteinase; PS - phosphatidylserine; SRA - scavenger receptor A; VCAM - vascular cell adhesion molecule; VEGF - vascular endothelial growth factor.

Process targeted	Targets	Target agents
Monocyte migration		
Reversible prelude with intima	Selectins	Microbubbles with antibodies
Receptors for chemotactic peptides	MCP-1	Radiolabeled MCP-1
Activation-dependent receptors	ICAM or VCAM	Antibodies; radiolabeled or on microbubbles
Subintimal activation of monocytes		
Lipid scavenging receptors	SRA I,II	Oxidized LDL
	FcγRIII	Radiolabeled non-specific IgG or Fc fragments
Other phagocyte receptors	PS receptor	PS-rich microbubbles
	Others	Superparamagnetic iron (USPIOs); nanoparticulate CT contrast
Immune activation	HLA expression	Radiolabeled antibody
Heightened metabolic activity	FDG	Positron-labeled FDG
Macrophage apoptosis		
Cell membrane	PS expression	Radiolabeled Annexin A5
Cell apoptosis pathways	Caspase substrate	Radiolabeled DEVD
Collateral products from macrophages		
Cytokines	MMPs	MMP inhibitor or substrate; radiolabeled or fluorochromes
Vasa vasorum or neovascularization	Integrins	Radiolabeled RDG peptide
	VGEF	Radiolabeled VGEF

Finally, PET imaging with F18-fluorodeoxyglucose (FDG) is currently considered to be one of the most promising imaging modalities for the identification of vulnerable lesions. FDG is a radionuclide tracer that competes with glucose for uptake into metabolically active cells, especially macrophages, and enables quantification via PET. Within carotid artery atherosclerotic plaques, Rudd et al. demonstrated with FDG PET that FDG was taken up by resident macrophages in atherosclerotic plaque but not by surrounding cellular plaque components.[89] The authors suggested that FDG may be capable of imaging and possibly even quantification of plaque inflammation. In addition, FDG PET could potentially be used to serially monitor changes in atherosclerotic plaque macrophage content. In an experimental rabbit model, Worthley and co-workers demonstrated that assessment of progression and/or regression of macrophage content in atherosclerotic plaques was feasible using this non-invasive technique.[90] In addition, Tahara et al. showed in 43 patients that FDG PET, co-registered with computed tomography data, was able to visualize significantly reduced plaque inflammation following 3 month treatment with simvastatin.[91]

However, thus far FDG imaging of the coronary arteries has been challenging because of cardiac motion, FDG uptake in the myocardium and limited resolution of PET. Possibly, co-registration of the functional images with high-resolution anatomical data obtained with MSCT in combination with dedicated protocols to suppress myocardial uptake could possibly overcome this limitation (Figure 15).[92] [93]
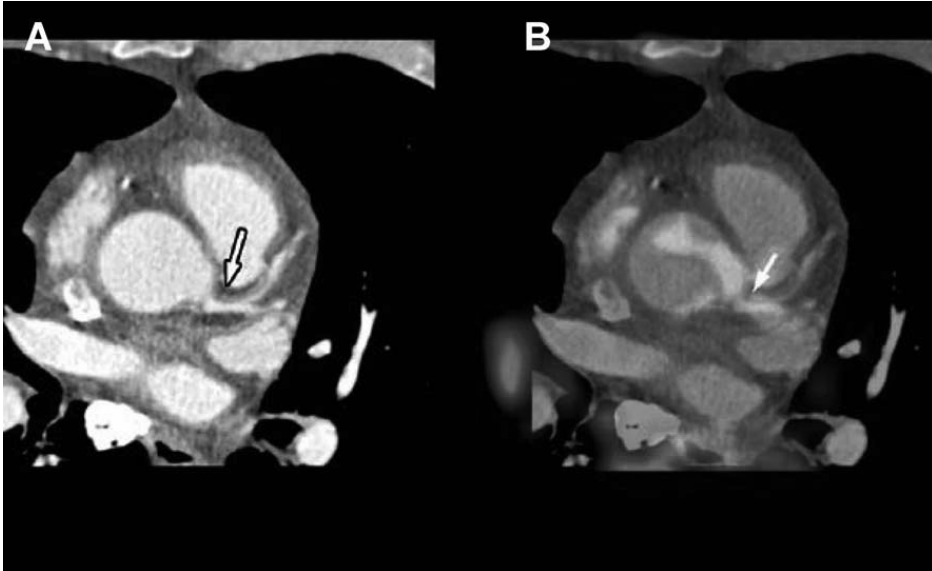
Figure 15. Example of the co-registration of functional imaging with F-18 fluorodeoxyglucose (FDG) positron emission tomography (PET) and anatomical imaging with multislice computed tomography (MSCT). (A) On MSCT axial images a non-calcified plaque in left main coronary artery (arrow) was identified. (B) Corresponding image after fusion with F-18 FDG PET, localizing the inflammatory PET signal with a maximal standard uptake value of 2.1 to the non-calcified plaque seen in the left coronary artery (arrow). Reprinted with permission from Alexanderson et al.[92]

SUMMARY AND CONCLUSION

Plaque rupture followed by coronary occlusion due to thrombosis is responsible for a large number of acute coronary events. Identification of lesions before they rupture would allow initiation of aggressive systemic or even local therapy and could potentially improve outcome. Due to absence of natural history data, the precursor of vulnerable lesions remains largely unknown and most details have been derived from retrospective post-mortem studies. On the basis of these investigations, it has been suggested that the most common substrate for superimposed thrombus formation is the thin capped fibroatheroma; a plaque with a large necrotic core and an inflamed thin fibrous cap (<65 mm thick) infiltrated by macrophages and lymphocytes.

As discussed in the current chapter, extensive effort is invested in the development of imaging tools to characterize coronary atherosclerosis with the ultimate goal of detecting vulnerable lesions. To this end, several techniques are currently under investigation, with each technique having specific advantages as well as limitations. Importantly, the clinical relevance in terms of predicting outcome and changing management remains to be established for all currently available techniques.

At present, invasive techniques, such as OCT and VH IVUS, provide the most detailed information and are currently employed in prospective natural history studies. Application of these techniques will remain largely restricted to symptomatic high-risk patients due to their invasive nature and a non-invasive technique would allow application on a wider scale. At present, non-invasive approaches cannot provide detailed characterization of the individual vulnerable coronary plaque. However, direct in vivo comparisons with invasive modalities may substantially improve our understanding and interpretation of non-invasive observations. Consequently, this information may be translated into enhanced strategies for risk stratification. In addition, the measurements of plaque vulnerability obtained with either invasive or non-invasive imaging techniques may be used as surrogate endpoint for prospective anti-atherosclerotic therapy trials.[32] Possibly, the combination of imaging techniques targeting both morphological and functional characteristics may be of particular value.

Evidently, large prospective studies are needed to further define the potential role of each imaging technique in the identification of vulnerable plaques. Moreover, much uncertainty remains on how these vulnerable lesions should be treated. In addition to increased intensity of systemic therapy, such as aspirin and statin therapy, also local or regional therapeutic approaches (such as plaque sealing) have been suggested. However, no robust data are currently available to support their effectiveness. Potentially, imaging techniques may be proven of great value in the development of such individually targeted treatment strategies.

OUTLINE OF THE THESIS

The aim of this thesis was to evaluate the role of imaging in the assessment and characterization of atherosclerosis and vulnerable plaque in the coronary arteries. Non-invasive computed tomography coronary angiography (CTA) is a relatively new technique for the evaluation of coronary atherosclerosis. Therefore, the performance of CTA in characterizing coronary atherosclerosis was assessed and was compared to invasive imaging techniques, in addition to determining the impact on clinical management.

In **Part 1**, the current advances of coronary CTA in characterizing atherosclerosis and vulnerable plaque were explored. **Chapter 2** explores the ability of the novel 320-row CTA to characterize different plaque components as compared to plaque imaging with invasive virtual histology intravascular ultrasound (VH IVUS). In **Chapter 3**, differences in

plaque composition were evaluated in relation to the degree of stenosis as assessed both non-invasively by CTA and invasively by VH IVUS. In **Chapter 4**, the spatial relationship between the site of greatest stenosis and site of greatest vulnerability was evaluated with VH IVUS on a per-vessel basis. The aim of **Chapter 5** was to systematically investigate the diagnostic performance of CTA for two endpoints, namely detecting significant stenosis (using invasive coronary angiography as the reference standard) versus detecting the presence of atherosclerosis (using IVUS as the reference of standard). Assessment of the length of coronary lesions was compared between CTA and quantitative coronary angiography in patients who underwent subsequent percutaneous coronary intervention (PCI) in **Chapter 6**. The purpose of the next chapters was to systematically compare high-risk plaque features on CTA, such as the pattern of calcifications (**Chapter 7**) and presence of positive remodeling (**Chapter 8**) and relate these characteristics on CTA to vulnerable plaque characteristics on VH IVUS.

In **Part 2**, the relation between characterization of atherosclerosis on CTA and the effect on clinical management was evaluated. **Chapter 9** focuses on the evolving role of coronary CTA (including coronary calcium scoring) on the diagnosis of patients with acute chest pain. In addition, an overview of a wide range of other CT applications is provided, including triple rule-out, evaluation of plaque composition, myocardial function, and perfusion. As CTA is inherently associated with patient radiation exposure, **Chapter 10** addresses effective strategies for radiation dose reduction. The diagnostic accuracy of 320-row CTA in the non-invasive evaluation of significant stenosis and atherosclerosis in patients referred for CTA as well as in patients presenting with acute chest pain is evaluated in **Chapter 11** and **Chapter 12**, respectively. **Chapter 13** evaluates the relation between the value of the calcium score and plaque characteristics (on CTA and VH IVUS) in patients with suspected acute coronary syndrome. The aim of **Chapter 14** was to evaluate the role of non-invasive CTA as a gatekeeper before invasive coronary angiography. Lastly, **Chapter 15** evaluates the value of CTA variables of atherosclerosis to predict the presence of ischemia on myocardial perfusion imaging.

REFERENCES

1. Falk E, Shah PK, Fuster V. Coronary plaque disruption. Circulation 1995;92:657-71.
2. van der Wal AC, Becker AE, van der Loos CM et al. Site of intimal rupture or erosion of thrombosed coronary atherosclerotic plaques is characterized by an inflammatory process irrespective of the dominant plaque morphology. Circulation 1994;89:36-44.
3. Virmani R, Kolodgie FD, Burke AP et al. Lessons from sudden coronary death: a comprehensive morphological classification scheme for atherosclerotic lesions. Arterioscler Thromb Vasc Biol 2000;20:1262-75.
4. Schaar JA, Muller JE, Falk E et al. Terminology for high-risk and vulnerable coronary artery plaques. Report of a meeting on the vulnerable plaque, June 17 and 18, 2003, Santorini, Greece. Eur Heart J 2004;25:1077-82.
5. Moreno PR, Falk E, Palacios IF et al. Macrophage infiltration in acute coronary syndromes. Implications for plaque rupture. Circulation 1994;90:775-8.
6. Gimbrone MA, Jr., Nagel T, Topper JN. Biomechanical activation: an emerging paradigm in endothelial adhesion biology. J Clin Invest 1997;99:1809-13.
7. Ross R. Atherosclerosis--an inflammatory disease. N Engl J Med 1999;340:115-26.
8. Kunsch C, Medford RM. Oxidative stress as a regulator of gene expression in the vasculature. Circ Res 1999;85:753-66.
9. Ambrose JA, Tannenbaum MA, Alexopoulos D et al. Angiographic progression of coronary artery disease and the development of myocardial infarction. J Am Coll Cardiol 1988;12:56-62.
10. White CW, Wright CB, Doty DB et al. Does visual interpretation of the coronary arteriogram predict the physiologic importance of a coronary stenosis? N Engl J Med 1984;310:819-24.
11. Garcia JA, Chen SY, Messenger JC et al. Initial clinical experience of selective coronary angiography using one prolonged injection and a 180 degrees rotational trajectory. Catheterization and Cardiovascular Interventions 2007;70:190-6.
12. Maddux JT, Wink O, Messenger JC et al. Randomized study of the safety and clinical utility of rotational angiography versus standard angiography in the diagnosis of coronary artery disease. Catheter Cardiovasc Interv 2004;62:167-74.
13. Hoffmann KR, Wahle A, Pellot-Barakat C et al. Biplane X-ray angiograms, intravascular ultrasound, and 3D visualization of coronary vessels. Int J Card Imaging 1999;15:495-512.
14. Di Mario C, The SH, Madretsma S et al. Detection and characterization of vascular lesions by intravascular ultrasound: an in vitro study correlated with histology. J Am Soc Echocardiogr 1992;5:135-46.
15. Gussenhoven EJ, Essed CE, Lancee CT et al. Arterial wall characteristics determined by intravascular ultrasound imaging: an in vitro study. J Am Coll Cardiol 1989;14:947-52.
16. Kostamaa H, Donovan J, Kasaoka S et al. Calcified plaque cross-sectional area in human arteries: correlation between intravascular ultrasound and undecalcified histology. Am Heart J 1999;137:482-8.
17. Siegel RJ. Histopathologic validation of angioscopy and intravascular ultrasound. Circulation 1991;84:109-17.
18. Potkin BN, Bartorelli AL, Gessert JM et al. Coronary artery imaging with Intravascular high-frequency ultrasound. Circulation 1990;81:1575-85.
19. Yamagishi M, Terashima M, Awano K et al. Morphology of vulnerable coronary plaque: insights from follow-up of patients examined by intravascular ultrasound before an acute coronary syndrome. J Am Coll Cardiol 2000;35:106-11.
20. Ge J, Baumgart D, Haude M et al. Role of intravascular ultrasound imaging in identifying vulnerable plaques. Herz 1999;24:32-41.

21. Kotani J, Mintz GS, Castagna MT et al. Intravascular ultrasound analysis of infarct-related and non-infarct-related arteries in patients who presented with an acute myocardial infarction. Circulation 2003;107:2889-93.

22. Rioufol G, Finet G, Ginon I et al. Multiple atherosclerotic plaque rupture in acute coronary syndrome: a three-vessel intravascular ultrasound study. Circulation 2002;106:804-8.

23. von Birgelen C, Klinkhart W, Mintz GS et al. Plaque distribution and vascular remodeling of ruptured and nonruptured coronary plaques in the same vessel: an intravascular ultrasound study in vivo. J Am Coll Cardiol 2001;37:1864-70.

24. von Birgelen C., Hartmann M, Mintz GS et al. Relationship between cardiovascular risk as predicted by established risk scores versus plaque progression as measured by serial intravascular ultrasound in left main coronary arteries. Circulation 2004;110:1579-85.

25. Sano K, Kawasaki M, Ishihara Y et al. Assessment of vulnerable plaques causing acute coronary syndrome using integrated backscatter intravascular ultrasound. J Am Coll Cardiol 2006;47:734-41.

26. Nair A, Kuban DB, Tuzcu EM et al. Coronary plaque classification with intravascular ultrasound radiofrequency data analysis. Circulation 2002;106:2200-6.

27. Nasu K, Tsuchikane E, Katoh O et al. Accuracy of in vivo coronary plaque morphology assessment: a validation study of in vivo virtual histology compared with in vitro histopathology. J Am Coll Cardiol 2006;47:2405-12.

28. Rodriguez-Granillo GA, Garcia-Garcia HM, Mc Fadden EP et al. In vivo intravascular ultrasound-derived thin-cap fibroatheroma detection using ultrasound radiofrequency data analysis. J Am Coll Cardiol 2005;46:2038-42.

29. Pundziute G, Schuijf JD, Jukema JW et al. Evaluation of plaque characteristics in acute coronary syndromes: non-invasive assessment with multi-slice computed tomography and invasive evaluation with intravascular ultrasound radiofrequency data analysis. Eur Heart J 2008;29:2373-81.

30. Rodriguez-Granillo GA, Serruys PW, Garcia-Garcia HM et al. Coronary artery remodelling is related to plaque composition. Heart 2006;92:388-91.

31. Valgimigli M, Rodriguez-Granillo GA, Garcia-Garcia HM et al. Distance from the ostium as an independent determinant of coronary plaque composition in vivo: an intravascular ultrasound study based radiofrequency data analysis in humans. Eur Heart J 2006;27:655-63.

32. Serruys PW, Garcia-Garcia HM, Buszman P et al. Effects of the direct lipoprotein-associated phospholipase A(2) inhibitor darapladib on human coronary atherosclerotic plaque. Circulation 2008;118:1172-82.

33. Jang IK, Bouma BE, Kang DH et al. Visualization of coronary atherosclerotic plaques in patients using optical coherence tomography: comparison with intravascular ultrasound. J Am Coll Cardiol 2002;39:604-9.

34. Tanaka A, Imanishi T, Kitabata H et al. Distribution and frequency of thin-capped fibroatheromas and ruptured plaques in the entire culprit coronary artery in patients with acute coronary syndrome as determined by optical coherence tomography. Am J Cardiol 2008;102:975-9.

35. Yabushita H, Bouma BE, Houser SL et al. Characterization of human atherosclerosis by optical coherence tomography. Circulation 2002;106:1640-5.

36. Jang IK, Tearney GJ, MacNeill B et al. In vivo characterization of coronary atherosclerotic plaque by use of optical coherence tomography. Circulation 2005;111:1551-5.

37. Kubo T, Imanishi T, Takarada S et al. Assessment of culprit lesion morphology in acute myocardial infarction: ability of optical coherence tomography compared with intravascular ultrasound and coronary angioscopy. J Am Coll Cardiol 2007;50:933-9.

38. Tearney GJ, Yabushita H, Houser SL et al. Quantification of macrophage content in atherosclerotic plaques by optical coherence tomography. Circulation 2003;107:113-9.

39. Raffel OC, Tearney GJ, Gauthier DD et al. Relationship between a systemic inflammatory marker, plaque inflammation, and plaque characteristics determined by intravascular optical coherence tomography. Arterioscler Thromb Vasc Biol 2007;27:1820-7.

40. Tearney GJ, Waxman S, Shishkov M et al. Three-dimensional coronary artery microscopy by intracoronary optical frequency domain imaging. JACC Cardiovasc Imaging 2008;1:752-61.

41. de Korte CL, Pasterkamp G, van der Steen AF et al. Characterization of plaque components with intravascular ultrasound elastography in human femoral and coronary arteries in vitro. Circulation 2000;102:617-23.

42. Schaar JA, de Korte CL, Mastik F et al. Characterizing vulnerable plaque features with intravascular elastography. Circulation 2003;108:2636-41.

43. Uchida Y, Nakamura F, Tomaru T et al. Prediction of acute coronary syndromes by percutaneous coronary angioscopy in patients with stable angina. Am Heart J 1995;130:195-203.

44. Takano M, Mizuno K, Yokoyama S et al. Changes in coronary plaque color and morphology by lipid-lowering therapy with atorvastatin: serial evaluation by coronary angioscopy. J Am Coll Cardiol 2003;42:680-6.

45. Margolis JR, Chen JT, Kong Y et al. The diagnostic and prognostic significance of coronary artery calcification. A report of 800 cases. Radiology 1980;137:609-16.

46. Agatston AS, Janowitz WR, Hildner FJ et al. Quantification of coronary Artery calcium using ultrafast computed tomography. J Am Coll Cardiol 1990;15:827-32.

47. Budoff MJ, Diamond GA, Raggi P et al. Continuous probabilistic prediction of angiographically significant coronary artery disease using electron beam tomography. Circulation 2002;105: 1791-6.

48. Haberl R, Becker A, Leber A et al. Correlation of coronary calcification and angiographically documented stenoses in patients with suspected coronary artery disease: results of 1,764 patients. J Am Coll Cardiol 2001;37:451-7.

49. Nallamothu BK, Saint S, Bielak LF et al. Electron-beam computed tomography in the diagnosis of coronary artery disease: a meta-analysis. Arch Intern Med 2001;161:833-8.

50. Greenland P, LaBree L, Azen SP et al. Coronary artery calcium score combined with Framingham score for risk prediction in asymptomatic individuals. JAMA 2004;291:210-5.

51. Detrano R, Guerci AD, Carr JJ et al. Coronary calcium as a predictor of coronary events in four racial or ethnic groups. N Engl J Med 2008;358:1336-45.

52. Budoff MJ, Shaw LJ, Liu ST et al. Long-term prognosis associated with coronary calcification: observations from a registry of 25,253 patients. J Am Coll Cardiol 2007;49:1860-70.

53. Achenbach S, Ropers D, Pohle K et al. Influence of lipid-lowering therapy on the progression of coronary artery calcification: a prospective evaluation. Circulation 2002;106:1077-82.

54. Schmermund A, Erbel R. Unstable coronary plaque and its relation to coronary calcium. Circulation 2001;104:1682-7.

55. Budoff MJ, Dowe D, Jollis JG et al. Diagnostic performance of 64-multidetector row coronary computed tomographic angiography for evaluation of coronary artery stenosis in individuals without known coronary artery disease: results from the prospective multicenter ACCURACY (Assessment by Coronary Computed Tomographic Angiography of Individuals Undergoing Invasive Coronary Angiography) trial. J Am Coll Cardiol 2008;52:1724-32.

56. Hoffmann U, Nagurney JT, Moselewski F et al. Coronary multidetector computed tomography in the assessment of patients with acute chest pain. Circulation 2006;114:2251-60.

57. Pohle K, Achenbach S, Macneill B et al. Characterization of non-calcified coronary atherosclerotic plaque by multi-detector row CT: comparison to IVUS. Atherosclerosis 2007;190:174-80.

58. Motoyama S, Kondo T, Sarai M et al. Multislice computed tomographic characteristics of coronary lesions in acute coronary syndromes. J Am Coll Cardiol 2007;50:319-26.

59. Henneman MM, Schuijf JD, Pundziute G et al. Noninvasive evaluation with multislice computed tomography in suspected acute coronary syndrome: plaque morphology on multislice computed tomography versus coronary calcium score. J Am Coll Cardiol 2008;52:216-22.

60. Min JK, Shaw LJ, Devereux RB et al. Prognostic value of multidetector coronary computed tomographic angiography for prediction of all-cause mortality. J Am Coll Cardiol 2007;50:1161-70.

61. Pundziute G, Schuijf JD, Jukema JW et al. Prognostic value of multislice computed tomography coronary angiography in patients with known or suspected coronary artery disease. J Am Coll Cardiol 2007;49:62-70.

62. van Werkhoven JM, Schuijf JD, Gaemperli O et al. Prognostic value of multislice computed tomography and gated single-photon emission computed tomography in patients with suspected coronary artery disease. J Am Coll Cardiol 2009;53:623-32.

63. Ibanez B, Cimmino G, Benezet-Mazuecos J et al. Quantification of serial changes in plaque burden using multi-detector computed tomography in experimental atherosclerosis. Atherosclerosis 2009;202:185-91.

64. Burgstahler C, Reimann A, Beck T et al. Influence of a lipid-lowering therapy on calcified and noncalcified coronary plaques monitored by multislice detector computed tomography: results of the New Age II Pilot Study. Invest Radiol 2007;42:189-95.

65. Earls JP, Berman EL, Urban BA et al. Prospectively gated transverse coronary CT angiography versus retrospectively gated helical technique: improved image quality and reduced radiation dose. Radiology 2008;246:742-53.

66. Husmann L, Valenta I, Gaemperli O et al. Feasibility of low-dose coronary CT angiography: first experience with prospective ECG-gating. Eur Heart J 2008;29:191-7.

67. Steigner ML, Otero HJ, Cai T et al. Narrowing the phase window width in prospectively ECG-gated single heart beat 320-detector row coronary CT angiography. Int J Cardiovasc Imaging 2009;25:85-90.

68. Fayad ZA, Nahar T, Fallon JT et al. In vivo magnetic resonance evaluation of atherosclerotic plaques in the human thoracic aorta: a comparison with transesophageal echocardiography. Circulation 2000;101:2503-9.

69. Hatsukami TS, Ross R, Polissar NL et al. Visualization of fibrous cap thickness and rupture in human atherosclerotic carotid plaque in vivo with high-resolution magnetic resonance imaging. Circulation 2000;102:959-64.

70. Skinner MP, Yuan C, Mitsumori L et al. Serial magnetic resonance imaging of experimental atherosclerosis detects lesion fine structure, progression and complications in vivo. Nat Med 1995;1:69-73.

71. Toussaint JF, LaMuraglia GM, Southern JF et al. Magnetic resonance images lipid, fibrous, calcified, hemorrhagic, and thrombotic components of human atherosclerosis in vivo. Circulation 1996;94:932-8.

72. Maynor CH, Charles HC, Herfkens RJ et al. Chemical shift imaging of atherosclerosis at 7.0 Tesla. Invest Radiol 1989;24:52-60.

73. Soila K, Nummi P, Ekfors T et al. Proton relaxation times in arterial wall and atheromatous lesions in man. Invest Radiol 1986;21:411-5.

74. Stuber M, Weiss RG. Coronary magnetic resonance angiography. J Magn Reson Imaging 2007;26:219-34.

75. Fayad ZA, Fuster V, Fallon JT et al. Noninvasive in vivo human coronary artery lumen and wall imaging using black-blood magnetic resonance imaging. Circulation 2000;102:506-10.

76. Kim WY, Stuber M, Bornert P et al. Three-dimensional black-blood cardiac magnetic resonance coronary vessel wall imaging detects positive arterial remodeling in patients with nonsignificant coronary artery disease. Circulation 2002;106:296-9.

77. Botnar RM, Stuber M, Lamerichs R et al. Initial experiences with in vivo right coronary artery human MR vessel wall imaging at 3 tesla. J Cardiovasc Magn Reson 2003;5:589-94.

78. Kooi ME, Cappendijk VC, Cleutjens KB et al. Accumulation of ultrasmall superparamagnetic particles of iron oxide in human atherosclerotic plaques can be detected by in vivo magnetic resonance imaging. Circulation 2003;107:2453-8.

79. Wasserman BA, Smith WI, Trout HH, III et al. Carotid artery atherosclerosis: in vivo morphologic characterization with gadolinium-enhanced double-oblique MR imaging initial results. Radiology 2002;223:566-73.

80. Yuan C, Kerwin WS, Ferguson MS et al. Contrast-enhanced high resolution MRI for atherosclerotic carotid artery tissue characterization. J Magn Reson Imaging 2002;15:62-7.

81. Tang TY, Muller KH, Graves MJ et al. Iron Oxide Particles for Atheroma Imaging. Arterioscler Thromb Vasc Biol 2009;29:1001-8.

82. Spuentrup E, Buecker A, Katoh M et al. Molecular magnetic resonance imaging of coronary thrombosis and pulmonary emboli with a novel fibrin-targeted contrast agent. Circulation 2005;111:1377-82.

83. Corti R, Fayad ZA, Fuster V et al. Effects of lipid-lowering by simvastatin on human atherosclerotic lesions: a longitudinal study by high-resolution, noninvasive magnetic resonance imaging. Circulation 2001;104:249-52.

84. Deguchi JO, Aikawa M, Tung CH et al. Inflammation in atherosclerosis: visualizing matrix metalloproteinase action in macrophages in vivo. Circulation 2006;114:55-62.

85. Gough PJ, Gomez IG, Wille PT et al. Macrophage expression of active MMP-9 induces acute plaque disruption in apoE-deficient mice. J Clin Invest 2006;116:59-69.

86. Schafers M, Riemann B, Kopka K et al. Scintigraphic imaging of matrix metalloproteinase activity in the arterial wall in vivo. Circulation 2004;109:2554-9.

87. Kolodgie FD, Petrov A, Virmani R et al. Targeting of apoptotic macrophages and experimental atheroma with radiolabeled annexin V: a technique with potential for noninvasive imaging of vulnerable plaque. Circulation 2003;108:3134-9.

88. Kietselaer BL, Reutelingsperger CP, Heidendal GA et al. Noninvasive detection of plaque instability with use of radiolabeled annexin A5 in patients with carotid-artery atherosclerosis. N Engl J Med 2004;350:1472-3.

89. Rudd JH, Warburton EA, Fryer TD et al. Imaging atherosclerotic plaque inflammation with [18F]-fluorodeoxyglucose positron emission tomography. Circulation 2002;105:2708-11.

90. Worthley SG, Zhang ZY, Machac J et al. In vivo non-invasive serial monitoring of FDG-PET progression and regression in a rabbit model of atherosclerosis. Int J Cardiovasc Imaging 2009; 25:251-7.

91. Tahara N, Kai H, Ishibashi M et al. Simvastatin attenuates plaque inflammation: evaluation by fluorodeoxyglucose positron emission tomography. J Am Coll Cardiol 2006;48:1825-31.

92. Alexanderson E, Slomka P, Cheng V et al. Fusion of positron emission tomography and coronary computed tomographic angiography identifies fluorine 18 fluorodeoxyglucose uptake in the left main coronary artery soft plaque. J Nucl Cardiol 2008;15:841-3.

93. Wykrzykowska J, Lehman S, Williams G et al. Imaging of Inflamed and Vulnerable Plaque in Coronary Arteries with 18F-FDG PET/CT in Patients with Suppression of Myocardial Uptake Using a Low-Carbohydrate, High-Fat Preparation. J Nucl Med 2009;50:563-8.

94. Yuan C, Mitsumori LM, Beach KW et al. Carotid atherosclerotic plaque: noninvasive MR characterization and identification of vulnerable lesions. Radiology 2001;221:285-99.

95. Narula J, Garg P, Achenbach S et al. Arithmetic of vulnerable plaques for noninvasive imaging. Nat Clin Pract Cardiovasc Med 2008;5 Suppl 2:S2-10.

96. Little WC, Constantinescu M, Applegate R et al. Can coronary angiography predict the site of a subsequent myocardial infarction in patients with mild-to-moderate coronary artery disease? Circulation 1988;78:1157-66.

97. Nobuyoshi M, Tanaka M, Nosaka H et al. Progression of coronary atherosclerosis: is coronary spasm related to progression? J Am Coll Cardiol 1991;18:904-10.

98. Giroud D, Li JM, Urban P et al. Relation of the site of acute myocardial infarction to the most severe coronary arterial stenosis at prior angiography. Am J Cardiol 1992;69:729-32.

99. Garcia JA, Movassaghi B, Casserly IP et al. Determination of optimal viewing regions for X-ray coronary angiography based on a quantitative analysis of 3D reconstructed models. Int J Cardiovasc Imaging 2008;25:455-62.

100. Corti R. Noninvasive imaging of atherosclerotic vessels by MRI for clinical assessment of the effectiveness of therapy. Pharmacol Ther 2006;110:57-70.

PART 1

Diagnosis of coronary
atherosclerosis
and vulnerable plaque

CHAPTER 2

Evaluation of Coronary Plaque Type and Composition with 320-Row Multidetector Computed Tomography: Comparison to Virtual Histology Intravascular Ultrasound

Joëlla E. van Velzen, Joanne D. Schuijf, Fleur R. de Graaf, Mark J. Boogers, Cornelis J. Roos, Martin J. Schalij, Lucia J. Kroft, Albert de Roos, Johan H.C. Reiber, Ernst E. van der Wall, J. Wouter Jukema, Jeroen J. Bax

ABSTRACT

Background: Recently, 320-row multidetector computed tomography angiography (CTA) has been introduced. However, the relation between plaque observations on 320-row CTA versus virtual histology intravascular ultrasound (VH IVUS) remains relatively unknown. Therefore, the objective of this study was to compare plaque observations on 320-row CTA to VH IVUS.

Methods: In total, 65 patients underwent 320-row CTA followed by VH IVUS. On CTA, three plaque types were identified: non-calcified, mixed and calcified. Attenuation values (Hounsfield Units (HU)) were measured in 3 regions of interest. On VH IVUS, plaque composition (% fibrotic, fibro-fatty, necrotic core, dense calcium) and presence of thin cap fibroatheroma (TCFA, more high risk) were evaluated.

Results: Overall, of the 272 plaques identified on CTA, 110 plaques (40%) were non-calcified, 142 plaques were mixed (52%) and 20 plaques (8%) were calcified. Non-calcified plaques demonstrated the lowest attenuation values (70 ± 37 HU), followed by mixed plaques (258 ± 219 HU) and calcified plaques (836 ± 226 HU). Plaque classification on CTA showed good agreement to VH IVUS. As compared with calcified plaques, non-calcified plaques contained more fibro-fatty tissue (54 ± 23% versus 47 ± 21%, p=0.001). Moreover, mixed and calcified plaques contained more dense calcium (9 ± 6% and 10 ± 7%, respectively) than non-calcified plaques (6 ± 6%, p<0.001). More necrotic core was present in mixed plaque (16 ± 8%) than in non-calcified (12 ± 7%) and calcified plaques (14 ± 7%)(p<0.001). Interestingly, mixed plaques most often corresponded to the presence of TCFA on VH IVUS (22%).

Conclusion: Plaque observations on 320-row CTA show good agreement to relative plaque composition on VH IVUS. Moreover, mixed plaques on 320-row CTA parallel the more high risk plaques on VH IVUS.

INTRODUCTION

Coronary multidetector computed tomography angiography (CTA) has generated great interest in recent years. The technique has been shown to have a high diagnostic performance in the non-invasive assessment of patients with known or suspected coronary artery disease (CAD).[1-3] An important advantage of coronary CTA is that not only luminal narrowing can be visualized but also atherosclerotic plaque composition in the arterial wall. Indeed, three different plaques types can be distinguished by CTA: non-calcified, mixed and calcified plaque. Interestingly, certain plaque characteristics on CTA have been associated with acute coronary syndromes. For instance, the presence of non-calcified and mixed coronary plaques has been related to acute coronary syndromes (ACS), whereas calcified plaques were related to stable CAD.[4] Nonetheless, plaque characterization with CTA has been notoriously demanding, particularly with earlier generation CTA systems because of limited spatial and temporal resolution.

Recently, a novel CTA system has been introduced equipped with 320-detector rows which can provide 16-cm anatomical coverage in one gantry rotation.[5] Accordingly, the 320-row system allows a volumetric scanning approach, covering the entire heart in a single heart beat. Additionally, volume scanning eliminates the problem of stair-step artifacts caused by inter-heartbeat variations as well as a reduction in cardiac motion artifacts often observed during step-and-shoot acquisition techniques and helical imaging. More importantly, volume scanning offers a distinct decrease in radiation dose and contrast administration in comparison with traditional helical scanning, as only one gantry rotation is needed to image the entire heart (350 ms).[6 7] Moreover, contrast is more homogenously distributed through the coronary arteries, thereby potentially improving the ability and reliability to characterize plaque composition.[8] Accordingly, these developments have resulted in overall improved image quality and diagnostic accuracy for the detection of CAD.[6 7]

However, no previous literature concerning the ability of plaque characterization in vivo with the new 320-detector row CTA technique has been published. Therefore, the aim of the present study was to evaluate the accuracy of coronary plaque characterization by the novel non-invasive 320-row CTA as compared to findings of invasive virtual histology intravascular ultrasound (VH IVUS).

METHODS

Patients and study protocol

The study group consisted of 65 symptomatic patients who presented at the outpatient clinic for the evaluation of chest pain and underwent non-invasive 320-row CTA followed by invasive coronary angiography and VH IVUS of 1 to 3 vessels. No interventions or changes in the clinical condition of the patients occurred between the examinations. Contra-indications for CTA were 1) (supra) ventricular arrhythmias, 2) renal insufficiency (glomerular filtration rate <30 ml/min), 3) known allergy to iodine contrast material, 4) severe claustrophobia, 5) pregnancy. Exclusion criteria for IVUS were severe vessel tortuousness, severe stenosis or vessel occlusion.

CTA

Data acquisition

CTA was performed using a 320-row CTA scanner (Aquilion ONE, Toshiba Medical Systems, Otawara, Japan) with 320 detector rows (each 0.50 mm wide) and a rotation time of 350 ms resulting in a spatial resolution of 0.5 mm and temporal resolution of 175 ms for half reconstruction. Beta-blocking medication (metoprolol 50 or 100 mg, single dose, 1 hour prior to CTA examination) were administered if the heart rate was ≥65 beats/min, unless contra-indicated. In addition, nitroglycerin (0.4 or 0.8 mg sublingual) was administered 5 minutes prior to CTA examination. For the 320-row contrast enhanced scan the entire heart was imaged in a single heartbeat, with a maximum of 16 cm cranio-caudal cover-age, using prospective ECG triggering. The phase window was adjusted according to the heart rate: if the heart rate was ≥60 beats/min the phase window was opened at 65-85% of R-R interval, if the heart rate was stable and <60 beats/min the phase window was opened at 70-80% of R-R interval. Tube voltage and current were adapted to body mass index (BMI) and thoracic anatomy. Tube voltage was 100 kV (BMI <23 kg/m^2), 120 kV (BMI, 23-35 kg/m^2), or 135 kV (BMI >35 kg/m^2) and maximal tube current was 400-580 mA (depending on body weight and thoracic anatomy). Contrast material was administered in a triple-phase protocol: first a bolus of 60 to 80 ml, followed by 40 ml of a 50:50 mixture of contrast and saline, followed by saline flush with a flow rate of 5-6 ml/sec (Iomeron 400 ®, Bracco, Milan, Italy). Automatic bolus arrival detection was applied in the left ventricle with a threshold of +180 Hounsfield Units. All images were acquired during an inspiratory breath-hold of approximately 4-8 seconds. Firstly, a data set was reconstructed at 75% of R-R interval, with a slice thickness of 0.50 mm and a reconstruction interval of 0.25 mm. In case of motion artifacts, multiple phases were reconstructed to obtain maximal diagnostic image quality. Subsequently, raw data sets were transferred to a remote work-station (Vitrea FX 1.0, Vital Images, Minnetonka, MN, USA). Radiation dose was quantified with a dose-length product conversion factor of 0.014 mSv/(mGy x cm).[9] As previously described, if scanning was performed prospectively full dose at 70-80% of R-R interval, estimated mean radiation dose was 3.9 ±1.3 mSv (range 2.7-6.2 mSv).[10] When scanning prospectively full dose at 65-85% of R-R interval, estimated mean radiation dose was 6.0 ±3.0 mSv (range 3.1-11.8 mSv).

Coronary plaque assessment

For data evaluation, 320-row CTA angiographic examinations were evaluated by 2 experi-enced readers including an interventional cardiologist blinded to conventional coronary angiography and VH IVUS findings. Agreement between observers was achieved in con-sensus. Firstly, general information on the coronary anatomy was obtained by evaluating three-dimensional volume rendered reconstructions. Secondly, the coronary arteries were evaluated using axial images, curved multiplanar reconstructions and maximum intensity projections. Furthermore, the coronary arteries were divided into segments according to the modified American Heart Association classification.[11] Each segment was evaluated

for the presence of any atherosclerotic plaque (defined as structures >1 mm^2 within and/or adjacent to the coronary artery lumen, which could be clearly distinguished from the vessel lumen).[12] Per segment one coronary plaque was selected at the site of the most severe luminal narrowing. Subsequently, axial slices were visually examined for the presence of significant luminal narrowing by determining the presence of ≥50% reduction of luminal diameter. To describe plaque composition, plaques were further classified as: 1) non-calcified plaque (plaques with lower CTA attenuation values as compared to contrast-enhanced lumen without any calcification), 2) mixed plaque (non-calcified and calcified elements in single plaque) 3) calcified plaque (plaques with high CTA attenuation values as compared to contrast-enhanced lumen). Of note, very small calcifications can still be missed by CTA.[13] As previously described, a good intra-observer agreement was observed for the classification of plaque type on CTA.[14][15] Furthermore, within the plaque, the CTA attenuation values measurements in Hounsfield Units (HU) were made using 3 circular regions of interest (area of 1.5 mm^2) that were placed in the center of the plaque. Consequently, the mean attenuation values (HU) were determined per plaque.

VH IVUS

Image acquisition

A dedicated IVUS-console (Volcano Corporation, Rancho Cordova, CA, USA) was used for the examination. Intracoronary nitrates were administrated prior to insertion of the IVUS catheter. VH IVUS was performed with a 20 MHz, 2.9 F phased-array IVUS catheter, (Eagle Eye, Volcano Corporation, Rancho Cordova, CA, USA) which was introduced distally in the coronary artery. A cine run was made before and after contrast injection to record the starting position of the IVUS catheter. Subsequently, motorized automated IVUS pullback was performed using a speed of 0.5 mm/s until the catheter reached the guiding catheter. Radiofrequency signals were collected at the R wave and images were stored on CD-ROM or DVD for off-line analysis. Of note, the typical resolution of a 20 MHz IVUS catheter is 80 microns axially and 200 to 250 microns laterally.[16]

Coronary plaque assessment

Offline analysis of the VH IVUS images was performed using dedicated software (pcVH 2.1 and VIAS 3.0, Volcano Corporation, Rancho Cordova, CA, USA). The lumen and the media-adventitia interface were defined by automatic contour detection and on all individual frames manual editing was performed. The four plaque components were differentiated into different color-codes (fibrotic tissue labeled in dark green, fibro-fatty in light green, necrotic core in red and dense calcium in white), as validated previously.[17] For each target plaque, plaque length was measured (mm).[16] Furthermore, plaques were visually qualitatively classified on 3 consecutive frames at the minimal lumen area site. Classification was obtained according to the following categorization:

(i) Pathological intimal thickening; defined as a mixture of fibrous and fibro-fatty tissues, a plaque burden ≥40% and <10% necrotic core and dense calcium.

(ii) Fibroatheroma; defined as having a plaque burden ≥40% and a confluent necrotic core occupying 10% of the plaque area or greater in 3 successive frames with evidence of an overlying fibrous cap.

(iii) TCFA; defined as a lesion with a plaque burden ≥40%, the presence of confluent necrotic core of >10%, and no evidence of an overlying fibrous cap in 3 successive frames.

(iv) Fibrocalcific plaque; defined as a lesion with a plaque burden ≥40%, being mainly composed of fibrotic tissue, having dense calcium >10% and a confluent necrotic core of <10% (higher amount accepted if necrotic core was located exclusively behind the accumulation of calcium).[18][19]

Statistical analysis

For each plaque type on CTA, the number and mean CTA attenuation values were assessed. On VH IVUS, relative plaque composition and plaque type was also assessed for each lesion. After initial plaque assessment, plaques on CTA were matched to plaques on VH IVUS using landmarks such as coronary ostia, side-branches and calcium deposits to allow accurate comparison between CTA and VH IVUS. Distances from the landmarks to the lesion were measured on curved multiplanar reconstructions on CTA and matched with the longitudinal images of VH IVUS. Plaque type classification on 320-row CTA was compared to both plaque composition and plaque type on VH IVUS. Finally, mean CTA attenuation values were compared between the various plaque types as assessed on VH IVUS. Continuous values were expressed as means (±standard deviation) and differences in plaque composition, type and Hounsfield units were assessed using a nested analysis of variance (ANOVA). Categorical values are expressed as number (percentages) and compared between groups with 2-tailed Chi-square test. A p-value of <0.05 was considered statistically significant. Statistical analysis was performed using SPSS 16.0 software (SPSS Inc., Chicago. Illinois).

RESULTS

Patient characteristics

The CTA and VH IVUS examinations were performed without complications in 65 patients. However, 3 patients were excluded due to non-diagnostic CTA image quality as a result of motion artifacts (n=2) and occurrence of an ectopic heart beat (n=1). Baseline patient characteristics of the remaining 62 patients are presented in Table 1. Mean heart rate was 57 ±7 beats/min. In total, 272 plaques were identified in which comparison between 320-row CTA and VH IVUS was possible. Fifty plaques (18%) corresponded to significant luminal narrowing on CTA.

Table 1. Patient characteristics of study population

	n (%)
Gender (M/F)	46 / 16
Age (years)	58 ±10
Risk factors for CAD	
Diabetes	13 (21%)
Hypertension	35 (57%)
Hypercholesterolemia	22 (36%)
Positive family history	31 (50%)
Current smoking	21 (34%)
Obese (BMI ≥30 kg/m^2)	9 (15%)
Previous CAD	
Previous myocardial infarction	15 (24%)
Previous PCI	16 (26)%
Heart rate (beats/min) during CTA	57 ±7

CAD; coronary artery disease, BMI; body mass index, PCI; percutaneous coronary intervention, CTA; multidetector computed tomography angiography.

Baseline 320-row CTA and VH IVUS results

Overall, of the 272 plaques identified on CTA, 110 plaques (40%) were non-calcified, 142 plaques were mixed (52%) and 20 plaques (8%) were calcified. Mean CTA attenuation value of the plaques was 224 ±222 HU. Non-calcified plaques demonstrated the lowest attenuation values (70 ±37 HU), followed by mixed plaques (258 ±219 HU) and calcified plaques (836 ±226 HU) (Figure 1).

VH IVUS examinations were acquired during invasive coronary angiography in 153 of the 186 available vessels (right coronary artery=51, left anterior descending coronary artery=56, left circumflex coronary artery=46). On VH IVUS, mean lesion length was 27.5 ±17.5 mm. Furthermore, the most prevalent plaque component was fibrotic tissue (52
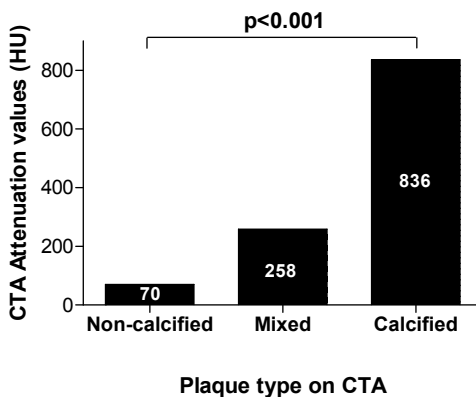
Figure 1. Comparison of attenuation values as measured in Hounsfield Units (HU) on 320-row multidetector computed tomography angiography (CTA) between the different plaque types on CTA. A significant difference in CTA attenuation values is demonstrated between non-calcified, mixed and calcified plaques on CTA (p<0.001).

±18%), followed by fibro-fatty tissue (28 ±14%), necrotic core (14 ±8%) and dense calcium (8 ±6%). The more vulnerable plaque type (TCFA) was present in 44 plaques (16%).

Comparison between 320-row CTA and VH IVUS

A good agreement was found when comparing plaque type classification on 320-row CTA to plaque composition on VH IVUS as demonstrated in Table 2. As compared with calcified plaques, non-calcified plaques contained significantly more fibro-fatty tissue on VH IVUS (54 ±23% versus 47 ±21% in calcified plaques, p=0.001). Moreover, mixed and calcified plaques on CTA contained significantly more dense calcium (9 ±6% and 10 ±7%, respectively) on VH IVUS than non-calcified plaques (6 ±6%, p<0.001). In addition, signifi-

Table 2. Comparison between plaque composition on virtual histology intravascular ultrasound (VH IVUS) and 320-row multidetector computed tomography angiography (CTA)

VH IVUS characteristics	Non-calcified plaques on CTA	Mixed plaques on CTA	Calcified plaques on CTA	p-value
Lesion length (mm)	29 ±20	27 ±16	24 ±15	0.64
Fibrotic (%)	54 ±23	51 ±16	47 ±21	0.001
Fibro-fatty (%)	18 ±15	18 ±13	20 ±13	0.62
Necrotic Core (%)	12 ±7	16 ±8	14 ±7	<0.001
Dense Calcium (%)	6 ±6	9 ±6	10 ±7	<0.001

VH IVUS, virtual histology intravascular ultrasound; CTA, multidetector computed tomography angiography

cantly more necrotic core was present in mixed plaque (16 ±8%) than in non-calcified (12 ±7%) and calcified plaques (14 ±7%)(p<0.001). Example of plaque evaluation on 320-row CTA as compared to VH IVUS is shown in Figure 2.

The results comparing plaque types on CTA against qualitively assessed plaque types on VH IVUS are reported in Table 3. As expected, pathological intimal thickening on VH IVUS was most often observed in non-calcified plaques (20 (21%)) as compared to mixed plaques (14 (9%), p=0.03) and calcified plaques (0 (0%)) on CTA. Interestingly, the more high risk plaques on VH IVUS (TCFA) were most often observed in mixed plaques on CTA (22%, Figure 3). Moreover, fibrocalcific plaques on VH IVUS were most often observed in the calcified plaques (9 (47%) versus 5 (5%) in non-calcified, p<0.001) on CTA.

Furthermore, mean CTA attenuation values were compared between the different plaque types as assessed on VH IVUS (Figure 4). As shown, the more advanced plaque types on VH IVUS corresponded to higher CTA attenuation values. Pathological intimal thickening had the lowest mean attenuation value of 141 ±124 HU, followed by the fibroatheroma (mean attenuation value of 209 ±205 HU), TCFA (mean attenuation value of 251 ±222) and in the fibrocalcific plaques (mean attenuation value of 387 ±293 HU) the highest attenuation values were found. Interestingly, CTA attenuation value measure-
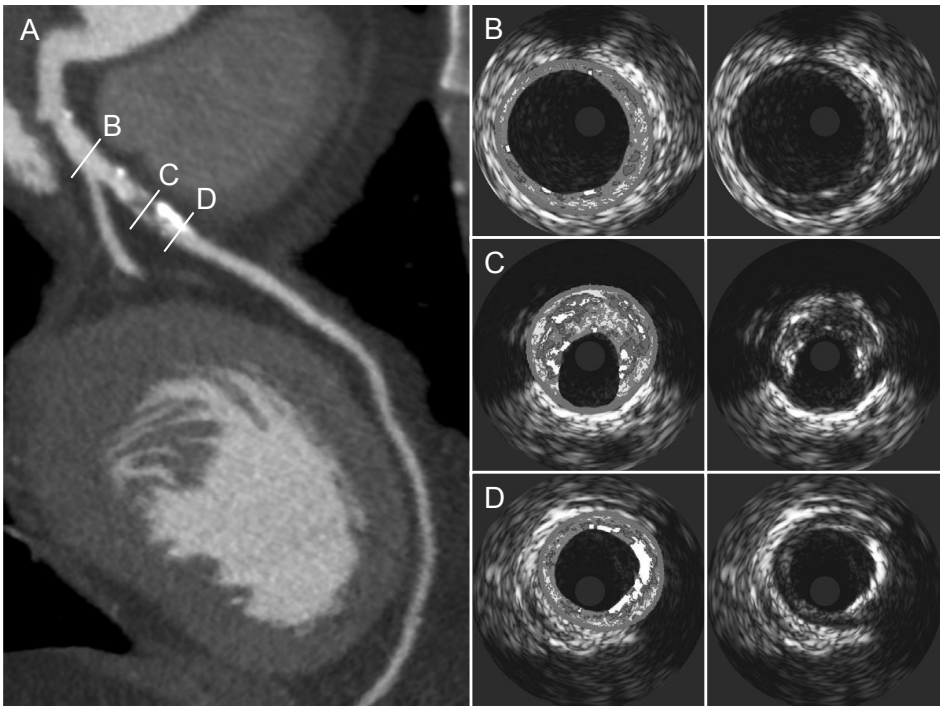
Figure 2. Example of comparison between plaque composition on 320-row multidetector computed tomography angiography (CTA) and virtual histology intravascular ultrasound (VH IVUS). In panel (A), a curved multiplanar reconstruction of the left anterior descending coronary artery is shown demonstrating no plaque at cross-section B and a mixed plaque at cross-section C and D. In panel (B, C and D) corresponding grayscale and VH IVUS images are shown. In panel (B), only minor intimal thickening is demonstrated. In panel (C), a plaque with a large plaque burden (≥40%), large necrotic core (≥10%) and no evidence of a fibrous cap is shown, suggesting the presence of a thin cap fibroatheroma. In panel (D) another cross-section is demonstrated showing extensive calcifications on both CTA and VH IVUS images.

Table 3. Comparison between plaque type on virtual histology intravascular ultrasound (VH IVUS) and 320-row multidetector computed tomography angiography (CTA)

VH IVUS plaque type	Non-calcified plaques on CTA	Mixed plaques on CTA	Calcified plaques on CTA	p-value
Presence PIT	20 (21%)	14 (9%)	0 (0%)	0.03
Presence FA	58 (62%)	73 (52%)	8 (42%)	0.58
Presence TCFA	11 (10%)	31 (22%)	2 (10%)	0.03
Presence FC	5 (5%)	23 (16%)	9 (47%)	<0.001

VH IVUS, virtual histology intravascular ultrasound; CTA, multidetector computed tomography; PIT, pathological intimal thickening; FA, fibroatheroma; TCFA, thin cap fibroatheroma; FC, fibrocalcific plaque
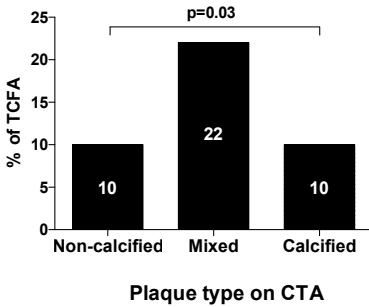
Figure 3. Comparison of presence (%) of thin cap fibroatheroma (TCFA) between the different plaque types on 320-row multidetector computed tomography angiography (CTA). Significantly more TCFA were present in mixed plaques (22%) as compared to non-calcified (10%) and calcified plaque (10%).
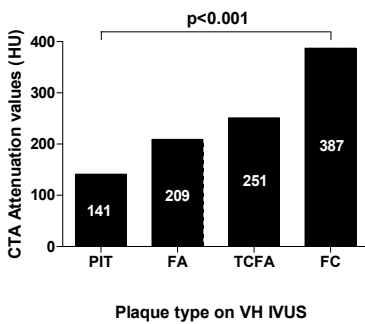
Figure 4. Comparison of attenuation values as measured in Hounsfield Units (HU) on 320-row multidetector computed tomography (CTA) between the different plaque types on virtual histology intravascular ultrasound (VH IVUS). A significant increase in CTA attenuation values is demonstrated for the more advanced plaque on VH IVUS. PIT, pathological intimal thickening; FA, fibroatheroma; TCFA, thin cap fibroatheroma; FC, fibrocalcific plaque.

ments of mixed plaques (258 ±219 HU) on CTA paralleled average attenuation values of TCFA (251 ±222 HU) on VH IVUS.

DISCUSSION

The present study evaluated the ability of plaque characterization on 320-row CTA as compared to invasive VH IVUS. In summary, the findings of the present study demonstrated that plaque characterization on 320-row CTA showed a good correlation with VH IVUS plaque characteristics. First, non-calcified plaques on 320-row CTA contained significantly more fibrotic tissue on VH IVUS than calcified plaques and mixed plaques on CTA. In addition, dense calcium on VH IVUS was most often observed in calcified plaques on CTA. Importantly, the highest amount of necrotic core (the more vulnerable plaque component) on VH IVUS was demonstrated in mixed plaque on 320-row CTA. Of particular interest was the finding that TCFA were most prevalent in mixed plaques, suggesting a possible higher degree of vulnerability in mixed plaques on CTA.

Second, the more advanced plaque types on VH IVUS corresponded to higher CTA attenuation values. Interestingly, CTA attenuation values of the more vulnerable plaque type (TCFA) on VH IVUS paralleled CTA attenuation values of the mixed plaques on 320-row CTA. However, these values still substantially overlapped as reflected by the large

standard deviations. Thus, distinction between the more subtle plaque features using CTA attenuation values does not seem feasible at this time.

Although 320-row CTA has only recently been introduced, preliminary data are available concerning the diagnostic performance of 320-row CTA.[20] De Graaf et al recently evaluated the diagnostic accuracy of 320-row CTA for detection of significant stenosis (defined as ≥50% luminal narrowing) in 64 patients using quantitative coronary angiography as the reference of standard.[6] The authors demonstrated an excellent diagnostic accuracy of 320-row for detection of significant stenosis, reporting sensitivity, specificity, and positive and negative predictive values on a patient basis of 100%, 88%, 92%, and 100%, respectively. Dewey et al also assessed the diagnostic accuracy 320-row CTA as compared to conventional coronary angiography in 30 patients.[7] The authors concluded that 320-row CTA has a high diagnostic accuracy for detection of significant stenosis while significantly reducing radiation dose.

The main advantage of the 320-row CTA, as compared to 64-row CTA, is the 16 cm anatomical coverage that can cover an entire organ, such as the heart, in a single gantry rotation. Indeed, 320-row CTA can accurately acquire images of the heart in a single beat (350 ms) as compared to the typical 6-10 seconds needed for 64-row systems.[21] Accordingly, this approach does not only lead to a marked reduction in radiation dose, it also eliminates helical acquisition artifacts. Additionally, due to the volume scanning approach, contrast is more homogenously distributed through the coronary arteries, thereby potentially improving the ability and reliability to characterize plaque composition with 320-row CTA. Nevertheless, the temporal (175 ms) and spatial resolution (0.5 mm) of the 320-row CTA systems remain similar to the latest generation 64-row CTA systems.[21]

Regarding plaque observations with CTA, several previous studies have correlated plaque composition on CTA to plaque characteristics on invasive IVUS. Initially, Pohle et al compared plaque composition on 16-row CTA to grayscale intravascular ultrasound in 32 patients.[22] The investigators identified 252 sites with non-calcified plaques on CTA and correlated the CTA attenuation values with invasive IVUS plaque characteristics. Interestingly, differences between subtle plaque features such as the more "vulnerable" lipid rich plaque (mean attenuation value of 58 ±43HU) and the more "stable" fibrous plaque (mean attenuation value of 121 ±34 HU) were demonstrated, although the overlap of attenuation values between individual characteristics were still substantial. Consequently, over the years newer generation CTA systems have been introduced with improved spatial and temporal resolution. Amongst others, Sun et al evaluated plaque characterization on 64-row CTA.[23] The investigators studied 26 patients with 40 lesions that underwent both 64-row CTA and IVUS and observed that although CTA was able to distinguish between fibrous and calcified plaques to a significant degree, there was no difference between lipid rich (mean attenuation value of 79 ±34 HU) and fibrous plaque components (mean attenuation value of 90 ±27 HU). When compared to histology, Chopard et al also demonstrated that differentiation between fibrous and lipid rich plaques with grayscale IVUS and 64-row CTA still remained limited.[24]

Only limited data are available regarding plaque composition assessment with VH IVUS in relation to CTA. In our institution, a previous comparison was made between CTA and VH IVUS, regarding the difference in plaque composition and vulnerability between lesions with significant (≥50% luminal narrowing) and non-significant stenosis on invasive coronary angiography in 78 patients. Interestingly, no evident relation existed between the degree of stenosis and plaque composition or vulnerability, as evaluated by CTA and VH IVUS.[25] In addition, Pundziute et al compared plaque composition between 64-row CTA and VH IVUS in 50 patients with 168 lesions.[26] Parallel to the current findings, the investigators also observed a good correlation between CTA and VH IVUS and demonstrated that TCFA was most often present in mixed plaque on CTA. However, the authors observed the largest amount of necrotic core in plaques deemed to be fully calcified on CTA, whereas in the current study necrotic core was largest in mixed plaques. This discrepancy can be possibly explained by differences in resolution between 64-row and 320-row CTA. Indeed, due to improved image quality, 320-row CTA could be superior in differentiating non-calcified elements within presence of calcified elements than 64-row CTA and thus allow more refined plaque characterization. Of note, dual-source CTA systems have recently been introduced that can operate two X-ray tubes at different kV settings. Accordingly, this may lead to more comprehensive characterization of atherosclerotic plaque, in particular the more calcified plaques.[27]

Several histopathological studies have observed that high-risk plaque features include the presence of a large necrotic core and thin fibrous cap (TCFA).[19 28 29] Indeed, the rupture of TCFA is thought to be the primary cause of ACS. There is an emerging need for imaging modalities that can identify atherosclerotic plaques with high-risk features, thus improving identification of patients that are at increased risk for events. In vivo, Rodriquez-Granillo et al demonstrated that VH IVUS was able to observe a higher degree of necrotic core and presence of TCFA in ACS patients as compared to patients with stable CAD.[30] In addition, VH IVUS could identify significantly more necrotic core in culprit lesions of patients presenting with ACS. However, VH IVUS is an invasive technique, restricted to patients referred for invasive coronary angiography and interventional procedures. Thus, a non-invasive modality that can identify patients at high risk would be preferred. Therefore, a number of previous studies have evaluated which plaque characteristics on CTA were related to increased plaque vulnerability. For instance, Pundziute et al compared plaque features on CTA between patients presenting with ACS and stable CAD and showed that mixed plaques were more prevalent in patients with ACS.[31] In addition, Motoyama et al compared plaque features of 38 patients with ACS to 33 patients with stable complaints.[32] Interestingly, features of mixed plaques such as spotty calcification and low attenuation non-calcified plaque elements were more often observed in patients with ACS. Importantly, when assessing the predictive value of plaque characteristics on CTA, the same authors demonstrated that these features (spotty calcifications, positive remodeling and low attenuation non-calcified plaque) were also prospectively related to the occurrence of ACS.[33] The aforementioned findings are in line with previous observations by IVUS suggesting that lesions containing smaller calcium deposits rather than extensive

calcifications are more often present in plaques related to ACS.[34 35] Of note, concerning the prognostic value of plaque composition on CTA, Pundziute et al demonstrated that mixed plaques were associated with more adverse events during follow-up.[36] Accordingly, these observations as well as our current findings further support the notion that lesions classified as mixed on CTA may have a higher likelihood of vulnerability.

However, with the latest generation 320-row CTA scanners, exact characterization of the lipid core and thin fibrous cap is not feasible at the moment. Nonetheless, although direct identification of TCFA may not be possible, non-invasive techniques may still be valuable, as they may identify patients with a higher likelihood of having vulnerable plaques at a relatively early stage and may provide an opportunity for intensified treatment strategies.

Limitations

The following limitations of the present study should be considered. First, the present study only evaluated 62 patients in a single center. Ideally, a larger patient population should be studied, preferably in a multicenter setting. Secondly, CTA is related with ionizing radiation exposure. Therefore, patients and image protocols should be carefully selected to prevent unnecessary exposure to radiation. Thirdly, severe calcifications on CTA can cause beam hardening and blooming artifacts and as a result can influence plaque classification. Similarly on VH IVUS, due to acoustic shadowing, it is difficult to assess plaque composition behind severe calcifications. Therefore, possibly small non-calcified elements within the more heavily calcified parts of the plaque may have been missed. Fourthly, descriptive studies have reported the influence of luminal contrast-enhancement on plaque attenuation values. However, in the present study we did not adjust for intra-coronary lumen contrast-enhancement as there is currently no validated algorithm available for this purpose. Lastly, no quantitative measurements were performed on plaque assessed with 320-row CTA, such as plaque volume, length and remodeling index, however, currently new dedicated software techniques are being developed to facilitate these measurements in the future.

Conclusion

Plaque observations on 320-row CTA show good agreement to relative plaque composition on VH IVUS. Moreover, mixed plaques on 320-row CTA parallel the more high risk plaques on VH IVUS.

REFERENCES

1. Meijboom WB, Meijs MF, Schuijf JD et al. Diagnostic accuracy of 64-slice computed tomography coronary angiography: a prospective, multicenter, multivendor study. J Am Coll Cardiol 2008;52: 2135-44.
2. Miller JM, Rochitte CE, Dewey M et al. Diagnostic performance of coronary angiography by 64-row CT. N Engl J Med 2008;359:2324-36.
3. Mowatt G, Cook JA, Hillis GS et al. 64-Slice computed tomography angiography in the diagnosis and assessment of coronary artery disease: systematic review and meta-analysis. Heart 2008; 94:1386-93.
4. Schuijf JD, Beck T, Burgstahler C et al. Differences in plaque composition and distribution in stable coronary artery disease versus acute coronary syndromes; non-invasive evaluation with multi-slice computed tomography. Acute Card Care 2007;9:48-53.
5. Hein PA, Romano VC, Lembcke A et al. Initial experience with a chest pain protocol using 320-slice volume MDCT. Eur Radiol 2009;19:1148-55.
6. De Graaf FR, Schuijf JD, Van Velzen JE et al. Diagnostic accuracy of 320-row multidetector computed tomography coronary angiography in the non-invasive evaluation of significant coronary artery disease. Eur Heart J 2010.
7. Dewey M, Zimmermann E, Deissenrieder F et al. Noninvasive coronary angiography by 320-row computed tomography with lower radiation exposure and maintained diagnostic accuracy: comparison of results with cardiac catheterization in a head-to-head pilot investigation. Circulation 2009;120:867-75.
8. Steigner ML, Mitsouras D, Whitmore AG et al. Iodinated contrast opacification gradients in normal coronary arteries imaged with prospectively ECG-gated single heart beat 320-detector row computed tomography. Circ Cardiovasc Imaging 2010;3:179-86.
9. Hausleiter J, Meyer T, Hermann F et al. Estimated radiation dose associated with cardiac CT angiography. JAMA 2009;301:500-7.
10. De Graaf FR, Schuijf JD, Van Velzen JE et al. Diagnostic accuracy of 320-row multidetector computed tomography coronary angiography in the non-invasive evaluation of significant coronary artery disease. Eur Heart J 2010.
11. Austen WG, Edwards JE, Frye RL et al. A reporting system on patients evaluated for coronary artery disease. Report of the Ad Hoc Committee for Grading of Coronary Artery Disease, Council on Cardiovascular Surgery, American Heart Association. Circulation 1975;51:5-40.
12. Leber AW, Knez A, Becker A et al. Accuracy of multidetector spiral computed tomography in identifying and differentiating the composition of coronary atherosclerotic plaques: a comparative study with intracoronary ultrasound. J Am Coll Cardiol 2004;43:1241-7.
13. van der Giessen AG, Gijsen FJ, Wentzel JJ et al. Small coronary calcifications are not detectable by 64-slice contrast enhanced computed tomography. Int J Cardiovasc Imaging 2010.
14. Klass O, Kleinhans S, Walker MJ et al. Coronary plaque imaging with 256-slice Multidetector Computed Tomography: interobserver variability of volumetric lesion parameters with semiautomatic plaque analysis software. Int J Cardiovasc Imaging 2010;26:711-20.
15. Pundziute G, Schuijf JD, Van Velzen JE et al. Assessment with multi-slice computed tomography and gray-scale and virtual histology intravascular ultrasound of gender-specific differences in extent and composition of coronary atherosclerotic plaques in relation to age. Am J Cardiol 2010;105:480-6.
16. Mintz GS, Nissen SE, Anderson WD et al. American College of Cardiology Clinical Expert Consensus Document on Standards for Acquisition, Measurement and Reporting of Intravascular Ultrasound Studies (IVUS). A report of the American College of Cardiology Task Force on Clinical Expert Consensus Documents. J Am Coll Cardiol 2001;37:1478-92.

17. Nasu K, Tsuchikane E, Katoh O et al. Accuracy of in vivo coronary plaque morphology assessment: a validation study of in vivo virtual histology compared with in vitro histopathology. J Am Coll Cardiol 2006;47:2405-12.

18. Carlier SG, Mintz GS, Stone GW. Imaging of atherosclerotic plaque using radiofrequency ultrasound signal processing. J Nucl Cardiol 2006;13:831-40.

19. Virmani R, Kolodgie FD, Burke AP et al. Lessons from sudden coronary death: a comprehensive morphological classification scheme for atherosclerotic lesions. Arterioscler Thromb Vasc Biol 2000;20:1262-75.

20. Rybicki FJ, Otero HJ, Steigner ML et al. Initial evaluation of coronary images from 320-detector row computed tomography. Int J Cardiovasc Imaging 2008;24:535-46.

21. Voros S. What are the potential advantages and disadvantages of volumetric CT scanning? J Cardiovasc Comput Tomogr 2009;3:67-70.

22. Pohle K, Achenbach S, Macneill B et al. Characterization of non-calcified coronary atherosclerotic plaque by multi-detector row CT: comparison to IVUS. Atherosclerosis 2007;190:174-80.

23. Sun J, Zhang Z, Lu B et al. Identification and quantification of coronary atherosclerotic plaques: a comparison of 64-MDCT and intravascular ultrasound. AJR Am J Roentgenol 2008;190:748-54.

24. Chopard R, Boussel L, Motreff P et al. How reliable are 40 MHz IVUS and 64-slice MDCT in characterizing coronary plaque composition? An ex vivo study with histopathological comparison. Int J Cardiovasc Imaging 2010;26:373-83.

25. Van Velzen JE, Schuijf JD, De Graaf FR et al. Plaque type and composition as evaluated non-invasively by MSCT angiography and invasively by VH IVUS in relation to the degree of stenosis. Heart 2009;95:1990-6.

26. Pundziute G, Schuijf JD, Jukema JW et al. Head-to-head comparison of coronary plaque evaluation between multislice computed tomography and intravascular ultrasound radiofrequency data analysis. JACC Cardiovasc Interv 2008;1:176-82.

27. Henzler T, Porubsky S, Kayed H et al. Attenuation-based characterization of coronary atherosclerotic plaque: Comparison of dual source and dual energy CT with single-source CT and histopathology. Eur J Radiol 2010.

28. Kolodgie FD. Pathologic assessment of the vulnerable human coronary plaque. Heart 2004;90: 1385-91.

29. Virmani R, Burke AP, Kolodgie FD et al. Pathology of the thin-cap fibroatheroma: a type of vulnerable plaque. J Intervent Cardiol 2003;16:267-72.

30. Rodriguez-Granillo GA, Garcia-Garcia HM, Mc Fadden EP et al. In vivo intravascular ultrasound-derived thin-cap fibroatheroma detection using ultrasound radiofrequency data analysis. Journal of the American College of Cardiology 2005;46:2038-42.

31. Pundziute G, Schuijf JD, Jukema JW et al. Evaluation of plaque characteristics in acute coronary syndromes: non-invasive assessment with multi-slice computed tomography and invasive evaluation with intravascular ultrasound radiofrequency data analysis. Eur Heart J 2008;29:2373-81.

32. Motoyama S, Kondo T, Sarai M et al. Multislice computed tomographic characteristics of coronary lesions in acute coronary syndromes. J Am Coll Cardiol 2007;50:319-26.

33. Motoyama S, Sarai M, Harigaya H et al. Computed tomographic angiography characteristics of atherosclerotic plaques subsequently resulting in acute coronary syndrome. J Am Coll Cardiol 2009;54:49-57.

34. Beckman JA, Ganz J, Creager MA et al. Relationship of clinical presentation and calcification of culprit coronary artery stenoses. Arterioscler Thromb Vasc Biol 2001;21:1618-22.

35. Ehara S, Kobayashi Y, Yoshiyama M et al. Spotty calcification typifies the culprit plaque in patients with acute myocardial infarction: an intravascular ultrasound study. Circulation 2004; 110:3424-9.

36. Pundziute G, Schuijf JD, Jukema JW et al. Prognostic value of multislice computed tomography coronary angiography in patients with known or suspected coronary artery disease. J Am Coll Cardiol 2007;49:62-70.

CHAPTER 3

Plaque Type and Composition as Evaluated Non-invasively by MSCT Angiography and Invasively by VH IVUS in Relation to the Degree of Stenosis

Joëlla E. van Velzen, Joanne D. Schuijf, Fleur R. de Graaf, Gaetano Nucifora, Gabija Pundziute, J. Wouter Jukema, Martin J. Schalij, Lucia J. Kroft, Albert de Roos, Johan H.C. Reiber, Ernst E. van der Wall, Jeroen J. Bax

ABSTRACT

Background: Imaging of coronary plaques has traditionally focused on evaluating degree of stenosis, as the risk for adverse cardiac events increases with stenosis severity. However, the relation between plaque composition and severity of stenosis remains largely unknown. Therefore, the objective of this study was to assess plaque composition (non-invasively by multislice computed tomography (MSCT) angiography and invasively by virtual histology intravascular ultrasound (VH IVUS)) in relation to degree of stenosis.

Methods: 78 patients underwent MSCT (identifying 3 plaque types; non-calcified, calcified, mixed) followed by invasive coronary angiography and VH IVUS. VH IVUS evaluated plaque burden, minimal lumen area and plaque composition (fibrotic, fibro-fatty, necrotic core, dense calcium) and plaques were classified as fibrocalcific, fibroatheroma, thin capped fibroatheroma (TCFA), pathological intimal thickening. For each plaque, percent stenosis was evaluated by quantitative coronary angiography. Significant stenosis was defined > 50% stenosis.

Results: Overall, 43 plaques (19%) corresponded to significant stenosis. Of the 227 plaques analyzed, 70 were non-calcified plaques (31%), 96 mixed (42%) and 61 calcified (27%) on MSCT. Plaque types on MSCT were equally distributed among significant and non-significant stenoses. VH IVUS identified that plaques with significant stenosis had higher plaque burden (67 ± 11% vs. 53 ± 12%, p<0.05) and smaller minimal lumen area (4.6 (3.8 - 6.8) mm² vs. 7.3 (5.4 - 10.5) mm², p<0.05). Interestingly, no differences were observed in % fibrotic, fibro-fatty, dense calcium and necrotic core. Non-significant stenoses were more frequently classified as pathological intimal thickening (46 (25%) vs. 3 (7%), p<0.05), although TCFA (more vulnerable plaque) was distributed equally (p=0.18).

Conclusion: No evident relation exists between the degree of stenosis and plaque composition or vulnerability, as evaluated non-invasively by MSCT and invasively by VH IVUS.

INTRODUCTION

Imaging of atherosclerosis has traditionally focused on evaluating the degree of stenosis, as the risk for adverse cardiac events increases with stenosis severity.[1] However, plaque composition rather than degree of stenosis may play a pivotal role in the development of acute atherothrombotic events and sudden cardiac death. Indeed, rupture of a vulnerable plaque (plaque with a large necrotic core, macrophage infiltration and thin fibrous cap) has been considered to be the primary cause of acute coronary syndromes (ACS).[2] In addition, it has been shown that almost two-thirds of vulnerable plaques are located in non-obstructive atherosclerotic lesions.[3][4] Moreover, non-obstructive lesions outnumber the more severely obstructive lesions and therefore account for the majority of ruptured plaques.[5][6] Possibly, direct visualisation of atherosclerosis rather than merely identifying obstructive disease may improve risk stratification for future events.

Multislice computed tomography (MSCT) has been demonstrated to be a promising tool for non-invasive assessment of atherosclerotic plaque burden and composition.[7] An important advantage of MSCT is that the technique not only visualizes luminal narrowing but can also identify atherosclerotic plaque in the arterial vessel wall.[7][8] Accordingly, in contrast to invasive coronary angiography, lesions that show outward (positive) remodeling without luminal narrowing can also be easily identified. In addition, information on plaque composition can be obtained and lesions can be differentiated into non-calcified, mixed or calcified. Interestingly, retrospective studies comparing plaque composition on MSCT between patients presenting with ACS and stable coronary artery disease (CAD) showed that non-calcified and mixed plaques were associated with ACS.[9][10]

With respect to invasive techniques, virtual histology intravascular ultrasound (VH IVUS) is a promising modality for the assessment of coronary plaque characteristics in vivo. VH IVUS has been validated against histopathology and shows good accuracy for the determination of different plaque components such as fibrotic, fibro-fatty, necrotic core and dense calcium.[11] The predictive accuracy of VH IVUS plaque composition assessment, when compared to histopathology, was 90.4% for fibrous, 92.8% for fibro-fatty, 89.5% for necrotic core, and 90.9% for dense calcium regions. Using this technique, it was demonstrated that differences in plaque composition can be related to particular clinical settings. Indeed, in a study by Rodriguez-Granillo et al., VH IVUS derived thin capped fibroatheroma (vulnerable plaque) were found more often in patients with ACS than patients with stable CAD.[12] Accordingly, VH IVUS may be useful for the evaluation of atherosclerotic plaque composition in vivo.

The purpose of this study was to evaluate if differences in plaque composition are related to the degree of stenosis. To this end, plaque composition was evaluated non-invasively by MSCT, followed by invasive evaluation using VH IVUS.

METHODS

Patients and study protocol

The study group consisted of 78 symptomatic patients who presented at the outpatient clinic (Leiden, the Netherlands) for the evaluation of chest pain and underwent MSCT coronary angiography followed within a month by clinically referred invasive coronary angiography and VH IVUS of 1 to 3 vessels. Contra-indications for MSCT were 1) (supra) ventricular arrhythmias, 2) renal insufficiency (glomerular filtration rate < 30 ml/min), 3) known allergy to iodine contrast material, 4) severe claustrophobia, 5) pregnancy. Exclusion criteria for IVUS were severe vessel tortuousness, severe stenosis or vessel occlusion. In each patient, the presence of CAD risk factors such as diabetes mellitus, systemic hypertension, hypercholesterolemia, positive family history, smoking and obesity, were recorded. The Framingham 10-year risk for hard CAD events was calculated as previously described in the National Cholesterol Education Program's Adult Treatment Panel III report.[13] Subsequently, the study population was then categorized as at low (< 10%), intermediate (10 - 20%) and high risk (> 20%).

MSCT

Data acquisition

MSCT coronary angiography was performed using either a 64-detector row helical scanner (Aquilion 64, Toshiba Multi-slice system, Toshiba Medical Systems, Otawara, Japan) or a 320-detector row volumetric scanner (Aquilion ONE, Toshiba Medical Systems, Otawara, Japan). Unless contra-indicated, if the heart rate ≥ 65 beats/min, beta-blockers (metoprolol 50 or 100 mg, single dose, 1 hour prior to examination) were administered. For the 64-slice contrast enhanced scan, collimation was 64 x 0.5 mm, tube voltage 100 to 135 kV and tube current 250 to 350 mA, depending on body shape. Non-ionic contrast material (Iomeron 400, Bracco, Milan, Italy) was administered with an amount of 80 to 110 ml followed by a saline flush with a flow rate of 5 ml/sec. For the 320-slice contrast enhanced scan the heart was imaged in a single heartbeat, using prospective triggering with exposure interval depending on the heart rate. Scan parameters were: 350 ms gantry rotation time, 100 to 135 kV tube voltage and a tube current of 400 to 580 mA, depending on body mass index. In total, 60 to 90 ml contrast material (Iomeron 400) was administered with a rate of 5 - 6 ml/sec followed by a saline flush. Subsequently, data sets were reconstructed and transferred to a remote workstation as previously described.[14]

Coronary plaque assessment

MSCT angiograms were evaluated using dedicated software (Vitrea 2.0 or Vitrea FX 1.0, Vital images, Minnetonka, MN, USA). MSCT angiographic examinations were evaluated in consensus by 2 experienced readers including an interventional cardiologist blinded to conventional coronary angiography and IVUS findings. According to the modified American Heart Association classification, coronary arteries were divided into 17 segments.[15]

Each segment was evaluated for the presence of any atherosclerotic plaque using axial and/or orthogonal images and curved multiplanar reconstructions. Structures > 1 mm^2 within and/or adjacent to the coronary artery lumen, which could be clearly distinguished from the vessel lumen, were defined as plaques.[7] Per segment one coronary plaque was selected at the site of the most severe luminal narrowing. To verify the presence of calcifications, the calcium score was evaluated prior to determining plaque composition. Plaques were further classified as: 1) non-calcified plaque (plaques with lower CT (computed tomography) attenuation compared to contrast-enhanced lumen without any calcification), 2) mixed plaque (non-calcified and calcified elements in single plaque) 3) calcified plaque (plaques with high CT attenuation compared to contrast-enhanced lumen).

Conventional coronary angiography

Conventional coronary angiography was performed according to standard protocols. Vascular access was obtained through the femoral approach according to the Seldinger technique with the use of a 6F or 7F sheath. Quantitative coronary angiography (QCA) analysis was performed by observer unaware of MSCT and IVUS findings with the use of QCA-CMS version 6.0 (Medis, Leiden, The Netherlands). For each plaque examined both with MSCT and VH IVUS, percent diameter stenosis as measured by quantitative coronary angiography was reported. Measurements were performed on at least two orthogonal projections. The highest percent diameter stenosis was used for further analysis. Significant stenosis was defined as > 50% stenosis.

VH IVUS

Image acquisition

VH IVUS examinations were acquired during coronary angiography in 136 of the 225 available vessels with the use of a dedicated IVUS-console (Volcano Corporation, Rancho Cordova, CA, USA). After administration of nitrates locally, VH IVUS was performed with a 20 MHz, 2.9 F phased-array IVUS catheter, (Eagle Eye, Volcano Corporation, Rancho Cordova, CA, USA) which was introduced distally in the coronary artery. A speed of 0.5 mm/s was used for motorized automated pullback until the catheter reached the guiding catheter. Images were stored on CD-ROM or DVD for off-line analysis.

Image analysis

VH IVUS analysis was performed by two experienced observers blinded to baseline patient characteristics with the use of dedicated software (pcVH 2.1, Volcano Corporation, Rancho Cordova, CA, USA). The lumen and the media-adventitia interface were defined by automatic contour detection and on all individual frames manual editing was performed. All four plaque components were differentiated into different color-codes (fibrotic tissue being labeled in dark green, fibro-fatty in light green, necrotic core in red and dense calcium in white), as validated previously.[16] For each frame, vessel and lumen area were

calculated and percentage plaque burden was calculated as plaque plus media cross sectional area (CSA) divided by external elastic membrane CSA multiplied by 100.[17] Plaque composition was calculated as percentage of the plaque burden.

Qualitative evaluation of plaque type was visually assed at the minimal lumen area site as assessed on IVUS using the following classification: (i) Pathological intimal thickening (PIT); defined as a mixture of fibrous and fibro-fatty tissues, a plaque burden ≥ 40% and < 10% necrotic core and dense calcium. (ii) Fibroatheroma (FA); defined as having a plaque burden ≥ 40% and a confluent necrotic core occupying 10% of the plaque area or greater in 3 successive frames with evidence of an overlying fibrous cap. (iii) Thin capped fibroatheroma (TCFA); defined as a lesion with a plaque burden ≥ 40%, the presence of confluent necrotic core of > 10%, and no evidence of an overlying fibrous cap. (iiii) Fibrocalcific plaque (FC); defined as a lesion with a plaque burden ≥ 40%, being mainly composed of fibrotic tissue, having dense calcium > 10% and a confluent necrotic core of < 10% (higher amount accepted if necrotic core was located exclusively behind the accumulation of calcium).[18] [19] To match plaques identified on MSCT with plaques identified on VH IVUS; landmarks such as coronary ostia, side-branches and calcium deposits were used. Distances from the landmarks to the lesion were measured on multiplanar reconstructions on MSCT and matched with the longitudinal images of VH IVUS.

Statistical analysis

Continuous values are expressed as means (± standard deviation) if normally distributed and compared with the 2-tailed t-test for independent samples. If not normally distributed, values are expressed as medians (interquartile range) and compared with the 2-tailed Mann-Whitney test. Categorical values are expressed as number (percentages) and compared between groups with 2-tailed Chi-square test. Binary logistic regression analysis was used to calculate the relation of significant stenosis with the different plaque types as identified on MSCT or VH IVUS. A p-value of < 0.05 was considered statistically significant. Statistical analysis was performed using SPSS 14.0 software (SPSS Inc., Chicago. Illinois).

RESULTS

Patients and study protocol

In total, 78 patients were identified that had undergone MSCT and invasive coronary angiography with VH IVUS. A patient example is provided in Figure 1. Three patients were excluded due to absence of any identifiable plaques on MSCT. In all patients MSCT angiograms and VH IVUS studies were of diagnostic image quality. Patient characteristics of the remaining 75 patients are summarized in Table 1. In 89 vessels (40%) VH IVUS could not be performed due to severe vessel stenosis, vessel tortuousness, vessel occlusion or time limitations in the catheterization laboratory. As a result, 136 vessels (60%) were available for analysis. In total, 227 plaques were identified on MSCT in which corresponding VH IVUS analysis was available. On QCA, the average percent stenosis of the plaques
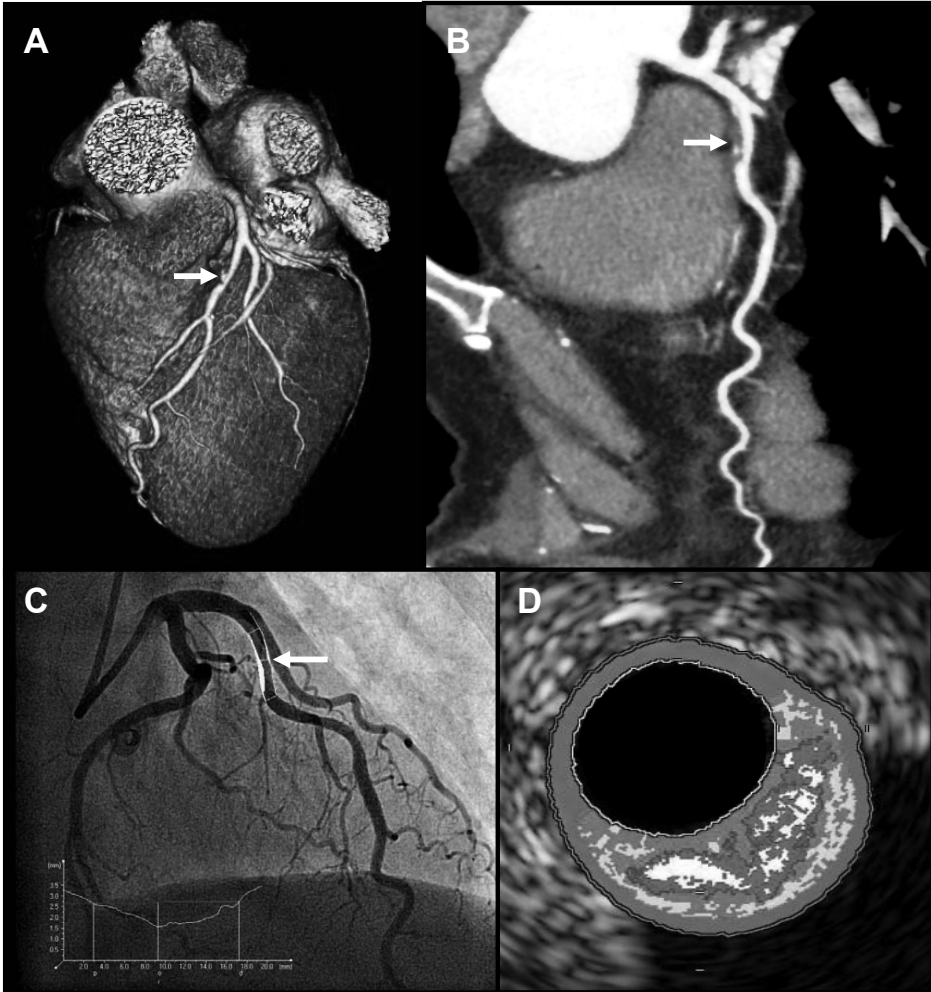
Figure 1. An example of combination of non-invasive imaging with 320-slice multislice computed tomography (MSCT) angiography and invasive imaging with coronary angiography and virtual histology intravascular ultrasound (VH IVUS). A 53 year old female was referred because of chest pain and intermediate risk profile, exercise testing was inconclusive and the patient was referred for anatomical evaluation by MSCT. An intermediate lesion in de mid left anterior descending coronary artery (LAD) was identified on MSCT. Consequently, the patient was further referred for coronary angiography combined with (VH) IVUS. (Panel A) Three-dimensional reconstruction depicting a lesion (arrow) with intermediate luminal narrowing in the mid LAD. (Panel B) Curved multiplanar reconstruction of the LAD and the corresponding lesion (arrow) showing a mixed plaque. (Panel C) The findings were confirmed on conventional coronary angiography and quantitative coronary angiography (QCA) analysis demonstrating luminal narrowing of 42% (arrow). (Panel D) Corresponding VH IVUS image showing a substantial amount of necrotic core (labelled in red).

was 29 ± 9%. Forty-three plaques (19%) corresponded to a significant stenosis (average percentage stenosis 61 ± 9%) and 184 plaques (81%) corresponded to a non-significant stenosis (average percentage stenosis 22 ± 2%).

Table 1. Patient characteristics of study population.

	n (%)
Gender (M / F)	43 / 32
Age (years)	59 ± 11
Risk factors for CAD (%)	
Diabetes Mellitus	22 (29%)
Hypertension	45 (60%)
Hypercholesterolemia	57 (76%)
Positive family history	33 (44%)
Current smoking	38 (51%)
Obese (BMI ≥ 30 kg/m^2)	14 (19%)
Previous CAD	
Previous myocardial infarction	20 (27%)
Framingham risk score (%)	
Low	45 (60%)
Intermediate	22 (29%)
High	8 (11%)
Heart rate (bpm) during MSCT	62 ± 9
Prevalence of significant CAD (defined as at least 1 stenosis with > 50% luminal narrowing on QCA)	29 (39%)

CAD; coronary artery disease, BMI; body mass index, MSCT; multislice computed tomography, QCA; quantitative coronary angiography.

Compositional characteristics in relation to angiographic degree of stenosis

Composition on MSCT

Of the 227 plaques analyzed, 70 were non-calcified plaques (31%), 96 were mixed (42%) and 61 were calcified (27%) on MSCT. The different plaque types as identified by MSCT were equally distributed among significant and non-significant stenoses (Figure 2). Plaque type on MSCT was not significantly related to stenosis (non-calcified plaque; OR (CI 95%) 0.9 (0.4 - 1.8), p=0.68, mixed plaque; OR (CI 95%) 1.5 (0.8 - 1.9), p=0.26); calcified plaque OR (CI 95%) 0.7 (0.3 - 1.7), p=0.41).

Composition on VH IVUS

In 136 vessels and 227 plaques, VH IVUS was successfully performed. The average plaque length analyzed was 22 ± 17 mm. Overall, the most prevalent plaque component was fibrotic tissue (52 ± 12%), followed by fibro-fatty tissue (22 ± 16%), necrotic core (15 ±
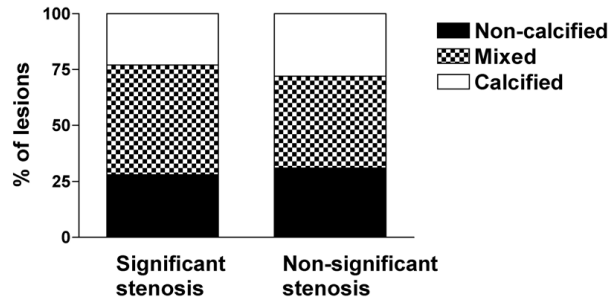
Figure 2. Bar graph demonstrating the relative distribution of different plaque types as determined by multislice computed tomography (MSCT) in lesions with significant and non-significant stenosis (p=ns).

9%) and dense calcium (11 ± 10%). As expected and can be derived from Table 2, plaques with a significant stenosis had a significantly higher plaque burden (67 ± 11% versus 53 ± 12%, p<0.05) and smaller minimum lumen area (4.6 (3.8 - 6.8) mm² versus 7.3 (5.4 - 10.5) mm², p<0.05) than compared to plaques without significant stenosis. Interestingly, no differences were observed in the amount of fibrotic tissue (51 ± 10% versus 53 ± 13%, p=0.62), fibro-fatty tissue (21 (9 - 33) % versus 18 (10 - 29) %, p=0.42), necrotic core (15 ± 8% versus 15 ± 9%, p=0.95) and dense calcium (8 (3 - 15) % versus 9 (3 - 15) %, p=0.77).

Table 2. Differences in plaque composition between lesions with significant and non-significant stenosis. MLA; minimal lumen area.

	Significant stenosis (n=43)	Non-significant stenosis (n=184)	P-value
Plaque burden (%)	67 ± 11	53 ± 12	<0.05
MLA mm²	4.6 (3.8 - 6.8)	7.3 (5.4 - 10.5)	<0.05
% Fibrotic	51 ± 10	53 ± 13	0.62
% Fibro-fatty	21 (9 - 33)	18 (10 - 29)	0.42
% Necrotic core	15 ± 8	15 ± 9	0.95
% Dense calcium	8 (3 -15)	9 (3 - 15)	0.77

Qualitative visual evaluation of coronary plaques revealed that pathological intimal thickening was more frequently observed in lesions with non-significant stenosis (3 (7%) versus 46 (25%), p<0.05), however, the more vulnerable plaques (thin capped fibroatheroma) were distributed equally (10 (23%) versus 27 (15%), p= 0.18) (Figure 3). Pathological intimal thickening was significantly related to non-significant stenosis (OR (CI 95%) for significant stenosis 0.2 (0.1 - 0.8), p=0.02), although there was no relation between the more vulnerable plaque types (thin capped fibroatheroma) and significant stenosis (OR (CI 95%) 1.8 (0.8 - 4.0), p=0.18).
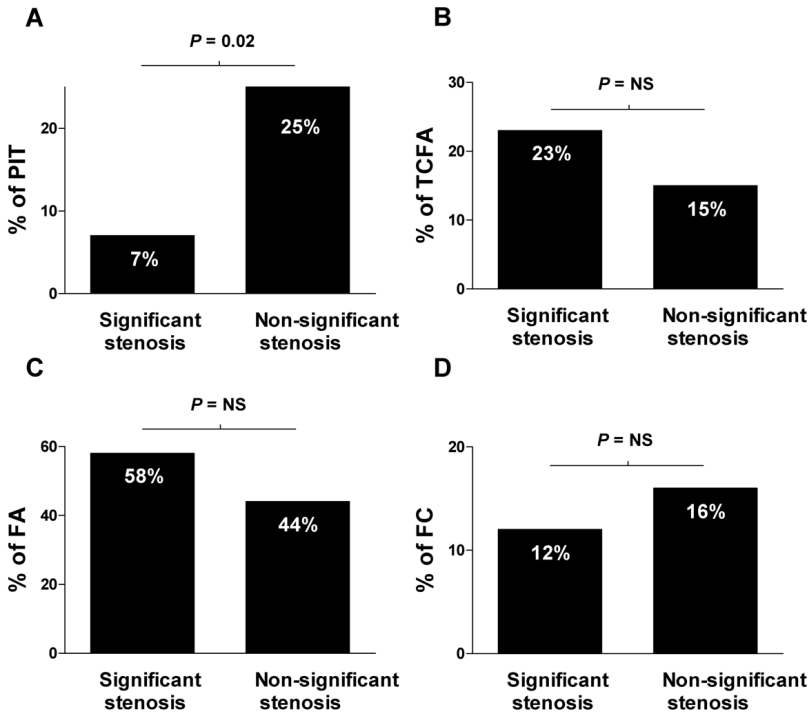
Figure 3. Differences in percentage of visually assessed plaque types on virtual histology intravascular ultrasound (VH IVUS) between lesions with significant and non-significant stenosis. Significantly more lesions classified as pathological intimal thickening (PIT) were present in non-significant stenosis as compared to significant stenosis (A). Percentage of fibroatheroma (FA), thin capped fibroatheroma (TCFA) and fibrocalcific (FC) plaques were not significantly different between lesions with significant and non-significant stenosis (C, B, D).

DISCUSSION

In the present study differences in plaque composition and vulnerability between lesions with significant and non-significant stenosis were assessed using non-invasive MSCT angiography and invasive VH IVUS. The main findings of coronary plaque characterization using MSCT and VH IVUS can be summarized as follows.

No differences in plaque composition between significant and non-significant stenosis were demonstrated non-invasively by MSCT and invasively by VH IVUS. MSCT showed that the proportion of non-calcified, mixed and calcified plaques were similar between significant and non-significant lesions. VH IVUS confirmed these findings, revealing no differences in plaque composition (fibrotic, fibro-fatty, necrotic core and dense calcium) between significant and non-significant stenosis. Importantly, no differences were observed in plaque vulnerability between significant and non-significant stenosis as demonstrated by an even distribution of thin capped fibroatheroma and percent necrotic core.

In the present study non-calcified, mixed and calcified plaques on MSCT were equally distributed between lesions with significant and non-significant stenosis. The observations on MSCT corresponded to the findings on VH IVUS, indicating that plaque composition did not differ between lesions with significant and non-significant stenosis. These results are in line with previous studies exploring plaque composition with grayscale IVUS in relation to luminal narrowing on coronary angiography.[20]

Nonetheless, qualitative evaluation of plaque type on VH IVUS revealed more early stage atherosclerosis in non-significant stenosis, as reflected by a higher prevalence of pathological intimal thickening. On the other hand, one would also expect to find more advanced plaque composition in lesions with significant stenosis, including a higher degree of calcium. Indeed, other non-invasive imaging techniques, such as calcium scoring on electron beam computed tomography, have demonstrated that calcium is more prevalent in patients with larger atherosclerotic plaque burden and that a moderate relation exists between the extent of coronary calcium and presence of obstructive CAD.[21] However in the present study, no differences were found between the prevalence of calcified plaques on MSCT in significant and non-significant stenosis. These findings were confirmed by an even distribution of dense calcium on VH IVUS. This could possibly be explained by the fact that there is a marked discrepancy between apparent angiographic luminal narrowing and actual extent of atherosclerosis. Indeed, due to compensatory enlargement or positive remodeling, a substantial build up of plaque can occur before resulting in luminal narrowing and reduction of blood flow. Therefore, plaque composition gradually becomes more advanced while remaining non-significant (in terms of luminal narrowing) for a considerable period of time. Of note, recently Sipahi and co-workers demonstrated that type of arterial remodeling (negative or positive) does not predict subsequent progression of atherosclerosis in patients undergoing statin therapy.[22] Interestingly, similar observations to our results were reported by Mintz et al. using IVUS. The authors reported that coronary calcium correlated well with plaque burden but not with angiographical luminal narrowing.[23] Accordingly, angiographic intermediate lesions were as likely to contain significant amounts of calcium as severe lesions.

Interestingly, also no difference in the proportion of non-calcified and mixed lesions was observed on MSCT among lesions with significant and non-significant stenosis. Although data are scarce, it has been suggested that non-calcified and mixed plaques on MSCT may be associated with increased plaque vulnerability.[10 24] Indeed, studies comparing plaque patterns on MSCT between patients presenting with ACS and stable CAD have consistently shown that non-calcified and mixed plaques are more prevalent in patients with ACS.[9 10] In addition, these lesions have been demonstrated to correspond with a larger amount of necrotic core and a higher prevalence of thin capped fibroatheroma on VH IVUS.[10] Accordingly, these observations suggest that the observation of non-calcified or mixed plaque on MSCT may potentially be of clinical relevance, regardless of stenosis severity.

Importantly, the observation of similar plaque composition between significant and non-significant stenosis translated into no differences in plaque vulnerability on VH IVUS, demonstrated by an even distribution of thin capped fibroatheroma and percent necrotic

core on VH IVUS. Similar observations have been reported by serial angiographic studies showing that vulnerability was poorly related to angiographic degree of luminal narrowing.[3 4 25] In line with these studies, investigations directly addressing plaque composition also reported a lack of agreement between plaque vulnerability and degree of stenosis. Using conventional grayscale IVUS, Yamagishi et al. prospectively examined coronary plaques with IVUS and found no differences in degree of luminal narrowing between plaques prior to ACS and plaques that remained stable.[26] In addition, Saam et al. studied carotid arteries of 192 subjects with non-invasive magnetic resonance plaque characterization and demonstrated that vulnerable lesions were equally present in lesions with significant and non-significant stenosis.[27]

Clinical implications

At present, MSCT is increasingly used in the evaluation of patients presenting with suspected CAD. Accordingly, the main objective in these patients is to determine the presence of significant stenosis in the coronary arteries and high diagnostic accuracies have been reported for this purpose.[28] In addition, data supporting its prognostic value are starting to emerge.[29 30] In several studies the presence of significant CAD on MSCT has been shown to result in a higher likelihood of coronary events. However, assessment of the presence, extent and type of atherosclerosis in addition to the degree of stenosis may potentially further refine risk stratification. In a preliminary prognostic study by Pundziute et al, the presence of non-significant stenosis was shown to be associated with worse outcome as compared to complete absence of any atherosclerosis.[31] Our current observations further support this concept, showing no difference in plaque composition and vulnerability between significant and non-significant lesions. Moreover, the incremental prognostic value of MSCT variables describing extent as well as type of atherosclerosis was recently evaluated by van Werkhoven et al.[30] Interestingly, the authors showed that the presence of substantial non-calcified plaque burden (regardless of stenosis severity) on MSCT was an independent predictor of adverse cardiac events providing incremental prognostic value over the presence of a significant stenosis.[30] Accordingly, these as well as our current observations may be of help in understanding the potential value of assessing plaque burden and plaque type on MSCT and suggest that evaluation of MSCT angiograms should not be restricted to assessment of luminal narrowing alone. Possibly, incorporation of information on the presence, extent, and composition of atherosclerosis may allow refined and more individualized risk stratification and thus improved identification of patients requiring more aggressive therapy. However, available data are scarce and need to be confirmed in larger patient cohorts.

Limitations

Imaging of severely stenotic or occluded lesions with IVUS is not possible. Therefore, the present study may not reflect the true spectrum of lesions with significant stenosis.

Conclusion

No evident relation between the degree of stenosis and plaque composition or vulnerability, as evaluated non-invasively by MSCT and invasively by VH IVUS, was observed. Evaluation of plaque composition may provide valuable information incremental to assessment of the degree of stenosis.

REFERENCES

1. Manoharan G, Ntalianis A, Muller O et al. Severity of coronary arterial stenoses responsible for acute coronary syndromes. Am J Cardiol 2009;103:1183-8.
2. Shah PK. Mechanisms of plaque vulnerability and rupture. J Am Coll Cardiol 2003;41:15-22S.
3. Ambrose JA, Tannenbaum MA, Alexopoulos D et al. Angiographic progression of coronary artery disease and the development of myocardial infarction. J Am Coll Cardiol 1988;12:56-62.
4. White CW, Wright CB, Doty DB et al. Does visual interpretation of the coronary arteriogram predict the physiologic importance of a coronary stenosis? N Engl J Med 1984;310:819-24.
5. Virmani R, Burke AP, Kolodgie FD et al. Pathology of the vulnerable plaque. J Am Coll Cardiol 2006;47:C13-C18.
6. Kullo IJ, Edwards WD, Schwartz RS. Vulnerable plaque: pathobiology and clinical implications. Ann Intern Med 1998;129:1050-60.
7. Leber AW, Knez A, Becker A et al. Accuracy of multidetector spiral computed tomography in identifying and differentiating the composition of coronary atherosclerotic plaques: a comparative study with intracoronary ultrasound. J Am Coll Cardiol 2004;43:1241-7.
8. Schroeder S, Kopp AF, Baumbach A et al. Noninvasive detection and evaluation of atherosclerotic coronary plaques with multislice computed tomography. J Am Coll Cardiol 2001;37:1430-5.
9. Henneman MM, Schuijf JD, Pundziute G et al. Noninvasive evaluation with multislice computed tomography in suspected acute coronary syndrome: plaque morphology on multislice computed tomography versus coronary calcium score. J Am Coll Cardiol 2008;52:216-22.
10. Pundziute G, Schuijf JD, Jukema JW et al. Evaluation of plaque characteristics in acute coronary syndromes: non-invasive assessment with multi-slice computed tomography and invasive evaluation with intravascular ultrasound radiofrequency data analysis. Eur Heart J 2008;29:2373-81.
11. Nair A, Kuban DB, Tuzcu EM et al. Coronary plaque classification with intravascular ultrasound radiofrequency data analysis. Circulation 2002;106:2200-6.
12. Rodriguez-Granillo GA, Garcia-Garcia HM, Mc Fadden EP et al. In vivo intravascular ultrasound-derived thin-cap fibroatheroma detection using ultrasound radiofrequency data analysis. J Am Coll Cardiol 2005;46:2038-42.
13. Executive Summary of The Third Report of The National Cholesterol Education Program (NCEP) Expert Panel on Detection, Evaluation, And Treatment of High Blood Cholesterol In Adults (Adult Treatment Panel III). JAMA 2001;285:2486-97.
14. Schuijf JD, Pundziute G, Jukema JW et al. Diagnostic accuracy of 64-slice multislice computed tomography in the noninvasive evaluation of significant coronary artery disease. Am J Cardiol 2006;98:145-8.
15. Austen WG, Edwards JE, Frye RL et al. A reporting system on patients evaluated for coronary artery disease. Report of the Ad Hoc Committee for Grading of Coronary Artery Disease, Council on Cardiovascular Surgery, American Heart Association. Circulation 1975;51:5-40.
16. Nasu K, Tsuchikane E, Katoh O et al. Accuracy of in vivo coronary plaque morphology assessment: a validation study of in vivo virtual histology compared with in vitro histopathology. J Am Coll Cardiol 2006;47:2405-12.
17. Mintz GS, Nissen SE, Anderson WD et al. American College of Cardiology Clinical Expert Consensus Document on Standards for Acquisition, Measurement and Reporting of Intravascular Ultrasound Studies (IVUS). A report of the American College of Cardiology Task Force on Clinical Expert Consensus Documents. J Am Coll Cardiol 2001;37:1478-92.
18. Carlier SG, Mintz GS, Stone GW. Imaging of atherosclerotic plaque using radiofrequency ultrasound signal processing. J Nucl Cardiol 2006;13:831-40.

19. Virmani R, Kolodgie FD, Burke AP et al. Lessons from sudden coronary death: a comprehensive morphological classification scheme for atherosclerotic lesions. Arterioscler Thromb Vasc Biol 2000;20:1262-75.

20. Hodgson JM, Reddy KG, Suneja R et al. Intracoronary ultrasound imaging: correlation of plaque morphology with angiography, clinical syndrome and procedural results in patients undergoing coronary angioplasty. J Am Coll Cardiol 1993;21:35-44.

21. O'Rourke RA, Brundage BH, Froelicher VF et al. American College of Cardiology/American Heart Association Expert Consensus document on electron-beam computed tomography for the diagnosis and prognosis of coronary artery disease. Circulation 2000;102:126-40.

22. Sipahi I, Tuzcu EM, Moon KW et al. Do the extent and direction of arterial remodelling predict subsequent progression of coronary atherosclerosis? A serial intravascular ultrasound study. Heart 2008;94:623-7.

23. Mintz GS, Pichard AD, Popma JJ et al. Determinants and correlates of target lesion calcium in coronary artery disease: a clinical, angiographic and intravascular ultrasound study. J Am Coll Cardiol 1997;29:268-74.

24. Motoyama S, Kondo T, Sarai M et al. Multislice computed tomographic characteristics of coronary lesions in acute coronary syndromes. J Am Coll Cardiol 2007;50:319-26.

25. Giroud D, Li JM, Urban P et al. Relation of the site of acute myocardial infarction to the most severe coronary arterial stenosis at prior angiography. Am J Cardiol 1992;69:729-32.

26. Yamagishi M, Terashima M, Awano K et al. Morphology of vulnerable coronary plaque: insights from follow-up of patients examined by intravascular ultrasound before an acute coronary syndrome. J Am Coll Cardiol 2000;35:106-11.

27. Saam T, Underhill HR, Chu B et al. Prevalence of American Heart Association type VI carotid atherosclerotic lesions identified by magnetic resonance imaging for different levels of stenosis as measured by duplex ultrasound. J Am Coll Cardiol 2008;51:1014-21.

28. Budoff MJ, Dowe D, Jollis JG et al. Diagnostic performance of 64-multidetector row coronary computed tomographic angiography for evaluation of coronary artery stenosis in individuals without known coronary artery disease: results from the prospective multicenter ACCURACY (Assessment by Coronary Computed Tomographic Angiography of Individuals Undergoing Invasive Coronary Angiography) trial. J Am Coll Cardiol 2008;52:1724-32.

29. Min JK, Shaw LJ, Devereux RB et al. Prognostic value of multidetector coronary computed tomographic angiography for prediction of all-cause mortality. J Am Coll Cardiol 2007;50:1161-70.

30. van Werkhoven JM, Schuijf JD, Gaemperli O et al. Prognostic value of multislice computed tomography and gated single-photon emission computed tomography in patients with suspected coronary artery disease. J Am Coll Cardiol 2009;53:623-32.

31. Pundziute G, Schuijf JD, Jukema JW et al. Prognostic value of multislice computed tomography coronary angiography in patients with known or suspected coronary artery disease. J Am Coll Cardiol 2007;49:62-70.

CHAPTER4

The Site of Greatest Vulnerability is Most Often Located Proximally to the Site of Most Severe Narrowing: A Virtual Histology Intravascular Ultrasound Study

Joëlla E. van Velzen, Michiel A. de Graaf, Fleur R. de Graaf, Joanne D. Schuijf, Jouke Dijkstra, Jeroen J. Bax, Johan H.C. Reiber, Martin J. Schalij, Ernst E. van der Wall, J.Wouter Jukema

ABSTRACT

Background: Previous angiographic studies have shown that almost two-thirds of vulnerable plaques are located in non-obstructive lesions. Possibly, the site of greatest vulnerability is not always located at the site of most severe stenosis. Therefore, the purpose of this study was to evaluate the difference in location between the site of greatest vulnerability and the site of most severe narrowing as assessed by virtual histology intravascular ultrasound (VH IVUS).

Methods: Overall, 77 patients (139 vessels) underwent VH IVUS. The site of greatest vulnerability was defined as the cross-section with the largest necrotic core area per vessel, the maximum necrotic core (Max NC) site. The site of most severe narrowing was defined as the minimum lumen area (MLA). Per vessel the distance from both the Max NC site and MLA site to the origo of the coronary artery was evaluated. In addition, the presence of a thin cap fibroatheroma (TCFA) was assessed.

Results: The mean difference (mm) between the MLA site and Max NC site was 10.8±20.6mm (P<0.001). Interestingly, the Max NC site was located at the MLA site in 7 vessels (5%) and proximally to the MLA site in 92 vessels (66%). Importantly, a higher % of TCFA was demonstrated at the Max NC site as compared to the MLA site (24% versus 9%, P<0.001).

Conclusion: The present findings demonstrate that the site of greatest vulnerability is rarely at the site of most severe narrowing. Most often, the site of greatest vulnerability is located proximally to the site of most severe narrowing.

INTRODUCTION

Previous angiographic studies have shown that almost two-thirds of vulnerable plaques are located in non-obstructive atherosclerotic lesions.[1][2] Nevertheless, at present, interventional strategies are mainly targeted towards management of acute coronary syndromes at the site of most severe luminal narrowing. Whether this approach adequately covers the more vulnerable regions remains uncertain. Thus far, the spatial relationship between the location of most severe narrowing and vulnerable rupture sites has not been fully elucidated.

Virtual histology intravascular ultrasound (VH IVUS) is a promising tool for the assessment of plaque composition.[3] Using spectral analysis of radiofrequency backscatter signals, this technique has the ability to evaluate 4 plaque components, namely fibrotic, fibro-fatty, necrotic core and calcified tissue. The accuracy of VH IVUS for the determination of plaque components has been validated against histopathology in human coronary arteries and was 90.4% for fibrous, 92.8% for fibro-fatty, 89.5% for necrotic core and 90.9% for dense calcium.[3][4] Recently, a large prospective multi-centre study by Stone et al. showed a strong predictive value of the presence of thin cap fibroatheroma (TCFA) on VH IVUS.[5] In a cohort of 697 patients, the presence of TCFA on VH IVUS was demonstrated to be an independent predictor of major adverse cardiovascular events.

The aim of the present study was to improve understanding of the spatial relationship between the location of the site of greatest vulnerability and the location of most severe narrowing. Therefore, we compared the location of the maximum necrotic core area (site of greatest vulnerability) with the location of the minimum lumen area (site of most severe narrowing) with VH IVUS.

METHODS

Patients

The study population consisted of 77 patients with chest pain referred for invasive coronary angiography (ICA). Patients were clinically referred for invasive coronary angiography because of known or suspected coronary artery disease (CAD). Referral for invasive coronary angiography was based on clinical presentation and/or imaging results. VH IVUS was performed to further evaluate the extent and severity of disease. Both patients presenting with stable chest pain and acute coronary syndrome (ACS) were evaluated. Patients with ACS included unstable angina and non-ST-segment elevation myocardial infarction defined according to the guidelines of the European Society of Cardiology[6] and the American College of Cardiology (ACC)/American Heart Association.[7] Patient data were prospectively collected in the departmental Cardiology Information System (EPD-Vision®, Leiden University Medical Center, Leiden, the Netherlands) and retrospectively analyzed. Contra-indications for VH IVUS were severe vessel tortuosity, severe luminal narrowing or (subtotal) vessel occlusion. In each patient the presence of CAD risk factors

such as diabetes, hypertension, hypercholesterolemia, positive family history, smoking and obesity, was recorded.

VH IVUS acquisition

VH IVUS was performed according to standard clinical protocol during ICA using a novel dedicated IVUS-console (s5[tm] Imaging system, Volcano Corporation, Rancho Cordova, CA, USA). After local intracoronary admission of 200 µg nitroglycerin, VH IVUS was performed with a 20 MHz, 2.9 F phased-array IVUS catheter (Eagle Eye, Volcano Corporation, Rancho Cordova, CA, USA). The IVUS catheter was positioned distally in the coronary artery and motorized automated IVUS pullback was performed using a speed of 0.5 mm/s until the catheter reached the guiding catheter. Images were obtained at the R-wave peak on the ECG. At an average heart rate of 60/min, the incremental distance between frames was approximately 0.5 mm. Cine runs were performed to record the starting position of the VH IVUS catheter. Images were stored on DVD for further offline analysis.

VH IVUS analysis

Images were analyzed offline using specially developed dedicated software for images acquired on the s5[tm] IVUS Imaging system (QCU- CMS 4.59, Medis, Leiden, The Netherlands). Vessels without evidence of major atherosclerotic plaque (plaque burden <40%) or with previous stent placement were excluded from further analysis. All IVUS examinations were evaluated by two experienced observers. First, the IVUS run was visually assessed to confirm that the pullback had been performed at a constant speed.

Second, contour detection of the external elastic membrane (EEM) and lumen was performed. The area enclosed by the contours of EEM and lumen was defined as plaque area. Percentage plaque burden was calculated as plaque cross-sectional area (CSA) plus media CSA divided by EEM CSA multiplied by 100 according to the American College of Cardiology Clinical Expert Consensus Document on Standards for Acquisition, Measurement and Reporting of Intravascular Ultrasound Studies (IVUS).[8] Subsequently, using radiofrequency backscatter analysis, four plaque components were differentiated into color codes as validated previously.[3] Accordingly, fibrotic tissue was labeled in dark green, fibro-fatty in light green, dense calcium in white and necrotic core in red.

The site of most severe narrowing was defined as the cross-section with the smallest cross-sectional lumen area in the entire vessel, the minimum lumen area site (MLA). Multiple definitions are available to define the site of greatest vulnerability on VH IVUS. As amount of necrotic core is quantifiable on VH IVUS, the site of greatest vulnerability was defined as the cross-section with the largest necrotic core area per vessel, the maximum necrotic core (Max NC) site. Subsequently, per vessel, the maximum necrotic core (Max NC) site and MLA site were identified. First, in each vessel the distance from both the Max NC site and MLA site to the ostium of the coronary artery was measured with a dedicated software tool in the longitudinal IVUS view. Distances were calculated based on the pullback speed of motorized automated pullback at a rate of 0.5 mm/s. Difference between both sites was calculated as distance from MLA site to origo minus distance from Max NC

site to origo. Furthermore, classification of plaque type and composition was performed at both the Max NC site and MLA site. Plaque components were reported as absolute values and percentages of plaque area. In addition, visual plaque type classification was obtained according to the following categorization:[9, 10]

1. Pathological intimal thickening; defined as a mixture of fibrotic and fibro-fatty tissues, a plaque burden ≥40% and <10% necrotic core and dense calcium.
2. Fibroatheroma; defined as having a plaque burden ≥40% and a confluent necrotic core occupying 10% of the plaque area or greater in three successive frames with evidence of an overlying fibrous cap.
3. TCFA; defined as a lesion with a plaque burden ≥40%, the presence of confluent necrotic core of >10%, and no evidence of a large fibrous cap.
4. Fibrocalcific plaque; defined as a lesion with a plaque burden ≥40%, with dense calcium >10% and a percentage necrotic core of <10% (higher amount accepted if necrotic core was located exclusively behind the accumulation of calcium).

Statistical analysis

Statistical analyses were performed using SPSS (version 17.0, SPSS Inc., Chicago, IL, USA). First, the spatial relationship (in mm) between Max NC and MLA site was assessed. In a sub-analysis, the impact of clinical presentation (patients with stable CAD versus patients with ACS) and the difference in length between the Max NC and MLA site was evaluated. Furthermore, differences in plaque composition and type between both the Max NC and MLA site were compared. When normally distributed, continuous variables were expressed as mean (± standard deviation) and compared with independent sample t-test for unpaired samples or the dependent t-test for paired samples. If not normally distributed, variables were presented as median and interquartile range. Unpaired samples were analyzed using non-parametric Mann-Whitney test and paired variables were analyzed with Wilcoxon signed rank tests. Categorical variables were expressed as numbers and percentages, and compared with the Chi-square test. A p-value of $p<0.05$ was considered significant.

RESULTS

Overall, 77 patients were evaluated. Patient characteristics are presented in Table 1. In total, 169 vessels were analyzed with VH IVUS, in 30 vessels (18%) previous PCI was performed and these vessels were therefore excluded. Thus, 139 vessels were included for further analysis.

The spatial relationship between the Max NC and MLA site is demonstrated in Figure 1. Interestingly, the Max NC site was located in the same location as the MLA site in only 7 vessels (5%). In the remaining vessels, the Max NC site was located proximally to the

Table 1. Patient characteristics of study population.

	n (%)
Age (years)	59 ± 10
Gender (% male)	64 (70%)
Risk factors for CAD	
Obesity (Body mass index ≥ 30 kg/m^2)	21 (23%)
Diabetes	27 (29%)
Hypertension†	54 (59%)
Hypercholesterolemia‡	47 (51%)
Family history of CAD	44 (48%)
Smoking	32 (35%)
Aspirin use	49 (53%)
Statin use	60 (65%)
Previous PCI	25 (27%)
Previous myocardial infarction	17 (19%)
Presentation with ACS	62 (67%)

Data are absolute values, percentages or means ± standard deviation.
†Defined as systolic blood pressure ≥140 mm Hg or diastolic blood pressure ≥90
mm Hg or the use of antihypertensive medication.
‡Serum total cholesterol ≥230 mg/dL or serum triglycerides ≥200 mg/dL or treatment with lipid
lowering drugs.
Abbreviations: CAD, coronary artery disease; ACS, acute coronary syndrome, PCI, percutaneous
coronary intervention.
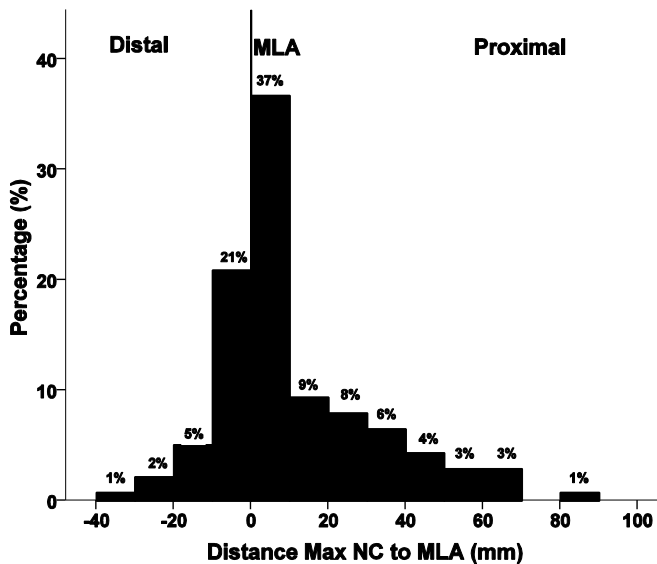
Figure 1. Spatial relationship of the maximum necrotic core site (Max NC) as compared to minimal lumen area (MLA). In the majority of vessels the site of Max NC is located proximal to site of MLA.

MLA site in 92 vessels (66%) and located distally from the MLA site in 40 vessels (29%). Accordingly, the mean difference (mm) between the MLA site and Max NC site was 10.8 ± 20.6 mm (P<0.001). Regarding the more proximally located Max NC sites, the mean difference between Max NC and MLA site was 19.6 ± 19.7 mm (P<0.001). Concerning the more distally located Max NC sites, the mean difference between Max NC site and MLA was 7.4 ± 7.8 mm (P<0.001). The differences in distance between Max NC site and MLA site were assessed between patients with ACS (n=52) and patients with stable CAD (n=25). Interestingly, no difference in distance between Max NC and MLA was observed (10.7 ± 20.5 mm for stable CAD vs. 10.9 ± 20.8 mm for patients with ACS, P=0.699). Figure 2 shows an example of a vessel with the site of greatest vulnerability located proximal to the MLA site.
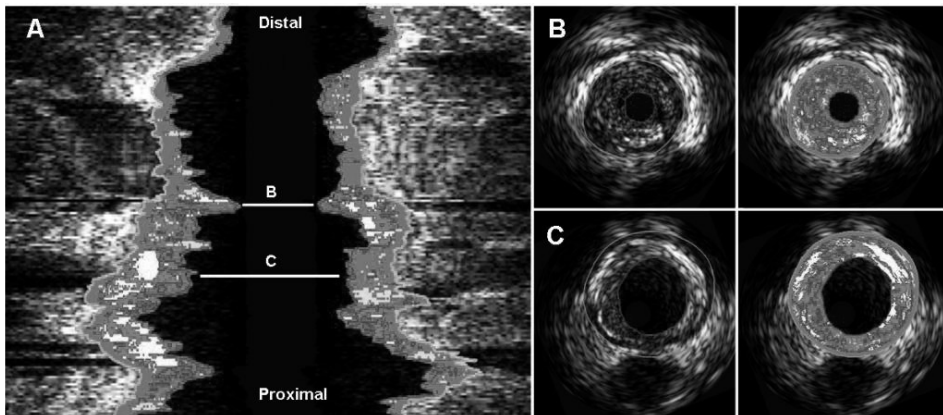
Figure 2. Example of a coronary artery with the site of maximum necrotic core (Max NC) located proximal from the minimal lumen area (MLA) site. Panel A demonstrates a longitudinal view of the intravascular ultrasound (IVUS) images. As demonstrated, the Max NC site (C) is not located at the minimum lumen area (MLA) site (B), but 16.4 mm proximal of the MLA site. Panel B shows the grayscale cross-sectional slices and the corresponding virtual histology IVUS images of the MLA site. Panel C shows the grayscale cross-sectional slices and the corresponding virtual histology IVUS images for the Max NC site. Interestingly, although the MLA site has significant luminal narrowing (lumen area of 2.1 mm2) the Max NC site demonstrated a thin cap fibroatheroma (TCFA).

The differences in absolute and relative plaque composition between the Max NC and MLA site are demonstrated in Table 2. As expected, the Max NC site contained significantly more necrotic core as compared to the MLA site (31% (23 - 40%) versus 19% (10 - 19%), P<0.001). Moreover, the MLA site contained significantly more fibrotic tissue than the Max NC site (57% (47 - 65%) versus 49% (41 - 57 %), P<0.001). Furthermore, the MLA site contained significantly more fibro-fatty tissue than the Max NC site (13% (6 - 24%) versus 6% (3 - 12%), P<0.001). Lastly, plaque burden was significantly larger at the MLA site than at Max NC site (63% (54 - 74%) versus 59% (43 - 68%), P<0.001).

Table 2. Comparison of plaque composition between maximum necrotic core (Max NC) site and minimum lumen area site (MLA).

VH IVUS plaque composition	Max NC site	MLA site	P-value
Lumen area (mm^2)	7.3 (5.1 - 10.9)	4.3 (3.1 - 6.9)	<0.001
Vessel area (mm^2)	18.7 (14.9 - 23.8)	14.0(10.4 - 17.4)	<0.001
Plaque area (mm^2)	11.2 (8.5 - 13.6)	8.9 (6.1 - 11.2)	<0.001
Plaque burden	59% (49 – 68%)	63% (54 – 74%)	<0.001
Fibrotic (mm^2)	3.8 (2.6 - 4.9)	3.2 (2.1 - 4.6)	0.01
Fibro-fatty (mm^2)	0.5 (0.2 - 1.0)	0.7 (0.2 - 1.5)	<0.001
Necrotic core (mm^2)	2.3 (1.5 - 3.1)	1.2 (0.5 - 1.8)	<0.001
Dense calcium (mm^2)	0.8 (0.3 - 1.3)	0.3 (0.1 - 0.8)	<0.001
Fibrotic	49% (41 – 57%)	57% (47 – 65%)	<0.001
Fibro-fatty	6% (3 – 12%)	13% (6 – 24%)	<0.001
Necrotic core	31% (24 – 40%)	19% (9 – 28%)	<0.001
Dense calcium	10% (5 – 16%)	6% (1 – 12%)	<0.001

Data are presented as medians and interquartile range

The difference in plaque type between MLA and Max NC sites was assessed. Interestingly, pathological intimal thickening was most often observed at the MLA site as compared to the Max NC site (26% versus 1%, P<0.001). In addition, lesions at the Max NC site were more often classified as a fibroatheroma than lesions at the MLA site (71% versus 60%, P=0.04). Furthermore, the percentage of fibrocalcific plaque was similar at both the MLA site and Max NC site (5% versus 4%, P=0.78). Importantly, as demonstrated in Figure 3, a significantly higher percentage of TCFA was present at Max NC site as compared to the MLA site (24% versus 9%, P<0.001). Moreover, if TCFA was identified at the Max NC site, only in 33% of cases the MLA site also demonstrated a TCFA. No significant differences were observed between plaque type and composition between proximal and distal Max NC sites (Table 3).
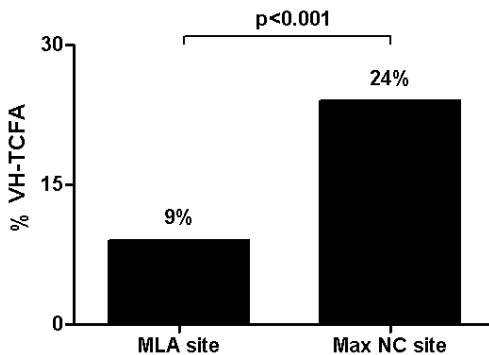
Figure 3. Difference in presence of thin cap fibroatheroma (TCFA) between minimum lumen area (MLA) site and maximum necrotic core (Max NC) site. As demonstrated, TCFA was significantly more often observed at the Max NC site as compared to the MLA site.

Table 3. Comparison of plaque composition and type between the maximum necrotic core (Max NC) site located proximal and distal from the minimum lumen area (MLA).

VH IVUS characteristics	Max NC site proximal to MLA site	Max NC site distal from MLA site	P-value
Plaque composition			
Fibrotic	49% (41 - 56%)	49% (39 - 58%)	0.96
Fibro-fatty	6% (3 – 12%)	5% (3 - 10%)	0.40
Necrotic core	31% (24 - 40%)	34% (24 - 39%)	0.74
Dense calcium	10% (6 – 14%)	10% (4 - 19%)	0.91
Plaque type			
Pathological intimal thickening	0 (0%)	1 (1%)	0.51
Fibroatheroma	32 (24%)	63 (48%)	0.18
Thin cap fibroatheroma	7 (5%)	23 (17%)	0.35
Fibrocalcific plaque	1 (1%)	5 (4%)	0.46

Data are presented as numbers, percentages, medians and interquartile range

DISCUSSION

The present study evaluated the spatial relationship between the site of most severe narrowing and greatest vulnerability with the use of invasive VH IVUS. Interestingly, it was demonstrated that the site of greatest vulnerability (defined as maximum necrotic core area) was rarely located at the site of most severe narrowing (defined as the minimum lumen area). Most often (in 66% of vessels), the site of greatest vulnerability was located proximal from the site of most severe narrowing. Of particular interest was the finding that a higher percentage of TCFA (plaque phenotype with high-risk of rupture) was demonstrated at the site of greatest vulnerability.

Histopathological studies have observed that high-risk plaque features include the presence of a large necrotic core, inflammatory cells at the shoulders of the plaque and a thin fibrous cap.[10] [11] Indeed, the rupture of a thin cap fibroatheroma is thought to be the primary cause of an acute coronary syndrome.[12] Moreover, several landmark angiographic studies have reported that the presence of plaque rupture was poorly related to angiographic degree of luminal narrowing.[1] [13] [14] As demonstrated during the follow up of patients admitted for acute myocardial infarction, almost two thirds of plaques prone to rupture were located in non flow-limiting atherosclerotic lesions, and only a minority were located in severely obstructed lesions.[1] Interestingly, the findings of the current study support this concept, demonstrating invasively with VH IVUS that the more vulnerable sites were not at the site of most severe narrowing, but were located more proximally. Therefore, it could be of importance to identify the presence of a high-risk lesion with either non-invasive or invasive modalities, even at sites without the presence of significant luminal narrowing.

Previous reports exploring the relation between the location of the site of most severe narrowing and site of greatest vulnerability using VH IVUS have demonstrated comparable findings.[15-17] Rodriguez et al. performed VH IVUS in 40 patients and assessed the difference in plaque characteristics between plaque rupture site and site of most severe narrowing.[17] Similar to the current findings, the authors demonstrated a significantly higher percentage of necrotic core at the plaque rupture site (16.8%) as compared with the site of most severe narrowing (11.8%). Consequently, the authors concluded that the plaque rupture sites had a worse plaque phenotype than the site of most severe narrowing. In addition, Konig et al. performed an analysis with VH IVUS in 48 patients and demonstrated that the site of severest stenosis was not always located at the site with the highest percentage necrotic core.[16] However, the aforementioned investigations performed an analysis on a per-lesion basis, whereas the present study investigated the entire vessel with VH IVUS. Indeed, a vessel-based analysis provides a more complete evaluation and relevant vulnerable plaque sites are less likely to be missed.

A possible explanation for the current findings could be the relation between presence of positive remodeling and plaque vulnerability. Indeed, compensatory enlargement of the vessel wall, including eccentric plaque growth, is strongly associated with necrotic core area, macrophage infiltration and the occurrence of acute cardiac events.[18 19] Also during in vivo VH IVUS studies, a similar connection between positive remodeling and plaque composition has been reported.[19 20] However, with traditional invasive coronary angiography, lesions with outward (positive) remodeling are frequently missed. Invasive coronary angiography is only able to show the contrast filled lumen and is unable to visualize atherosclerosis in the arterial wall (with the exception of large calcifications) and reference segments.[21] As a consequence, coronary angiography alone will not detect the exact location of the site of greatest vulnerability in the majority of patients. Furthermore, due to the difference in location between the site of most severe narrowing and the site of greatest vulnerability, percutaneous coronary intervention (PCI) of the high risk lesion will be less accurate. Incomplete coverage of a high-risk lesion can lead to increased rates of in-stent restenosis, dissection and stent thrombosis.[22 23] Therefore, identification of the site of greatest vulnerability, in addition to the site of most severe narrowing, could possibly be of importance for clinical management and outcome. In addition, PCI is most often performed in flow-limiting lesions in order to relieve chest pain symptoms. However, no consensus exists regarding the type of treatment for vulnerable regions and systemic anti-atherosclerotic measures (statins) are currently preferred. Nevertheless, studies are ongoing evaluating other alternatives (e.g. bio-absorbable stents) for effective treatment of vulnerable plaque regions.[24]

The following limitations of the present study should be considered. First, the present study only evaluated 77 patients in a single center. Ideally, a larger patient population should be studied, preferably in a multicenter setting. Secondly, due to acoustic shadowing it is difficult to assess plaque composition behind severe calcifications on VH IVUS. Therefore, possibly small non-calcified elements within the more heavily calcified parts of the plaque may have been missed. Lastly, detection of the thin fibrous cap (<65 µm)

is not yet feasible as VH IVUS has limited radial resolution of only 100 µm. A technique such as optical coherence tomography (OCT) imaging would permit these measurements; however, OCT was not performed in the present study.

Conclusion

The present findings demonstrate that the site of greatest vulnerability is rarely at the site of most severe narrowing. Moreover, the site of greatest vulnerability is frequently located proximal from the site of most severe narrowing. Potentially, due to insufficient identification of the high risk lesion, a vulnerable site might remain concealed.

REFERENCES

1. Ambrose JA, Tannenbaum MA, Alexopoulos D et al. Angiographic progression of coronary artery disease and the development of myocardial infarction. J Am Coll Cardiol 1988;12:56-62.
2. Glaser R, Selzer F, Faxon DP et al. Clinical progression of incidental, asymptomatic lesions discovered during culprit vessel coronary intervention. Circulation 2005;111:143-9.
3. Nasu K, Tsuchikane E, Katoh O et al. Accuracy of in vivo coronary plaque morphology assessment: a validation study of in vivo virtual histology compared with in vitro histopathology. J Am Coll Cardiol 2006;47:2405-12.
4. Nair A, Kuban BD, Tuzcu EM et al. Coronary plaque classification with intravascular ultrasound radiofrequency data analysis. Circulation 2002;106:2200-6.
5. Stone GW, Maehara A, Lansky AJ et al. A prospective natural-history study of coronary atherosclerosis. N Engl J Med 2011;364:226-35.
6. Bassand JP, Hamm CW, Ardissino D et al. Guidelines for the diagnosis and treatment of non-ST-segment elevation acute coronary syndromes. Eur Heart J 2007;28:1598-660.
7. Braunwald E, Antman EM, Beasley JW et al. ACC/AHA 2002 guideline update for the management of patients with unstable angina and non-ST-segment elevation myocardial infarction-- summary article: a report of the American College of Cardiology/American Heart Association task force on practice guidelines (Committee on the Management of Patients With Unstable Angina). J Am Coll Cardiol 2002;40:1366-74.
8. Mintz GS, Nissen SE, Anderson WD et al. American College of Cardiology Clinical Expert Consensus Document on Standards for Acquisition, Measurement and Reporting of Intravascular Ultrasound Studies (IVUS). A report of the American College of Cardiology Task Force on Clinical Expert Consensus Documents. J Am Coll Cardiol 2001;37:1478-92.
9. Carlier SG, Mintz GS, Stone GW. Imaging of atherosclerotic plaque using radiofrequency ultrasound signal processing. J Nucl Cardiol 2006;13:831-40.
10. Virmani R, Kolodgie FD, Burke AP et al. Lessons from sudden coronary death: a comprehensive morphological classification scheme for atherosclerotic lesions. Arterioscler Thromb Vasc Biol 2000;20:1262-75.
11. Kolodgie FD, Virmani R, Burke AP et al. Pathologic assessment of the vulnerable human coronary plaque. Heart 2004;90:1385-91.
12. Shah PK. Mechanisms of plaque vulnerability and rupture. J Am Coll Cardiol 2003;41:15S-22S.
13. Giroud D, Li JM, Urban P et al. Relation of the site of acute myocardial infarction to the most severe coronary arterial stenosis at prior angiography. Am J Cardiol 1992;69:729-32.
14. Little WC, Constantinescu M, Applegate RJ et al. Can coronary angiography predict the site of a subsequent myocardial infarction in patients with mild-to-moderate coronary artery disease? Circulation 1988;78:1157-66.
15. Kaple RK, Maehara A, Sano K et al. The axial distribution of lesion-site atherosclerotic plaque components: an in vivo volumetric intravascular ultrasound radio-frequency analysis of lumen stenosis, necrotic core and vessel remodeling. Ultrasound Med Biol 2009;35:550-7.
16. Konig A, Bleie O, Rieber J et al. Intravascular ultrasound radiofrequency analysis of the lesion segment profile in ACS patients. Clin Res Cardiol 2010;99:83-91.
17. Rodriguez-Granillo GA, Garcia-Garcia HM, Valgimigli M et al. Global characterization of coronary plaque rupture phenotype using three-vessel intravascular ultrasound radiofrequency data analysis. Eur Heart J 2006;27:1921-7.
18. Burke AP, Kolodgie FD, Farb A et al. Morphological predictors of arterial remodeling in coronary atherosclerosis. Circulation 2002;105:297-303.
19. Varnava AM, Mills PG, Davies MJ. Relationship between coronary artery remodeling and plaque vulnerability. Circulation 2002;105:939-43.

20. Rodriguez-Granillo GA, Serruys PW, Garcia-Garcia HM et al. Coronary artery remodelling is related to plaque composition. Heart 2006;92:388-91.
21. Mintz GS, Painter JA, Pichard AD et al. Atherosclerosis in angiographically "normal" coronary artery reference segments: an intravascular ultrasound study with clinical correlations. J Am Coll Cardiol 1995;25:1479-85.
22. Fujii K, Carlier SG, Mintz GS et al. Stent underexpansion and residual reference segment stenosis are related to stent thrombosis after sirolimus-eluting stent implantation: an intravascular ultrasound study. J Am Coll Cardiol 2005;45:995-8.
23. Okabe T, Mintz GS, Buch AN et al. Intravascular ultrasound parameters associated with stent thrombosis after drug-eluting stent deployment. Am J Cardiol 2007;100:615-20.
24. Wykrzykowska JJ, Onuma Y, Serruys PW. Advances in stent drug delivery: the future is in bioabsorbable stents. Expert Opin Drug Deliv 2009;6:113-26.

CHAPTER 5

Diagnostic Performance of Non-Invasive Multidetector Computed Tomography Coronary Angiography to Detect Coronary Artery Disease using Different Endpoints; Detection of Significant Stenosis versus Detection of Atherosclerosis

Joëlla E. van Velzen, Joanne D. Schuijf, Fleur R. de Graaf, Eric Boersma, Gabija Pundziute, Fabrizio Spanó Mark J. Boogers, Martin J. Schalij, Lucia J. Kroft, Albert de Roos, J. Wouter Jukema, Ernst E. van der Wall, Jeroen J. Bax

ABSTRACT

Background: The positive predictive value of multidetector computed tomography angiography (CTA) for detecting significant stenosis remains limited. Possibly CTA may be more accurate in the evaluation of atherosclerosis rather than in the evaluation of stenosis severity. However, a comprehensive assessment of the diagnostic performance of CTA in comparison to both conventional coronary angiography (CCA) and intravascular ultrasound (IVUS) is lacking. Therefore, the aim of the study was to systematically investigate the diagnostic performance of CTA for 2 endpoints, namely detecting significant stenosis (using CCA as the reference standard) versus detecting the presence of atherosclerosis (using IVUS as reference of standard).

Methods: A total of 100 patients underwent CTA followed by both CCA and IVUS. Only those segments in which IVUS imaging was performed were included for CTA and QCA analysis. On CTA, each segment was evaluated for significant stenosis (defined as ≥50% luminal narrowing), on CCA significant stenosis was defined as a stenosis ≥50%. Secondly, on CTA, each segment was evaluated for atherosclerotic plaque, atherosclerosis on IVUS was defined as a plaque burden of ≥40% on cross-sectional area.

Results: CTA correctly ruled out significant stenosis in 53 of 53 (100%) patients. However, 9 patients (19%) were incorrectly diagnosed as having significant lesions on CTA resulting in sensitivity, specificity, positive and negative predictive values of 100%, 85%, 81% and 100%. CTA correctly ruled out the presence of atherosclerosis in 7 patients (100%) and correctly identified the presence of atherosclerosis in 93 patients (100%). No patients were incorrectly classified, resulting in sensitivity, specificity, positive and negative predictive values of 100%.

Conclusion: The present study is the first to confirm using both CCA and IVUS that the diagnostic performance of CTA is superior in the evaluation of the presence or the absence of atherosclerosis when compared with the evaluation of significant stenosis.

INTRODUCTION

With the introduction of multidetector computed tomography angiography (CTA) technology, non-invasive imaging of coronary anatomy has become possible. The technique has developed rapidly and is increasingly used for the evaluation of coronary artery disease (CAD), although the precise role of CTA in the assessment of CAD has not been adequately defined yet. On the basis of the high specificity and the high negative predictive value, CTA has an excellent ability of ruling out significant CAD.[1-3]

However, relatively low positive predictive values have been reported and frequently the presence of a significant stenosis that is observed on CTA is not confirmed on conventional coronary angiography (CCA).[4] This discrepancy between CTA and CCA has been attributed to the inferior spatial and temporal resolution of CTA when compared with CCA and at present it seems that the technique remains inferior to CCA. However, one could also question the use of CCA as a reference standard. In contrast to the luminographic approach of CCA, CTA is a cross-sectional or tomographic imaging technique. As a result, CTA allows direct visualization of the coronary vessel wall and thus the presence of coronary atherosclerosis. It is anticipated that precisely this information will become increasingly important in the evaluation and subsequent management of patients with CAD.[5] Possibly the true strength of coronary CTA may therefore lie in the evaluation of atherosclerosis rather than evaluation of significant stenosis.

Thus far diagnostic accuracy studies have only evaluated the performance of CTA using invasive CCA as the standard of reference.[1 3 4] Nonetheless, it is conceivable that CTA may perform better when compared with IVUS (using atherosclerosis as endpoint) than when compared with CCA (using significant stenosis as endpoint). However, thus far no studies have addressed this issue by combing these endpoints in a large cohort of patients. Such a comprehensive evaluation would provide valuable information to further understand how CTA should be used in clinical practice. Therefore, the purpose of this study was to provide a systematic evaluation concerning both the diagnostic accuracy for the detection of significant stenosis (using CCA as the reference standard) and the diagnostic accuracy for the detection of atherosclerosis (using IVUS as the reference standard) in a large cohort of patients.

METHODS

Patients and study protocol

The study group consisted of 106 patients without known CAD who were clinically referred for coronary CTA because of chest pain or elevated risk profile. On the basis of imaging results and clinical presentation patients were referred for CCA in combination with IVUS of 1 - 3 vessels and enrolled in the present study. Contra-indications for CTA were 1) (supra) ventricular arrhythmias, 2) renal insufficiency (glomerular filtration rate <30 ml/min), 3) known allergy to iodine contrast material, 4) severe claustrophobia, 5) pregnancy. Exclusion

criteria for IVUS were severe vessel tortuousness, severe stenosis or vessel occlusion. In each patient, the presence of CAD risk factors including diabetes, systemic hypertension, hypercholesterolemia, positive family history, smoking and obesity, were recorded. Patients were classified as having a low, intermediate or high pre-test likelihood of CAD using the method described by Diamond and Forrester.[6] The study protocol was approved by the institutional ethics committee, and informed consent was obtained in all patients.

Multidetector computed tomography angiography

Data acquisition

Beta-blocking medication (metoprolol 50 or 100 mg, single oral dose, 1 hour prior to examination) was administered in case of a heart rate ≥65 beats/min and in the absence of contra-indications. CTA was performed using either a 64-detector row helical scanner (Aquilion 64, Toshiba Medical Systems, Toshiba Medical Systems, Otawara, Japan) or a 320-detector row volumetric scanner (Aquilion ONE, Toshiba Medical Systems, Otawara, Japan). For the 64-row contrast-enhanced scan, collimation was 64 x 0.5 mm, tube voltage 100 - 135 kV and tube current 250 - 350 mA, depending on body posture. Non-ionic contrast material (Iomeron 400, Bracco, Milan, Italy) was administered with an amount of 80 - 110 ml followed by a saline flush with a flow rate of 5 ml/s. Data acquisition was performed during an inspiratory breath hold of ~ 8 - 10 seconds. Datasets were reconstructed from the retrospectively gated raw data, the best phase was reconstructed with an interval of 0.3 mm. Using a single test slice reconstructed throughout the various phases of the heart cycle, other suitable R-R intervals were examined for additional reconstructions.

For the 320-row contrast-enhanced scan the heart was imaged in a single heartbeat, using prospective triggering with exposure interval depending on the heart rate. Scan parameters were: 350 ms gantry rotation time, 100 - 135 kV tube voltage, and a tube current of 400 - 580 mA, depending on body mass index (BMI). In total, 60 - 90 ml contrast material (Iomeron 400) was administered with a flow rate of 5 - 6 ml/s followed by a saline flush. Automatic peak enhancement detection in the left ventricle was used for timing of the bolus using a threshold of +180 Hounsfield Units. Data acquisition was performed during an inspiratory breath hold of ~ 4 - 6 seconds. Subsequently, data sets were reconstructed and transferred to a remote workstation as previously described.[7]

Data analysis

CTA scans were evaluated using dedicated software (Vitrea 2.0 or Vitrea FX 1.0, Vital images, Minnetonka, MN, USA). CTA examinations were evaluated by two experienced readers (blinded to CCA and IVUS results). Disagreement between readers was resolved in consensus. Three-dimensional rendered reconstructions were used to obtain general information on the anatomy of the coronary arteries. Coronary arteries were subsequently divided into 17 segments according to a modified American Heart Association classification.[8] First, to evaluate the presence of significant stenosis, each segment was evaluated

for the presence of luminal narrowing using axial and/or orthogonal images and curved multiplanar reconstructions. Atherosclerotic lesions were deemed significant stenosis if resulting in ≥50% luminal narrowing. Lesions below this threshold were considered to be non-significant. Second, to evaluate the presence of atherosclerosis, each segment was evaluated for the presence of any atherosclerotic plaque on axial and/or orthogonal images and curved multiplanar reconstructions. Structures >1 mm^2 within and/or adjacent to the coronary artery lumen, which could be clearly distinguished from the vessel lumen, were defined as atherosclerotic plaque.[9]

Conventional and quantitative coronary angiography (QCA)

CCA was performed according to standard protocols. QCA analysis was performed on a segmental basis by an observer unaware of CTA and IVUS findings with the use of QCA-CMS version 6.0 (Medis, Leiden, The Netherlands). QCA was performed only in those segments with plaque. Plaque on invasive CCA was defined as any evidence of luminal narrowing of any degree, clinically significant or not, or evidence of calcification on angiogram before or after contrast injection.[10] The tip of the catheter was used for calibration and for each segment examined both with CTA and IVUS, the reference diameter and minimum luminal diameter were measured and percentage diameter stenosis was reported. Measurements were performed on at least two orthogonal projections and the highest percentage diameter stenosis was used for further analysis. Significant stenosis was defined as ≥50% luminal narrowing.

Intravascular ultrasound

Image acquisition

IVUS examinations were acquired during CCA in 219 of the 300 available vessels with the use of a dedicated IVUS-console (Volcano Corporation, Rancho Cordova, CA, USA). IVUS was performed with a 20 MHz, 2.9 F phased-array IVUS catheter (Eagle Eye, Volcano Corporation, Rancho Cordova, CA, USA), which was introduced distally in the coronary artery under fluoroscopic guidance, after administration of nitrates locally. A motorized automated pullback with a continuous speed of 0.5 mm/s was used until the catheter reached the guiding catheter. Cine runs before and after contrast injections were performed to confirm the position of the IVUS catheter. Images were stored on CD-ROM or DVD for offline analysis.

Image analysis

IVUS analysis was performed by two blinded observers. Lumen and external elastic membrane (EEM) contours were manually traced to determine lumen area and EEM area (QCU-CMS, version 4.5, Leiden, the Netherlands). In each segment, the site with minimum lumen area (mm^2) was identified. Additionally, cross-sectional area measurements of EEM, lumen area and percentage plaque burden (plaque and media area / EEM area multiplied by 100) were performed. The measurements were performed in accordance with the
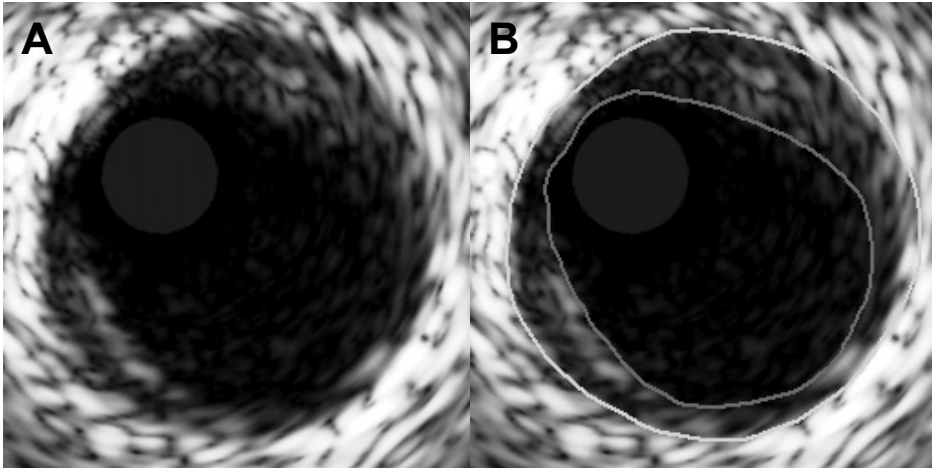
Figure 1. Example of intravascular ultrasound IVUS) cross-sectional image without (A) and with border detection (B). Cross-sectional image of coronary atherosclerosis with vessel border (green) and lumen (red) border tracing demonstrated in panel B. The IVUS image corresponds to a plaque burden of 41%.

IVUS guidelines of the American College of Cardiology.[11] The presence of visually evident atherosclerosis on IVUS was defined as a plaque burden of ≥40% cross-sectional area on at least three consecutive frames.[12] An example of an IVUS cross-sectional image with a plaque burden of ≥40% is demonstrated in Figure 1.

Statistical analysis

Only those segments in which IVUS imaging was performed were included for CTA and QCA analysis. First, the diagnostic accuracy (sensitivity, specificity, positive and negative predictive values including 95% confidence intervals) of CTA for the detection of significant stenosis (luminal narrowing ≥50% on CCA) was calculated on segmental, vessel and patient basis. CCA was the standard of reference for detection of significant stenosis and a segment, vessel or patient was classified as true positive if a significant stenosis was identified correctly by CTA. Second, the diagnostic accuracy (sensitivity, specificity, positive and negative predictive values including 95% confidence intervals) of CTA for the detection of atherosclerosis (plaque burden ≥40% on cross-sectional area on IVUS) was calculated on segmental, vessel and patient basis. IVUS was the standard of reference for the detection of atherosclerosis and a segment, vessel, or patient was classified as true positive if the presence of atherosclerosis was identified correctly by CTA. In the analysis on a vessel basis, the left main was considered part of the left anterior descending artery (LAD) and the intermediate branch was considered part of the left circumflex artery (LCx). Initially, the diagnostic accuracy was determined excluding segments of non-diagnostic image quality. In a subsequent analysis, non-diagnostic segments were included in the analysis and were considered positive for stenosis and atherosclerosis. Differences between the diagnostic accuracy for the two different endpoints were considered significant at the

0.05 level if 95% confidence intervals did not overlap. Continuous values were expressed as means (± standard deviation) if normally distributed and compared with the two-tailed t-test for independent samples. If not normally distributed, values were expressed as medians and interquartile range (IQR) and compared with the 2-tailed Mann-Whitney test. A p-value of <0.05 was considered statistically significant.

To account for possible clustering of coronary artery segments and vessels within patients, the generalized estimating equation (GEE) method was applied for stenosis and atherosclerosis evaluation. When compared to QCA, CTA was scored as significant stenosis present (luminal narrowing ≥50% and non-diagnostic segments) or absent (luminal narrowing <50%). When compared to IVUS, CTA was scored as atherosclerosis present (including non-diagnostic segments) or absent. First, regular binary logistic regression analysis was performed to evaluate the predictive value of CTA for the presence of significant stenosis on QCA and the predictive value of CTA for presence of atherosclerosis on IVUS. Second, to adjust for clustering of segments within patient, GEE analyses were

Table 1. Patient characteristics of the study.

Gender (male/female)	64/36
Age (years)	57 ± 11
Risk factors for CAD (%)	
Diabetes	29 (29%)
Hypertension	60 (60%)
Hypercholesterolaemia	62 (62%)
Positive family history	44 (44%)
Current smoking	47 (47%)
Obese (BMI ≥30 kg/m^2)	21 (21%)
Symptoms (%)	
Typical angina	27 (27%)
Atypical angina	27 (27%)
Non-anginal chest pain	46 (46%)
Pre-test likelihood (%)	
Low	24 (24%)
Intermediate	57 (57%)
High	19 (19%)
Prevalence segments with ≥50% luminal narrowing on QCA	58 (11%)
Prevalence segments with ≥40% plaque burden on IVUS	329 (65%)

BMI; body mass index, QCA; quantitative coronary angiography; IVUS, intravascular ultrasound

performed with proc GENMOD with a binominal distribution for the outcome variable, the link function specified as logit, and patients as separate subjects. In both analyses the parameters of estimation and the standard error were virtually identical, suggesting that

no clustering within patients was present. Statistical analysis was performed using SPSS 14.0 software (SPSS Inc., Chicago. Illinois, USA).

RESULTS

Patient characteristics

In the study population of 106 patients, overall image quality on CTA was reduced in 6 patients (6%). Reasons for reduced image quality were the presence of motion artifacts, increased noise due to a high BMI, elevated heart rate and breathing. Accordingly, these patients were not included in the analysis. Patient characteristics of the remaining 100 patients are presented in Table 1. The average age of the patient group was 57 ± 11 years and 64 were male (64%). The majority of patients (57%) had an intermediate pre-test likelihood for CAD. The average interval between CTA and CCA including IVUS was 61 ± 73 days. In total, in 528 segments both CTA and invasive data (CCA and IVUS analysis) were available (right coronary artery = 72, left anterior descending coronary artery = 87, left circumflex coronary artery = 60). Image quality was insufficient in 18 segments (3%) because of small vessel size (n= 8), a high BMI resulting in increased noise (n=3) and motion artifacts (n=7) and these segments were excluded. For this study estimated mean radiation dose for the 320-row CTA was 3.2 ± 1.1 mSv if scanned full dose at 75% of R-R interval. In patients who were scanned full dose at 65-85% of R-R interval, estimated mean radiation dose was 7.1 ± 1.7 mSv. For the 64-row CTA the estimated mean radiation dose was 18.1 ± 5.9 mSv in patients scanned for the full R-R interval, retrospectively gated.

Diagnostic accuracy of CTA for the detection of significant stenosis

The diagnostic accuracy of CTA (with 95% confidence intervals) for the detection of significant stenosis on a segment, vessel and patient basis excluding and including non-diagnostic segments is presented in Table 2. When excluding non-diagnostic segments, the presence of stenosis was correctly ruled out by CTA in 435 of 452 segments, without significant stenosis on CCA, whereas 57 of the 58 segments were correctly classified as having a significant stenosis. However, CTA overestimated a total of 17 lesions deemed non-significant on CCA and underestimated 1 lesion which was significant on CCA. On a segmental basis, this resulted in a sensitivity and specificity of respectively 98% and 96%, and positive and negative predictive values of 77% and 99%, respectively. On a vessel basis, a total of 47 vessels out of the 219 vessels were identified as significant stenosis on CCA. CTA correctly identified all the 47 vessels as significant (100%). In the remaining 172 vessels, CTA correctly identified 158 vessels as non-significant (92%). However, 14 vessels were overestimated as significant CAD by CTA. On a vessel basis, this resulted in a sensitivity and specificity of respectively 100% and 92%, and positive and negative predictive values of 77% and 100%, respectively. On a patient basis, CTA correctly ruled out significant CAD in 53 of 62 (85%) patients without significant stenosis on CCA. Additionally, CTA

Table 2. Diagnostic accuracy for the detection of significant stenosis, excluding and including non-diagnostic segments.

	Segmental Analysis	Vessel Analysis	Patient Analysis
Excluding non-diagnostic segments			
Sensitivity	57/58 (98%, 95%-100%)	47/47 (100%)	38/38 (100%)
Specificity	435/452 (96%, 94%-97%)	158/172 (92%, 88%-96%)	53/62 (85%, 78%-93%)
PPV	57/74 (77%, 69%-85%)	47/61 (77%, 67%-88%)	38/47 (81%, 71%-90%)
NPV	435/436 (99.7%, 99%-100%)	158/158 (100%)	53/53 (100%)
Diagnostic Accuracy	492/510 (96%, 95%-98%)	205/219 (94%, 90%-97%)	91/100 (92%, 86%-96%)
Including non-diagnostic segments			
Sensitivity	60/61 (98%, 95%-100%)	47/47 (100%)	38/38 (100%)
Specificity	435/467 (93%, 91%-95%)	149/172 (87%, 82%-92%)	53/62 (85%, 78%-93%)
PPV	60/92 (65%, 55%-75%)	47/70 (67%, 56%-78%)	38/47 (81%, 71%-90%)
NPV	435/436 (99.7%, 99%-100%)	149/149 (100%)	53/53 (100%)
Diagnostic Accuracy	495/528 (94%, 92%-96%)	196/219 (90%, 85%-94%)	91/100 (92%, 86%-96%)

Accuracy and 95% confidence intervals of CTA to detect significant stenosis using CCA as the standard of reference [segmental (n=510), vessel (n=219) and patient (n=100) analysis], excluding and including non-diagnostic segments.
PPV; positive predictive value, NPV; negative predictive value.

correctly identified 38 of 38 patients (100%) with one or more significant lesions. However, nine patients (19%) were incorrectly classified as having significant lesions on CTA.

Diagnostic accuracy of CTA for the detection of atherosclerosis

The diagnostic accuracy of CTA (with 95% confidence intervals) for the detection of athero-sclerosis on a segment, vessel and patient basis, excluding and including non-diagnostic segments is presented in Table 3. In the 510 evaluated segments, median minimal lumen area was 6.7 mm^2 (IQR 4.5 - 10.1 mm^2), median EEM area was 14.0 mm^2 (IQR 10.0 - 20.0 mm^2) and median percentage plaque burden was 42% (IQR 34 - 50%). When excluding non-diagnostic segments, 329 segments with atherosclerosis were detected by IVUS, of which 326 were correctly identified by CTA (sensitivity 99%). CTA incorrectly classified three segments as without atherosclerosis. In addition, of the 181 segments considered without atherosclerosis by IVUS, atherosclerosis was correctly excluded in 179 segments by CTA (specificity 99%) and two segments were incorrectly classified as positive for atherosclerosis. On a vessel basis, 172 vessels out of 173 vessels which were deemed positive for atherosclerosis by IVUS were correctly identified by CTA (99%). Moreover, CTA correctly ruled out presence of atherosclerosis in the 45 out of 46 vessels deemed nega-tive for atherosclerosis by IVUS. Thus, CTA overestimated only one vessel as positive and underestimated one vessel as negative for atherosclerosis. On a vessel basis, this resulted in a sensitivity and specificity of respectively, 99% and 98% and a positive and negative predictive value of 99% and 98%, respectively. On a patient basis CTA correctly ruled out the presence of atherosclerosis in 7 patients (100%), and correctly identified the presence

Table 3. Diagnostic accuracy for the detection of atherosclerosis, excluding and including non-diagnostic segments.

	Segmental Analysis	Vessel Analysis	Patient Analysis
Excluding non-diagnostic segments			
Sensitivity	326/329 (99%, 98%-100%)	172/173 (99%, 98%-100%)	93/93 (100%)
Specificity	179/181 (99%, 97%-100%)	45/46 (98%, 94%-100%)	7/7 (100%)
PPV	326/328 (99%, 99%-100%)	172/173 (99%, 98%-100%)	93/93 (100%)
NPV	179/182 (98%, 97%-100%)	45/46 (98%, 94%-100%)	7/7 (100%)
Diagnostic Accuracy	505/510 (99%, 98%-99.8%)	217/219 (99%, 98%-100%)	100/100 (100%)
Including non-diagnostic segments			
Sensitivity	343/346 (99%, 98%-100%)	172/173 (99%, 98%-100%)	93/93 (100%)
Specificity	179/182 (98%, 97%-100%)	45/46 (98%, 94%-100%)	7/7 (100%)
PPV	343/346 (99%, 98%-100%)	172/173 (99%, 98%-100%)	93/93 (100%)
NPV	179/182 (98% (97%-100%)	45/46 (98 %, 94%-100%)	7/7 (100%)
Diagnostic Accuracy	522/528 (99%, (98%-99.7%)	217/219 (98%, 99%-100%)	100/100 (100%)

Accuracy and 95% confidence intervals of CTA for the detection of atherosclerosis, with IVUS as the standard of reference [segmental (n=510), vessel (n=219) and patient (n=100) analysis], excluding and including non-diagnostic segments.
PPV; positive predictive value, NPV; negative predictive value.
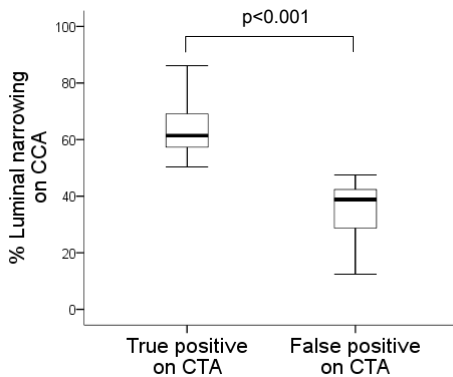
Figure 2A. Difference in percentage luminal narrowing between true and false positives for detection of significant stenosis on multidetector computed tomography angiography (CTA). Box plot graph illustrating the difference in percentage luminal narrowing on conventional coronary angiography (CCA) between true positive (median = 61%) and false positive (median = 39%) lesions for significant stenosis on CTA.
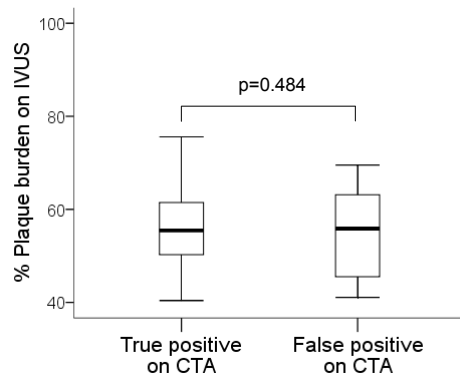
Figure 2B. Difference in percentage plaque burden between true and false positives for significant stenosis on multidetector computed tomography angiography (CTA).
Boxplot illustrating the difference in percentage plaque burden on intravascular ultrasound (IVUS) between lesions true positive (median = 56%) and false positive (median = 56%) for significant stenosis on CTA.

of atherosclerosis in 93 patients (100%) resulting in sensitivity, specificity, positive and negative predictive values of 100%.

Quantitative analysis of CCA and IVUS characteristics of lesions with correct and incorrect diagnosis of significant stenosis on CTA

To explore the differences between lesions correctly identified as a significant stenosis by CTA (true positives) and lesions incorrectly identified as significant lesions by CTA (false positives), CCA, and IVUS characteristics were compared. As demonstrated in Figure 2A, percentage luminal narrowing on CCA was significantly higher in true positives when compared with false positives (61% (IQR 57 - 70%) versus 39% (IQR 28 - 43%) p<0.001).
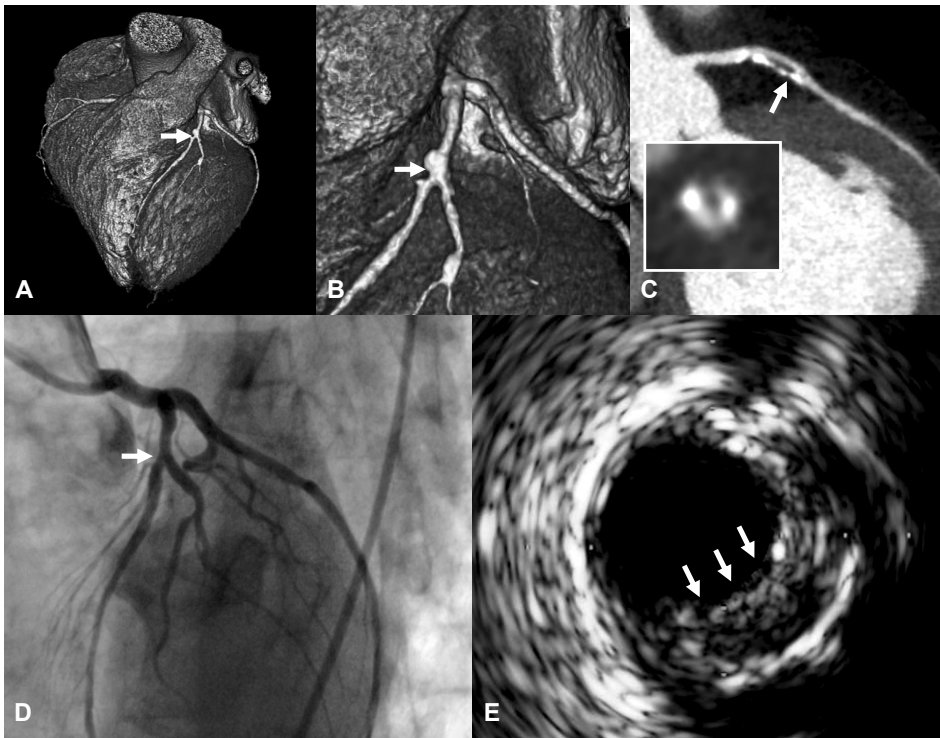
Figure 3. Case example of a 65 year old male with extensive coronary artery disease (CAD) as demonstrated by 320-row multidetector computed tomography angiography (CTA) and intravascular ultrasound (IVUS) while conventional coronary angiography (CCA) showed no significant CAD. (A) 3D volume rendered reconstruction providing an overview of the left anterior descending coronary artery (LAD) showing signs of extensive atherosclerosis in the mid LAD (arrow). (B) An enlargement of the mid LAD demonstrating presence of extensive calcifications. (C) Multiplanar reconstruction of the LAD demonstrating the presence of diffuse atherosclerosis in the mid LAD (arrow) with luminal narrowing, enlargement showing cross-sectional view of the LAD with calcified and non-calcified elements. (D) CCA demonstrating no signs of significant luminal narrowing in the LAD. (E) IVUS cross-sectional image of the mid LAD confirming the presence of extensive atherosclerosis with calcifications (arrows) and a plaque burden of ≥40%.

However, minimal lumen area on IVUS was not significantly different between true positives and false positives (3.9 mm^2 (IQR 3.0 - 5.6 mm^2) versus 4.1 mm^2 (IQR 3.6 - 7.6 mm^2), p=0.136). More importantly, plaque burden on IVUS was not significantly different between true and false positives (56% (IQR 50 - 62%) versus 56% (IQR 46 - 63%), p=0.484) implying that substantial atherosclerosis is present in lesions that are falsely classified as positive for stenosis on CTA despite the absence of significant luminal narrowing (Figure 2B). A case example of a patient with stenosis on CTA in the absence of significant stenosis on CCA is provided in Figure 3.

DISCUSSION

The present study is the first to perform a comprehensive evaluation of the diagnostic performance of CTA. We systematically investigated the diagnostic accuracy of CTA for the detection of significant stenosis (with CCA as the reference standard) as well as for the detection of atherosclerosis (using IVUS as the reference standard) in a large patient population. In the current study, regarding the accuracy of CTA to detect significant stenosis, a negative predictive value of 100% and a diagnostic accuracy of 92% were observed on a patient level. Importantly, no patients with significant stenosis were missed. Nevertheless, nine patients (9% of the total population) were incorrectly classified as having a significant stenosis resulting in a limited positive predictive value of 81%. However, when the definition of disease was changed from significant stenosis (gold standard CCA) to the presence of atherosclerosis (gold standard IVUS), the performance of CTA improved and an excellent diagnostic accuracy was observed. Further exploration of lesions incorrectly classified as having significant stenosis on CTA confirmed the presence of substantial plaque burden in these segments. The findings of the present study demonstrate that CTA may be superior in the evaluation of the presence or the absence of visually evident atherosclerosis on IVUS when compared with the evaluation of significant stenosis. Accordingly, CTA may therefore perform better in the assessment of atherosclerosis rather than the evaluation of stenosis severity. Conceivably, precisely this information on atherosclerosis, which cannot be derived from CCA, may become increasingly important in the definition and subsequent management of CAD.[5]

The present observations regarding the diagnostic accuracy for detection of significant stenosis are in line with the previous literature using 64-row CTA.[1 3] Recently in a multicentre trial, the diagnostic performance of 64-row CTA was investigated in 230 symptomatic patients with suspected CAD, reporting a sensitivity and specificity of 95% and 83% on a patient basis, respectively.[1] However, while in this study the negative predictive value (on a patient basis) was high (99%), a relatively low positive predictive value of 64% was reported. Indeed, due to limitations in spatial resolution it has been established that CTA cannot precisely grade the severity of stenosis and frequently overestimates the degree of luminal narrowing. Similarly, in the present study, 17 segments were incorrectly identified as having significant stenosis leading to a positive predictive value for detecting significant

stenosis of only 77% on segmental basis and 81% on patient basis. Therefore, while CTA remains an excellent tool for ruling out the presence of significant stenosis, a substantial proportion of lesions are overestimated, thereby resulting in incorrect diagnosis.

Importantly, when changing the definition of CAD from the presence of significant stenosis to the presence of atherosclerosis, the overestimated lesions were no longer false positive studies. Comparison with IVUS revealed that in all of these patients despite the absence of significant luminal narrowing, substantial plaque burden was present. Accordingly, CTA had excellent diagnostic accuracy for the detection of atherosclerosis when compared with IVUS. Importantly, no patients with visually evident atherosclerosis (as determined on IVUS) were missed nor was the presence of atherosclerosis incorrectly diagnosed. On a segmental and vessel level, only slightly lower values were observed. Accurate assessment of atherosclerosis with CTA has previously been demonstrated in several investigations. When compared with histology, a good correlation for detecting and characterizing atherosclerotic plaque was reported.[13] In vivo, Leber et al observed a sensitivity and specificity for 16-row CTA of respectively 85% and 92% to detect coronary lesions as determined on IVUS.[9] Evaluation of the characteristics of lesions missed on CTA revealed that particularly small plaques located in distal segments were not identified. In contrast, larger and proximally located plaques, which may be considered more clinically relevant, were accurately detected.

Clinical implications

At present, CCA is the gold standard for detecting severely stenotic lesions and remains the basis for referral for surgical and catheter-based revascularization. However, CCA has a tendency to underestimate total atherosclerotic plaque burden (partly due to positive remodeling) and more detailed characterization of atherosclerosis is not feasible at present. Currently, the gold standard for assessing and quantifying coronary artery plaque burden is IVUS. Nevertheless, the use of this invasive technique is restricted to patients with a high likelihood of having significant lesions requiring intervention. In contrast, non-invasive CTA will typically be used in lower likelihood patients and thus to evaluate the presence of CAD in more early stages. This technique has been proved very useful in the clinical setting and particularly due to the high negative predictive value it can accurately rule out the presence of significant disease in the majority of patients with a low to intermediate pre-test risk profile. While the technique accurately rules out the presence of significant stenosis, the limited positive predictive value (potentially resulting in unnecessary invasive procedures) has been a cause of concern. However in this regard, two issues are important to acknowledge. First, as demonstrated in the current study, coronary segments false positive for significant stenosis may not necessarily be false positive for atherosclerosis. Accordingly, these findings may still be considered relevant for risk stratification and initiation of anti-atherosclerotic measures. Second, regardless of the actual severity of the detected lesion, functional testing remains essential to determine the haemodynamical consequences of the lesion.[14] The presence and extent of ischaemia rather than an estimate of luminal narrowing should invariably serve as the

basis for further referral for CCA and possible revascularization. Considering these issues, it is conceivable that the emphasis of CTA, which traditionally has been on the evaluation of significant stenosis, may shift towards the evaluation of atherosclerosis.

As demonstrated in our systematic comparison of CTA with both CCA and IVUS, the diagnostic accuracy of CTA for detecting the presence of atherosclerosis was superior over the detection of significant stenosis. In fact, the ability of CTA to accurately exclude the presence of atherosclerosis may be considered superior over other non-invasive techniques. Importantly, supporting data are emerging that patients without any evidence of atherosclerotic plaques on CTA have excellent prognosis that is maintained over a relatively long period of time.[15 16] In these patients, CTA may obviate the need for further testing and unnecessary aggressive therapy. In contrast, patients with atherosclerotic plaques on CTA have been shown to have worse outcome. These patients may thus benefit from intensified treatment, while further evaluation with functional testing remains essential to determine the need for revascularization. On the basis of these and the current observations, it is conceivable therefore that shifting the use of CTA from mere stenosis assessment towards evaluation of atherosclerosis may have several advantages for clinical management and may allow improved risk stratification.

Limitations

In the current study, only patients with sufficient CTA image quality for the evaluation of both the presence of significant stenosis and atherosclerosis were included. In addition, a verification bias could be present, as in a limited number of cases patients were referred for CCA on the basis of CTA findings. Moreover, in the present study, no nitroglycerine was administered before the CT scan. Furthermore, concerns have been raised about CTA radiation dose, especially with respect to the long term effects. However, the recent introduction of single heart beat imaging (320-row CTA), dose modulation and particularly prospective triggering have drastically reduced patient radiation dose. Future research will most likely focus on further decreasing radiation exposure while maintaining good image quality.

Conclusion

The present study is the first to perform a comprehensive evaluation of the diagnostic accuracy of CTA for the detection of significant stenosis and for the presence of atherosclerosis. In this regard, the diagnostic accuracy of CTA for the detection of the presence of atherosclerosis was superior over the detection of significant stenosis. Possibly, the emphasis of CTA should shift towards the evaluation of atherosclerosis rather than mere stenosis severity.

REFERENCES

1. Budoff MJ, Dowe D, Jollis JG et al. Diagnostic performance of 64-multidetector row coronary computed tomographic angiography for evaluation of coronary artery stenosis in individuals without known coronary artery disease: results from the prospective multicenter ACCURACY (Assessment by Coronary Computed Tomographic Angiography of Individuals Undergoing Invasive Coronary Angiography) trial. J Am Coll Cardiol 2008;52:1724-32.
2. Meijboom WB, Meijs MF, Schuijf JD et al. Diagnostic accuracy of 64-slice computed tomography coronary angiography: a prospective, multicenter, multivendor study. J Am Coll Cardiol 2008;52: 2135-44.
3. Miller JM, Rochitte CE, Dewey M et al. Diagnostic performance of coronary angiography by 64-row CT. N Engl J Med 2008;359:2324-36.
4. Mowatt G, Cook JA, Hillis GS et al. 64-Slice computed tomography angiography in the diagnosis and assessment of coronary artery disease: systematic review and meta-analysis. Heart 2008;94:1386-93.
5. Mark DB, Berman DS, Budoff MJ et al. ACCF/ACR/AHA/NASCI/SAIP/SCAI/SCCT 2010 expert consensus document on coronary computed tomographic angiography: a report of the American College of Cardiology Foundation Task Force on Expert Consensus Documents. J Am Coll Cardiol 2010;55:2663-99.
6. Diamond GA, Forrester JS. Analysis of probability as an aid in the clinical diagnosis of coronary-artery disease. N Engl J Med 1979;300:1350-8.
7. Schuijf JD, Pundziute G, Jukema JW et al. Diagnostic accuracy of 64-slice multislice computed tomography in the noninvasive evaluation of significant coronary artery disease. Am J Cardiol 2006;98:145-8.
8. Austen WG, Edwards JE, Frye RL et al. A reporting system on patients evaluated for coronary artery disease. Report of the Ad Hoc Committee for Grading of Coronary Artery Disease, Council on Cardiovascular Surgery, American Heart Association. Circulation 1975;51:5-40.
9. Leber AW, Knez A, Becker A et al. Accuracy of multidetector spiral computed tomography in identifying and differentiating the composition of coronary atherosclerotic plaques: a comparative study with intracoronary ultrasound. J Am Coll Cardiol 2004;43:1241-7.
10. Butler J, Shapiro M, Reiber J et al. Extent and distribution of coronary artery disease: a comparative study of invasive versus noninvasive angiography with computed angiography. Am Heart J 2007;153:378-84.
11. Mintz GS, Nissen SE, Anderson WD et al. American College of Cardiology Clinical Expert Consensus Document on Standards for Acquisition, Measurement and Reporting of Intravascular Ultrasound Studies (IVUS). A report of the American College of Cardiology Task Force on Clinical Expert Consensus Documents. J Am Coll Cardiol 2001;37:1478-92.
12. Virmani R, Kolodgie FD, Burke AP et al. Lessons from sudden coronary death: a comprehensive morphological classification scheme for atherosclerotic lesions. Arterioscler Thromb Vasc Biol 2000;20:1262-75.
13. Nikolaou K, Becker CR, Wintersperger BJ et al. [Evaluating multislice computed tomography for imaging coronary atherosclerosis]. Radiologe 2004;44:130-9.
14. Schuijf JD, Wijns W, Jukema JW et al. Relationship between noninvasive coronary angiography with multi-slice computed tomography and myocardial perfusion imaging. J Am Coll Cardiol 2006;48:2508-14.
15. Pundziute G, Schuijf JD, Jukema JW et al. Prognostic value of multislice computed tomography coronary angiography in patients with known or suspected coronary artery disease. J Am Coll Cardiol 2007;49:62-70.

16. van Werkhoven JM, Schuijf JD, Gaemperli O et al. Prognostic value of multislice computed tomography and gated single-photon emission computed tomography in patients with suspected coronary artery disease. J Am Coll Cardiol 2009;53:623-32.

CHAPTER 6

Non-invasive Assessment of
Atherosclerotic Coronary Lesion
Length using Multidetector
Computed Tomography Angiography:
Comparison to Quantitative
Coronary Angiography

Joëlla E. van Velzen, Michiel A. de Graaf, Agnieska Ciarka, Fleur R. de Graaf, Martin J. Schalij, Lucia J. Kroft, Albert de Roos, J. Wouter Jukema, Johan H.C. Reiber, Joanne D. Schuijf, Jeroen J. Bax, Ernst E. van der Wall

ABSTRACT

Background: Multidetector computed tomography angiography (CTA) provides information on plaque extent and stenosis in the coronary wall. More accurate lesion assessment may be feasible with CTA as compared to invasive coronary angiography (ICA). Accordingly, lesion length assessment was compared between ICA and CTA in patients referred for CTA who underwent subsequent percutaneous coronary intervention (PCI).

Methods: 89 patients clinically referred for CTA and were subsequently referred for ICA and PCI. On CTA, lesion length was measured from the proximal to the distal shoulder of the plaque. Quantitative coronary angiography (QCA) was performed to analyze lesion length. Stent length was recorded for each lesion.

Results: In total, 119 lesions were retrospectively identified. Mean lesion length on CTA was 21.4±8.4 mm and on QCA 12.6±6.1 mm. Mean stent length deployed was 17.4±5.3 mm. Lesion length on CTA was significantly longer than on QCA (difference 8.8±6.7 mm, p<0.001). Moreover, lesion length visualized on CTA was also significantly longer than mean stent length (CTA lesion length-stent length was 4.2±8.7 mm, p<0.001).

Conclusion: Lesion length assessed by CTA is longer than that assessed by ICA. Possibly, CTA provides more accurate lesion length assessment than ICA and may facilitate improved guidance of percutaneous treatment of coronary lesions.

INTRODUCTION

Invasive coronary angiography (ICA) has been traditionally used for evaluation of the presence and severity of coronary artery disease (CAD). Accordingly, the technique has been extensively utilized to guide further treatment strategies, such as percutaneous coronary intervention (PCI) with stent placement. In particular, the choice for stent length and diameter is frequently decided on the basis of the 2-dimensional ICA images. However, although ICA has an excellent ability to visualize the lumen and severity of luminal narrowing, the presence of atherosclerotic plaque in the arterial wall cannot be accurately visualized.[1] The chosen stent length may not always match the true atherosclerotic plaque length and could potentially lead to insufficient stent coverage of the plaque and possible development of post-stent complications such as arterial dissection, in-stent restenosis and stent thrombosis.[2-4]

Several studies comparing ICA to intravascular ultrasound (IVUS) have shown that ICA indeed underestimates plaque extent.[1 5 6] Multidetector computed tomography angiography (CTA) is increasingly used to non-invasively evaluate the presence of CAD[7 8], and a growing number of patients referred for ICA will have previously undergone non-invasive evaluation by CTA. A particular strength of this modality is that it is able to not only visualize luminal narrowing but also the extent of atherosclerotic plaque in the arterial wall.[9 10] Accordingly, in patients with previous CTA, who subsequently underwent ICA and PCI, lesion length on CTA was compared to length on ICA.

METHODS

Patients

A total of 89 patients were retrospectively analyzed, who were clinically referred for CTA and had subsequent ICA and PCI with stent implantation. All clinical data were retrieved from the departmental Cardiology Information System (EPD-Vision®, Leiden University Medical Center). In each patient, the presence of CAD risk factors such as diabetes, systemic hypertension, hypercholesterolemia, positive family history, smoking and obesity, were noted.

Multidetector computed tomography coronary angiography

Data acquisition

Contra-indications for CTA were 1) (supra) ventricular arrhythmias, 2) renal insufficiency (glomerular filtration rate<30 ml/min), 3) known allergy to iodine contrast material, 4) severe claustrophobia, 5) pregnancy. Patients received beta-blocking medication (50-100 mg metoprolol orally, or 5-10 mg intravenously) 1 hour before CTA examination if the heart rate was above 65 beats per minute, unless contra-indicated. Forty-seven patients were scanned on a 64-detector row helical scanner (Aquilion 64, Toshiba Medical Systems,

Otawara, Japan). Scan parameters were: 400 ms gantry rotation time, 100 to 135 kV tube voltage and a tube current of 250 to 350 mA, depending on body shape. Thirty-six patients were scanned on a 320-detector row volumetric scanner (Aquilion ONE, Toshiba Medical Systems, Otawara, Japan). The heart was imaged in a single heartbeat, using prospective triggering with exposure interval depending on the heart rate. Scan parameters were: 350 ms gantry rotation time, 100 to 135 kV tube voltage and a tube current of 400 to 580 mA, depending on body mass index. In total, 60 to 90 ml contrast material (Iomeron 400, Bracco, Milan, Italy) was administered with a rate of 5 - 6 ml/sec followed by a saline flush. Subsequently, data sets were reconstructed in the best available phase and transferred to a remote workstation.

CTA lesion length assessment

Post-processing of the CTA scans was performed on a dedicated workstation (Vitrea FX 2.0.2, Vital images Minnetonka, MN, USA). Coronary anatomy was assessed in a standardized manner by dividing the coronary artery tree into 17 segments according to the modified American Heart Association classification. CTA lesion length was evaluated in consensus by 2 experienced readers who were blinded to quantitative coronary angiography (QCA) lesion length findings. Firstly, the location of lesions was identified on ICA. To match lesions identified on ICA with lesions on CTA, landmarks such as coronary ostia, side-branches and calcium deposits were used. A plaque on CTA was defined as a structure ≥1mm^2 in the coronary artery lumen.[11] Secondly, on CTA, lesion length was determined on curved multiplanar reconstructions (MPR's) in two different angles for every lesion in which PCI was performed. Lesion length (mm) was measured on CTA from the proximal
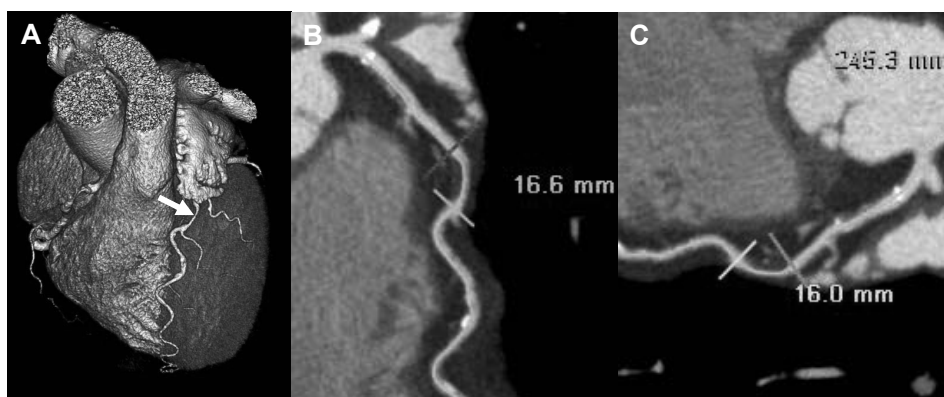
Figure 1. Example of atherosclerotic lesion length measurement in two different views on multidetector computed tomography angiography images with the use of a dedicated software tool. In panel (A), a 3 dimensional volume rendered reconstruction of the heart with the left anterior descending coronary artery (LAD) is shown (arrow). (B) In panel (B) lesion length measurement is performed of a non-calcified lesion in the mid LAD. In this view, lesion length measured was 16.6 mm. In panel (C), lesion length measurement is performed of the same lesion, however in a different angle. In this view, lesion length measured was 16.0 mm.

to distal shoulder of the plaque with a dedicated Vitrea software display tool (Vitrea FX 2.0.2, Minnetonka, MN, USA) (Figure 1). A tandem lesion within 4 mm of the edge of lesion was considered as part of the lesion. The average of these two measurements was taken as the final CTA lesion length. Radiation dose was quantified with a dose-length product conversion factor of 0.014 mSv/(mGy·cm).[12] For the 320-row CTA, patients with a low heart rate (<60 bpm) were scanned full dose at 70-80% of R-R interval and estimated mean radiation dose was 3.2 ± 1.1 mSv. Patients with a higher heart rate (60-65 bpm) were scanned full dose at 65-85% of R-R interval and estimated mean radiation dose was 7.1 ± 1.7 mSv. For the 64-row CTA: The estimated mean radiation dose was 18.1 ± 5.9 mSv, all performed with retrospective gating.

Quantitative coronary angiography

QCA analysis was performed by observer unaware of CTA findings with the use of QCA-CMS version 6.0 (Medis, Leiden, The Netherlands). Prior to measuring lesion length, images were calibrated with use of the contrast filled catheter. Subsequently, per lesion, the two best orthogonal projections were chosen on which measurements were performed to minimize foreshortening. Consequently, lesion length (mm) was measured from the proximal shoulder to the distal shoulder of the lesion. The longest length measured on QCA was used for further analysis. In addition, highest percent diameter stenosis as measured by QCA was reported for each lesion. The choice and size of stent used were left to the discretion of operator. Per lesion, stent diameter and length were reported. If more than one stent was planned, the total stent length of all combined stents deployed was used.

Statistical analysis

Continuous variables were expressed as mean and standard deviation, and categorical data were expressed in numbers and percentages. Paired variables were analyzed with Wilcoxon signed rank tests. Statistical analysis was performed using SPSS software (version 16.0, SPSS inc., Chicago, IL, USA). A p-value<0.05 was considered statistically significant.

RESULTS

Of the 89 patients, 4 were excluded in which the target lesion length was not quantifiable on CTA. These lesions were either a total chronic occlusion (n=2) or in-stent restenosis (n=2). Furthermore, 2 patients were excluded due to impaired CTA image quality. Consequently, 83 patients (59 males (71%), mean age 62 ±10 years) and 119 lesions were included in the analysis. Baseline patient characteristics are described in Table 1. The average time interval between CTA and PCI was 63 ±110 days. As determined by QCA, the mean percent stenosis of the lesions was 71 ±11%. Overall, lesions were most often located in the left anterior descending coronary artery (56 lesions, 47%) followed by the left circumflex coronary artery (35 lesions, 29%) and the right coronary artery (28 lesions,

Table 1. Patient characteristics (n=83).

	n (%)
Age (mean ±standard deviation)	62 ±10
Gender (male/female)	59/24
Obesity (BMI ≥ 30 kg/m^2)	12 (14%)
Diabetes	18 (22%)
Hypertension	44 (53%)
Hypercholesterolemia	28 (34%)
Family History	37 (45%)
Smoking	33 (40%)
Previous stent (%)	18 (22%)
Complications during PCI	
Edge dissection	6 (7%)
Stent thrombosis*	1 (1%)

BMI, body mass index
* Defined as definite, probable and possible stent thrombosis within 1 month

24%). Concerning plaque composition, 27 lesions (23%) were non-calcified, 72 lesions (60%) were mixed and 20 lesions (17%) were calcified.

Lesion length

The mean lesion length measured on CTA was 21.4 ±8.4 mm, as compared to a mean lesion length on QCA of 12.5 ±6.1 mm resulting in a mean difference (CTA lesion length - QCA lesion length) of 8.8 ±6.7 mm. Only 2 lesions were longer on QCA than on CTA, however the difference between these 2 lesions was only minor (13.2 mm on CTA versus 14.3 mm on QCA and 5.7 mm on CTA versus 6.7 mm on QCA). Overall, mean CTA lesion length was significantly longer than mean QCA lesion length (p<0.001), as demonstrated in Figure 2. At Bland-Altman analysis, mean differences (±SD) of 8.8 ±6.7 mm were observed between CTA and ICA, with 95% limits of agreement ranging from -4.3 to 22.0
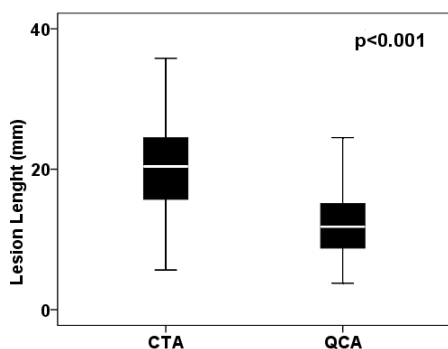
Figure 2. Box plot showing the difference between lesion length assessment on multidetector computed tomography angiography (CTA) and quantitative coronary angiography (QCA). Lesion length assessment is less on QCA as compared to CTA (p<0.001).
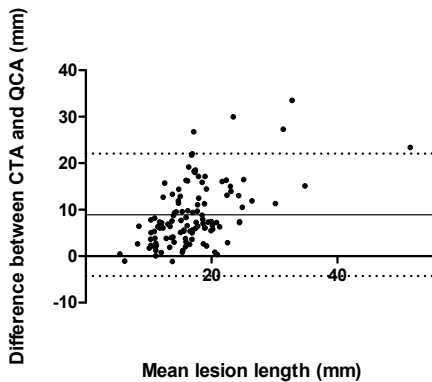
Figure 3. Bland-Altman plot of lesion length (mm) shows the difference between each pair plotted against the average value of the same pair (solid line, mean value of difference; dotted line, mean value of differences ± 2 SDs).

(Figure 3). The mean diameter of stents deployed was 3.1 ±0.3 mm, ranging from 3.0 mm to 4.0 mm. The length of stents deployed ranged from 8.0 mm to 33.0 mm (mean 17.5 ±5.3 mm). Accordingly, lesion length on CTA was also significantly longer than mean stent length (CTA lesion length - stent length was 4.2 ±8.7 mm, p<0.001). Furthermore, mean stent length exceeded lesion length on QCA; stent length - QCA lesion length was 4.8 ±6.2 mm (p<0.001).

DISCUSSION

Comparison between ICA and non-invasive CTA demonstrated that lesion length measured by CTA was substantially longer than lesion length measured by ICA. In addition, lesion length on CTA was compared to the stent length selected for PCI. Interestingly, lesion length measured by CTA significantly exceeded the mean length over which the stent was deployed.

There are only very limited data regarding lesion length measurement with CTA. Soon et al compared atherosclerotic lesion length between ICA and CTA (16-slice) in 30 patients and 44 lesions and observed that lesion length was significantly longer on CTA than on ICA with a median difference of 9.8 mm (95% confidence interval of 7.3-13.3).[13] Moreover, the finding that ICA significantly underestimates atherosclerotic lesion length has also been demonstrated by Yamagishi et al, who compared atherosclerotic lesion length on ICA to grayscale IVUS, the current gold standard for the evaluation of atherosclerosis.[5] The authors demonstrated that lesion length on ICA (mean lesion length of 12.4 ±6.1 mm) was significantly shorter than lesion length measured by IVUS (mean lesion length of 16.3 ±8.9 mm).

Although angiographically detected coronary atherosclerosis has been linked to outcome in several clinical trials [14-17], it has been suggested that ICA considerably underestimates the overall extent of CAD.[18] Indeed, when compared to IVUS, the presence of angiographic disease did not reflect true atherosclerotic plaque burden.[1] Mintz et al

compared the detection of atherosclerosis on ICA to IVUS and found that only 7% of segments described as normal on ICA were truly without any atherosclerotic plaque on IVUS.[1] Conversely, non-invasive CTA has been shown to provide accurate evaluation of coronary plaque burden,[9] [19-21] with a good correlation for detecting and characterizing atherosclerotic plaque in comparison to histology.[22-24] Moreover, Leber et al demonstrated a sensitivity and specificity of 16-slice CTA for the detection of coronary lesions as determined on IVUS of 85% and 92%, respectively.[11] However, small plaques located in distal segments were more difficult to evaluate, particularly in CTA scans with reduced image quality.[11]

The large difference between ICA and CTA lesion length assessment can be explained by the excellent ability of CTA to visualize plaque and vessel remodelling in the arterial wall, in contrast to ICA. Indeed, ICA only shows the contrast filled lumen and is unable to visualize the arterial wall (with the exception of large calcifications), and reference segments may not be optimally evaluated by ICA.[25] Indeed, with traditional invasive coronary angiography, lesions with outward (positive) remodeling are frequently underestimated or missed. Moreover, CTA is not hampered by limitations of angiographic projection such as foreshortening or difficulties in case of tortuous vessels. However, it is of importance to identify the presence of atherosclerosis even at sites without significant luminal narrowing, and some acute coronary syndromes may be triggered by sudden disruption of atherosclerotic plaques that caused neither significant luminal narrowing nor chest pain complaints before the event.[26] It has been suggested that the most rupture prone part of the plaque is not at the maximum point of luminal narrowing but actually located in the shoulders of the plaque.[27] Accordingly, it is important to assess the entire plaque length.

It has also been demonstrated that insufficient coverage of the target lesion increases the risk for in-stent restenosis and stent thrombosis. Fujii et al. retrospectively evaluated lesion characteristics using IVUS leading to stent thrombosis after PCI.[2] The authors observed that stent thrombosis occurred in stents with significantly more residual plaque upstream and downstream from the stent as compared to lesions without stent thrombosis. Okabe et al explored which IVUS related findings predicted the risk for the development of stent thrombosis.[3] The authors observed that residual disease at the edge of the stent was associated with subsequent stent thrombosis. Of note, a higher residual plaque burden proximal from the stent has also been associated with increased rates of in-stent restenosis.[4] Accordingly, optimal assessment of the lesion length may improve success and outcome of interventional procedures.[28]

Limitations

Several limitations need to be addressed. First, there was a time-interval between CTA and PCI during which atherosclerosis may have progressed. Second, only lesions subsequently treated by PCI were included in the study. Therefore, the current observations are only based on lesions with a high grade stenosis. Third, in the current study QCA was not part of the clinical routine of the laboratory and the difference between the CTA lesion length and the stent length chosen reflects the discrepancy between stent length driven by visual

assessment. Furthermore, the attending interventional cardiologist did not incorporate lesion topography on CTA before performing PCI. However, future studies should be performed to evaluate the value and improved outcome of CTA lesion assessment prior to PCI.

Conclusion

Lesion length assessed by CTA is longer than lesion length assessed by ICA, which may facilitate improved guidance of percutaneous treatment of coronary lesions.

REFERENCES

1. Mintz GS, Painter JA, Pichard AD et al. Atherosclerosis in angiographically "normal" coronary artery reference segments: an intravascular ultrasound study with clinical correlations. J Am Coll Cardiol 1995;25:1479-85.
2. Fujii K, Carlier SG, Mintz GS et al. Stent underexpansion and residual reference segment stenosis are related to stent thrombosis after sirolimus-eluting stent implantation: an intravascular ultrasound study. J Am Coll Cardiol 2005;45:995-8.
3. Okabe T, Mintz GS, Buch AN et al. Intravascular ultrasound parameters associated with stent thrombosis after drug-eluting stent deployment. Am J Cardiol 2007;100:615-20.
4. Liu XB, Qian JY, Zhang F et al. Intravascular ultrasound assessment of sirolimus-eluting stent restenosis or thrombosis after stent implantation. Zhonghua Xin Xue Guan Bing Za Zhi 2009;37: 397-401.
5. Yamagishi M, Hosokawa H, Saito S et al. Coronary disease morphology and distribution determined by quantitative angiography and intravascular ultrasound--re-evaluation in a cooperative multicenter intravascular ultrasound study (COMIUS). Circ J 2002;66:735-40.
6. Porter TR, Sears T, Xie F et al. Intravascular ultrasound study of angiographically mildly diseased coronary arteries. J Am Coll Cardiol 1993;22:1858-65.
7. Meijboom WB, van Mieghem CA, Mollet NR et al. 64-slice computed tomography coronary angiography in patients with high, intermediate, or low pretest probability of significant coronary artery disease. J Am Coll Cardiol 2007;50:1469-75.
8. Meijboom WB, Meijs MF, Schuijf JD et al. Diagnostic accuracy of 64-slice computed tomography coronary angiography: a prospective, multicenter, multivendor study. J Am Coll Cardiol 2008;52: 2135-44.
9. Achenbach S, Moselewski F, Ropers D et al. Detection of calcified and noncalcified coronary atherosclerotic plaque by contrast-enhanced, submillimeter multidetector spiral computed tomography: a segment-based comparison with intravascular ultrasound. Circulation 2004;109: 14-7.
10. Kass M, Glover CA, Labinaz M et al. Lesion characteristics and coronary stent selection with computed tomographic coronary angiography: a pilot investigation comparing CTA, QCA and IVUS. J Invasive Cardiol 2010;22:328-34.
11. Leber AW, Knez A, Becker A et al. Accuracy of multidetector spiral computed tomography in identifying and differentiating the composition of coronary atherosclerotic plaques: a comparative study with intracoronary ultrasound. J Am Coll Cardiol 2004;43:1241-7.
12. Hausleiter J, Meyer T, Hermann F et al. Estimated radiation dose associated with cardiac CT angiography. JAMA 2009;301:500-7.
13. Soon KH, Farouque HM, Chaitowitz I et al. Discrepancy between computed tomography coronary angiography and selective coronary angiography in the pre-stenting assessment of coronary lesion length. Australas Radiol 2007;51:440-5.
14. Bigi R, Cortigiani L, Colombo P et al. Prognostic and clinical correlates of angiographically diffuse non-obstructive coronary lesions. Heart 2003;89:1009-13.
15. Califf RM, Phillips HR, III, Hindman MC et al. Prognostic value of a coronary artery jeopardy score. J Am Coll Cardiol 1985;5:1055-63.
16. Cashin-Hemphill L, Mack WJ, Pogoda JM et al. Beneficial effects of colestipol-niacin on coronary atherosclerosis. A 4-year follow-up. JAMA 1990;264:3013-7.
17. Schuler G, Hambrecht R, Schlierf G et al. Regular physical exercise and low-fat diet. Effects on progression of coronary artery disease. Circulation 1992;86:1-11.

18. Butler J, Shapiro M, Reiber J et al. Extent and distribution of coronary artery disease: a comparative study of invasive versus noninvasive angiography with computed angiography. Am Heart J 2007;153:378-84.

19. Becker CR, Nikolaou K, Muders M et al. Ex vivo coronary atherosclerotic plaque characterization with multi-detector-row CT. Eur Radiol 2003;13:2094-8.

20. Petranovic M, Soni A, Bezzera H et al. Assessment of nonstenotic coronary lesions by 64-slice multidetector computed tomography in comparison to intravascular ultrasound: evaluation of nonculprit coronary lesions. J Cardiovasc Comput Tomogr 2009;3:24-31.

21. Schepis T, Marwan M, Pflederer T et al. Quantification of noncalcified coronary atherosclerotic plaques with Dual Source Computed Tomography: comparison to intravascular ultrasound. Heart 2009.

22. Nikolaou K, Becker CR, Muders M et al. Multidetector-row computed tomography and magnetic resonance imaging of atherosclerotic lesions in human ex vivo coronary arteries. Atherosclerosis 2004;174:243-52.

23. Schroeder S, Kuettner A, Wojak T et al. Non-invasive evaluation of atherosclerosis with contrast enhanced 16 slice spiral computed tomography: results of ex vivo investigations. Heart 2004; 90:1471-5.

24. Schroeder S, Kuettner A, Leitritz M et al. Reliability of differentiating human oronary plaque morphology using contrast-enhanced multislice spiral computed tomography: a comparison with histology. J Comput Assist Tomogr 2004;28:449-54.

25. Mintz GS, Pichard AD, Kent KM et al. Interrelation of coronary angiographic reference lumen size and intravascular ultrasound target lesion calcium. Am J Cardiol 1998;81:387-91.

26. Virmani R, Burke AP, Kolodgie FD et al. Pathology of the thin-cap fibroatheroma: a type of vulnerable plaque. J Intervent Cardiol 2003;16:267-72.

27. Virmani R, Kolodgie FD, Burke AP et al. Lessons from sudden coronary death: a comprehensive morphological classification scheme for atherosclerotic lesions. Arterioscler Thromb Vasc Biol 2000;20:1262-75.

28. Hecht HS. Applications of multislice coronary computed tomographic angiography to percutaneous coronary intervention: how did we ever do without it? Catheter Cardiovasc Interv 2008; 71:490-503.

CHAPTER 7

Comprehensive Assessment
of Spotty Calcifications
on Computed Tomography
Angiography: Comparison to Plaque
Characteristics on Intravascular
Ultrasound with Radiofrequency
Backscatter Analysis

Joëlla E. van Velzen, Fleur R. de Graaf, Michiel A. de Graaf, Joanne D. Schuijf, Lucia J. Kroft, Albert de Roos, Johan H.C. Reiber, Jeroen J. Bax, J. Wouter Jukema, Eric Boersma, Martin J. Schalij, Ernst E. van der Wall

ABSTRACT

Background: The purpose of the study was to systematically compare calcification patterns in plaques on computed tomography angiography (CTA) with plaque characteristics on intravascular ultrasound with radiofrequency backscatter analysis (IVUS-VH).

Methods: In total, 108 patients underwent CTA and IVUS-VH. On CTA, calcification patterns in plaques were classified as non-calcified, spotty or dense calcifications. Plaques with spotty calcifications were differentiated into small spotty (< 1 mm), intermediate spotty (1 - 3 mm) and large spotty calcifications (≥ 3 mm). Plaque characteristics deemed more high-risk on IVUS-VH were defined by % necrotic core (NC) and presence of thin cap fibroatheroma (TCFA).

Results: Overall, 300 plaques were identified both on CTA and IVUS-VH. % NC was significantly higher in plaques with small spotty calcifications as compared to non-calcified plaques (20% vs. 13%, p=0.006). In addition, there was a trend for a higher % NC in plaques with small spotty calcifications than in plaques with intermediate spotty calcifications (20% vs. 14%, p=0.053). Plaques with small spotty calcifications had the highest % TCFA as compared to large spotty and dense calcifications (31% vs. 9% and 31% vs. 6%, p<0.05).

Conclusion: Plaques with small spotty calcifications on CTA were related to plaque characteristics deemed more high-risk on IVUS-VH. Therefore, CTA may be valuable in the assessment of the vulnerable plaque.

INTRODUCTION

Computed tomography angiography (CTA) is a rapidly evolving technique that has the ability to non-invasively and accurately detect significant coronary artery stenosis and coronary atherosclerotic plaque.[1-5] A potentially interesting application of CTA would be the identification of patients or lesions that have an increased likelihood of plaque rupture leading to acute coronary events. Several previous studies have identified specific plaque characteristics which are frequently observed with CTA in patients presenting with acute coronary syndrome (ACS).[6-8] Among these characteristics, a spotty pattern of calcifications has been related to the presence of ACS.[6-8] Indeed, preliminary data with CTA demonstrated that culprit lesions in patients with ACS had a higher prevalence of smaller spotty calcifications than target lesions in patient with stable complaints.[9] Moreover, the presence of spotty calcifications on CTA were associated with a higher likelihood of developing ACS.[8]

More detailed information on plaque characteristics can be obtained by intravascular ultrasound with radiofrequency backscatter analysis (IVUS-VH).[10 11] This technique was developed to improve grayscale intravascular ultrasound tissue characterization and provide detailed quantitative information on plaque composition in vivo.[12 13] Additionally, the presence of thin cap fibroatheroma (TCFA) on IVUS-VH was demonstrated to be independently predictive of major cardiovascular events during follow-up.[14]

However, the relation between calcification patterns on CTA and plaque characteristics on IVUS-VH has not been previously reported. Furthermore, in previous studies, the definition of spotty calcification on CTA has been variable. Indeed, definitions for spotty calcification on CTA have ranged from presence of any calcified material embedded in non-calcified plaque to a specific threshold regarding the size of calcification. Subsequently, due to the inconsistency of definitions, comparability of spotty calcifications on CTA between investigations is hampered. Therefore, the purpose of the study was to perform a systematic evaluation of plaques with different calcification patterns on CTA and relate this to plaque characteristics on IVUS-VH.

METHODS

Patient population and study protocol

A total of 108 patients were included in this evaluation who underwent CTA prior to invasive coronary angiography with IVUS-VH of 1 to 3 vessels, as part of clinical protocol. For this retrospective evaluation, consecutive patients were selected as part of an ongoing registry addressing the relative merits of CTA in relation to other imaging techniques.[15] Patient with chest pain were referred for imaging for the non-invasive evaluation of coronary artery disease (CAD), according to clinical protocol. Thereafter, patients were referred for invasive coronary angiography in combination with IVUS-VH based on the patient's clinical presentation and/or imaging results to further evaluate the extent and severity

of CAD. During invasive coronary angiography, an experienced interventional cardiologist decided whether IVUS studies should be performed. Clinical history was evaluated between the CTA examination and invasive coronary angiography to ensure that neither acute coronary syndromes nor worsening of angina occurred between examinations. Exclusion criteria for CTA examination were: (i) (supra) ventricular arrhythmias, (ii) renal failure (glomerular filtration rate < 30 mL/min), (iii) known allergy to iodine contrast material, (iv) severe claustrophobia, (v) pregnancy. Patient data were prospectively collected in the departmental Cardiology Information System (EPD-Vision©, Leiden University Medical Center, Leiden, the Netherlands) and retrospectively analyzed. Our institutional review board does not require its approval and written informed consent for retrospective technical analysis of data, as was the case for this study. In each patient, the presence of risk factors for CAD and medication (use of aspirin, statins, beta-blocking medication and angiotensin-converting enzyme (ACE) inhibitors) were recorded.

CTA

Image acquisition

CTA examination was performed using either a 64-row helical scanner (Aquilion 64, Toshiba Medical Systems, Toshiba Medical Systems, Otawara, Japan) or a 320-row volumetric scanner (Aquilion ONE, Toshiba Medical Systems, Otawara, Japan). If the patient's heart rate was ≥ 65 beats/minute and no contra-indications existed, beta-blocking medication (metoprolol 50 or 100 mg, single oral dose, 1 hour prior to examination) was administered. Scan parameters for the 64-row contrast enhanced scan were: 400 ms gantry rotation time, collimation of 64 x 0.5 mm, tube voltage of 100 - 135 kV and tube current of 250 - 350 mA, depending on body posture. Non-ionic contrast material (Iomeron 400, Bracco, Milan, Italy or Ultravist 370, Bayer Schering Pharma AG Berlin, Germany) was administered with an amount of 80 - 110 ml followed by a saline flush with a flow rate of 5 ml/s. Datasets were reconstructed from the retrospectively gated raw data, the best phase was reconstructed with an interval of 0.3 mm. Using a single test slice reconstructed throughout the various phases of the heart cycle, other suitable R - R intervals were examined for additional reconstructions. Concerning the 320-row contrast enhanced scan; imaging was performed in a single volume using prospective triggering with exposure interval depending on the heart rate. If the heart rate was ≥ 60 beats/min, the phase window was set 65 - 85% of R - R interval, if the heart rate was stable and < 60 beats/min the phase window was set at 70 - 80% of R - R interval. Scan parameters were: 350 ms gantry rotation time, 320 x 0.5 mm collimation, 100 - 135 kV tube voltage and a tube current of 400 - 580 mA, depending on body mass index (BMI). Overall, 60 - 90 ml contrast material (Iomeron 400, Bracco, Milan, Italy) was administered with a rate of 5 - 6 ml/s followed by a saline flush. Data acquisition was performed during an inspiratory breath hold of approximately 4 - 10 seconds. Subsequently, images were reconstructed in the best phase of the R - R interval and transferred to a remote workstation for post-processing.

Image analysis

CTA datasets were evaluated using dedicated software (Vitrea 2.0 or Vitrea FX 1.1 Vital images, Minnetonka, MN, USA). Analysis was performed with the use of available post-processing tools such as cross-sectional axial slices and multiplanar reconstructions. One experienced reader, blinded to the IVUS-VH results, evaluated the CTA datasets. The coronary arteries were divided into 17 segments according to the modified American Heart Association classification.[16] Each segment was evaluated for the presence of any atherosclerotic plaque. Structures > 1 mm² within and/or adjacent to the coronary artery lumen, which could be clearly distinguished from the vessel lumen, were defined as atherosclerotic plaque.[3]

Calcification patterns in plaques on CTA were classified morphologically as non-calcified, spotty calcifications or dense calcifications. Non-calcified plaques were defined as a plaque with low CT attenuation located in the vessel wall in at least 2 independent image planes and clearly distinguishable from the contrast-enhanced lumen and pericardial tissue without any calcification.[17] Plaques with spotty calcifications were defined as follows: length (extent in the longitudinal direction of the vessel) of the calcification < 3/2 of vessel diameter and width (extent of the calcification perpendicular to the longitudinal direction of the vessel) of the calcification < 2/3 of vessel diameter, as previously described (Figure 1).[17] Plaques with spotty calcification were further differentiated according to their length (extent of the calcification parallel to the longitudinal direction of the vessel on curved multiplanar reconstruction) into small spotty (< 1 mm), intermediate spotty (1 - 3 mm) and large spotty calcifications (≥ 3 mm) as measured with caliper function (for illustration see Figure 2).[18] Dense calcifications were defined as a plaque with high CT density, completely calcified and with calcifications present bilateral on cross-sectional axial slices.
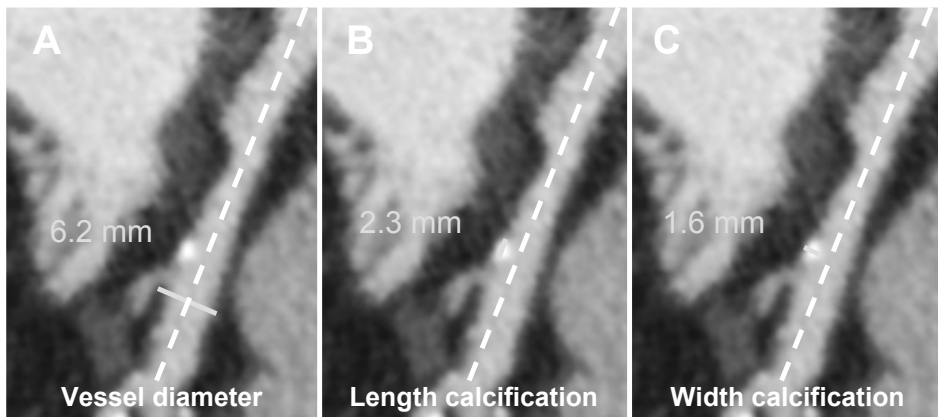
Figure 1. Example of measurement of spotty calcification. Plaques with spotty calcifications were defined as follows: length (extent in the longitudinal direction of the vessel) of the calcification < 3/2 of vessel diameter and width (extent of the calcification perpendicular to the longitudinal direction of the vessel) of the calcification < 2/3 of vessel diameter. (A) Measurement of vessel diameter (blue line) perpendicular to long vessel axis (dashed white line). (B) Measurement of length of calcification (blue line) parallel to long vessel axis (dashed white line). (C) Measurement of width of calcification (blue line) perpendicular to long vessel axis (dashed line).
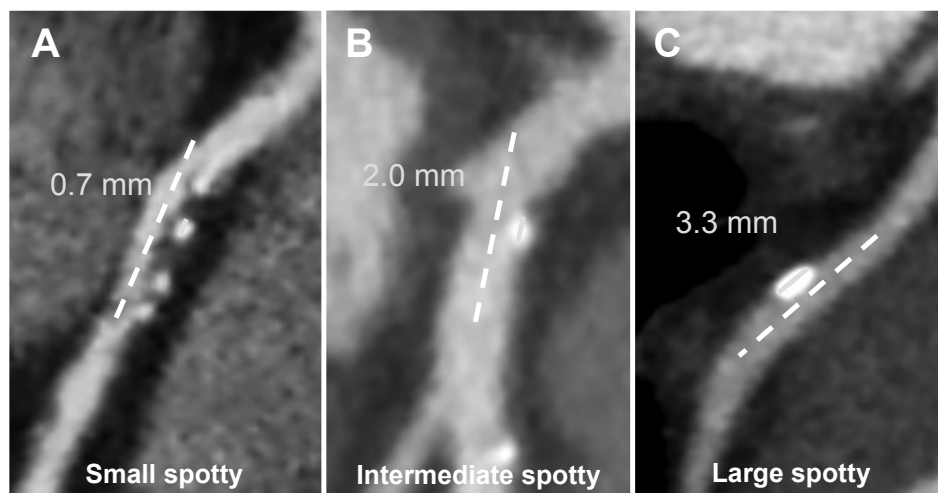
Figure 2. Illustration of the different types of spotty calcification. (A) Small spotty calcification (< 1 mm). (B) Intermediate spotty calcification (1-3 mm). (C) Large spotty calcification (> 3 mm)

Invasive IVUS-VH

Image acquisition

Conventional invasive coronary angiography was performed according to standard protocols. IVUS examinations were acquired with a 20 MHz, 2.9 F phased-array IVUS catheter, (Eagle Eye, Volcano Corporation, Rancho Cordova, CA, USA) and a dedicated IVUS-console (Volcano Corporation, Rancho Cordova, CA, USA) after intracoronary administration of nitroglycerine. Under fluoroscopic guidance, the IVUS catheter was introduced distally in the coronary artery and a motorized automated pullback with a continuous speed of 0.5 mm/s was used until the catheter reached the guiding catheter. Images were stored on CD-ROM or DVD for off-line analysis.

Image analysis

IVUS-VH analysis was performed by two experienced observers blinded to baseline patient characteristics and CTA findings with the use of dedicated software (QCU-CMS, version 4.59, Medis Medical Imaging Systems, Leiden, The Netherlands). First, contour detection (lumen and media interface) was performed manually with the use of cross-sectional views to provide compositional output.[19] Secondly, on a frame-by-frame basis, the four different tissue components were differentiated and labeled with four different color-codes (fibrotic tissue was labeled in dark green, fibro-fatty tissue in light green, necrotic core in red and dense calcium in white), as validated previously.[10] The mean percentage of each plaque component was obtained in the full length of the lesion observed on the CTA examination. A lesion on intravascular ultrasound imaging was defined as at least three consecutive frames with a plaque burden of at least 40%.[20] In addition, the presence of the thin cap fibroatheroma (TCFA) was evaluated on a per-lesion basis. TCFA
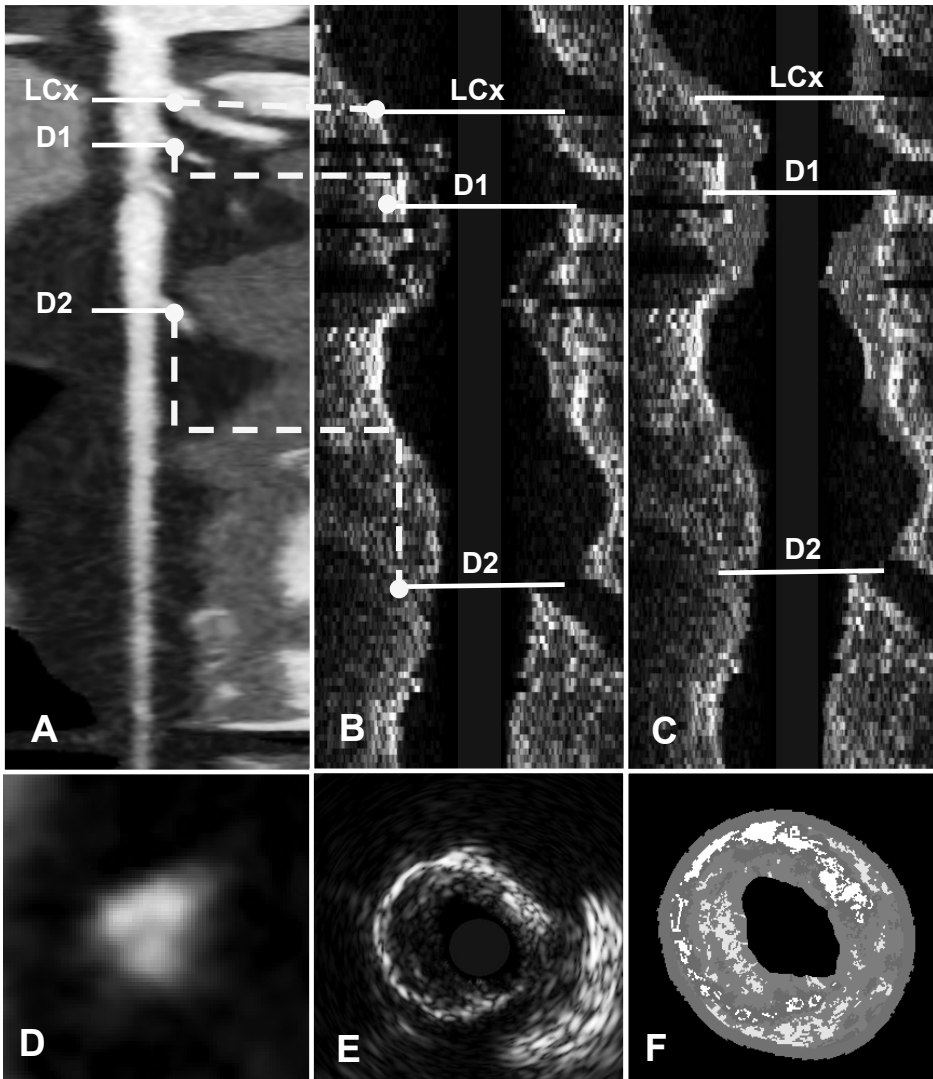
Figure 3. Example of anatomical matching of computed tomography angiography (CTA) with intravascular ultrasound with radiofrequency backscatter analysis (IVUS-VH) datasets. (A) Straightened multiplanar reconstruction of left anterior descending coronary artery in which various landmarks have been identified (left circumflex artery (LCx), first and second diagonal branch (D1 and D2). (B, C) Corresponding grayscale intravascular ultrasound and IVUS-VH datasets in longitudinal view in which identical landmarks have been matched to CTA dataset (yellow dashed line). Corresponding cross-sectional view of minimal lumen area on CTA (D) and IVUS-VH (E,F).

was defined as a lesion with a plaque burden ≥ 40%, presence of >10% confluent necrotic core on three consecutive frames and necrotic core in contact with the lumen for along the lumen circumference.[14 21 22] High-risk plaque characteristics on IVUS-VH were defined by % of necrotic core and presence of TCFA.

To ensure that identical plaques were assessed by CTA and IVUS-VH, coronary ostia and side branches were used as landmarks and distances from the landmarks to the target lesions were measured (Figure 3). On CTA, distances were measured using multiplanar reconstructions. On IVUS-VH, longitudinal reconstructed ECG triggered datasets were used to measure the difference between corresponding plaque and landmarks. After
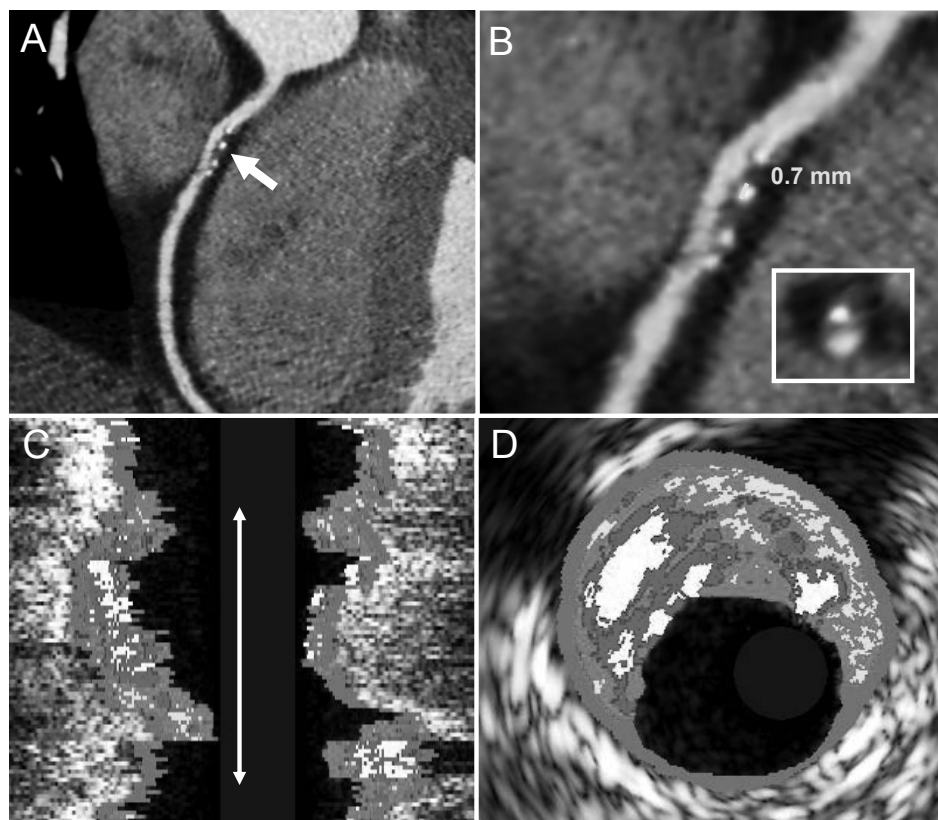
Figure 4. Example of small spotty calcifications as assessed on computed tomography angiography (CTA) with high-risk plaque characteristics on intravascular ultrasound with radiofrequency backscatter analysis (IVUS-VH). (A) Multiplanar reconstruction of the right coronary artery (RCA) demonstrating a plaque with non-calcified elements and spotty calcifications (arrow). (B) Enlargement of the same plaque demonstrating a spotty calcification with a length of 0.7 mm. (C) Longitudinal reconstructed ECG triggered IVUS-VH run with superimposed color coded map. The plaque (white arrow) corresponds to the same plaque on CTA demonstrating a large necrotic core and multiple small spotty calcifications. (D) Cross-sectional axial image of the same plaque demonstrating calcifications (white) and a large necrotic core (red) indicating presence of a thin cap fibroatheroma (TCFA).
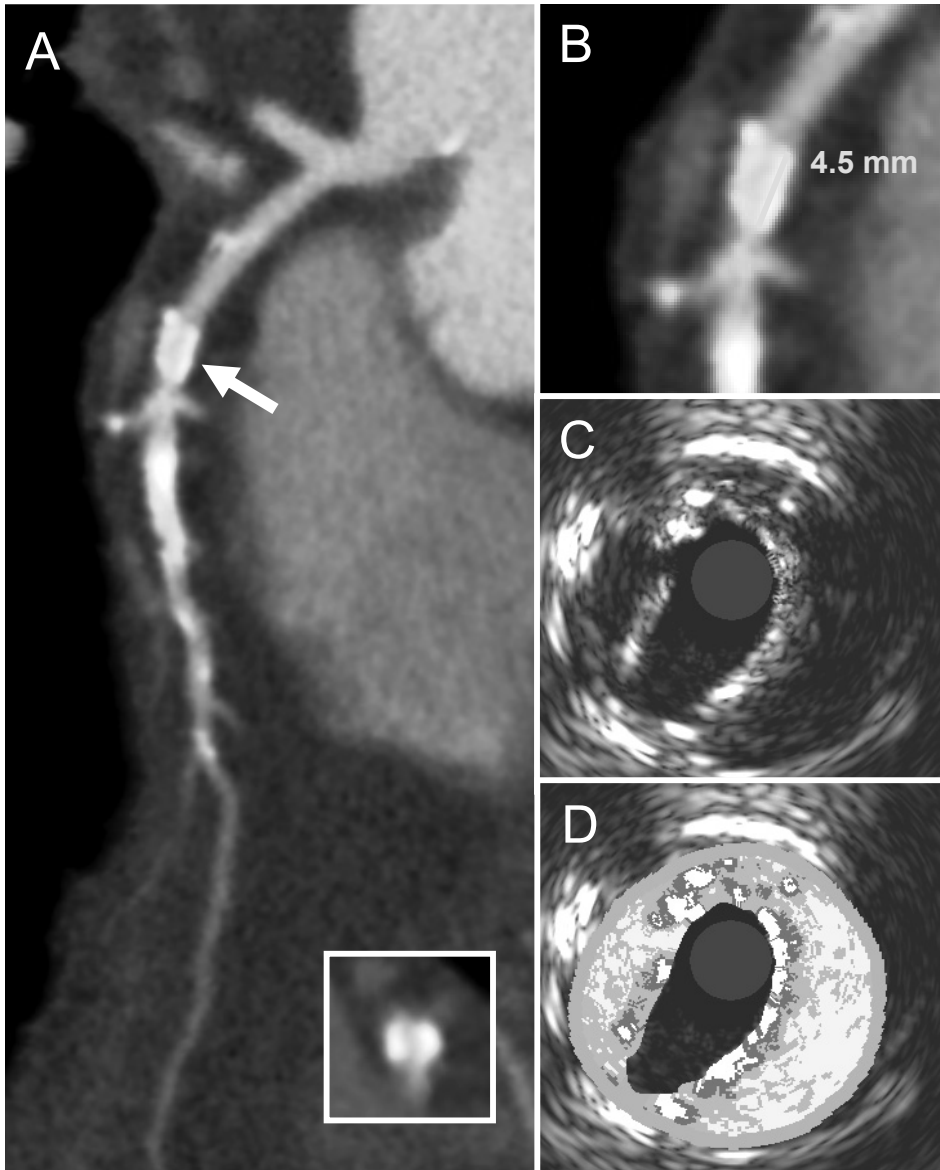
Figure 5. Example of a plaque with dense calcifications on computed tomography angiography (CTA) with corresponding grayscale and intravascular ultrasound with radiofrequency backscatter analysis (IVUS-VH) images. (A) Curved multiplanar reconstruction of the right coronary artery (RCA) demonstrating a plaque with dense calcifications (arrow). Inlay showing cross-sectional axial image of the same plaque with calcifications present bilateral of the coronary artery. (B) Enlargement of the same plaque reporting the length of the calcification (4.5 mm). (C) Grayscale IVUS image demonstrating a heavily calcified plaque with corresponding IVUS-VH image (D) showing a plaque with heavy calcifications (white).

alignment of plaques on CTA and IVUS-VH, we identified matching slices between the 2 modalities and could determine the proximal and distal end of a lesion. Examples of different calcification patterns on CTA with corresponding IVUS-VH images are demonstrated in Figure 4 and 5.

Statistical analysis

Plaques available on both CTA and IVUS-VH were included in the lesion based analysis. Plaque composition (% fibrotic, fibro-fatty, necrotic core and dense calcium) and presence of TCFA was compared between lesions with different calcification patterns on CTA (non-calcified, small spotty calcifications, intermediate spotty calcifications, large spotty calcifications and dense calcifications). If normally distributed, continuous values were expressed as means (± standard deviation) and differences in plaque composition and type were assessed using an analysis of variance (ANOVA). If not normally distributed, values were expressed as medians (interquartile range (IQR)) and differences in plaque composition and type were assessed using the Kruskall-Wallis test. To account for possible clustering of coronary artery plaques within patients, the generalized estimating equation (GEE) method was applied to evaluate the differences in plaque characteristics between the groups of different calcification patterns on CTA (non-calcified, small spotty calcifications, intermediate spotty calcifications, large spotty calcifications and dense calcium). This was performed with proc GENMOD with a binominal distribution for the outcome variable, the link function specified as a logistical (presence of TCFA) or a linear (% fibrotic, fibro-fatty, necrotic core and dense calcium) distribution and patients as separate subjects. Due to lack of power, we did not perform post-hoc analysis. A p-value of < 0.05 was considered statistically significant. Statistical analysis was performed using SPSS 17.0 software (SPSS Inc., Chicago. Illinois).

RESULTS

Out of a total of 108 patients, 33 patients (31%) were scanned with a 64-row CTA scanner and 75 patients (69%) with a 320-row CTA scanner. Baseline patient characteristics are provided in Table 1. In summary, 80 patients (74%) were male and mean age was 57 ± 10 years. IVUS-VH examination was successfully performed in 264 vessels (81%) of the available 324 vessels without complications (right coronary artery (RCA), n=88; left anterior descending coronary artery (LAD), n=98; left circumflex coronary artery (LCx), n=78). In the remaining vessels, IVUS imaging could not be performed due to severe vessel tortuousity, severe stenosis, vessel occlusion or due to time-constraints in the cathlab

Baseline CTA and IVUS-VH results

In total, 799 plaques were demonstrated on CTA and in 300 plaques (38%) IVUS-VH was also available. Of the 300 plaques identified on CTA, 78 plaques (26%) were non-calcified, 39 plaques (13%) had small spotty calcifications (< 1 mm), 96 plaques (32%)

Table 1. Baseline patient characteristics

Number of patients	108
Age (years)	57 ± 10
Male gender	80 (74%)
Stable angina/Suspected acute coronary syndrome	38 / 70
Hypertension†	63 (58%)
Hypercholesterolemia‡	55 (51%)
Diabetes	29 (27%)
Smoking	43 (40%)
Family history of CAD	49 (45%)
Obesity (≥ 30 kg/m^2)	21 (19%)
Medication at time of referral	
Aspirin	61 (57%)
Statins	69 (64%)
ACE inhibitor	53 (49%)
Beta-blockers	58 (54%)
Previous myocardial infarction	22 (20%)
Previous PCI	29 (27%)

Data are absolute values, percentages or means ± standard deviation.
†Defined as systolic blood pressure ≥140 mm Hg or diastolic blood pressure ≥ 90 mm Hg or the use of antihypertensive medication.
‡Serum total cholesterol ≥ 230 mg/dL or serum triglycerides ≥ 200 mg/dL or treatment with lipid lowering drugs.
Abbreviations: CAD, coronary artery disease; ACE, angiotensin converting enzyme; PCI, percutaneous coronary intervention

had intermediate spotty calcifications (1 - 3 mm), 54 plaques (18%) had large spotty calcifications (≥ 3 mm) and 33 plaques (11%) had dense calcifications. On IVUS-VH, the average plaque length analyzed was 26 ± 18 mm. The most prevalent plaque component was fibrotic tissue (58%, IQR 50 - 63%), followed by necrotic core (15%, IQR 10 - 21%), fibro-fatty tissue (13%, IQR 8 - 21%), and dense calcium (6%, IQR 3 - 10%). Visual plaque assessment revealed that 52 plaques (17%) were classified as TCFA.

Comparison of calcification patterns on CTA and plaque composition on IVUS-VH

The results comparing calcification patterns on CTA against relative plaque composition on IVUS-VH are reported in Table 2. Small spotty calcifications contained less fibro-fatty tissue (9%, IQR 6 - 15%) as compared to non-calcified plaques (12%, IQR 8 - 22%), intermediate spotty calcifications (13%, IQR 7 - 21%), large spotty calcifications (15%, IQR 9 - 25%) and dense calcifications (20%, IQR 13 - 25%, p<0.05). In line with this observation, the more calcified plaques contained significantly more dense calcium on IVUS-VH than the non-calcified plaques (9%, IQR 6 - 11% versus 3%, IQR 1 - 6%, p<

Table 2. Plaque composition on intravascular ultrasound with radiofrequency backscatter analysis (IVUS-VH) is reported in relation to the different calcification patterns on computed tomography angiography (CTA).

	Non-calcified	Small spotty (< 1 mm)	Intermediate spotty (1 - 3 mm)	Large spotty (≥ 3 mm)	Dense calcifications	Global p-value
% Fibrotic	61 (55 - 68)	56 (50 - 63)	58 (50 - 64)	54 (49 - 59)	54 (49 - 59)	< 0.001
% Fibro-fatty	12 (8 - 22)*	9 (6 - 15)	13 (7 - 21)*	15 (9 - 25)*	20 (13 - 25)*	< 0.001
% Necrotic Core	13 (6 - 20)*	20 (12 - 24)	14 (9 - 21)**	17 (13 - 21)	14 (12 - 22)	0.003
% Dense calcium	3 (1 - 6)*	7 (4 - 13)	6 (3 - 10)	9 (6 - 13)	9 (6 - 11)	< 0.001

Data in parentheses are percentages with 95% confidence intervals.

* p-value < 0.05, individual groups compared to plaques with small spotty calcifications as reference group

** p-value=0.053, individual group compared to plaques with small spotty calcifications as reference group

0.001). More importantly, necrotic core was significantly higher in plaques with small spotty calcifications (20%, IQR 12 - 24%) as compared to non-calcified plaques (13%, IQR 6 - 20%, p=0.006). In addition, there was a trend for a higher percentage of necrotic core in plaques with small spotty calcifications than in plaques with intermediate spotty calcifications (p=0.053). Moreover, as demonstrated in Figure 6, plaques with small spotty calcifications were demonstrated to have a high percentage of TCFA (31%) as compared to large spotty calcifications (9%) and dense calcifications (6%, p<0.05). In addition, there was a trend for plaques with small spotty calcifications to have a higher percentage of TCFA than plaques with intermediate spotty calcifications (17%, p=0.073). However, no significant difference was demonstrated between the percentage of TCFA in plaques with small spotty calcifications and non-calcified plaques (p=0.37).
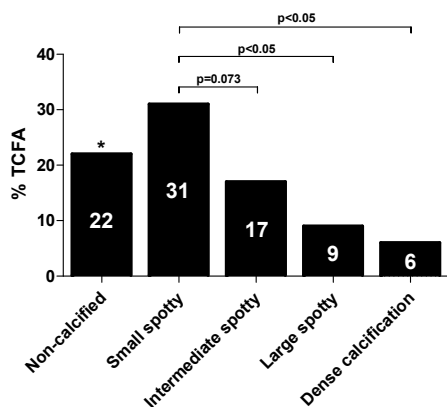
Figure 6. Bar graph represents the percentage of thin cap fibroatheroma (TCFA) in relation to the different calcification patterns on computed tomography angiography (CTA). As is shown, in particular plaques with small spotty calcifications on CTA contain the highest percentage of TCFA as compared to large spotty calcifications and dense calcium. (*) Small spotty calcifications did not have more TCFA than non-calcified plaques (p=ns).

DISCUSSION

The present study systematically evaluated the relation between different calcification patterns on CTA and plaque characteristics on invasive IVUS-VH. It was demonstrated that plaques with spotty calcifications, in particular the smaller spotty calcifications (< 1 mm) had plaque characteristics deemed high-risk on IVUS-VH, as defined by a higher % of necrotic core and presence of TCFA.

Interestingly, the present findings are in line with histopathological studies which have reported that lesions associated with acute coronary events are often not heavily calcified.[20][21][23] Burke et al studied the degree of calcification in serial sections of coronary arteries in sudden coronary death cases and observed that plaque ruptures showed relatively little calcification and that most acute plaque ruptures resulting in sudden death occurred in areas of only mild speckled calcification.[21] Furthermore, smaller calcium deposits on grayscale IVUS have been related to more unstable clinical presentation such as unstable angina and myocardial infarction. Beckman et al measured the arc of calcium in lesions of 78 patients and found that the average arc of calcium was greatest (32 ± 7°) in patients with stable angina, less (15 ± 4°) in patients with unstable angina, and least (10 ± 5°) in patients with acute myocardial infarction (p< 0.014).[24] In line with these findings, van der Hoeven et al studied 60 patients with acute myocardial infarction on grayscale IVUS and demonstrated that small calcified spots (arc < 45°, length < 1.5 mm) were more common in the culprit lesions as compared to the adjacent distal and proximal segments.[18] Accordingly, Ehara et al confirmed the findings in a larger patient population of 178 patients with grayscale IVUS.[25] The authors found that not only the frequency of calcium deposits was significantly different between patients with stable, unstable angina and myocardial infarction but also calcium deposits were significantly longer in patients with stable angina (mean length of 4.3 ± 3.2 mm) as compared to patients with unstable angina (mean length of 1.9 ± 1.8) and myocardial infarction (mean length of 2.2 ± 1.6). Thus, these findings support the concept that there may be a significant difference in the pattern of coronary calcifications, particularly with respect to size and length of the deposits, among patients with stable and unstable angina.

Non-invasively, calcium scoring with electron beam computed tomography (EBCT) showed similar findings. Although a higher calcium score has been related to larger plaque areas and worse prognosis[26], when comparing coronary calcium scores of patients with stable angina to patients with acute myocardial infarction, significant differences were observed.[27] Extensive calcium was more often present in the coronary arteries of patients with chronic stable angina, whereas patients with acute myocardial infarction demonstrated a more diffuse pattern of calcifications. More interestingly, using contrast-enhanced CTA, the presence of spotty calcifications were frequently present in lesions of patients with ACS but rarely observed in culprit lesions of patients with stable CAD.[9] Similarly, Motoyama et al demonstrated both retrospectively and prospectively with CTA that non-calcified plaques with spotty calcifications and positive remodelling were associated with a higher likelihood of the development of ACS.[7][8] However, unlike the present study,

the aforementioned findings were not related to invasive observations. Interestingly, a previous study by our institution evaluated the association between plaque composition on CTA and the presence of high-risk features on IVUS-VH in a smaller population of 50 patients.[28] It was demonstrated that the more high-risk plaques (TCFA) were most often present in mixed plaques (32%) on CTA. Although similar to the current findings, the % of TCFA in mixed plaques was higher in the previous evaluation than in the current study. This could probably be explained by difference in the size and baseline characteristics of the patient population. In addition, the amount of dense calcium in the current study is somewhat lower than reported in other studies. However, this could be explained by the inclusion of a substantial number (65%) of patients presenting with acute coronary syndrome, known to have substantially less calcified arteries.

Interestingly, earlier investigations have used various definitions of spotty calcifications on CTA. For instance, some investigations described spotty calcification as any calcified material embedded within a non-calcified plaque, whereas other use a threshold of calcified material less than 3 mm in size.[7 9 29] However, a comprehensive approach for the evaluation of the extent of the spotty calcifications on CTA is preferred, thereby improving reproducibility and use in risk stratification. The strength of the current study is that a systematic approach for the evaluation of spotty calcifications was applied, demonstrating that indeed the smaller spotty calcifications were related to the plaque characteristics deemed more high-risk such as necrotic core and presence of TCFA.

Importantly, the findings are clinically relevant considering that CTA is increasingly used for the assessment of CAD and the use of this technique is extended from assessment of stenosis to the evaluation of the vessel wall. Nevertheless, even with the latest generation CTA scanners, exact identification of the lipid core and thin fibrous cap is not feasible at the moment. Therefore, assessment of spotty calcification on CTA may be beneficial for individualized risk stratification in combination with other high-risk features such as cardiovascular risk factors and biomarkers. Perhaps, CTA has a potential application in the context of identifying the "vulnerable" patient at risk for ACS. However, the clinical and prognostic impact of these findings has to be evaluated in future prospective studies.

Limitations

First, due to the limitations of intravascular ultrasound, not all plaques on CTA were also evaluated by IVUS-VH. In addition, detection of the thin fibrous cap (< 65 μm) is not yet feasible as IVUS-VH has a limited radial resolution of only 100 μm. Furthermore, it has been suggested that dense calcium on IVUS-VH is related to artifacts in the form of a halo of necrotic core surrounding dense calcium. However, no standardized method for correcting for this issue is currently available. Additionally, no other high risk plaque characteristics were assessed on CTA. Potentially, incorporating other CTA variables such as degree of stenosis and overall plaque burden, may allow for better risk stratification. In addition, this study performed a retrospective analysis of data possibly introducing a bias with regards to lesion selection. Future evaluations examining on the relationship between calcification patterns on CTA and IVUS-VH characteristics should be performed

in a more prospective manner. Moreover, reproducibility information on the measurement of calcification on CTA was not provided. Lastly, CTA is inherently associated with radiation exposure. However, recently, dose-saving algorithms and prospective ECG triggering were introduced to substantially reduce radiation dose.[30]

Conclusion

The current study demonstrated that plaques with small spotty calcifications on CTA were related to plaque characteristics deemed more high-risk on invasive IVUS-VH. Therefore, CTA may be valuable in the assessment of the vulnerable plaque.

REFERENCES

1. Achenbach S, Giesler T, Ropers D et al. Detection of coronary artery stenoses by contrast-enhanced, retrospectively electrocardiographically-gated, multislice spiral computed tomography. Circulation 2001;103:2535-8.

2. Budoff MJ, Dowe D, Jollis JG et al. Diagnostic performance of 64-multidetector row coronary computed tomographic angiography for evaluation of coronary artery stenosis in individuals without known coronary artery disease: results from the prospective multicenter ACCURACY (Assessment by Coronary Computed Tomographic Angiography of Individuals Undergoing Invasive Coronary Angiography) trial. J Am Coll Cardiol 2008;52:1724-32.

3. Leber AW, Knez A, Becker A et al. Accuracy of multidetector spiral computed tomography in identifying and differentiating the composition of coronary atherosclerotic plaques: a comparative study with intracoronary ultrasound. J Am Coll Cardiol 2004;43:1241-7.

4. Miller JM, Rochitte CE, Dewey M et al. Diagnostic performance of coronary angiography by 64-row CT. N Engl J Med 2008;359:2324-36.

5. Van Velzen JE, Schuijf JD, De Graaf FR et al. Diagnostic performance of non-invasive multidetector computed tomography coronary angiography to detect coronary artery disease using different endpoints: detection of significant stenosis vs. detection of atherosclerosis. Eur Heart J 2011;32:637-45.

6. Hoffmann U, Moselewski F, Nieman K et al. Noninvasive assessment of plaque morphology and composition in culprit and stable lesions in acute coronary syndrome and stable lesions in stable angina by multidetector computed tomography. Journal of the American College of Cardiology 2006;47:1655-62.

7. Motoyama S, Kondo T, Sarai M et al. Multislice computed tomographic characteristics of coronary lesions in acute coronary syndromes. J Am Coll Cardiol 2007;50:319-26.

8. Motoyama S, Sarai M, Harigaya H et al. Computed tomographic angiography characteristics of atherosclerotic plaques subsequently resulting in acute coronary syndrome. J Am Coll Cardiol 2009;54:49-57.

9. Pflederer T, Marwan M, Schepis T et al. Characterization of culprit lesions in acute coronary syndromes using coronary dual-source CT angiography. Atherosclerosis 2010;211:437-44.

10. Nasu K, Tsuchikane E, Katoh O et al. Accuracy of in vivo coronary plaque morphology assessment: a validation study of in vivo virtual histology compared with in vitro histopathology. J Am Coll Cardiol 2006;47:2405-12.

11. Pundziute G, Schuijf JD, Jukema JW et al. Type 2 diabetes is associated with more advanced coronary atherosclerosis on multislice computed tomography and virtual histology intravascular ultrasound. J Nucl Cardiol 2009;16:376-83.

12. Nair A, Kuban DB, Tuzcu EM et al. Coronary plaque classification with intravascular ultrasound radiofrequency data analysis. Circulation 2002;106:2200-6.

13. Voros S, Rinehart S, Qian Z et al. Prospective validation of standardized, 3-dimensional, quantitative coronary computed tomographic plaque measurements using radiofrequency backscatter intravascular ultrasound as reference standard in intermediate coronary arterial lesions: results from the ATLANTA (assessment of tissue characteristics, lesion morphology, and hemodynamics by angiography with fractional flow reserve, intravascular ultrasound and virtual histology, and noninvasive computed tomography in atherosclerotic plaques) I study. JACC Cardiovasc Interv 2011;4:198-208.

14. Stone GW, Maehara A, Lansky AJ et al. A prospective natural-history study of coronary atherosclerosis. N Engl J Med 2011;364:226-35.

15. Van Velzen JE, Schuijf JD, De Graaf FR et al. Plaque type and composition as evaluated non-invasively by MSCT angiography and invasively by VH IVUS in relation to the degree of stenosis. Heart 2009;95:1990-6.

16. Austen WG, Edwards JE, Frye RL et al. A reporting system on patients evaluated for coronary artery disease. Report of the Ad Hoc Committee for Grading of Coronary Artery Disease, Council on Cardiovascular Surgery, American Heart Association. Circulation 1975;51:5-40.

17. Kitagawa T, Yamamoto H, Horiguchi J et al. Characterization of noncalcified coronary plaques and identification of culprit lesions in patients with acute coronary syndrome by 64-slice computed tomography. JACC Cardiovasc Imaging 2009;2:153-60.

18. van der Hoeven BL, Liem SS, Oemrawsingh PV et al. Role of calcified spots detected by intravascular ultrasound in patients with ST-segment elevation acute myocardial infarction. Am J Cardiol 2006;98:309-13.

19. Mintz GS, Nissen SE, Anderson WD et al. American College of Cardiology Clinical Expert Consensus Document on Standards for Acquisition, Measurement and Reporting of Intravascular Ultrasound Studies (IVUS). A report of the American College of Cardiology Task Force on Clinical Expert Consensus Documents. J Am Coll Cardiol 2001;37:1478-92.

20. Virmani R, Kolodgie FD, Burke AP et al. Lessons from sudden coronary death: a comprehensive morphological classification scheme for atherosclerotic lesions. Arterioscler Thromb Vasc Biol 2000;20:1262-75.

21. Burke AP, Weber DK, Kolodgie FD et al. Pathophysiology of calcium deposition in coronary arteries. Herz 2001;26:239-44.

22. Carlier SG, Mintz GS, Stone GW. Imaging of atherosclerotic plaque using radiofrequency ultrasound signal processing. J Nucl Cardiol 2006;13:831-40.

23. Virmani R, Burke AP, Kolodgie FD et al. Pathology of the thin-cap fibroatheroma: a type of vulnerable plaque. J Intervent Cardiol 2003;16:267-72.

24. Beckman JA, Ganz J, Creager MA et al. Relationship of clinical presentation and calcification of culprit coronary artery stenoses. Arterioscler Thromb Vasc Biol 2001;21:1618-22.

25. Ehara S, Kobayashi Y, Yoshiyama M et al. Spotty calcification typifies the culprit plaque in patients with acute myocardial infarction: an intravascular ultrasound study. Circulation 2004; 110:3424-9.

26. Detrano R, Guerci AD, Carr JJ et al. Coronary calcium as a predictor of coronary events in four racial or ethnic groups. N Engl J Med 2008;358:1336-45.

27. Shemesh J, Stroh CI, Tenenbaum A et al. Comparison of coronary calcium in stable angina pectoris and in first acute myocardial infarction utilizing double helical computerized tomography. Am J Cardiol 1998;81:271-5.

28. Pundziute G, Schuijf JD, Jukema JW et al. Head-to-head comparison of coronary plaque evaluation between multislice computed tomography and intravascular ultrasound radiofrequency data analysis. JACC Cardiovasc Interv 2008;1:176-82.

29. Utsunomiya H, Yamamoto H, Kunita E et al. Combined presence of aortic valve calcification and mitral annular calcification as a marker of the extent and vulnerable characteristics of coronary artery plaque assessed by 64-multidetector computed tomography. Atherosclerosis 2010;213: 166-72.

30. Herzog BA, Wyss CA, Husmann L et al. First head-to-head comparison of effective radiation dose from low-dose 64-slice CT with prospective ECG-triggering versus invasive coronary angiography. Heart 2009;95:1656-61.

CHAPTER 8

Positive Remodeling on Coronary Computed Tomography as a Marker for Plaque Vulnerability on Virtual Histology Intravascular Ultrasound

Eleanore S.J. Kröner, Joëlla E. van Velzen, Mark J. Boogers, Hans-Marc J. Siebelink, Martin J. Schalij, Lucia J. Kroft, Albert de Roos, Ernst E. van der Wall, J. Wouter Jukema, Johan H.C. Reiber, Joanne D. Schuijf, Jeroen J. Bax

ABSTRACT

Background: Coronary computed tomography angiography (CTA) allows direct evaluation of the vessel wall and thus positive remodeling, which is a marker of vulnerability. The purpose of this study was to assess the association between positive remodeling on CTA and vulnerable plaque characteristics on virtual histology intravascular ultrasound (VH IVUS).

Methods: A total of 45 patients (78% male, age 58 ±11 years) underwent CTA followed by VH IVUS. On CTA, the remodeling index (RI) was determined for each lesion by a blinded observer using quantitative analysis. Positive remodeling was defined based on RI ≥1.0. Percentage necrotic core and presence of thin-capped fibroatheroma (TCFA) were used as markers for plaque vulnerability on VH IVUS.

Results: In total, 99 atherosclerotic plaques were evaluated, of which 37 lesions (37.4%) were identified as having positive remodeling on CTA. Higher levels of plaque vulnerability were identified in lesions with positive remodeling as compared to lesions without positive remodeling. Percentage necrotic core was significantly higher in lesions with positive remodeling (15.7% ±7.8%) as compared to lesions without this characteristic (10.2% ±7.2%) ($p<0.001$). Furthermore, significantly more TCFA lesions were identified in positively remodeled lesions (n=16; 43.2%) than in lesions without positive remodeling (n=3; 4.8%) ($p<0.001$).

Conclusion: Lesions with positive remodeling on CTA are associated with increased levels of plaque vulnerability on VH IVUS, including a higher percentage necrotic core and a higher prevalence of TCFA. Accordingly, evaluation of remodeling on CTA may provide a valuable marker for plaque vulnerability.

INTRODUCTION

Non-invasively, coronary computed tomography angiography (CTA) has emerged as a promising modality to detect coronary atherosclerosis. The technique allows for direct evaluation of the coronary artery vessel wall, thereby enabling to some extent non-invasive evaluation of plaque morphology and composition.[1] Due to technical restrictions, CTA cannot provide detailed visualization of fibrous cap thickness or necrotic core size. However, the presence of positive remodeling, which is an important surrogate marker of vulnerability,[2,3] can be reliably assessed.[4-6] Moreover, previous studies have demonstrated a relation between positive remodeling as assessed on CTA and presentation with acute coronary syndrome (ACS).[5,6] However, a direct comparison of plaque remodeling on CTA and plaque characteristics on virtual histology intravascular ultrasound (VH IVUS) has not yet been performed. The purpose of this study was to assess the association between positive remodeling on CTA and vulnerable plaque characteristics on VH IVUS.

METHODS

Patient population

The patient population consisted of 45 patients who underwent both CTA and invasive coronary angiography in combination with VH IVUS. Patients were clinically referred for CTA because of known or suspected coronary artery disease (CAD), followed by invasive coronary angiography and VH IVUS. Referral for invasive coronary angiography was based on clinical presentation and/or imaging results. VH IVUS was performed to further evaluate the extent and severity of disease in order to determine further management more precisely and elucidate possible discrepancies between non-invasive and invasive angiographic findings. Contra-indications for CTA were (1) (supra) ventricular arrhythmias, (2) renal insufficiency (glomerular filtration rate<30ml/min, (3) known allergy to iodinated contrast agents, (4) severe claustrophobia, (5) pregnancy. Exclusion criteria for IVUS were severe vessel tortuosity, severe stenosis or vessel occlusion. Risk factors for CAD were derived from existing patient medical record data. For this retrospective evaluation, patients with good to moderate image quality on CTA and available quantitative analyses were selected from an ongoing registry.[7]

CTA and VH IVUS acquisition

CTA was performed using either a 64-detector row (n=34) helical scanner or a 320-detector row (n=11) volumetric scanner (Aquilion 64 or Aquilion ONE, Toshiba Medical Systems, Otawara, Japan) as previously described.[8,9] Patients with an elevated heart rate (≥65 beats/min) were administered beta-blockers (oral metoprolol 50 or 100mg, single dose, 1 hour before examination), if not contra-indicated. Unless contra-indicated, nitroglycerin 0.4mg sublingual was administered immediately before contrast injection. During the CTA examination the mean heart rate was 57 ±8 beats per minute. An initial data set was

reconstructed at 75% of the R-R interval, with a slice thickness of 0.50 mm and a reconstruction interval of 0.25 mm. In case of motion artifacts, additional reconstructions were explored to obtain images with most optimal image quality for evaluation. For processing and evaluation CTA data were transferred to an off-line workstation.

The VH IVUS examinations were performed during invasive coronary angiography. Invasive coronary angiography was performed according to standard protocols. Patients were administered nitroglycerin intracoronary before induction of the IVUS catheter (Eagle Eye, Volcano Corporation, Rancho Cordova, CA, USA). The ultrasound catheter was positioned in the coronary artery, and motorized pull back at a speed of 0.5 mm/s was used until the catheter reached the guiding catheter. The VH IVUS data were stored digitally and assessed offline.

CTA and VH IVUS analysis

The CTA examinations were evaluated by an independent and experienced observer who was blinded to the VH IVUS results, using a dedicated and extended version of the QAngio CT software (QAngio CT 1.1, Medis medical imaging systems, Leiden, The Netherlands).[10] On CTA data sets, the dedicated software was used to detect both lumen and vessel wall contours. According to the modified American Heart Association classification, coronary arteries were divided into 17 segments.[11] Only segments that were available on both VH IVUS and CTA were analyzed. Coronary plaques were defined as structures >1 mm^2 within and/or adjacent to the coronary artery lumen, which could be clearly distinguished from the vessel lumen.[12] Per segment, coronary plaque was selected at the site of the most severe luminal narrowing. The detected lumen and vessel wall contours were used for automated quantitative measurements of coronary plaques. At the level of the minimal lumen area (MLA), the remodeling index (RI) was calculated by dividing the cross-sectional vessel wall area by the corresponding reference area. The cross-sectional reference area was determined in the normal appearing reference area as close as possible to the respective coronary lesion. The presence of positive remodeling was defined as a RI ≥1.0.[13]

The VH IVUS analysis was performed by two experienced observers who were blinded to baseline patient characteristics and CTA results, with the use of dedicated software (pcVH2.1, Volcano Corporation, Rancho Cordova, CA, USA). The previously described 17-segment model was used to ensure that similar plaques were analyzed with CTA and VH IVUS. Side branches and coronary ostia were used as anatomical markers.

For each lesion identified on both CTA and VH IVUS, MLA and corresponding vessel area were determined. In addition, percentage plaque burden was calculated as plaque cross-sectional area divided by the vessel cross-sectional area multiplied by 100.[14] Four different plaque components, namely fibrotic tissue, fibro-fatty, necrotic core and dense calcium, were differentiated into different color codes. The different plaque components were calculated as percentage of the plaque burden. Plaque type was determined on VH IVUS using a classification based on the differentiation of the four plaque components as described previously.[7] In total, four different plaque types were identified, namely pathological intimal thickening, fibroatheroma, fibrocalcific plaque and thin capped

fibroatheroma (TCFA). TCFA lesions were defined as lesions with a plaque burden ≥40%, the presence of confluent necrotic core of >10%, and no evidence of an overlying fibrous cap.[7] Both the percentage necrotic core and the presence of TCFA were used to determine plaque vulnerability on VH IVUS.[15]

Statistical analysis

Statistical analysis was performed using SPSS 18.0 (SPSS, Inc., Chicago, Illinois). Continuous data are represented as means (±SD). Categorical data are expressed as absolute numbers or percentages. Segments available on both CTA and VH IVUS were included in the lesion-based analysis. Plaque vulnerability on VH IVUS (as defined by the percentage necrotic core and the presence of TCFA) was assessed in lesions with positive remodeling (RI ≥1.0) on CTA and compared to the remaining lesions that did not show positive remodeling (RI <1.0) on CTA. Comparisons were performed by chi-square analysis. A p value of <0.05 was considered statistically significant.

Table 1. Patient characteristics (n=45)

Age (years)	58 ±11
Men/women	35/10
Heart rate during CTA (beats per minute)	57 ±8
Stable angina/Suspected acute coronary syndrome	27/18
At least one stenosis with >50% diameter narrowing on invasive coronary angiography)	32 (71%)
No. of vessels diseased: 1	17 (53%)
No. of vessels diseased: 2	6 (19%)
No. of vessels diseased: 3	9 (28%)
Cardiovascular risk factors	
Diabetes Mellitus	10 (22%)
Hypertension†	29 (64%)
Hypercholesterolemia‡	26 (58%)
Current Smoker	20 (44%)
Obesity¥	8 (18%)

Data are absolute values or means ± standard deviation.
Data in parentheses are percentages.
†Defined as systolic blood pressure ≥140 mm Hg or diastolic blood pressure ≥90 mm Hg or the use of antihypertensive medication.
‡Serum total cholesterol ≥230 mg/dL or serum triglycerides ≥200 mg/dL or treatment with Lipid lowering drugs.
¥Body mass index ≥30 kg/m^2
CTA: coronary computed tomography angiography

RESULTS

In total, 45 patients (78% male, age 57.8 ±11 years) who underwent CTA followed by VH IVUS were enrolled retrospectively. Characteristics of the patient population are provided in Table 1. In all patients CTA and VH IVUS studies were of sufficient imaging quality for analysis. In total, 99 plaques were identified on both CTA and the corresponding available VH IVUS analyses. Of theses 99 atherosclerotic plaques, 37 lesions (37.4%) were classified as positive remodeled (RI ≥1.0) on CTA. In the remaining 62 lesions (62.6%) no positive remodeling (RI <1.0) was observed. On VH IVUS, the most prevalent plaque component was fibrotic tissue (52% ±16%), followed by fibro-fatty tissue (19% ±12%), necrotic core (13% ± 8%) and dense calcium (8% ±9%). Qualitative evaluation of coronary lesions on VH IVUS revealed the presence of pathological intimal thickening, fibroatheroma and fibrocalcific lesions in respectively 37 (37.4%), 30 (30.3%) and 13 (13.1%) of lesions. Finally, TCFA were identified in 19 lesions (19.2%).

Lesions identified as positive remodeled (RI ≥1.0) on CTA had a significantly higher plaque burden on VH IVUS as compared to lesions without positive remodeling (RI <1.0) as shown in Table 2. Percentage necrotic core was also significantly higher in the positive remodeled lesions (RI ≥1.0) as compared to lesions without positive remodeling (RI <1.0). No differences in relation to the presence or absence of positive remodeling on CTA were observed in the percentage of fibrotic tissue, fibro fatty tissue and dense calcium.

Table 2. VH IVUS characteristics between lesions with and without positive remodeling on CTA

Plaque characteristics on VH IVUS	Presence of positive remodeling on CTA	Absence of positive remodeling on CTA	p value
Minimal lumen area (mm2)	8 ±4	9 ±5	0.38
Vessel area* (mm2)	16 ±6	15 ±6	0.24
Plaque burden (%)	51 ±10	41 ±16	<0.001
Fibrotic (%)	55 ±9	51 ±19	0.18
Fibro-Fatty (%)	20 ±11	18 ±13	0.58
Necrotic core (%)	16 ±8	10 ±7	0.001
Dense calcium (%)	9 ±6	7 ±11	0.25

Data are represented as mean ± standard deviation
*at minimal lumen area
CTA: computed tomography coronary angiography; VH IVUS: virtual histology intravascular ultrasound

Qualitative evaluation of plaque types as shown in Figure 1, revealed an equal distribution of the presence of fibroatheroma (9 (24%) versus 21 (34%), p=0.32) between lesions with positive remodeling (RI ≥1.0) as compared to lesions without positive remodeling (RI <1.0). Furthermore, no significant difference of the presence of fibrocalcific plaques (3 (8%) versus 10 (16%), p=0.36) were observed between the two groups. Pathological
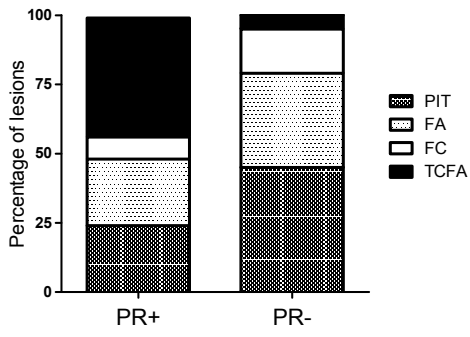
Figure 1. Relative distribution of visually assessed plaque types on VH IVUS between lesions with positive remodeling and lesions without positive remodeling on CTA. Significantly more lesions classified as PIT were present in lesions without positive remodeling. Percentage of FA and FC were not significantly different between lesions with positive remodeling and lesions without positive remodeling. Significantly more TCFA lesions were identified in lesions with positive remodeling on CTA. (Abbreviations: PR+, lesions with positive remodeling (RI ≥1.0) on CTA; PR −, lesions without positive remodeling (RI <1.0) on CTA; PIT, pathological intimal thickening; FA, fibroatheroma; FC, fibrocalcific lesions; TCFA, thin-capped fibroatheroma.)
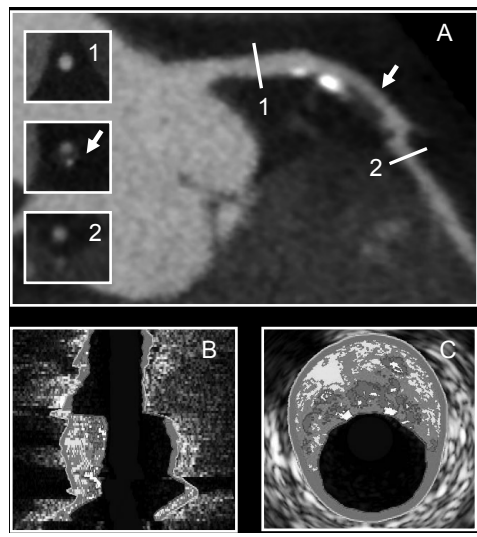
Figure 2. An example of a lesion with positive remodeling on 320-row CTA and corresponding findings on VH IVUS. (A) Curved multiplanar reconstruction of the left anterior descending coronary artery showing a large plaque in the proximal segment of the vessel. The diameter of the vessel at the plaque site is larger as compared to the diameter at the reference sections (1,2), indicating the presence of positive remodeling. (B and C) Corresponding longitudinal (B) and cross-sectional (C) VH IVUS images demonstrate indeed an outward-remodeled lesion, with a large plaqueburden (69%) and a large amount of necrotic core (19%), labeled in red, corresponding to a TCFA lesion.

intimal thickening was significantly more often observed in lesions without positive remodeling (RI ≥1.0) on CTA; 28 lesions (45%) without positive remodeling (RI <1.0) on CTA were classified as showing pathological intimal thickening as compared to 9 lesions (24%) with positive remodeling (RI ≥1.0) on CTA (p=0.04). Importantly, as shown in Figure 1, 16 lesions (43.2%) with positive remodeling (RI ≥1.0) on CTA were identified as TCFA. In contrast, only 3 lesions (4.8%) without positive remodeling (RI <1.0) on CTA were classified as TCFA (p<0.001). An example of a lesion with positive remodeling (RI ≥1.0) on CTA and corresponding findings on VH IVUS is provided in Figure 2.

DISCUSSION

In the present study, positive remodeling on CTA was related to vulnerable plaque characteristics on VH IVUS. Lesions with positive remodeling on CTA were shown to have a significantly higher plaque burden on VH IVUS. A larger amount of necrotic core and a higher prevalence of TCFA were found in lesions with positive remodeling on CTA.

The current findings are consistent with previous investigations, showing that compensatory enlargement of the vessel wall, including eccentric plaque growth, is strongly associated with necrotic core area and macrophage infiltration.[15 16] Indeed, histopathological data have confirmed that vulnerable plaques are almost always associated with positive remodeling.[17-19] Also during in vivo VH IVUS studies, a similar connection between positive remodeling and plaque composition has been reported.[20] In 41 patients, Rodriguez-Granillo et al. described a significantly larger percentage of necrotic core in positively remodeled vessels as compared to vessels with negative remodeling. Furthermore, 56% of positively remodeled lesions were classified as TCFA, indicating a higher risk phenotype. In the current study, non-invasive imaging with CTA was used to identify the presence of positive remodeling. Previous studies have shown that reliable assessment of remodeling on CTA is feasible.[4-6 21] Achenbach et al. determined RI in 44 patients with high-quality CTA data sets and observed higher indices in nonstenotic (<50% diameter reduction) as compared to stenotic lesions.[4] In a subset of patients, measurements on CTA were verified against IVUS, revealing a close correlation (r^2=0.82). Consequently, several studies have explored whether the presence of positive remodeling on CTA may indicate an increased likelihood of vulnerability. Interestingly, lower attenuation values on CTA have been observed in lesions with positive remodeling as compared to lesions without this phenomenon.[21] In turn, a correlation between lower attenuation values on CTA and increased lipid-rich and necrotic core content on IVUS has been observed.[12 22] Accordingly, these observations indirectly suggested that positively remodeled lesions on CTA may have a higher proportion of necrotic core, a hypothesis that was tested in the current study. In addition, the presence of positive remodeling on CTA has been related to clinical presentation with ACS.[5 23] Two retrospective studies investigated the differences in coronary plaque features between ACS patients and patients presenting with stable angina pectoris.[5 23] As compared to lesions in stable patients, culprit lesions in ACS displayed more non-calcified plaque, spotty calcifications and higher remodeling indices. Moreover, in a prospective study in 1.059 patients with a follow-up duration of 27 ±10 months, patients with plaques showing both positive remodeling and a low attenuation value on CTA were found to have a higher likelihood of developing ACS over time[6]. In contrast, absence of lesions with these characteristics on CTA conferred an excellent outcome.

Currently, the use of CTA is gradually shifting from assessment of degree of stenosis to evaluation of atherosclerotic plaque burden and risk assessment. The present study showed that lesions identified as positive remodeled on CTA were associated with plaque vulnerability on VH IVUS. Accordingly, more comprehensive assessment of the coronary

artery vessel wall, including evaluation of positive remodeling, may potentially allow more individualized risk stratification, based on CTA.

The following limitations need to be acknowledged. This feasibility study is a retrospective analysis in selected optimal conditions. Only patients with a CTA data set of diagnostic image quality were included and assessment of remodeling may be more difficult in data sets with lower image quality. Accordingly, our current findings are based on a relatively small study population and need to be validated in a larger, more challenging study population. Our observations indicate that with increasing remodeling index, the likelihood of TCFA also increases. However, this observation does not implicate that a lesion with a remodeling index of ≥1.0 is per definition a vulnerable lesion. Possibly, additional markers are needed to predict the presence of a vulnerable lesion with higher accuracy. Of note, other characteristics of vulnerable plaque on CTA were not analyzed in this particular study. Importantly, while the presence of positive remodeling on CTA may have value for risk stratification in addition to clinical characteristics and other CTA variables, the implications of this particular observation for prognosis and therapeutic management remain to be determined. Finally, the radiation exposure associated with CTA currently still restricts its widespread use. Notably however, novel dose-saving algorithms and recent technical improvements have led to substantial dose reductions.[24]

Positive Remodeling as Marker for Vulnerability

REFERENCES

1. Schroeder S, Kopp AF, Baumbach A et al. Non-invasive characterisation of coronary lesion morphology by multi-slice computed tomography: a promising new technology for risk stratification of patients with coronary artery disease. Heart 2001;85:576-578.

2. Smits PC, Pasterkamp G, Quarles van Ufford MA et al. Coronary artery disease: arterial remodelling and clinical presentation. Heart 1999;82:461-464.

3. Varnava AM, Mills PG, Davies MJ. Relationship between coronary artery remodeling and plaque vulnerability. Circulation 2002;105:939-943.

4. Achenbach S, Ropers D, Hoffmann U et al. Assessment of coronary remodeling in stenotic and nonstenotic coronary atherosclerotic lesions by multidetector spiral computed tomography. J Am Coll Cardiol 2004;43:842-847.

5. Motoyama S, Kondo T, Sarai M et al. Multislice computed tomographic characteristics of coronary lesions in acute coronary syndromes. J Am Coll Cardiol 2007;50:319-326.

6. Motoyama S, Sarai M, Harigaya H et al. Computed tomographic angiography characteristics of atherosclerotic plaques subsequently resulting in acute coronary syndrome. J Am Coll Cardiol 2009;54:49-57.

7. van Velzen JE, Schuijf JD, de Graaf FR et al. Plaque type and composition as evaluated non-invasively by MSCT angiography and invasively by VH IVUS in relation to the degree of stenosis. Heart 2009;95:1990-1996.

8. Schuijf JD, Pundziute G, Jukema JW et al. Diagnostic accuracy of 64-slice multislice computed tomography in the noninvasive evaluation of significant coronary artery disease. Am J Cardiol 2006;98:145-148.

9. de Graaf FR, Schuijf JD, van Velzen JE et al. Diagnostic accuracy of 320-row multidetector computed tomography coronary angiography in the non-invasive evaluation of significant coronary artery disease. Eur Heart J 2010;31:1908-1915.

10. Boogers MJ, Schuijf JD, Kitslaar PH et al. Automated quantification of stenosis severity on 64-slice CT: a comparison with quantitative coronary angiography. J Am Coll Cardiol Cardiovasc Imaging 2010;3:699-709.

11. Austen WG, Edwards JE, Frye RL et al. A reporting system on patients evaluated for coronary artery disease. Report of the Ad Hoc Committee for Grading of Coronary Artery Disease, Council on Cardiovascular Surgery, American Heart Association. Circulation 1975;51:5-40.

12. Leber AW, Knez A, Becker A et al. Accuracy of multidetector spiral computed tomography in identifying and differentiating the composition of coronary atherosclerotic plaques: a comparative study with intracoronary ultrasound. J Am Coll Cardiol 2004;43:1241-1247.

13. American College of Cardiology Clinical Expert Consensus Document on Standards for Acquisition, Measurement and Reporting of Intravascular Ultrasound Studies (IVUS). A report of the American College of Cardiology Task Force on Clinical Expert Consensus Documents developed in collaboration with the European Society of Cardiology endorsed by the Society of Cardiac Angiography and Interventions. Eur J Echocardiogr 2001;2:299-313.

14. Mintz GS, Nissen SE, Anderson WD et al. American College of Cardiology Clinical Expert Consensus Document on Standards for Acquisition, Measurement and Reporting of Intravascular Ultrasound Studies (IVUS). A report of the American College of Cardiology Task Force on Clinical Expert Consensus Documents. J Am Coll Cardiol 2001;37:1478-1492.

15. Fuster V, Moreno PR, Fayad ZA et al. Atherothrombosis and high-risk plaque: part I: evolving concepts. J Am Coll Cardiol 2005;46:937-954.

16. Fuster V, Fayad ZA, Moreno PR et al. Atherothrombosis and high-risk plaque: Part II: approaches by noninvasive computed tomographic/magnetic resonance imaging. J Am Coll Cardiol 2005; 46:1209-1218.

17. Schaar JA, Muller JE, Falk E et al. Terminology for high-risk and vulnerable coronary artery plaques. Report of a meeting on the vulnerable plaque, June 17 and 18, 2003, Santorini, Greece. Eur Heart J 2004;25:1077-1082.

18. Falk E, Shah PK, Fuster V. Coronary plaque disruption. Circulation 1995;92:657-671.

19. Virmani R, Kolodgie FD, Burke AP et al. Lessons from sudden coronary death: a comprehensive morphological classification scheme for atherosclerotic lesions. Arterioscler Thromb Vasc Biol 2000;20:1262-1275.

20. Rodriguez-Granillo GA, Serruys PW, Garcia-Garcia HM et al. Coronary artery remodelling is related to plaque composition. Heart 2006;92:388-391.

21. Schmid M, Pflederer T, Jang IK et al. Relationship between degree of remodeling and CT attenuation of plaque in coronary atherosclerotic lesions: an in-vivo analysis by multi-detector computed tomography. Atherosclerosis 2008;197:457-464.

22. Pohle K, Achenbach S, MacNeill B et al. Characterization of non-calcified coronary atherosclerotic plaque by multi-detector row CT: comparison to IVUS. Atherosclerosis 2007;190:174-180.

23. Pflederer T, Marwan M, Schepis T et al. Characterization of culprit lesions in acute coronary syndromes using coronary dual-source CT angiography. Atherosclerosis 2010;211:437-444.

24. Hausleiter J, Meyer T, Hermann F et al. Estimated radiation dose associated with cardiac CT angiography. JAMA 2009;301:500-507.

PART 2

Imaging of coronary
atherosclerosis and clinical
management

CHAPTER 9

Monitoring and Investigations in ICCU: CT Angiography and other Applications of CT

Joëlla E. van Velzen, Joanne D. Schuijf, Lucia J. Kroft, Jeroen J. Bax

SUMMARY

Patients presenting with acute chest pain constitute a common and important diagnostic challenge. Therefore, interest has been raised in using computed tomography (CT) for non-invasive visualization of coronary artery disease in patients presenting with acute chest pain. Due to rapid developments in coronary CT angiography technology, high diagnostic accuracies for detecting coronary stenosis can be obtained. Additionally, CT is an excellent modality in patients whose symptoms suggest other non-coronary causes of acute chest pain such as aortic aneurysms, aortic dissection or pulmonary embolism. Furthermore, acquisition of the coronary arteries, thoracic aorta and pulmonary arteries in a single CT examination is feasible, allowing "triple rule-out". Finally, other applications such as the evaluation of plaque composition, myocardial function and perfusion are currently under investigation and may also become valuable in the setting of acute chest pain. However, although CT shows great potential in evaluating patients with acute chest pain, more randomized clinical trials are needed to determine the value of this technique in this challenging patient population.

INTRODUCTION

Since the introduction of computed tomography (CT) in the early 1970s the technique has evolved into an essential imaging tool in general medicine. With this technique, non-invasive high resolution cross-sectional imaging of internal structures such as the brain, thorax and abdomen was permitted, thereby gradually replacing the more invasive radiographic techniques.[1] Moreover, CT angiography has evolved as a very accurate tool
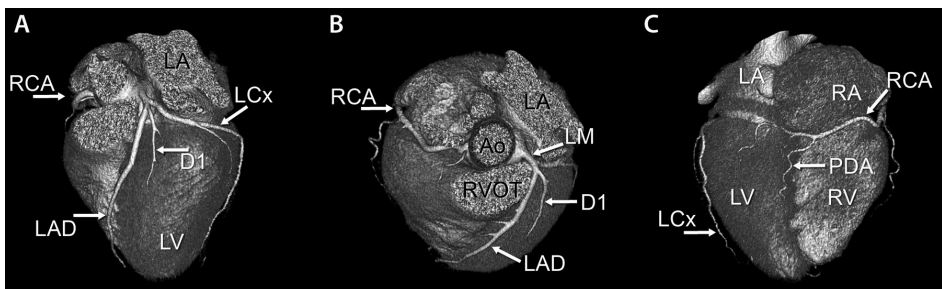
Figure 1. Surface rendered volumetric 3D images of the coronary arteries and side-branches providing a 3D overview of the coronary artery tree and their relative position to the underlying cardiac structures, including the left ventricle (LV) and right ventricle (RV). (A) Anterior view of the left circulation demonstrating the left anterior descending coronary artery (LAD) with first diagonal branch (D1). Moreover, the left circumflex coronary artery (LCx) can be identified. The left atrium (LA) and right ventricular outflow tract (RVOT) can be also appreciated in this view. (B) Cranial view demonstrating a volume rendered image of right coronary artery (RCA) and left main coronary artery (LM) and their main branches originating from the right and left coronary cusp, respectively. (C) Posterior view of the RCA and the posterior descending coronary artery (PDA).

for the visualization of the aorta and pulmonary arteries. However, high quality imaging of the coronary arteries remained challenging due to small vessel size, movement and tortuous anatomy requiring high temporal, spatial and contrast resolution. In the late 1990s, the first 4-slice spiral CT scanner was developed with sufficient resolution to allow visualization of the coronary arteries. Preliminary investigations using these earlier generation multislice CT scanners established the potential of multislice CT for detecting significant coronary stenosis in comparison to conventional coronary angiography (CCA).[2-4] Since then, coronary multislice CT angiography has developed into a promising non-invasive alternative to invasive CCA. With each successive generation of scanners from 4-slice to the present 64-slice and even 320-slice scanners, temporal and spatial resolution improved markedly due to faster gantry rotation times, thinner detectors and volumetric coverage. These new developments currently allow motion free visualisation of the entire coronary artery tree with high diagnostic accuracy for detecting coronary stenosis (Figure 1).[5 6]

Owing to these rapid developments, interest has been raised in using CT for the evaluation of patients presenting with acute chest pain. In the intensive coronary care unit (ICCU), acute chest pain is the most common clinical presentation of coronary artery disease (CAD). The diagnosis of acute coronary syndrome (ACS) is straightforward in high risk patients with typical chest pain, typical electrocardiography (ECG) changes, and elevation of serum cardiac enzymes, whereas it is difficult in patients presenting with atypical chest pain, non-diagnostic or normal ECG and normal initial cardiac enzymes. Indeed, up to 8% of patients with ACS are misdiagnosed and inappropriately discharged home.[7] Conversely, only a minority of "low risk" patients (i.e., those with initially normal electro-cardiograms and cardiac enzymes) actually suffer from myocardial ischemia.[8] Therefore, most patients presenting with acute chest pain are evaluated with serial ECGs and cardiac enzymes followed by a rest and/or stress-imaging study. However, this approach leads to many unnecessary hospital admissions and is both time-consuming and expensive and thus, resource-intensive. Therefore, a non-invasive and rapid examination to establish or exclude CAD as the underlying cause of symptoms could substantially improve the clinical care of patients admitted to the ICCU, reducing hospital admissions and costs. For this purpose, coronary CT angiography may constitute an attractive modality as it offers relatively simple and fast image acquisition.

This chapter will focus on the evolving role of coronary CT angiography (including coronary calcium scoring) in the diagnosis of patients with acute chest pain. Furthermore, the role of CT in diagnosing other important causes of acute chest pain, concerning the great vessels such as aortic aneurysms, acute aortic dissection, and pulmonary emboli, will be addressed. Lastly, an overview of a wide range of other CT applications is provided including triple rule-out, evaluation of plaque composition, myocardial function and perfusion.

CORONARY CT ANGIOGRAPHY: TECHNIQUE, ACQUISITION AND POST-PROCESSING

CT is an imaging modality which has an X-ray source (tube) and detectors on opposite sides of a gantry that continuously rotates around the patient. During the CT scan the patient is moved through the gantry. Subsequently, the X-ray source emits photons collimated into a fan beam which are, after partial absorption and dispersion, reabsorbed by the detectors. Computer systems process these data into three-dimensional (3D) volumetric information, which can be transferred to CT workstations and be evaluated using multiple post-processing techniques. Fast image acquisition is essential for the acquirement of motion-free images and as multiple factors influence CT quality, proper patient preparation and appropriate CT acquisition techniques are critical to guarantee diagnostic image quality.

Patient preparation

Proper patient preparation is important for obtaining diagnostic image quality. Therefore, before referring a patient for coronary CT angiography, a short patient history should be taken. Overall, a history of a severe allergic reaction to contrast agents, impaired renal function (glomerular filtration rate < 30 ml/min), presence of atrial fibrillation and pregnancy are considered contra-indications. The patient should refrain from food and liquids preferably three hours before the examination, to prevent nausea as a reaction to the contrast agent. Moreover, a low and stable heart rate in the range of approximately 50 to 60 beats per minute is preferred during image acquisition. To achieve a low and stable heart rate, beta-blocking medication is frequently administered prior to the examination, unless contra-indicated. Lastly, to ensure for rapid delivery of the contrast agent bolus for coronary CT angiography, an intravenous catheter should be present for delivery of the contrast agent, preferably in the right antecubital vein (18-20 gauge).

ECG triggering and image acquisition

The range of the current 64-slice scanners is not large enough to cover the entire heart in one rotation and therefore several heart cycles are needed to image the entire heart. To compensate for cardiac motion and synchronize the start of the systole, ECG gating is needed to obtain phase-compatible images. Currently, there are two approaches of scanning the beating heart; with retrospective gating and prospective triggering (Figure 2). Firstly, retrospective ECG gating collects data during the whole R-R interval in several heart beats with 64-slice scanners. Afterwards, the most optimal phase in which the coronary arteries have the least motion artifacts can be selected, most often being in mid diastole. As data acquisition is throughout the cardiac cycle, ventricular function can be analyzed as well. A newer scanning technique is prospective triggering in which the start of scanning is triggered by the R-wave and the scanning is performed only during diastole or another pre-specified part of the cardiac cycle. An advantage is that the patient is exposed to less radiation.[9] A disadvantage is that, afterwards, one has limited ability to

Retrospective gating

Propective triggering

= Beam on
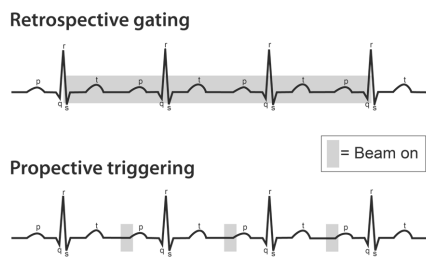
Figure 2. Figure showing the mechanism of retrospective ECG gating versus prospective ECG triggering. With retrospective gating data are continuously acquired while simultaneously recording the ECG of the patient. Therefore, retrospective reconstruction can be performed in every phase of the R-R interval. With prospective triggering, the X-ray beam is on only during a pre-selected phase of the R-R interval and reconstruction can only be performed in the scanned phase, for example in mid diastole (70 - 80% of R-R interval).

correct any motion artifacts that occurred due to changes in heart rate or arrhythmias. Prospective triggering with dose modulation can be used for coronary artery imaging (full dose at the mid diastole of the cardiac cycle) in combination with ventricular function analysis (low dose throughout the other parts of the cardiac cycle).

Depending on the scanner type, imaging can be performed in helical ("spiral") mode with continuous table movement and continuous or modulated acquisition, or in step-and-shoot mode with multiple volumetric acquisitions reconstructed into a single dataset. A wide-volume detector allows full cardiac acquisition in a single gantry rotation, e.g. a 320-detector row scanner that allows a maximum of 16 cm scan-range in a single rotation.[10]

When positioning the patient, this should be in a supine position with both arms above the head. The ECG leads are best positioned above and below the level of the scan surface to prevent streak artifacts. Importantly, to make sure that the entire heart is imaged, the CT examination must start from approximately 1-2 cm below the carina to 2 cm below the apex. Of note, if other structures (e.g. pulmonary arteries, aorta, bypass grafts) need to be visualized, a larger scan length should be selected.

For coronary calcium scoring, a low-dose ECG triggered non contrast-enhanced scan is performed before the contrast-enhanced CT examination and reconstructed to 3 mm slices. Additionally, this scan can be used to determine the proper location and scan range for coronary CT imaging. For a regular 64-slice scanner, a rapid infusion of 60 - 100 ml of contrast material with a flow-rate of 5 ml/s is used, followed by a saline flush. Typical scan parameters are: a pitch of 0.375, rotation time of 333-500 ms, tube voltage of 120 kV and tube current of 300 mAs. When using a bolus-triggered start of the CT scan, the start is automatically initiated if the preset contrast-enhancement threshold level in the descending aorta is reached. Alternatively, a test bolus injection can be used to determine the contrast transit time. Subsequently, data acquisition is performed at half-inspiratory breath hold of approximately 10 seconds.

Post-processing and evaluation

After data acquisition, images are reconstructed and sent to a dedicated workstation for post-processing. If a non contrast-enhanced dataset is acquired, coronary calcium score can be quantified according to the Agatston method on a vessel and patient basis.[11] Commonly, coronary CT angiography datasets are reconstructed with continuous images using thin increments (typically 0.5 - 0.6 mm slice thickness). Retrospectively gated axial images can be reconstructed in any phase of the cardiac cycle. However, when prospective triggering was used, images can only be reconstructed in the pre-specified R-R acquisition interval. Most often reconstructions are performed in the relatively motion-free phase of mid diastole (70 - 80% of R-R interval) which is generally least affected by motion artifacts.

For post-processing, various types of algorithms are available. The thin axial slices are considered the source information of CT imaging (Figure 3). Accordingly, the cardiac structures and coronary arteries can be easily evaluated by scrolling through the images in axial
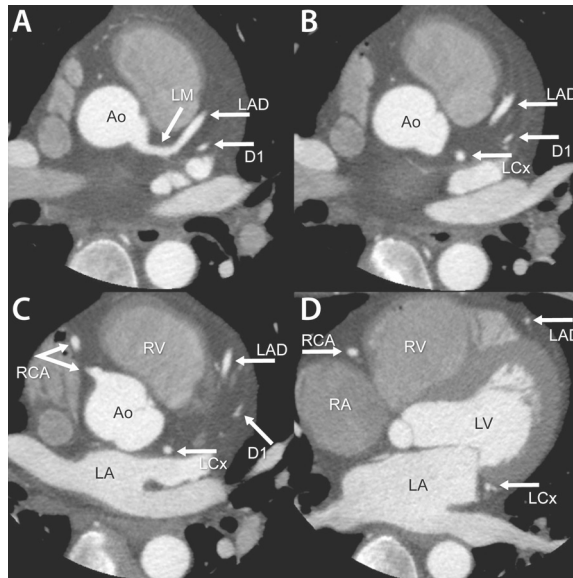
Figure 3. Typical example of axial contrast-enhanced images (0.5 mm slice thickness), which can be used to evaluate cardiac structures (such as the left ventricle (LV), left atrium (LA), right ventricle (RV) and aorta (Ao)) and coronary arteries by scrolling through the slices in the cranio-caudal direction. Four images have been selected to demonstrate to anatomy of the heart. (A) Axial image showing the left main (LM) coronary artery at the level of the ostium which arises from the left coronary cusp and bifurcates first into the left anterior descending coronary artery (LAD). (B) Slightly more distal axial image showing the left circumflex coronary artery (LCx) and the first diagonal branch (D1) which has originated from the LAD. (C) Axial image demonstrating the origin of the right coronary artery (RCA) from the right coronary cusp and the mid segments of the LCx, LAD and D1. (D) Axial image at midventricular level which shows the mid segment of the right coronary artery (RCA) and distal segments of the LAD and LCx (the latter is seen in the left atrioventricular groove).

direction (Online supplemental movie 1). Additionally, curved multiplanar reconstructions (MPR) allow visualization of the entire coronary artery in a single image which is useful for depicting the entire coronary lumen and evaluating degree of stenosis. Furthermore, maximum intensity projections (MIP) can be reconstructed which represent a series of contiguous CT slices stacked into a single image ("slab"). Moreover, MIPs are very suitable for assessment of longer length of vessel segments and may facilitate in evaluating the degree of stenosis. Lastly, 3D volume rendering provides a 3D image of the heart and vessels (Online supplemental movie 2). An excellent overview of the coronary anatomy is provided, although 3D volume rendering is generally not used for assessing the degree of stenosis.

A systematic approach is important when evaluating a coronary CT angiogram. If coronary calcium scoring has been performed, the Agatston score is reported on a patient and vessel basis. In addition, the patient based Agatston score is commonly placed in a percentile rank based on the known distribution of coronary calcium scores in relation to patient age and sex to facilitate interpretation of the coronary calcium score. With regard to the coronary CT angiogram, the quality of the scan should be mentioned as this influences the diagnostic certainty of the study. Findings are commonly reported similar to the traditional CCA report. Typically, the coronary segments are described as normal, mild (< 30% wall irregularities), non-significant (30 - 50% stenosis), significant (> 50% stenosis), severe stenosis (> 70%) and occlusion. Presence and patency of stents and bypasses are reported, if evaluable. Segments effected by severe calcifications, motion and breathing artifacts should also be mentioned in the report.

CORONARY CALCIUM SCORE

It has been widely verified that presence of coronary calcifications only occurs in the presence of coronary atherosclerosis.[12] Both electron beam computed tomography (EBCT) and multislice CT have been used over the past years for the non-invasive evaluation of coronary calcifications, both demonstrating high sensitivities for the detection of CAD. An example of coronary calcium scoring is provided in Figure 4.[13][14] For quantification of the coronary calcifications, the Agatston method (a method that multiplies the calcified area by a density factor based on the highest Hounsfield values within this area) has been traditionally used.[11] Total coronary calcium scores are generally divided into normal (zero calcium), mild (1 - 100), moderate (100 - 400) and severe (> 400).[15] Although newer quantification methods have been introduced (calcified volume (mm^3) and mass (mg) measurements), no clinical studies have provided data using these methods.

Coronary calcium score in general population

Several population based studies have demonstrated that the calcium score increases with higher age thereby reflecting the natural progression of atherosclerosis. In addition, men tend to have higher coronary calcium scores than women of similar age. Therefore, when interpreting the coronary calcium score, it should be ranked in percentiles according to the
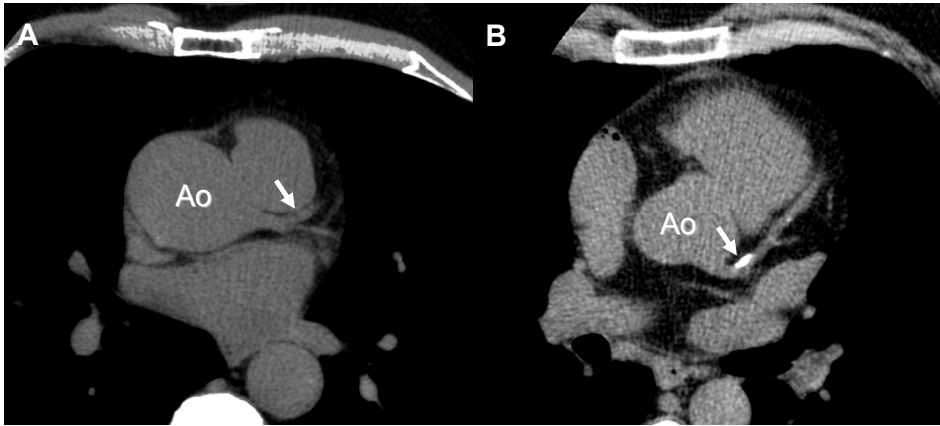
Figure 4. Example of coronary calcium scoring with non contrast-enhanced computed tomography. Calcium deposits can be recognized as bright white structures located in the coronary arteries. (A) An example of a patient without calcium (arrow) in the proximal left anterior descending coronary artery (LAD). (B) An example of a patient with extensive calcifications in the proximal LAD (arrow). Ao; aorta.

distribution within age and sex.[13 16] Moreover, the relation between the presence of obstructive CAD and presence and extent of coronary calcium has been extensively studied.[17] The presence of coronary calcifications was demonstrated to have a high sensitivity and negative predictive value for the presence of obstructive disease, however a very limited specificity was reported.[17 18] Indeed, extensive calcifications (resulting in a high coronary calcium score) can be present even in the absence of significant luminal narrowing. Therefore, although high coronary calcium scores are often associated with obstructive CAD, the technique may be more suited to provide an estimate of total plaque burden rather than stenosis severity. Interestingly, numerous investigations have shown that the extent of coronary calcium burden translates into prognostic information. Coronary calcium scoring has therefore been proposed as a tool for stratifying cardiac risk. In fact, several large trials have reported that elevated coronary calcium scores have predictive value for cardiovascular events, both independently and incrementally to cardiovascular risk factors.[19 20]

Coronary calcium score in patients with ACS

In the specific clinical setting of acute chest pain, a few initial investigations with EBCT have been conducted to assess the value of coronary calcium scoring; however, the number of patients in these studies was relatively limited.[21-23] Georgiou et al performed a prospective observational study of 192 patients with acute chest pain and demonstrated that the presence of coronary calcium was a strong predictor of future cardiac events.[21] In addition, the authors elegantly demonstrated that the absence of coronary calcifications had a very low risk for future cardiac events (< 1%). Moreover, McLaughlin et al performed coronary calcium scoring in 134 patients with suspected ACS and a normal or non-diagnostic ECG. The authors found that the absence of calcium had a high negative predictive value (98%) for ruling out the presence of ACS.[23]

Nevertheless, when comparing coronary calcium scores of patients with stable angina to patients with acute myocardial infarction, significant differences have been observed.[24] Extensive calcium was more often present in the coronary arteries of patients with chronic stable angina, whereas patients with acute myocardial infarction demonstrated only mildly calcified or non-calcified culprit arteries. Similar results were shown in a study by Henneman et al who showed that in 40 patients suspected of ACS coronary calcium was absent in 13 patients (33%).[25] Importantly, in 5 (39%) of the 13 patients without coronary calcium, significant CAD was identified on CCA (example shown in Figure 5). Thus, particularly in the acute setting, absence of coronary calcification may not invariably imply the absence of atherosclerotic plaque. Moreover, the presence of coronary calcification does not by definition explain the actual cause of chest pain. Evidently, there is a need for more research to define the role of coronary calcium scoring in patients with acute chest pain. The current guidelines therefore do not recommend coronary calcium scoring as a screening method for patients suspected of ACS.[26] However, in asymptomatic patients initially classified as being at intermediate risk, knowledge of the extent of coronary calcium may be valuable for refining risk stratification and determining further management.

Figure 5. Example of a patient presenting with suspected ACS in which calcium scoring and contrast-enhanced coronary CT angiography was performed to exclude coronary artery disease. Although no calcium was demonstrated by the calcium score (A), an obstructive non-calcified plaque with a super-imposed thrombus in the right coronary artery (RCA) was detected on coronary CT angiography (B,C). The volume rendered 3D reconstruction (B) and curved multiplanar reconstruction (C) show an occlusion in the mid segment of the RCA (white arrows). (D) This finding was confirmed on invasive conventional coronary angiography (white arrow). Ao; aorta, LAD; left anterior descending coronary artery, LCx; left circumflex coronary artery. Reprinted with permission from Henneman et al.[25]

Right coronary artery

Left anterior descending coronary artery

Left circumflex coronary artery

Figure 6. Example of coronary CT angiography performed to rule out ACS in a 43 year old male admitted because of acute chest pain and intermediate risk profile. Curved multiplanar reconstructions (MPRs) in two different views of the right coronary artery, left anterior descending coronary artery and left circumflex coronary artery are shown demonstrating normal coronary arteries.

CORONARY CT ANGIOGRAPHY

Evaluation of CAD in general population with coronary CT angiography

With the current generation 64-slice scanners with improved temporal and spatial resolution a good diagnostic accuracy for detection of obstructive CAD both in proximal coronary vessels and smaller distal vessels has been observed. Indeed, a high sensitivity (ranging from 85 - 99%) and specificity (ranging from 83 - 90%) of 64-slice CT angiography for the detection of obstructive lesions as compared to CCA has been demonstrated.[5] [6 27] More importantly, due to the high negative predictive value, coronary CT angiography has an excellent ability to exclude significant CAD (Figure 6). Accordingly, if patients show normal coronary arteries on coronary CT angiography no further testing is required and patients can be reassured. However, a significant limitation of CT angiography remains the relatively low positive predictive value (ranging from 64 to 93%). As a result, atherosclerotic lesions are still frequently being overestimated on CT which occasionally may lead to unnecessary referral for invasive CCA. Moreover, it should be noted that the diagnostic performance of CT coronary angiography is influenced by the pre-test likelihood of significant CAD (Table 1). Indeed, a recent study showed that the benefit from this non-invasive modality is highest in patients with a low to intermediate pre-test likelihood for CAD due to its excellent ability to rule out obstructive CAD.[28] Similar results were recently published by Henneman et al demonstrating that coronary CT was able to rule out coronary atherosclerosis in 58% of patients with low pre-test likelihood.[29] However, in patients with a high pre-test likelihood, CT was often abnormal and CAD was ruled out in only 17% of patients. Consequently, the remaining 83% of patients with a high pre-test likelihood and abnormalities on coronary CT angiography still required further functional and/or invasive testing. Therefore, to avoid layered testing and delayed diagnosis, these patients should be directly referred for either functional testing or invasive CCA. Accordingly, current guidelines state that if the pre-test likelihood of CAD is high, invasive CCA remains the test of first choice and the additional value of non-invasive coronary angiography may be limited.

Table 1. Diagnostic accuracy of 64-slice CT angiography for detection for significant stenosis (≥ 50%) according to pre-test probability. As can be derived from the table, patients with a low to intermediate likelihood benefit the most from non-invasive coronary CT angiography as the sensitivity and specificity (and negative predictive value to rule out CAD) is higher in these patients. Data adapted from Meijboom et al.[28]

Pre-test probability	N	Sensitivity	Specificity	PPV	NPV
Low	66	100%	93%	78%	100%
Intermediate	83	100%	84%	80%	100%
High	105	98%	74%	93%	89%

Evaluation of CAD in patients with suspected ACS with coronary CT angiography

A major advantage of coronary CT angiography is that it is a non-invasive, fast and accurate modality for ruling out the presence of CAD and severe stenosis, features that are particularly useful in the emergency department. Several investigations have assessed the value of coronary CT angiography in patients presenting with ACS (an example is provided in Figure 7). Preliminary studies investigating the efficacy of CT in the diagnosis of ACS were performed with 4- and 16-slice systems.[30][31] Ghersin et al studied 62 patients
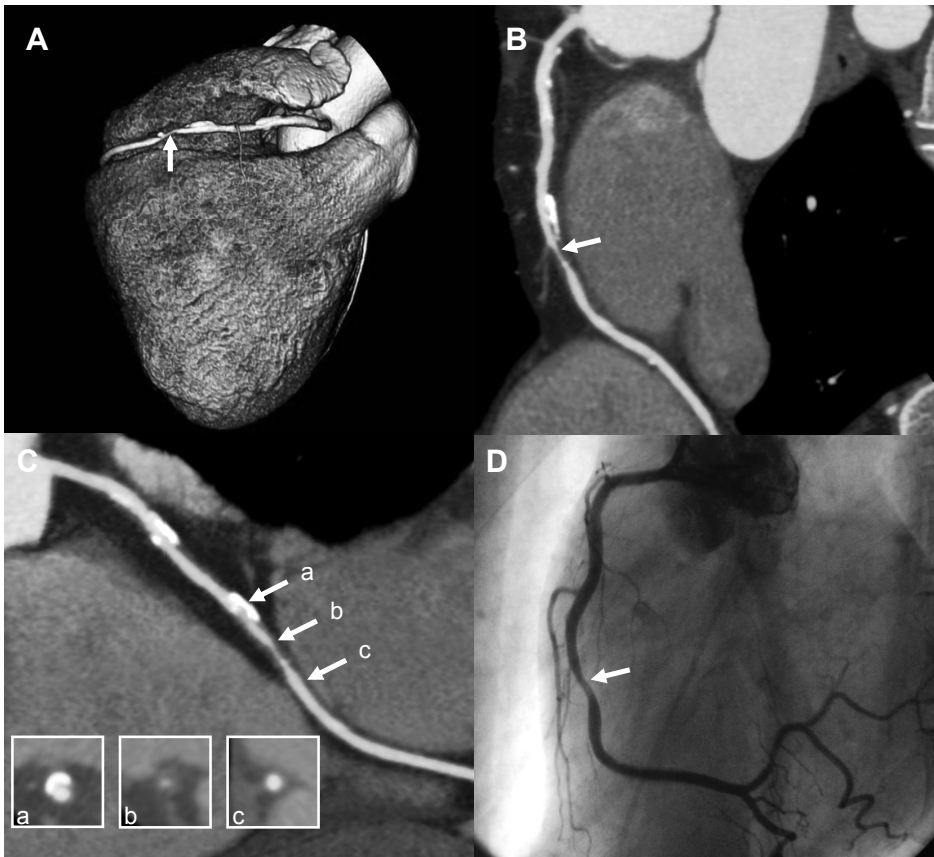
Figure 7. Example of non-invasive coronary angiography with computed tomography in a patient presenting with suspected ACS. In (A), a 3D volume rendered reconstruction is provided, showing a large dominant right coronary artery (RCA) with signs of luminal narrowing (white arrow). (B) A curved multiplanar reconstruction (MPR) of the RCA is shown demonstrating the presence of significant luminal narrowing in the mid segment (arrow). (C) Another curved MPR in a different view, revealing the presence of significant stenosis (arrows). Cross-sectional CT images (inlays) show the presence of calcified plaque proximal to the stenosis (a), exclusively non-calcified plaque within the stenosis (b), and no coronary plaque distal from the stenosis (c). (D) Conventional coronary angiography confirming the presence of significant luminal narrowing of the RCA (arrow).

Table 2. Studies assessing the diagnostic accuracy of dedicated coronary 64-slice CT angiography in patients presenting with acute chest pain in the emergency department.

	N	Pre-test probability	% ACS	Sensitivity	Specificity	PPV	NPV
Hoffman et al.[33]	103	Low	14%	100%	82%	47%	100%
Gallagher et al.[39]	85	Low	8%	86%	92%	50%	99%
Rubinstein et al.[36]	58	Intermediate	34%	100%	92%	87%	100%
Goldstein et al.[32]	99	Low	8%	100%	74%	25%	100%
Hoffman et al.[34]	368	Low	8%	100%	84%	35%	100%

ACS; acute coronary syndrome, PPV; positive predictive value, NNP; negative predictive value

hospitalized with suspected ACS and found a moderate sensitivity (80%) and specificity (89%) for the detection of significant CAD (defined as ≥ 50% luminal narrowing).[30] Subsequent studies have been performed using 64-slice systems (Table 2), with higher spatial and temporal resolution, evaluating coronary plaque and stenosis in patients presenting with ACS.[32-36] For instance, Rubinshtein and colleagues evaluated the efficacy of coronary CT angiography for initial triage in 58 patients with suspected ACS and assessed clinical outcomes during a follow-up of 15 months.[36] During the follow-up period, no deaths or myocardial infarctions occurred in the 35 patients discharged from the emergency department after initial triage and with normal CT findings. The authors concluded that coronary CT angiography had a high positive predictive value for diagnosing ACS, whereas a normal CT study predicted a low rate of major adverse cardiovascular events and favourable outcome during follow-up. Most recently, the ROMICAT (Rule Out Myocardial Infarction using Computed Assisted Tomography) trial evaluated 368 patients suspected of ACS and demonstrated that 50% of patients with acute chest pain with a low to intermediate likelihood of ACS were free of CAD by coronary CT angiography and had no ACS. The authors concluded that given the large number of such patients, initial evaluation with coronary CT angiography may significantly improve patient management in the emergency department. These results are in line with most studies signifying that coronary CT angiography is useful and safe in ruling out CAD and facilitates early and accurate release of patients with acute chest pain.[32-36] Additionally, CT evaluation reduced diagnostic time, lowered costs and required fewer repeat investigations when compared to standard of care.[32] Of note, the majority of patients included in the abovementioned studies were classified as having a low to intermediate risk for ACS (normal or non-diagnostic ECG and normal first cardiac enzymes). In addition, the presence of a significant stenosis on coronary CT does not by definition confirm the presence of ACS. Importantly, there is no additional role for coronary CT angiography in patients with evident myocardial infarction. Naturally, high risk patients should immediately be referred for invasive CCA and coronary CT angiography would only cause significant delay. At present, there are no formal guidelines for the use of CT in patients with acute chest pain, although appropriateness criteria and consensus documents have recently been published.[37 38] Currently, more large randomized clinical trials should be performed to determine the accuracy and benefits of coronary CT

angiography for triage of patients with acute chest pain prior to implementation of this technique. However, in the future, initial evaluation with coronary CT angiography may play an important role, especially in a population with low to intermediate risk for ACS in whom the incremental value of non-invasive imaging may have a significant impact on patient management.

CT ANGIOGRAPHY OF AORTA AND PULMONARY ARTERIES

Non-cardiac causes of acute chest pain concerning vascular structures in the thorax such as aortic aneurysms, dissection, pulmonary emboli and pathology of the chest wall can be easily visualized by CT angiography. CT angiography of other vascular beds than the heart is less complex if non ECG gating techniques are used. ECG gating may be used to improve image quality. In addition, contrast-enhancement in the blood pool is required to visualize the vascular structures; therefore intravenous contrast is still needed. Several common principles should be applied to all imaging protocols to provide optimal diagnostic image quality such as bolus-timing for optimization of contrast delivery in the vessel, fast high resolution acquisition and administration of approximately 60 - 120 ml of contrast material (dependent on patient size, contrast agent used and scanner type) injected at rapid infusion rates (4 – 5 ml/s).

Thoracic aortic aneurysm

In general, an ascending aortic diameter equal to or greater than 4 cm (when younger than 60 years old) is considered an aneurysm (Figure 8). Atherosclerosis is, as expected, the most frequent cause of thoracic aneurysms (70%). Two different types of thoracic aortic aneurysms can be identified according to their pathological features. First, a true aneurysm, in which all three layers of the vessel wall are involved (intima, media and adventitia) and which is characterized by a fusiform shape (Figure 8). Secondly, a false aneurysm (or pseudo-aneurysm), in which the intima is disrupted and the blood is contained by the adventitia. CT angiography is the most robust tool for evaluating aortic aneurysms and some key features should be evaluated when using CT such as maximal aortic diameter, presence of thrombus, shape and extent of the aneurysm, involvement of aortic branches, relationship to adjacent structures and presence of aortic calcifications. As in 23% of cases a thoracic aneurysm co-exists with an abdominal aortic aneurysm, evaluation of the whole aorta should be performed. Most importantly, CT shows excellent accuracy for characterizing important features of aneurysms.[40]

Aortic dissection

Aortic dissection is the most common disorder of the acute aortic syndromes and also has the highest mortality rate. Aortic dissection occurs when a tear in the media layer allows blood to enter within and along the vessel wall and results in separation of the layers of the aorta. In most patients, an intima disruption is present that leads to the
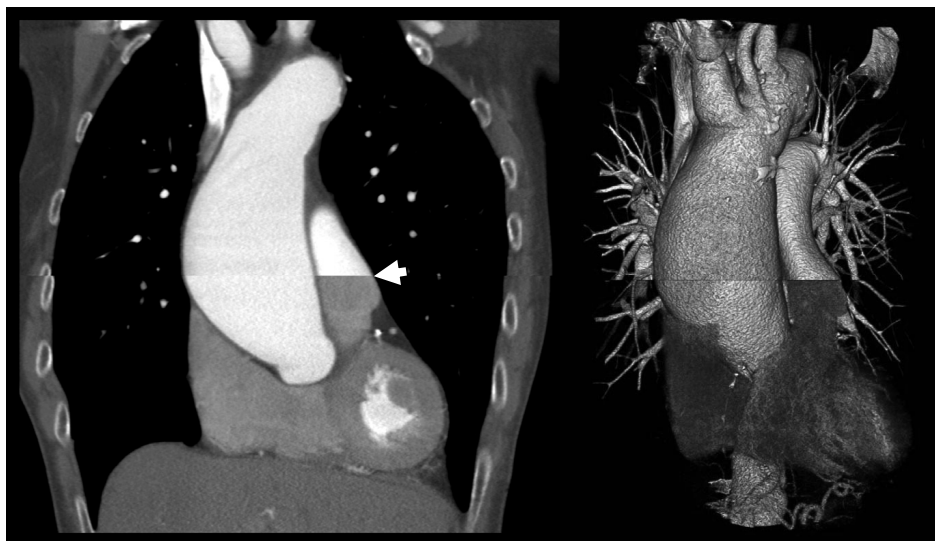
Figure 8. Electrocardiography (ECG)-gated thoracic computed tomography (CT) showing an aneurysm of the ascending aorta in a coronal view and 3D volume rendering representation. Acquisition was performed by 2 x 16 cm volume rotations with a 320-detector-row CT scanner. As a result of the time delay between the two rotations in combination with short contrast bolus injection, a difference in pulmonary artery contrast-enhancement can be observed (arrowhead). The pulmonary artery contrast difference does not hamper evaluation of the aorta. Note the sharp reconstruction of the ascending aorta using ECG-gating at end-systole at a cardiac frequency of 75 beats per minute.

development of a true and false lumen, separated by a "flap". There are currently two classification systems: the De Bakey classification and the Stanford classification. The De Bakey type I dissection involves both the ascending and descending thoracic aorta. The De Bakey type II dissection only involves the ascending aorta while the De Bakey type III dissection only involves the descending aorta. The Stanford system is more clinically useful and uses the following classification: In Stanford type A the dissection is located in the ascending aorta and aortic arch, either with or without involvement of the descending aorta, while Stanford type B dissections are limited to the descending aorta alone. Type A acute aortic dissection has the worst prognosis and generally should be immediately surgically repaired to avoid fatal complications.

When aortic dissection is suspected, urgent high resolution imaging is required to confirm the diagnosis. For this purpose; CT angiography, magnetic resonance imaging (MRI) and transesophageal echocardiography (TEE) have been shown to be equally accurate for confirming or excluding the diagnosis of thoracic aortic dissection.[41] Currently, CT angiography is the most commonly used technology for the assessment of patients suspected of aortic dissection (Figure 9). Indeed, CT angiography has an excellent sensitivity and specificity of almost 100% for the detection of aortic dissection, as has been reported by various studies.[42 43] CT scanning protocols for patients suspected of thoracic aortic dissection should include unenhanced (for depicting intramural hematoma) and
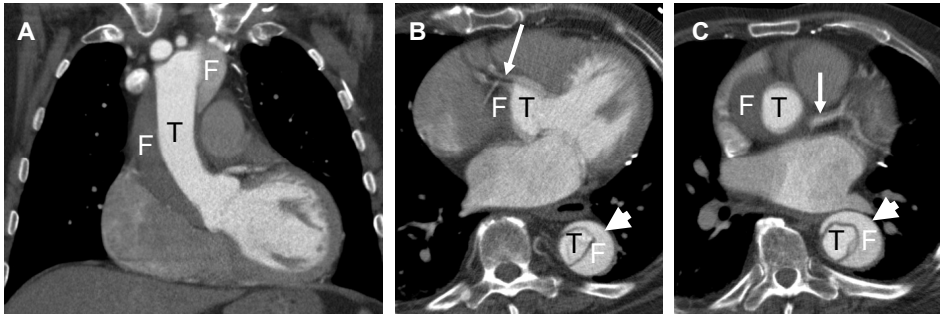
Figure 9. Thoracic computed tomography (CT) angiography showing a type A aortic dissection (A). The right coronary artery is contrast-enhanced and has its origin from the true lumen (arrow, B). The right coronary artery has double appearance due to motion artefacts in this non-electrocardiography (ECG) gated scan. The left main coronary artery stem (arrow, C) is also contrast-enhanced and had its origin from the true lumen. Carotid and subclavian arteries as well as the visceral arteries all had their origin from the true lumen. Note the almost complete disruption between the true and false lumen of the descending aorta (arrowheads B, C). F, false lumen; T, true lumen.

contrast-enhanced image acquisition with visualization of the entire aorta. The key features of dissection on contrast-enhanced images are: a flap separating two lumens (usually the convexity of the intimal flap is towards the false lumen), contrast arriving in the true lumen first followed by the false lumen, slower flow in the false lumen and presence of pleural and/ or pericardial effusion. CT should also be used to accurately locate the position of the intimal tear site, as this is important for the surgical approach.

Pulmonary embolism

The renowned Wells' clinical decision rule is used to risk stratify patients suspected of pulmonary embolism.[44] This is a scoring method based on various clinical risk factors and stratifies patients as low, intermediate or high risk. If a patient has a score of greater than four, further testing is required. CT pulmonary angiography has been demonstrated to provide high diagnostic accuracy for the detection of pulmonary embolism and patients with a high-quality negative CT examination do not require further examination.[45] [46] On CT, pulmonary emboli are shown as filling defects in the contrast-enhanced central or (sub)segmental pulmonary arteries (Figure 10). Currently, contrast-enhanced CT pulmonary angiography is the imaging method of choice for the detection of pulmonary emboli and thus replacing ventilation-perfusion imaging.

TRIPLE RULE-OUT CT

The concept of the "triple rule-out" protocol is to simultaneously exclude all three potentially life threatening causes of acute chest pain, such as ACS or myocardial infarction, acute aortic dissection and pulmonary embolism, in one single CT examination. A triple
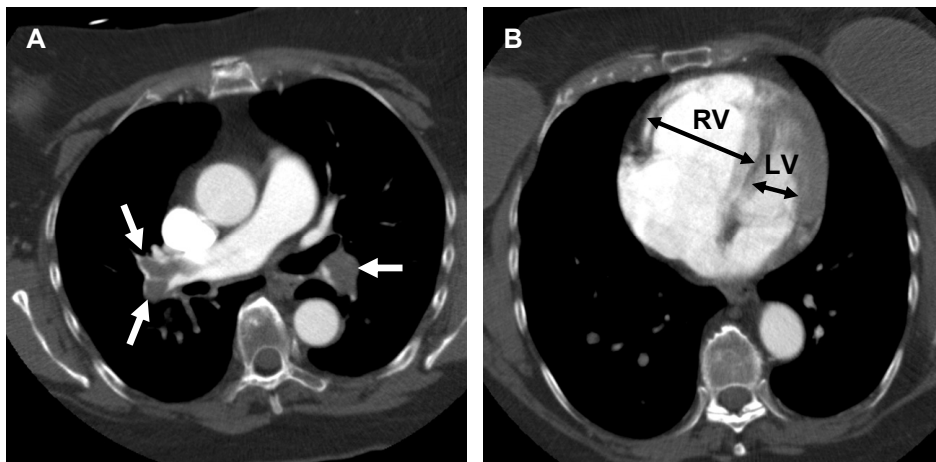
Figure 10. Patient with acute pulmonary embolism and high embolus-load. Massive emboli in the left and right pulmonary arteries can be observed (arrows, A). Note severe dilatation of the right ventricle (RV, B) with interventricular septum shift to the left and compression of the left ventricle (LV) due to high embolus load. Normally the RV diameter does not exceed that of the LV.

rule-out scan protocol includes coverage of the entire thorax cavity including the aortic arch. Although 16-slice scanners have allowed for the adequate evaluation of coronary arteries, these systems were not fast enough to provide a high resolution scan of the entire thorax in addition to an ECG gated scan of the coronary arteries. Newer, state-of-the-art 64-slice scanners with wider anatomic coverage are able to scan the entire thorax including the pulmonary arteries, thoracic aorta and coronary arteries in a single breath hold of approximately 15 - 20 seconds. However, an important technical challenge of a "triple rule-out" scan protocol is to ensure that high contrast-enhancement is present simultaneously in both the right and left circulation to evaluate the pulmonary and aorta including the coronary arteries. Recent data reporting the implementation of a tri-phasic contrast injection protocol (first bolus of 100 ml of at 5 ml/s, followed by a second bolus of 30 ml contrast at 3 ml/s, followed by a saline flush) showed promising results with satisfactory contrast-enhancement of coronary, aortic, and pulmonary vasculature in a single breath hold.[47] Potentially, this new approach may improve the triage of patients presenting to the emergency department with acute chest pain, and provide a faster algorithm to make a diagnosis. However, it is crucial that patients should be carefully selected to ensure the appropriate use of a triple rule-out CT protocol. Indeed, as the triple rule-out protocol may involve retrospective gating of the entire thorax, radiation dose is high, even more than the radiation dose observed in dedicated coronary CT angiography.[48] [49] Prospective gating techniques may reduce radiation dose, but cannot be applied effectively in patients with high heart rates. Therefore, patients with symptoms highly suggestive for either ACS, acute pulmonary embolism or acute aortic dissection, should be referred for a work-up specifically designed for this purpose (such as invasive CCA if a patient has a high risk for ACS). Notably, presence of a significant stenosis on CT angiography does not

automatically confirm the presence of ACS. In the remaining patients with uncertain cause of the acute chest pain complaints, a triple rule-out protocol can be considered. Initial studies suggest that a triple rule-out CT angiography protocol for evaluation of patients with acute chest pain is feasible and that quantitative parameters of image quality may be comparable to the conventional, dedicated coronary and pulmonary CT angiography protocols.[50][51] A study evaluating the diagnostic value of triple rule-out with 64-slice CT in the emergency department demonstrated that this technique facilitated the differential diagnosis of chest pain.[50] In total, 55 patients underwent 64-slice CT angiography and in 22 patients (40%) a definite diagnosis was made (pulmonary embolism (n = 10), coronary stenosis (n = 9), and aortic dissection (n = 1)). Furthermore, a recent study demonstrated that the triple rule-out protocol could potentially identify a subset of patients with acute chest pain who can safely be discharged from the emergency department without adverse events during a 30-day follow-up.[52] Indeed, more randomized control trials are needed to determine whether this protocol is safe, cost-effective, and improves clinical decision making before routine use of such a technique can be justified.

OTHER APPLICATIONS OF CT

Evaluation of plaque composition

An important advantage of coronary CT angiography is that not only luminal narrowing can be visualized but also atherosclerotic plaque composition. Three different plaques types can be distinguished by coronary CT; non-calcified plaque, mixed plaque and calcified plaque. More interestingly, plaque composition on coronary CT angiography has been linked to clinical presentation. Indeed, non-calcified and mixed plaques have been shown to be more prevalent in patients with ACS whereas extensively calcified plaques have been associated with stable CAD.[53] In addition, it has been suggested that certain plaque features have prognostic value. In prospective studies, non-calcified plaques with low attenuation values, positive remodeling and spotty calcifications have been associated with subsequent development of ACS (Figure 11).[54][55] Although further characterization of non-calcified plaque remains challenging, more improvements are expected, possibly allowing for improved identification of patients at risk.[56]

Evaluation of myocardial function

Another particular advantage of CT angiography is that it allows assessment of cardiac function. If data have been collected during the whole cardiac cycle, images can be retrospectively reconstructed in several phases. The end-systolic and end-diastolic phases can then be used to determine end-systolic and end-diastolic volumes to derive left ventricular ejection fraction. Indeed, numerous studies have shown that global left ventricular function by CT correlates well with echocardiography and MRI although a slight tendency of CT to overestimate end-systolic volumes and thus slightly underestimate left ventricular ejection fraction has been reported.[57][58] In addition, regional wall motion
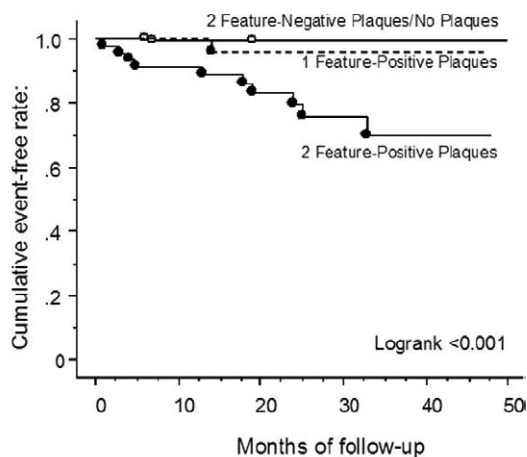
Figure 11. Kaplan-Meier curve demonstrating the cumulative event free rate for development of ACS on the basis of plaque features which include positive vessel remodelling and low-attenuation plaques. Patient stratification was performed according to the presence of 2- and 1-feature positive, and 2-feature negative plaques/no plaques. Interestingly, 2-feature positive plaques show significant worse survival than 1-feature positive or 2-feature negative plaques. Reprinted with permission from Motoyama et al.[55]

abnormalities can be reliably evaluated as compared to MRI.[59] However, as images should be acquired throughout the cardiac cycle, left ventricular function protocols are associated with increased radiation exposure. Accordingly, the necessity of function measurements with CT should be carefully determined in each patient.

Evaluation of myocardial infarction

Over recent years, MRI has been successfully employed to image the presence of infarcted myocardium with delayed enhancement imaging. However, several studies have demonstrated that the presence of myocardial infarction can be also identified on CT.[60] Due to the pharmokinetics of the contrast material a difference between the accumulation of contrast in infarcted and normal myocardium can be visualized. Accordingly, early hypoenhancement can be observed on the CT images during the first pass of contrast medium at the area of infarcted myocardium. In addition, delayed hyperenhancement of infarcted tissue can be detected similar to MRI. Interestingly, a good correlation between infarct imaging with CT and other imaging modalities such as MRI and nuclear imaging has been demonstrated.[60-62] Moreover, a good correlation between enhancement patterns (both early hypoenhancement and late hyperenhancement) and recovery of myocardial function at a follow-up of 3 months was found, suggesting that CT may be useful to predict myocardial functional recovery after infarction.[63] However, it is important to realize that in general, delayed enhancement imaging with CT requires additional imaging and thus involves additional radiation exposure. Also, a larger amount of contrast agent is

required for delayed enhancement imaging as compared to imaging the coronary arteries alone.

Evaluation of myocardial perfusion

A major limitation of coronary CT angiography is that the hemodynamical significance of atherosclerotic lesions cannot be assessed. Indeed, functional information is of particular importance in regard to lesions with borderline luminal narrowing. Interestingly, due to recent developments in scanner technology, it has become possible to image myocardial perfusion and to determine the presence of ischemia through perfusion imaging during stress.[64] The technique is based on myocardial tissue attenuation changes during the infusion of contrast medium. Consequently, CT perfusion imaging can detect the presence of myocardial perfusion defects during stress that resolve during rest, indicating the presence of ischemia. Recent studies have been published demonstrating the feasibility of stress-rest myocardial perfusion imaging with CT in humans.[65-67] Blankstein et al demonstrated using 64-slice CT that an adenosine stress CT protocol can identify stress-induced myocardial perfusion defects with a diagnostic accuracy comparable to SPECT.[65] Additionally, the average radiation with this protocol was similar to the SPECT radiation dose. In addition, George et al showed that using both 64-slice and 256-slice CT that the combination of coronary CT angiography and adenosine perfusion CT allowed detection of hemodynamically relevant lesions with high diagnostic accuracy.[66] Importantly, the combination of both anatomical and functional data may improve the diagnostic accuracy of CT and optimize patient management. However, before CT perfusion imaging can be implemented in daily clinical practice, its accuracy should be confirmed in additional, larger prospective studies.

EXTRACARDIAC FINDINGS

Beyond evaluating the coronary arteries, other cardiac findings and/or extracardiac findings may be identified during coronary CT angiography. Interestingly, extracardiac

Figure 12. Large diaphragmatic hernia causing intra-thoracic located stomach (between arrows). Large diaphragmatic hernia may cause chest complaints resembling those of coronary artery disease.

findings provide an explanation for chest pain complaints in 4% to 8% of patients (Figure 12)[68 69] or may be incidental findings not related to chest complaints. Several studies have shown that extracardiac findings are present in a large proportion of patients (approximately 50%).[68-71] However, many of these findings are not significant and do not require follow-up or treatment, such as an incidental small calcified pulmonary nodule or calcified lymph nodes. However, 2% to 5% of patients do have significant findings requiring immediate further diagnostic action, such as a suspected malignancy which may necessitate immediate therapeutic actions, or the presence of acute pulmonary embolism or pneumonia.[68 70 72 73] Other findings, e.g., pulmonary nodules with low suspicion for malignancy, may require non-urgent further investigation or follow up.[74] It is estimated that the patient population requiring further follow-up comprises approximately 15% of patients undergoing coronary CT angiography.[68-71 75 76]

For coronary artery assessment, a zoomed-in small field-of-view focused on the heart is reconstructed as to obtaining maximal spatial resolution for evaluation. However, this focused view only reveals 36% of the total chest volume, whereas 70% of the total chest volume has been exposed to radiation.[73] Substantially more significant extracardiac pathology is found on maximum full-field reconstructions than on small-field reconstructions.[70] Therefore the maximum full-field reconstructions should be reviewed for optimal identification of extracardiac pathology.[68 70 71 73]

LIMITATIONS AND FUTURE DEVELOPMENTS

Limitations

Coronary CT angiography has several major limiting factors that effects its usefulness in patients admitted to the emergency department and the ICCU. The technique is particularly limited in patients with an irregular heart rhythm, elevated heart rate and a high body mass index. Indeed, the heart rate and regularity of the rhythm is closely related to image quality and accuracy of coronary stenosis assessment. Therefore, it is essential to provide adequate pre-medication with beta-blockers (orally or intravenously) to reduce the heart rate below 65 beats/min for optimal image quality. Moreover, coronary CT angiography has particularly been criticized to be an important source of ionizing radiation in the population. The effective radiation dose with retrospective 64-slice CT coronary angiography is estimated to range approximately from 7 to 23 mSv.[77] However, with the use of ECG dose modulation, a method that reduces tube current during systole, a radiation dose reduction of 30 to 50% can be achieved.[49] Moreover, prospective ECG triggered CT angiography has been shown to reduce radiation dose by 80% often resulting in effective radiation doses of < 3 mSv.[78] Notably, the triple rule-out CT angiography protocol is associated with an even higher radiation dose than with dedicated coronary CT and mean radiation doses of 18 mSv have been reported. However, when implementing ECG dose modulation, the mean radiation dose can be reduced to < 10 mSv.[79] In addition, contrast administration is associated with nephrotoxicity and adverse reactions. Therefore,

it is essential to verify that renal function is not impaired prior to referring patients for contrast-enhanced CT angiography studies.

Future developments

CT technology is evolving quickly. Most recently 256- and 320-detector row scanners have been introduced, which have higher volume coverage and improved temporal and spatial resolution.[10 80] Complete volume coverage of the heart in a single heart beat is possible thereby reducing the motion artifacts in patients with irregular heart rates. Furthermore, additional radiation dose reduction has been achieved with the implementation of prospective ECG triggering by scanning only during a small pre-defined phase of the R-R interval. Moreover, dual-source CT systems with 2 × 128 detector rows have been introduced demonstrating a high temporal resolution of 75 ms (approximately half of the temporal resolution of the fastest 64-slice CT) making it possible to freeze cardiac motion and obtain diagnostic quality images of the coronary arteries regardless of heart rate. Initial studies with dual-source coronary CT in patients presenting with chest pain have reported high negative predictive values of almost 100% for detecting coronary artery stenoses, even in patients with higher heart rates.[81] Most recently, high-pitch ECG triggered ("Flash Spiral") dual-source CT scanners have shown promising results. The novelty of this technique lies in the very high pitch which results in fast image acquisition without cardiac motion artifacts and a very low radiation exposure (mean estimated effective radiation dose of 1.0 ±0.3 mSv).[82] Nevertheless, as these techniques are relatively new, only limited data are currently available. Prospective studies are needed to validate these novel applications of CT for use in standard clinical practice.

PERSONAL PERSPECTIVE

Preliminary data suggest that coronary CT angiography has the potential to evaluate patients with acute chest pain and possibly improve diagnosis and management strategies. Improvements in technology (faster gantry rotation times, thinner detectors, volumetric coverage) and consequential improvement in image quality have resulted in a high diagnostic accuracy for detecting obstructive CAD in stable patients with low to intermediate likelihood. However, despite the excellent negative predictive value for ruling out of CAD, there are still a considerable number of false positive studies. Moreover, another drawback is that at present the hemodynamical significance of a lesion cannot be evaluated. Nevertheless, there are some features distinctive for coronary CT angiography which renders this technique very suitable for use in the diagnostic work-up of patients presenting with acute chest pain. The technique is non-invasive, relatively fast and simple to use and generally widely available. Furthermore, contrast-enhanced CT angiography is the imaging modality of choice regarding the detection of non-coronary causes of acute chest pain such as aortic aneurysms, aortic dissection, or pulmonary embolism. Notably, radiation exposure is a major concern which needs to be carefully considered when

referring patients for coronary CT angiography. However, newer CT systems are available with dose saving innovations such a prospective triggering and dose modulation, allowing substantial radiation dose reduction. Overall, large randomized controlled trials are needed to assess the safety, efficacy and cost-effectiveness of the use of coronary CT angiography in patients with acute chest pain, before an evidence based recommendation can be made.

CONCLUSION

A major advantage of coronary CT angiography is that it is a non-invasive, fast and accurate modality for ruling out the presence of CAD and severe stenosis, features that are particularly useful in the emergency department. Recent investigations have demonstrated that use of coronary CT angiography is very promising in the diagnostic work-up of patients presenting with acute chest pain. Accordingly, if patients show normal coronary arteries on coronary CT angiography no further additional testing is required and patients can be reassured. Moreover, a normal CT angiography without any sign of CAD appears to be associated with a good short-term prognosis. However, the presence of some degree of coronary atherosclerosis might not fully exclude the presence of ACS and therefore further investigations are still needed. Nevertheless, coronary CT angiography is an excellent modality in patients whose symptoms suggest other non-coronary causes of acute chest pain such as aortic aneurysms, aortic dissection or pulmonary embolism. Accordingly, coronary CT angiography has much promise for evaluation of patients with acute chest pain, but it requires further investigation to determine its role in this setting.

REFERENCES

1. Hounsfield GN. Computerized transverse axial scanning (tomography). 1. Description of system. Br J Radiol 1973;46:1016-22.
2. Achenbach S, Giesler T, Ropers D et al. Detection of coronary artery stenoses by contrast-enhanced, retrospectively electrocardiographically-gated, multislice spiral computed tomography. Circulation 2001;103:2535-8.
3. Knez A, Becker CR, Leber A et al. Usefulness of multislice spiral computed tomography angiography for determination of coronary artery stenoses. Am J Cardiol 2001;88:1191-4.
4. Nieman K, Oudkerk M, Rensing BJ et al. Coronary angiography with multi-slice computed tomography. Lancet 2001;357:599-603.
5. Budoff MJ, Dowe D, Jollis JG et al. Diagnostic performance of 64-multidetector row coronary computed tomographic angiography for evaluation of coronary artery stenosis in individuals without known coronary artery disease: results from the prospective multicenter ACCURACY (Assessment by Coronary Computed Tomographic Angiography of Individuals Undergoing Invasive Coronary Angiography) trial. J Am Coll Cardiol 2008;52:1724-32.
6. Miller JM, Rochitte CE, Dewey M et al. Diagnostic performance of coronary angiography by 64-row CT. N Engl J Med 2008;359:2324-36.
7. Lee TH, Goldman L. Evaluation of the patient with acute chest pain. N Engl J Med 2000;342: 1187-95.
8. Reilly BM, Evans AT, Schaider JJ et al. Impact of a clinical decision rule on hospital triage of patients with suspected acute cardiac ischemia in the emergency department. JAMA 2002;288: 342-50.
9. Earls JP, Berman EL, Urban BA et al. Prospectively gated transverse coronary CT angiography versus retrospectively gated helical technique: improved image quality and reduced radiation dose. Radiology 2008;246:742-53.
10. Dewey M, Zimmermann E, Deissenrieder F et al. Noninvasive coronary angiography by 320-row computed tomography with lower radiation exposure and maintained diagnostic accuracy: comparison of results with cardiac catheterization in a head-to-head pilot investigation. Circulation 2009;120:867-75.
11. Agatston AS, Janowitz WR, Hildner FJ et al. Quantification of coronary artery calcium using ultrafast computed tomography. J Am Coll Cardiol 1990;15:827-32.
12. Margolis JR, Chen JT, Kong Y et al. The diagnostic and prognostic significance of coronary artery calcification. A report of 800 cases. Radiology 1980;137:609-16.
13. McClelland RL, Chung H, Detrano R et al. Distribution of coronary artery calcium by race, gender, and age: results from the Multi-Ethnic Study of Atherosclerosis (MESA). Circulation 2006; 113:30-7.
14. Rumberger JA, Simons DB, Fitzpatrick LA et al. Coronary artery calcium area by electron-beam computed tomography and coronary atherosclerotic plaque area. A histopathologic correlative study. Circulation 1995;92:2157-62.
15. Greenland P. ACCF/AHA 2007 clinical expert consensus document on coronary artery calcium scoring by computed tomography in global cardiovascular risk assessment and in evaluation of patients with chest pain: a report of the American College of Cardiology Foundation Clinical Expert Consensus Task Force (ACCF/AHA Writing Committee to Update the 2000 Expert Consensus Document on Electron Beam Computed Tomography) developed in collaboration with the Society of Atherosclerosis Imaging and Prevention and the Society of Cardiovascular Computed Tomography. J Am Coll Cardiol 2007;49:378-402.
16. Hoff JA, Chomka EV, Krainik AJ et al. Age and gender distributions of coronary artery calcium detected by electron beam tomography in 35,246 adults. Am J Cardiol 2001;87:1335-9.

17. Haberl R, Becker A, Leber A et al. Correlation of coronary calcification and angiographically documented stenoses in patients with suspected coronary artery disease: results of 1,764 patients. J Am Coll Cardiol 2001;37:451-7.

18. Budoff MJ, Diamond GA, Raggi P et al. Continuous probabilistic prediction of angiographically significant coronary artery disease using electron beam tomography. Circulation 2002;105: 1791-6.

19. Budoff MJ, Shaw LJ, Liu ST et al. Long-term prognosis associated with coronary calcification: observations from a registry of 25,253 patients. J Am Coll Cardiol 2007;49:1860-70.

20. Greenland P, LaBree L, Azen SP et al. Coronary artery calcium score combined with Framingham score for risk prediction in asymptomatic individuals. JAMA 2004;291:210-5.

21. Georgiou D, Budoff MJ, Kaufer E et al. Screening patients with chest pain in the emergency department using electron beam tomography: a follow-up study. J Am Coll Cardiol 2001;38: 105-10.

22. Laudon DA, Vukov LF, Breen JF et al. Use of electron-beam computed tomography in the evaluation of chest pain patients in the emergency department. Ann Emerg Med 1999;33:15-21.

23. McLaughlin VV, Balogh T, Rich S. Utility of electron beam computed tomography to stratify patients presenting to the emergency room with chest pain. Am J Cardiol 1999;84:327-8, A8.

24. Shemesh J, Stroh CI, Tenenbaum A et al. Comparison of coronary calcium in stable angina pectoris and in first acute myocardial infarction utilizing double helical computerized tomography. Am J Cardiol 1998;81:271-5.

25. Henneman MM, Schuijf JD, Pundziute G et al. Noninvasive evaluation with multislice computed tomography in suspected acute coronary syndrome: plaque morphology on multislice computed tomography versus coronary calcium score. J Am Coll Cardiol 2008;52:216-22.

26. Bertrand ME, Simoons ML, Fox KA et al. Management of acute coronary syndromes in patients presenting without persistent ST-segment elevation. Eur Heart J 2002;23:1809-40.

27. Mowatt G, Cook JA, Hillis GS et al. 64-Slice computed tomography angiography in the diagnosis and assessment of coronary artery disease: systematic review and meta-analysis. Heart 2008; 94:1386-93.

28. Meijboom WB, van Mieghem CA, Mollet NR et al. 64-slice computed tomography coronary angiography in patients with high, intermediate, or low pretest probability of significant coronary artery disease. J Am Coll Cardiol 2007;50:1469-75.

29. Henneman MM, Schuijf JD, van Werkhoven JM et al. Multi-slice computed tomography coronary angiography for ruling out suspected coronary artery disease: what is the prevalence of a normal study in a general clinical population? Eur Heart J 2008.

30. Ghersin E, Litmanovich D, Dragu R et al. 16-MDCT coronary angiography versus invasive coronary angiography in acute chest pain syndrome: a blinded prospective study. AJR Am J Roentgenol 2006;186:177-84.

31. Sato Y, Matsumoto N, Ichikawa M et al. Efficacy of multislice computed tomography for the detection of acute coronary syndrome in the emergency department. Circ J 2005;69:1047-51.

32. Goldstein JA, Gallagher MJ, O'Neill WW et al. A randomized controlled trial of multi-slice coronary computed tomography for evaluation of acute chest pain. J Am Coll Cardiol 2007;49: 863-71.

33. Hoffmann U, Nagurney JT, Moselewski F et al. Coronary multidetector computed tomography in the assessment of patients with acute chest pain. Circulation 2006;114:2251-60.

34. Hoffmann U, Bamberg F, Chae CU et al. Coronary computed tomography angiography for early triage of patients with acute chest pain: the ROMICAT (Rule Out Myocardial Infarction using Computer Assisted Tomography) trial. J Am Coll Cardiol 2009;53:1642-50.

35. Hollander JE, Chang AM, Shofer FS et al. One-year outcomes following coronary computerized tomographic angiography for evaluation of emergency department patients with potential acute coronary syndrome. Acad Emerg Med 2009;16:693-8.

36. Rubinshtein R, Halon DA, Gaspar T et al. Usefulness of 64-slice cardiac computed tomographic angiography for diagnosing acute coronary syndromes and predicting clinical outcome in emergency department patients with chest pain of uncertain origin. Circulation 2007;115:1762-8.

37. Hendel RC, Patel MR, Kramer CM et al. ACCF/ACR/SCCT/SCMR/ASNC/NASCI/SCAI/SIR 2006 appropriateness criteria for cardiac computed tomography and cardiac magnetic resonance imaging: a report of the American College of Cardiology Foundation Quality Strategic Directions Committee Appropriateness Criteria Working Group, American College of Radiology, Society of Cardiovascular Computed Tomography, Society for Cardiovascular Magnetic Resonance, American Society of Nuclear Cardiology, North American Society for Cardiac Imaging, Society for Cardiovascular Angiography and Interventions, and Society of Interventional Radiology. J Am Coll Cardiol 2006;48:1475-97.

38. Stillman AE, Oudkerk M, Ackerman M et al. Use of multidetector computed tomography for the assessment of acute chest pain: a consensus statement of the North American Society of Cardiac Imaging and the European Society of Cardiac Radiology. Eur Radiol 2007;17:2196-207.

39. Gallagher MJ, Ross MA, Raff GL et al. The diagnostic accuracy of 64-slice computed tomography coronary angiography compared with stress nuclear imaging in emergency department low-risk chest pain patients. Ann Emerg Med 2007;49:125-36.

40. Hartnell GG. Imaging of aortic aneurysms and dissection: CT and MRI. J Thorac Imaging 2001; 16:35-46.

41. Shiga T, Wajima Z, Apfel CC et al. Diagnostic accuracy of transesophageal echocardiography, helical computed tomography, and magnetic resonance imaging for suspected thoracic aortic dissection: systematic review and meta-analysis. Arch Intern Med 2006;166:1350-6.

42. Hayter RG, Rhea JT, Small A et al. Suspected aortic dissection and other aortic disorders: multi-detector row CT in 373 cases in the emergency setting. Radiology 2006;238:841-52.

43. Sommer T, Fehske W, Holzknecht N et al. Aortic dissection: a comparative study of diagnosis with spiral CT, multiplanar transesophageal echocardiography, and MR imaging. Radiology 1996;199:347-52.

44. Wells PS, Anderson DR, Ginsberg J. Assessment of deep vein thrombosis or pulmonary embolism by the combined use of clinical model and noninvasive diagnostic tests. Semin Thromb Hemost 2000;26:643-56.

45. Schoepf UJ, Holzknecht N, Helmberger TK et al. Subsegmental pulmonary emboli: improved detection with thin-collimation multi-detector row spiral CT. Radiology 2002;222:483-90.

46. Stein PD, Fowler SE, Goodman LR et al. Multidetector computed tomography for acute pulmonary embolism. N Engl J Med 2006;354:2317-27.

47. Vrachliotis TG, Bis KG, Haidary A et al. Atypical chest pain: coronary, aortic, and pulmonary vasculature enhancement at biphasic single-injection 64-section CT angiography. Radiology 2007;243:368-76.

48. McCollough CH, Primak AN, Saba O et al. Dose performance of a 64-channel dual-source CT scanner. Radiology 2007;243:775-84.

49. Hausleiter J, Meyer T, Hadamitzky M et al. Radiation dose estimates from cardiac multislice computed tomography in daily practice: impact of different scanning protocols on effective dose estimates. Circulation 2006;113:1305-10.

50. Johnson TR, Nikolaou K, Wintersperger BJ et al. ECG-gated 64-MDCT angiography in the differential diagnosis of acute chest pain. AJR Am J Roentgenol 2007;188:76-82.

51. White CS, Kuo D, Kelemen M et al. Chest pain evaluation in the emergency department: can MDCT provide a comprehensive evaluation? AJR Am J Roentgenol 2005;185:533-40.

52. Takakuwa KM, Halpern EJ. Evaluation of a "triple rule-out" coronary CT angiography protocol: use of 64-Section CT in low-to-moderate risk emergency department patients suspected of having acute coronary syndrome. Radiology 2008;248:438-46.

53. Pundziute G, Schuijf JD, Jukema JW et al. Evaluation of plaque characteristics in acute coronary syndromes: non-invasive assessment with multi-slice computed tomography and invasive evaluation with intravascular ultrasound radiofrequency data analysis. Eur Heart J 2008;29: 2373-81.

54. van Werkhoven JM, Schuijf JD, Gaemperli O et al. Incremental prognostic value of multi-slice computed tomography coronary angiography over coronary artery calcium scoring in patients with suspected coronary artery disease. Eur Heart J 2009;30:2622-9.

55. Motoyama S, Sarai M, Harigaya H et al. Computed tomographic angiography characteristics of atherosclerotic plaques subsequently resulting in acute coronary syndrome. J Am Coll Cardiol 2009;54:49-57.

56. Barreto M, Schoenhagen P, Nair A et al. Potential of dual-energy computed tomography to characterize atherosclerotic plaque: ex vivo assessment of human coronary arteries in comparison to histology. J Cardiovasc Comput Tomogr 2008;2:234-42.

57. Wu YW, Tadamura E, Yamamuro M et al. Estimation of global and regional cardiac function using 64-slice computed tomography: a comparison study with echocardiography, gated-SPECT and cardiovascular magnetic resonance. Int J Cardiol 2008;128:69-76.

58. Dewey M, Muller M, Eddicks S et al. Evaluation of global and regional left ventricular function with 16-slice computed tomography, biplane cineventriculography, and two-dimensional transthoracic echocardiography: comparison with magnetic resonance imaging. J Am Coll Cardiol 2006;48:2034-44.

59. Annuar BR, Liew CK, Chin SP et al. Assessment of global and regional left ventricular function using 64-slice multislice computed tomography and 2D echocardiography: a comparison with cardiac magnetic resonance. Eur J Radiol 2008;65:112-9.

60. Henneman MM, Schuijf JD, Dibbets-Schneider P et al. Comparison of multislice computed tomography to gated single-photon emission computed tomography for imaging of healed myocardial infarcts. Am J Cardiol 2008;101:144-8.

61. Gerber BL, Belge B, Legros GJ et al. Characterization of acute and chronic myocardial infarcts by multidetector computed tomography: comparison with contrast-enhanced magnetic resonance. Circulation 2006;113:823-33.

62. Mahnken AH, Koos R, Katoh M et al. Assessment of myocardial viability in reperfused acute myocardial infarction using 16-slice computed tomography in comparison to magnetic resonance imaging. J Am Coll Cardiol 2005;45:2042-7.

63. Lessick J, Dragu R, Mutlak D et al. Is functional improvement after myocardial infarction predicted with myocardial enhancement patterns at multidetector CT? Radiology 2007;244:736-44.

64. Nagao M, Matsuoka H, Kawakami H et al. Detection of myocardial ischemia using 64-slice MDCT. Circ J 2009;73:905-11.

65. Blankstein R, Shturman LD, Rogers IS et al. Adenosine-induced stress myocardial perfusion imaging using dual-source cardiac computed tomography. J Am Coll Cardiol 2009;54:1072-84.

66. George RT, rbab-Zadeh A, Miller JM et al. Adenosine stress 64- and 256-row detector computed tomography angiography and perfusion imaging: a pilot study evaluating the transmural extent of perfusion abnormalities to predict atherosclerosis causing myocardial ischemia. Circ Cardiovasc Imaging 2009;2:174-82.

67. Kido T, Kurata A, Higashino H et al. Quantification of regional myocardial blood flow using first-pass multidetector-row computed tomography and adenosine triphosphate in coronary artery disease. Circ J 2008;72:1086-91.

68. Lehman SJ, Abbara S, Cury RC et al. Significance of cardiac computed tomography incidental findings in acute chest pain. Am J Med 2009;122:543-9.

69. Onuma Y, Tanabe K, Nakazawa G et al. Noncardiac findings in cardiac imaging with multidetector computed tomography. J Am Coll Cardiol 2006;48:402-6.

70. Aglan I, Jodocy D, Hiehs S et al. Clinical relevance and scope of accidental extracoronary findings in coronary computed tomography angiography: A cardiac versus thoracic FOV study. Eur J Radiol 2009.

71. Kirsch J, Araoz PA, Steinberg FB et al. Prevalence and significance of incidental extracardiac findings at 64-multidetector coronary CTA. J Thorac Imaging 2007;22:330-4.

72. Chia PL, Kaw G, Wansaicheong G et al. Prevalence of non-cardiac findings in a large series of patients undergoing cardiac multi-detector computed tomography scans. Int J Cardiovasc Imaging 2009;25:537-43.

73. Haller S, Kaiser C, Buser P et al. Coronary artery imaging with contrast-enhanced MDCT: extra-cardiac findings. AJR Am J Roentgenol 2006;187:105-10.

74. MacMahon H, Austin JH, Gamsu G et al. Guidelines for management of small pulmonary nodules detected on CT scans: a statement from the Fleischner Society. Radiology 2005;237:395-400.

75. Cademartiri F, Malago R, Belgrano M et al. Spectrum of collateral findings in multislice CT coronary angiography. Radiol Med 2007;112:937-48.

76. Law YM, Huang J, Chen K et al. Prevalence of significant extracoronary findings on multislice CT coronary angiography examinations and coronary artery calcium scoring examinations. J Med Imaging Radiat Oncol 2008;52:49-56.

77. Hausleiter J, Meyer T, Hermann F et al. Estimated radiation dose associated with cardiac CT angiography. JAMA 2009;301:500-7.

78. Husmann L, Valenta I, Gaemperli O et al. Feasibility of low-dose coronary CT angiography: first experience with prospective ECG-gating. Eur Heart J 2008;29:191-7.

79. Takakuwa KM, Halpern EJ, Gingold EL et al. Radiation dose in a "triple rule-out" coronary CT angiography protocol of emergency department patients using 64-MDCT: the impact of ECG-based tube current modulation on age, sex, and body mass index. AJR Am J Roentgenol 2009;192:866-72.

80. Motoyama S, Anno H, Sarai M et al. Noninvasive coronary angiography with a prototype 256-row area detector computed tomography system: comparison with conventional invasive coronary angiography. J Am Coll Cardiol 2008;51:773-5.

81. Johnson TR, Nikolaou K, Becker A et al. Dual-source CT for chest pain assessment. Eur Radiol 2008;18:773-80.

82. Lell M, Marwan M, Schepis T et al. Prospectively ECG-triggered high-pitch spiral acquisition for coronary CT angiography using dual source CT: technique and initial experience. Eur Radiol 2009;19:2576-83.

CHAPTER 10

Reduction of Radiation Dose using 80 kV Tube Voltage: a Feasible Strategy?

Ernst E. van der Wall, Joëlla E. van Velzen, Fleur R. de Graaf, J. Wouter Jukema

Computed tomography (CT) coronary angiography has become a highly accurate noninvasive approach for delineation of the presence and severity of coronary atherosclerosis.[1-9] Cardiac CT is optimally suited for the evaluation of patients with a low or intermediate risk of coronary disease, allowing the non-invasive rule-out of coronary disease at relatively low cost and risk.[10-18] However, the appropriate radiation dose remains an important issue in cardiac CT. On one hand, a too low radiation dose may result in a high level of image noise and therefore in non-diagnostic images. On the other hand, using higher radiation exposure levels may put patients at unnecessary risk of radiation damage.[19-26] Effective strategies to reduce radiation dose, such as prospective gating, heart rate control, ECG-correlated modulation of the tube current, and tube voltage below 100 kV, are becoming more and more applied in the clinical situation.[27-31]

Recently, Buechel et al.[32] evaluated a large group of 612 patients referred for CT coronary angiography by 64-slice computed tomography. Intravenous metoprolol (2 to 30 mg) was administered if necessary to achieve a target heart rate below 65 beats/min. Using prospective ECG-triggering a mean effective radiation dose of 1.8 ± 0.6 mSv was obtained with a diagnostic image quality in 96.2% of segments. The authors concluded that low-dose CT coronary angiography by prospective ECG-triggering is feasible in the vast majority of an every-day population, whereby a heart rate below 62 beats/min favors diagnostic image quality. Blankstein et al.[33] investigated the effective radiation dose and image quality of 100 kV versus 120 kV tube voltage among patients referred for cardiac dual source CT imaging in 294 consecutive patients. They convincingly demonstrated that use of low kV resulted in a substantial reduction of radiation dose without compromising image quality. The effective radiation dose for the 100 kV and 120 kV scans was 8.5 and 15.4 mSv, respectively. In the recently published PROTECTION II trial, Hausleiter et al.[34] studied 400 non-obese patients undergoing CT angiography with either 100 kV or 120 kV CT coronary angiography. The study specifically examined the impact of a reduction in tube voltage to 100 kV using 64-slice CT angiography systems from three different manufacturers. It was demonstrated that a further 31% reduction in radiation exposure could be obtained with 100 kV tube voltage settings while image quality was preserved. Zhang et al.[35] prospectively evaluated image quality parameters, contrast volume and radiation dose at the 100 kV tube voltage setting during CT coronary angiography using a 320-row computed tomography scanner. The effective radiation dose was 2.12 ± 0.19 mSv for 100 kV, being a reduction of 54% compared to 4.61 ± 0.82 mSv for 120 kV. Diagnostic image quality was achieved in 98.2% of coronary segments with 100 kV and 98.6% of coronary segments with 120 kV. Therefore, the 100 kV setting allowed significant reductions in contrast material volume and effective radiation dose while maintaining adequate diagnostic image quality.

In the International Journal of Cardiovascular Imaging, Wang et al.[36] investigated the feasibility of a body mass index-adapted low-dose 80 kV scan protocol using prospectively ECG-triggered high-pitch spiral coronary CT angiography in 106 patients referred for coronary CT angiography to rule out coronary artery disease. The image quality and dose performance were compared with 100 kV and 120 kV tube settings. The authors

demonstrated that an adequate diagnostic image quality was obtained in more than 98% of coronary segments using the 80, 100, and 120 kV tube voltage settings (p = 0.482). Image noise was significantly higher with 80 kV compared to 100 kV and 120 kV tube voltage settings. The effective dose using 80 kV (0.36 ± 0.03 mSv) was significantly lower than that using 100 kV (0.86 ± 0.08 mSv), or the 120 kV tube voltage setting (1.77 ± 0.18 mSv). Use of a tube voltage of 80 kV for patients with a body mass index ≤ 22.5 kg/m² resulted in a further dose reduction of 58% and 80% compared with 100 kV and 120 kV protocols, while maintaining diagnostic image quality. Particularly in patients with slim body shape, a further reduction of tube voltage to 80 kV may be advisable. The authors concluded that 80 kV high-pitch spiral coronary CT angiography is feasible for patients with body mass index ≤ 22.5 kg/m². The authors also suggested that the amount of contrast material could be decreased, reducing contrast media-associated nephropathy and avoiding the obscuration of calcification caused by excessively high Hounsfield value. To further reduce the high image noise, they introduced iterative reconstruction in clinical routine practice. Consequently, the authors propose a combination of a low kV scan protocol, reduced contrast material injection protocol, and iterative reconstruction for an acceptable low radiation dose together with preserved image quality.

The above-mentioned findings by Wang et al.[36] have been underscored by Abada et al.[37], who used a 64-slice CT 80 kV tube voltage setting in 11 patients with body weight < 60 kg. The authors reported a dose reduction by up to 88% without a negative influence on image quality. Achenbach et al.[38] reported a case of 74-year-old patient with 63 kg body weight using 80 kV tube voltage and showed adequate diagnostic image quality and a dose reduction of 80% compared with a standard 120 kV tube voltage setting. In summary, the study by Wang et al.[36] validly demonstrates that further reduction in tube current may be feasible for reducing radiation exposure in patients undergoing CT coronary angiography.

REFERENCES

1. Schuijf JD, Bax JJ, van der Wall EE (2005) Non-invasive visualization of the coronary arteries with multi-detector row computed tomography; influence of technical advances on clinical applicability. Int J Cardiovasc Imaging 21:343–345
2. Groen JM, Greuter MJ, Vliegenthart R et al (2008) Calcium scoring using 64-slice MDCT, dual source CT and EBT: a comparative phantom study. Int J Cardiovasc Imaging 24:547–556
3. Dirksen MS, Bax JJ, de Roos A et al (2002) Usefulness of dynamic multislice computed tomography of left ventricular function in unstable angina pectoris and comparison with echocardiography. Am J Cardiol 90:1157-1160
4. van de Veire NR, Schuijf JD, De Sutter J et al (2006) Non-invasive visualization of the cardiac venous system in coronary artery disease patients using 64-slice computed tomography. J Am Coll Cardiol 48:1832-1838
5. Roeters van Lennep JE, Westerveld HT, Erkelens DW, van der Wall EE (2002) Risk factors for coronary heart disease: implications of gender. Cardiovasc Res 53:538-549
6. van der Wall EE, Heidendal GA, den Hollander W, Westera G, Roos JP (1980) I-123 labeled hexadecenoic acid in comparison with thallium-201 for myocardial imaging in coronary heart disease. A preliminary study. Eur J Nucl Med 5:401–405
7. Groothuis JG, Beek AM, Meijerink MR, Brinckman SL, Hofman MB, van Rossum AC (2010) Towards a noninvasive anatomical and functional diagnostic work-up of patients with suspected coronary artery disease. Neth Heart J 18:270–273
8. van Mieghem CA, de Feyter PJ (2009) Combining noninvasive anatomical imaging with invasive functional information: an unconventional but appropriate hybrid approach. Neth Heart J 17: 292–294
9. Knaapen P, de Haan S, Hoekstra OS et al (2010) Cardiac PET-CT: advanced hybrid imaging for the detection of coronary artery disease. Neth Heart J 18:90–98
10. van der Wall EE, van Dijkman PR, de Roos A et al (1990) Diagnostic significance of gadolinium-DTPA (diethylenetriamine penta-acetic acid) enhanced magnetic resonance imaging in thrombolytic treatment for acute myocardial infarction: its potential in assessing reperfusion. Br Heart J 63:12–17
11. Wijpkema JS, Dorgelo J, Willems TP et al (2007) Discordance between anatomical and functional coronary stenosis severity. Neth Heart J 15:5–11
12. van de Wal RM, van Werkum JW, le Cocq d'Armandville MC et al (2007) Giant aneurysm of an aortocoronary venous bypass graft compressing the right ventricle. Neth Heart J 15:252–254
13. de Leeuw JG, Wardeh A, Sramek A, van der Wall EE (2007) Pseudo-aortic dissection after primary PCI. Neth Heart J 15:265–266
14. Nollen GJ, Groenink M, Tijssen JG, Van Der Wall EE, Mulder BJ (2004) Aortic stiffness and diameter predict progressive aortic dilatation in patients with Marfan syndrome. Eur Heart J 25: 1146-1152
15. ten Kate GJ, Wuestink AC, de Feyter PJ (2008) Coronary artery anomalies detected by MSCT-angiography in the adult. Neth Heart J 16:369–375
16. Bakx AL, van der Wall EE, Braun S, Emanuelsson H, Bruschke AV, Kobrin I (1995) Effects of the new calcium antagonist mibefradil (Ro 40-5967) on exercise duration in patients with chronic stable angina pectoris: a multicenter, placebo-controlled study. Ro 40-5967 International Study Group. Am Heart J 130:748–757
17. Schuijf JD, Bax JJ, van der Wall EE (2007) Anatomical and functional imaging techniques: basically similar or fundamentally different? Neth Heart J 15:43–44
18. Juwana YB, Wirianta J, Suryapranata H, de Boer MJ (2007) Left main coronary artery stenosis undetected by 64-slice computed tomography: a word of caution. Neth Heart J 15:255–256

19. van der Laarse A, Kerkhof PL, Vermeer F et al (1988) Relation between infarct size and left ventricular performance assessed in patients with first acute myocardial infarction randomized to intracoronary thrombolytic therapy or to conventional treatment. Am J Cardiol 61:1–7

20. Ertas¸ G, van Beusekom HM, van der Giessen WJ (2009) Late stent thrombosis, endothelialisation and drug-eluting stents. Neth Heart J 17:177–180

21. Bleeker GB, Schalij MJ, Boersma E et al (2007) Relative merits of M-mode echocardiography and tissue Doppler imaging for prediction of response to cardiac resynchronization therapy in patients with heart failure secondary to ischemic or idiopathic dilated cardiomyopathy. Am J Cardiol 99:68–74

22. Ypenburg C, van der Wall EE, Schalij MJ, Bax JJ (2008) Imaging in cardiac resynchronisation therapy. Neth Heart J 16:S36–S40

23. Nemes A, Geleijnse ML, van Geuns RJ et al (2008) Dobutamine stress MRI versus threedimensional contrast echocardiography: it's all black and white. Neth Heart J 16:217–218

24. van der Geest RJ, Niezen RA, van der Wall EE, de Roos A, Reiber JH (1998) Automated measurement of volume flow in the ascending aorta using MR velocity maps: evaluation of inter- and intraobserver variability in healthy volunteers. J Comput Assist Tomogr 22:904–911

25. van Rugge FP, Boreel JJ, van der Wall EE et al (1991) Cardiac first-pass and myocardial perfusion in normal subjects assessed by sub-second Gd-DTPA enhanced MR imaging. J Comput Assist Tomogr 15:959–965

26. van der Wall, Vliegen HW, de Roos A, Bruschke AV (1995) Magnetic resonance imaging in coronary artery disease. Circulation 92:2723–2739

27. Underwood SR, Bax JJ, vom Dahl J et al (2004) Study Group of the European Society of Cardiology. Imaging techniques for the assessment of myocardial hibernation. Report of a Study Group of the European Society of Cardiology. Eur Heart J 25:815-836

28. Portegies MC, Schmitt R, Kraaij CJ et al (1991) Lack of negative inotropic effects of the new calcium antagonist Ro 40-5967 in patients with stable angina pectoris. J Cardiovasc Pharmacol 18:746–751

29. Zhang LJ, Yang GF, Huang W, Zhou CS, Chen P, Lu GM (2010) Incidence of anomalous origin of coronary artery in 1879 Chinese adults on dual-source CT angiography. Neth Heart J 18: 466-470

30. van der Wall EE (2009) CT angiography, underuse, overuse, or appropriate use? Neth Heart J 17: 223

31. Rogalla P, Blobel J, Kandel S et al (2010) Radiation dose optimisation in dynamic volume CT of the heart: tube current adaptation based on anterior-posterior chest diameter. Int J Cardiovasc Imaging 26:933-940

32. Buechel RR, Husmann L, Herzog BA et al (2011) Low-dose computed tomography coronary angiography with prospective electrocardiogram triggering: Feasibility in a large population. J Am Coll Cardiol 57:332-336

33. Blankstein R, Bolen MA, Pale R et al (2010) Use of 100 kV versus 120 kV in Cardiac Dual source computed tomography: effect on radiation dose and image quality. Int J Cardiovasc Imaging. [Epub ahead of print]

34. Hausleiter J, Martinoff S, Hadamitzky M et al (2010) Image Quality and Radiation Exposure With a Low Tube Voltage Protocol for Coronary CT Angiography Results of the PROTECTION II Trial. JACC Cardiovasc Imaging 3:1113-1123

35. Zhang C, Zhang Z, Yan Z, Xu L, Yu W, Wang R. 320-row CT coronary angiography: effect of 100-kV tube voltages on image quality, contrast volume, and radiation dose. Int J Cardiovasc Imaging. 2011 Oct;27(7):1059-68

36. Wang D, Hu X, Zhang S et al. Image quality and dose performance of 80 kV low dose scan protocol in high-pitch spiral coronary CT angiography: feasibility study. Int J Cardiovasc Imaging. [Epub ahead of print]

37. Abada HT, Larchez C, Daoud B, Sigal-Cinqualbre A, Paul JF (2006) MDCT of the coronary arteries: feasibility of low-dose CT with ECG-pulsed tube current modulation to reduce radiation dose. AJR Am J Roentgenol 186 (6 Suppl 2):S387-390
38. Achenbach S, Anders K, Kalender WA (2008) Dual-source cardiac computed tomography: image quality and dose considerations. Eur Radiol 18:1188-1198

Chapter 10

CHAPTER 11

Diagnostic Accuracy of 320-Row Multidetector Computed Tomography Coronary Angiography in the Non-Invasive Evaluation of Significant Coronary Artery Disease

Fleur R. de Graaf, Joanne D. Schuijf, Joëlla E. van Velzen, Lucia J. Kroft, Albert de Roos, Johannes H.C. Reiber, Eric Boersma, Martin J. Schalij, Fabrizio Spano,, J. Wouter Jukema, Ernst E. van der Wall, Jeroen J. Bax

ABSTRACT

Background: Multidetector computed tomography coronary angiography (CTA) has emerged as a feasible imaging modality for non-invasive assessment of coronary artery disease (CAD). Recently, 320-row CTA systems were introduced, with 16-cm anatomical coverage, allowing image acquisition of the entire heart within a single heart beat. The aim of the present study was to assess the diagnostic accuracy of 320-row CTA in patients with known or suspected CAD.

Methods: A total of 64 patients (34 male, mean age 61 ± 16 years) underwent CTA and invasive coronary angiography. All CTA scans were evaluated for the presence of obstructive coronary stenosis by a blinded expert, and results were compared to quantitative coronary angiography (QCA).

Results: Four patients were excluded from initial analysis due to non-diagnostic image quality. Sensitivity, specificity, positive and negative predictive values to detect ≥ 50% luminal narrowing on a patient basis were 100%, 88%, 92% and 100%, respectively. Moreover, sensitivity, specificity, positive and negative predictive values to detect ≥ 70% luminal narrowing on a patient basis were 94%, 95%, 88% and 98%, respectively. With inclusion of non-diagnostic imaging studies, sensitivity, specificity, positive and negative predictive values to detect ≥ 50% luminal narrowing on a patient basis were 100%, 81%, 88% and 100%, respectively.

Conclusion: The current study shows that 320-row CTA allows accurate non-invasive assessment of significant CAD.

INTRODUCTION

Cardiovascular disease is the leading cause of morbidity and mortality in the Western world. Early detection of coronary artery disease (CAD) is of vital importance as timely treatment may significantly reduce morbidity and mortality. Although invasive coronary angiography remains the standard of reference for the evaluation of CAD, multidetector computed tomography coronary angiography (CTA) has recently emerged as a robust imaging modality for the non-invasive evaluation of CAD.[1] With sub-millimeter spatial resolution this technique allows detailed visualization of luminal narrowing as well as atherosclerotic changes within the coronary vessel wall. Advances in CTA technology have led to continuous improvements in image quality as well as reduction in radiation dose and contrast material. Recently, 320-row CTA systems were introduced, with enhanced cranio-caudal volume coverage as compared to 64-row systems. With 16-cm anatomical coverage (0.5 mm x 320 detectors), this new generation of CTA scanners allows image acquisition of the entire heart within a single gantry rotation and heart beat. Accordingly, wide volume CTA, in combination with prospective image acquisition, allows for a marked decrease in scan time and time of breath-hold, resulting in decreased radiation dose and contrast material as compared to retrospective helical imaging requiring multiple heart beats. In addition, improved temporal resolution and scan time result in an overall reduction of cardiac motion artifacts' and eliminate the problem of stair-step artifacts', observed during step-and-shoot acquisition techniques and helical imaging.[2-5]

The diagnostic accuracy of 320-row CTA in the evaluation of significant coronary artery stenosis has not been previously reported. Therefore, the purpose of the current study was to evaluate the diagnostic accuracy of 320-row CTA in the identification of significant CAD, compared to invasive coronary angiography as the standard of reference.

METHODS

Patient population

The study population consisted of 64 patients (34 male, mean age 61 ± 16 years) who were scheduled for invasive coronary angiography and in whom also CTA was performed. Referral for CTA of patients scheduled for conventional coronary angiography was based on patient eligibility and availability of the CT scanner. Exclusion criteria for CTA examination were: 1) (supra)ventricular arrhythmias, 2) renal failure (glomerular filtration rate < 30 ml/min), 3) known allergy to iodine contrast material, 4) severe claustrophobia, 5) pregnancy. Diagnostic invasive coronary angiography served as the standard of reference. Patients with total calcium score > 1000 or previous coronary artery bypass grafting (CABG) were excluded from the study. Based on these exclusion criteria, 2 patients with atrial fibrillation were excluded from CTA. Furthermore, 8 patients with previous CABG and 16 patients with a total calcium score exceeding 1000 were excluded from the study. The mean interval between invasive coronary angiography and CTA was 23 ± 32 days. No interventions or changes in the clinical

condition of the patients occurred between the examinations. Table 1 presents an overview of the main clinical characteristics of the study population. The study was conducted in accordance with the principles of the Declaration of Helsinki. All patients gave written informed consent to the study protocol, which was approved by the local Ethics Committee.

Table 1. Clinical characteristics of the study population

Number of patients	64
Age (yrs)	61 ± 16
Men / women	34 / 30
Average calcium score (Agatston)	184 ± 223
BMI [*] (kg/m²)	26 ± 3
Family history of CAD [†]	27 (42%)
Diabetes	13 (20%)
Hypertension	41 (64%)
Hypercholesterolemia	29 (45%)
Current smoker	12 (19%)
Previous myocardial infarction	15 (23%)
Anterior wall	2 (3%)
Inferior wall	10 (15%)
Posterior wall	3 (5%)
Previous percutaneous coronary intervention	18 (28%)
Number of coronary arteries with ≥ 50% luminal narrowing on angiographic examination	
None	27 (42%)
1	25 (39%)
2	9 (14%)
3	3 (5%)

[*] BMI, Body Mass Index; [†] CAD, coronary artery disease

CTA data acquisition

CTA studies were performed using a 320-row CTA scanner (Aquilion ONE, Toshiba Medical Systems, Otawara, Japan) with 320 detector rows (each 0.5 mm wide) and a gantry rotation time of 350 ms. Metoprolol was administered orally (50-100 mg depending on heart rate) 1 hour before data acquisition to patients with a heart rate exceeding 65 beats per minute (bpm), unless contraindicated. The entire heart was imaged in a single heart beat, with a maximum of 16 cm cranio-caudal coverage. During the scan, the ECG was registered simultaneously for prospective triggering of the data. The phase window was set at 65-85% of R-R interval in patients with a heart rate ≥ 60 bpm, and 75% of R-R interval in patients with stable heart rate < 60 bpm. In patients requiring LV function measurements, prospective ECG triggered dose modulation was used, scanning an entire cardiac cycle and attaining maximal tube current at 75% (when stable heart rate < 60 bpm) or 65-85% (when heart rate ≥ 60 bpm) of R-R interval. When prospective dose modulation was used,

the tube current outside of the pre-defined interval was 25% of the maximal tube current.

Tube voltage and current were adapted to body mass index (BMI) and thoracic anatomy. Tube voltage was 100 kV (BMI < 23 kg/m²), 120 kV (BMI 23 - 35 kg/m²) or 135 kV (BMI ≥ 35 kg/m²) and maximal tube current was 400-580 mA (depending on body weight and thoracic anatomy). A tri-phasic injection of intra-venous contrast was used and the total amount of non-ionic contrast media (Iomeron 400; Bracco, Milan, Italy) injected into the antecubital vein was 60-80 ml (depending on body weight). First, 50-70 ml of contrast media was administered at a flow rate of 5.0 or 6.0 ml/s, followed by 20 ml of 50% con-trast/saline. Subsequently, a saline flush of 25 ml was administered at a flow rate of 3.0 ml/s. In order to synchronize the arrival of the contrast media and the scan, bolus arrival was detected using automated peak enhancement detection in the left ventricle using a threshold of +180 Hounsfield Units. All images were acquired during an inspiratory breath-hold of approximately 5 seconds. An initial data set was reconstructed at 75% of R-R interval, with a slice thickness of 0.50 mm and a reconstruction interval of 0.25 mm. If multiple phases were obtained, additional reconstructions were explored in case of motion artifacts in order to obtain images with the least motion artifacts. For processing and evaluation, images were transferred to a remote workstation with dedicated CTA analysis software (Vitrea FX 1.0, Vital Images, Minnetonka, MN, USA). CTA was performed successfully in all patients without complications. During the CTA examination mean heart rate (± SD) was 60 ± 11 bpm. Radiation dose was quantified with a dose-length product conversion factor of 0.014 mSv/(mGy×cm) as described.[6]

When scanning prospectively, full dose at 75% of R-R interval, estimated mean radia-tion dose was 3.9 ± 1.3 mSv (range 2.7 - 6.2 mSv). When scanning prospectively, full dose at 65-85% of R-R interval, estimated mean radiation dose was 6.0 ± 3.0 mSv (range 3.1 – 11.8 mSv). The estimated mean radiation dose for prospectively ECG triggered modulated scans was 10.8 ± 2.8 mSv (range 4.5 – 14.2 mSv). The average investigation time for the CTA acquisitions was approximately 20 minutes.

CTA image analysis

CTA image analysis was performed by 2 observers in consensus, experienced in the evaluation of CTA and blinded to the invasive coronary angiography data. First, general information regarding the status and anatomy of the coronary arteries was obtained using three-dimensional volume rendered reconstructions. Subsequently, axial slices were visu-ally examined for the presence of significant narrowing by determining the presence of ≥ 50% and ≥ 70% reduction of luminal diameter as recommended by the SCCT guidelines for the interpretation and reporting of CTA.[7] CTA analysis was assisted by curved multipla-nar reconstructions of all vessels. Data was analyzed on a segmental, vessel and patient basis. Coronary anatomy was assessed in a standardized manner by dividing the coronary artery tree into 17 segments according to a modified American Heart Association clas-sification.[8] Each segment was determined interpretable or uninterpretable and evaluated for the presence of ≥ 50% and ≥ 70% stenosis. Subsequently vessel based analysis was performed. In case 1 segment was uninterpretable, an intention to diagnose strategy was

applied. However, if more than 1 segment in a single vessel was deemed uninterpretable, the vessel was considered to be of non-diagnostic image quality. Finally, a patient based analysis was performed using a similar approach. In case 1 vessel was uninterpretable, an intention to diagnose strategy was applied. However, if more than 1 vessel was uninterpretable, the entire scan was considered to be of non-diagnostic image quality. Accordingly, diagnostic image quality, the presence of ≥ 50% and the presence of ≥ 70% stenosis were assessed on a segmental, vessel and patient level. Of note, the presence of restenosis in a stented segment was identified by reduced or complete absence of contrast within the stent as well as reduced or absent runoff of contrast distally to the stented segment.

Invasive coronary angiography analysis

Invasive coronary angiography was performed according to standard techniques. Angiograms were assessed by an experienced observer blinded to the results of CTA. The available coronary segments were identified on the basis of the American Heart Association guidelines. The same segmental model with identical definitions was used for both the invasive coronary angiography and CTA analysis. Subsequently, all segments were visually classified as normal (no atherosclerosis or minor wall irregularities with ≤ 20% luminal narrowing) or abnormal (presence of stenosis with > 20% luminal narrowing). All segments visually scored as abnormal were quantified using a dedicated and validated quantitative coronary angiography (QCA) software package (QAngioXA 6.0, CA-CMS, Medis Medical Imaging Systems, Leiden, The Netherlands). Each segment was evaluated for the presence of significant stenosis by determining the presence of ≥ 50% and ≥ 70% luminal diameter reduction in the angiographic view with most severe luminal narrowing. Obstructive CAD was defined as luminal narrowing of ≥ 50% on QCA analysis.

Statistical analysis

Data were analyzed on segment, vessel and patient basis. Sensitivity, specificity and positive and negative predictive values, including 95% confidence intervals (CI), for the detection of ≥ 50% and ≥ 70% luminal narrowing on invasive coronary angiography were calculated. In an initial analysis, the diagnostic accuracy was determined excluding segments, vessels or patients of non-diagnostic image quality. In a subsequent analysis, non-diagnostic segments, vessels or patients were included in the analysis, and were considered positive (≥ 50% luminal narrowing). In the analysis on a vessel basis, the left main was considered part of the left anterior descending artery (LAD) and the intermediate branch was considered part of the left circumflex artery (LCx). Continuous data were expressed as mean ± standard deviation (SD). Statistical analyses were performed using SPSS software version 16 (SPSS, Inc., Chicago, Illinois). A value of $p < 0.05$ was considered statistically significant and all reported p-values were two-sided. Generalized estimating equation (GEE) method was applied for stenosis evaluation (for both the presence of ≥ 50% and ≥ 70% stenosis) to account for clustering of coronary artery segments within patients. The GEE analyses were performed with proc GENMOD with a binominal distribution for the outcome variable, the link function specified as logit, and patients as separate subjects.

RESULTS

Segment analysis

In a total of 839 segments available for analysis, invasive coronary angiography identified 72 segments containing significant stenosis. However, 12 segments (1%) were uninterpretable as a result of: motion artifacts (n=7), extensive calcifications (n=2), vessel of small diameter (n=2) and blooming artifact due to stent (n=1). Eight uninterpretable segments were located in the right coronary artery (RCA) (segment 1, n=2; segment 2, n=3; segment 3, n=2; segment 4, n=1), two uninterpretable segments were located in the LCx (segment 11, n=1; segment 13, n=1) and two uninterpretable segments were located in the LAD (segment 7, n=1; and segment 8, n=1). In the remaining 827 segments, CTA analysis correctly ruled out significant stenosis in 735 segments. In a total of 62 segments, significant lesions were correctly identified on CTA, while 21 segments deemed non-obstructive on coronary angiography, were incorrectly classified as obstructive by CTA. Consequently, the sensitivity and specificity for the detection of ≥ 50% stenosis on a segment basis were 87% and 97%, respectively, and positive and negative predictive values were 75% and 99% respectively. The diagnostic accuracy for the detection of ≥ 50% luminal narrowing excluding and including non-diagnostic segments, as well as the diagnostic performance for the detection of ≥ 70% luminal narrowing are shown in Tables 2 and 3, respectively. As determined with GEE analyses, the presence of a significant stenosis on CTA was highly predictive for the presence of a significant stenosis on CAG, both for ≥ 50% luminal narrowing (odds ratio (OR) 5.5, 95% CI 4.6 - 6.5) and ≥ 70% luminal narrowing (OR 7.7, 95% CI 5.6 - 9.8).

Table 2. Diagnostic accuracy of 320-row CTA for the detection of ≥ 50% coronary stenosis.

	Segment Analysis	Vessel Analysis	Patient Analysis
Excluding non-diagnostic segments, vessels and patients			
Non-diagnostic	12/839, 1%	2/177, 1%	4/64, 6%
Sensitivity	62/71 (87%, 80%-95%)	48/51 (94%, 88%-100%)	35/35 (100%)
Specificity	735/756 (97%, 96%-98%)	114/124 (92%, 87%-97%)	22/25 (88%, 75%-100%)
PPV	62/83 (75%, 65%-84%)	48/58 (83%, 73%-92%)	35/38 (92%, 84%-100%)
NPV	735/744 (99%, 98%-99.6%)	114/117 (97%, 95%-100%)	22/22 (100%)
Diagnostic Accuracy	797/827 (96%, 95%-98%)	162/175 (93%, 89%-96%)	57/60 (95%, 89%-100%)
Including non-diagnostic segments, vessels and patients			
Sensitivity	63/72 (88%, 80%-95%)	48/51 (94%, 88%-100%)	37/37 (100%)
Specificity	735/767 (96%, 94%-97%)	114/126 (90%, 85%-96%)	22/27 (81%, 67%-96%)
PPV	63/95 (66%, 57%-76%)	48/60 (80%, 70%-90%)	37/42 (88%, 78%-98%)
NPV	735/744 (99%, 98%-99.6%)	114/117 (97%, 95%-100%)	22/22 (100%)
Diagnostic Accuracy	798/839 (95%, 94%-97%)	162/177 (92%, 87%-96%)	59/64 (92%, 86%-99%)

Data are absolute values used to calculate percentages. Data in parenthesis are percentages with 95% confidence intervals. Patients with scans of non-diagnostic image quality were excluded from vessel and segment analysis.
CI, confidence interval; CTA, computed tomography angiography; NPV, negative predictive value; PPV, positive predictive value.

Vessel analysis

In 177 vessels evaluated, a total of 51 significantly obstructed vessels were identified on invasive coronary angiography. In total, 2 vessels (1%) were rendered non-diagnostic on CTA analysis due to motion artefacts in a patient with increased HR during acquisition (RCA, n=1) and small vessel lumen (LCx, n=1). In the remaining 175 vessels, CTA correctly ruled out significant stenosis in 114 vessels. One or more significant lesions were correctly identified by CTA in 48 vessels, whereas CTA overestimated lesion size in 10 vessels. The absence of significant stenosis was incorrectly identified by CTA in only 3 vessels (LAD, n=2; LCx n=1), resulting in a sensitivity and specificity of 94% and 92%, respectively. Positive and negative predictive values were 83% and 97%, respectively. The diagnostic accuracy for the detection of ≥ 50% luminal narrowing excluding and including non-diagnostic vessels, as well as the diagnostic performance for the detection of ≥ 70% luminal narrowing are depicted in Tables 2 and 3.

Table 3. Diagnostic accuracy of 320-row CTA for the detection of ≥ 70% coronary stenosis.

	Segment Analysis	Vessel Analysis	Patient Analysis
Non-diagnostic	12/839, 1%	2/177, 1%	4/64, 6%
Sensitivity	23/24 (96%, 88%-100%)	17/18 (94%, 84%-100%)	15/16 (94%, 82%-100%)
Specificity	795/803 (99%, 98%-99.7%)	153/157 (97%, 95%-99.9%)	42/44 (95%, 89%-100%)
PPV	23/31 (74, 59%-90%)	17/21 (81%, 64%-98%)	15/17 (88%, 73%-100%)
NPV	795/796 (99.9%, 99.6%-100%)	153/154 (99%, 98%-100%)	42/43 (98%, 93%-100%)
Diagnostic Accuracy	818/827 (99%, 98%-99.6%)	170/175 (97%, 95%-99.6%)	57/60 (95%, 89%-100%)

Data are absolute values used to calculate percentages. Data in parenthesis are percentages with 95% confidence intervals. Patients with scans of non-diagnostic image quality were excluded from vessel and segment analysis.
CI, confidence interval; CTA, computed tomography angiography; NPV, negative predictive value; PPV, positive predictive value.

Patient analysis

Out of 64 CTA examinations, four scans (6%) were of non-diagnostic image quality caused by: severe motion artifacts due to extra-systole during image acquisition (n=1) and an unexpected rise in HR during contrast administration (n=1), poor contrast attenuation (n=1) and heavy calcifications (n=1). In the remaining 60 CTA examinations, invasive coronary angiography identified 35 patients with obstructive CAD. All patients (100%) were correctly identified by CTA. However, in one patient, CTA incorrectly identified a significant lesion in the RCA, while an actual obstructive lesion in the LAD was underestimated. In another patient, CTA underestimated a stenosis in the LAD while obstructive CAD in the RCA was correctly identified. In a third patient, CTA underestimated a stenosis in the LCx while obstructive CAD in the LAD was correctly identified. In all other patients, the correct stenosis was identified by CTA. In addition, in a total of 22 patients, CTA correctly ruled out the presence of significant CAD. Only 3 patients were incorrectly diagnosed

with obstructive CAD on CTA. In two patients, a heavily calcified lesion was incorrectly classified as obstructive (LAD, n=1; RCA, n=1). In a third patient, a 40% stenosis of the second diagonal branch was incorrectly deemed obstructive on CTA. Importantly, however, on a patient basis, no patients with significant CAD were missed by CTA. Therefore, the sensitivity and specificity for the detection of ≥ 50% stenosis on a patient basis was 100% and 88% respectively. In addition, positive and negative predictive values were 92% and 100%, respectively. Table 2 presents an overview of diagnostic accuracy and negative and positive predictive values excluding and including non-diagnostic CTA examinations. In addition, Table 3 presents an overview of the diagnostic accuracy for the detection of ≥ 70% coronary stenosis.

DISCUSSION

The present study demonstrated excellent diagnostic accuracy for the assessment of obstructive CAD using 320-row CTA. On a patient level, a negative predictive value of 100% and a diagnostic accuracy of 95% were shown for the detection of ≥ 50% stenosis. When including scans of non-diagnostic image quality, the patient based diagnostic accuracy was 92% while the negative predictive value remained 100%. Importantly, no patients with significant CAD were missed using 320-row CTA. Furthermore, the excellent negative predictive value on segment, vessel and patient basis suggests that CTA might be particularly valuable in the exclusion of significant CAD. These results are in line with previous published data on the performance of 64-row CTA.[9-12]

In addition, excellent diagnostic performance for the evaluation of stenosis ≥ 70% was observed using 320-row CTA, with a negative predictive value of 98% and a diagnostic accuracy of 95% on a patient basis. These findings are in line with previously published data using a 70% stenosis cut-off in the evaluation of CAD using 64-row CTA.[12]

At present, limited data are available on the diagnostic accuracy of 320-row CTA. Previously, a case report has been published directly comparing 320-row CTA and invasive coronary angiography, reporting excellent agreement between the two investigations in a single patient.[13] Furthermore, in a study by Rybicki et al, consistently excellent image quality was observed in over 89% of segments in 40 consecutive patients referred for 320-row CTA.[3] In four of these patients, the observations on CTA were confirmed on invasive coronary angiography.

Technological advancements

Although diagnostic accuracy of 320-row CTA may be comparable to the performance of 64-row scanners, advantages of this new technology lie in improved image acquisition as well as reduced radiation dose compared to retrospectively gated 64-row CTA. For the first time since the introduction of CTA technology, 16-cm volumetric data acquisition within a single gantry rotation has become possible, allowing full cardiac imaging within a single gantry rotation, even in patients with an enlarged heart. Accordingly, single heart beat

Figure 1 Non-invasive coronary angiography using 320-row CTA revealing the absence of significant CAD.
Panel A shows a 3-dimensional volume rendered reconstruction of the heart, providing an overview of the left anterior descending artery (LAD), proximal left circumflex artery (LCx) and proximal right coronary artery (RCA). Panel B, C and D represent the curved multiplanar reconstructions of a normal RCA, LAD and LCx, respectively, without significant CAD. Panel E and F show the corresponding vessels on invasive coronary angiography.

image acquisition allows for a significant reduction of contrast material and breath-hold time (with a total breath-hold time of 5 s) as compared to CTA systems requiring multiple heart beats to image the entire heart. Figures 1 and 2 represent examples of single heart beat CTA of patients with normal coronary arteries and 3-vessel disease, respectively.

Furthermore, 320-row systems have increased temporal resolution (350 ms per gantry rotation) which reduces cardiac motion artifacts. Although certain types of 64-row systems have a slightly higher temporal resolution (330 ms per gantry rotation), these systems can only cover a small volume (3.2 cm) in a single heart beat.[14] Similarly, dual-source systems, with even superior temporal resolution (83 ms), allow limited cranio-caudal coverage per rotation.[15] In contrast, 320-row CTA allows volumetric data acquisition with full cardiac coverage in a single rotation, eliminating the problem of stair-step artifacts associated with helical and step-and-shoot scanning techniques.

Figure 2 Non-invasive coronary angiography with 320-row CTA revealing 3-vessel disease. Panel A represents a 3-dimensional volume rendered reconstruction of the heart, with an overview of the left anterior descending artery (LAD) and left circumflex artery (LCx), revealing multi-vessel disease (arrows). Panel B shows the curved multiplanar reconstruction of the right coronary artery (RCA) with two significant atherosclerotic lesions (arrows). Panel C reveals multiple severe lesions (arrows) in the proximal segment of the LAD. In panel D, a severe lesion (arrow) in the LCx is shown. Panel E and F are invasive coronary angiograms confirming all findings (arrows).

Recently, several new approaches have been developed to reduce CTA radiation dose. First, dose modulation was introduced, allowing tube current modulation throughout the cardiac cycle[16], decreasing radiation exposure at the cost of increased image noise during low tube current. Subsequently, prospective ECG triggering became available, allowing data acquisition during a narrow pre-defined portion of the R-R interval (usually end-diastolic phase when the heart is relatively motion-free), resulting in a substantial reduction in radiation dose.[17] Importantly, volumetric data acquisition used by 320-row CTA may further reduce radiation exposure by eliminating helical oversampling.[18] Indeed, in the current study, using 320-row CTA in combination with prospective ECG triggering, radiation doses as low as 2.7 mSv were achieved in patients with a low and stable heart rate, while diagnostic image quality was maintained in 94% of patients scanned. Moreover, a recent investigation by Steigner and colleagues, using 320-row CTA in combination with

prospective ECG triggering in the evaluation of 41 patients, concluded that a phase window width of 10% may reduce radiation dose (to an estimated 5.3 mSv) while maintaining diagnostic image quality in over 90% of patients.[19] Therefore, compared to retrospectively gated 64-row CTA, prospectively gated 320-row CTA may considerably reduce radiation exposure to the patient, while maintaining good image quality. Of note, even lower mean radiation doses have been reported recently in studies using new-generation 64-row CTA with prospectively ECG triggered step-and-shoot technology. These studies, however, were performed using maximal dose reduction by using tube voltages with a maximum of 100 or 120 kV as well as performing image acquisition during a minimal phase window of only 75% of the cardiac cycle.[20 21] Other technical advances, such as adaptive collimation and high-pitch spiral acquisition may also allow significant radiation reduction using scanning techniques requiring multiple heart beats.[22 23]

Limitations

Despite promising initial results, the following limitations to the present study should be considered. First, CTA is inherently associated with radiation exposure. Concerns have been raised about radiation dose, especially with respect to the long term sequelae in younger people and women of childbearing age.[24] Accordingly, careful patient selection is warranted and conservative imaging protocols, with respect to radiation dose, should be aimed for. Second, the present study was conduced in a relatively small group of patients. In addition, CTA was performed in patients referred for invasive coronary angiography, creating a selection bias of patients with a relatively high prevalence of significant CAD. Thus, the present diagnostic performance was achieved in an intermediate-to-high prevalence patient population. As a result, the current data may not be directly applicable to patients with a low-to-intermediate prevalence of CAD. Third, at present, quantitative methods to analyze CTA are limited. Nevertheless, development of dedicated quantification techniques is ongoing, and may substantially improve objectivity and reproducibility of the degree of stenosis observed on CTA. Fourth, as a single-centre study, the generalizability of the present results is limited. Last, as CTA and invasive coronary angiography analysis were performed blinded, differences in segment allocation may have occurred. Although differences in segment classification may have affected the results on a segment basis, the effect on vessel and particularly patient basis may have been negligible.

Future directions

Prospective studies in larger patient populations are required to further establish the diagnostic accuracy 320-row CTA in the detection of CAD in a low-to-intermediate likelihood population. Moreover, 320-row CTA acquisition protocols for optimal image acquisition and decreased radiation dose need to be further defined. As CTA technology continues to develop, future research will most likely continue to focus on further decreasing radiation exposure, while maintaining high image quality.

Conclusion

The current study demonstrates that 320-row CTA is highly sensitive for the detection of significant CAD. Importantly, on a patient basis, no patients with significant CAD ≥ 50% were missed. The high negative predictive value suggests this technique is particularly reliable for the exclusion of significant CAD.

Diagnostic accuracy of 320-row CTA

1. Sun Z, Jiang W. Diagnostic value of multislice computed tomography angiography in coronary artery disease: a meta-analysis. Eur J Radiol 2006;60:279-86.

2. Hein PA, Romano VC, Lembcke A et al. Initial experience with a chest pain protocol using 320-slice volume MDCT. Eur Radiol 2009;19:1148-55.

3. Rybicki FJ, Otero HJ, Steigner ML et al. Initial evaluation of coronary images from 320-detector row computed tomography. Int J Cardiovasc Imaging 2008;24:535-46.

4. Rybicki FJ, Melchionna S, Mitsouras D et al. Prediction of coronary artery plaque progression and potential rupture from 320-detector row prospectively ECG-gated single heart beat CT angiography: Lattice Boltzmann evaluation of endothelial shear stress. Int J Cardiovasc Imaging 2009;25:289-99.

5. Voros S. What are the potential advantages and disadvantages of volumetric CT scanning? J Cardiovasc Comput Tomogr 2009;3:67-70.

6. Valentin J. Managing patient dose in multi-detector computed tomography(MDCT). ICRP Publication 102. Ann ICRP 2007;37:1-79.

7. Raff GL, Abidov A, Achenbach S et al. SCCT guidelines for the interpretation and reporting of coronary computed tomographic angiography. J Cardiovasc Comput Tomogr 2009;3:122-36.

8. Austen WG, Edwards JE, Frye RL et al. A reporting system on patients evaluated for coronary artery disease. Report of the Ad Hoc Committee for Grading of Coronary Artery Disease, Council on Cardiovascular Surgery, American Heart Association. Circulation 1975;51:5-40.

9. Meijboom WB, Meijs MF, Schuijf JD et al. Diagnostic accuracy of 64-slice computed tomography coronary angiography: a prospective, multicenter, multivendor study. J Am Coll Cardiol 2008;52:2135-44.

10. Mowatt G, Cook JA, Hillis GS et al. 64-Slice computed tomography angiography in the diagnosis and assessment of coronary artery disease: systematic review and meta-analysis. Heart 2008;94:1386-93.

11. Miller JM, Rochitte CE, Dewey M et al. Diagnostic performance of coronary angiography by 64-row CT. N Engl J Med 2008;359:2324-36.

12. Budoff MJ, Dowe D, Jollis JG et al. Diagnostic performance of 64-multidetector row coronary computed tomographic angiography for evaluation of coronary artery stenosis in individuals without known coronary artery disease: results from the prospective multicenter ACCURACY (Assessment by Coronary Computed Tomographic Angiography of Individuals Undergoing Invasive Coronary Angiography) trial. J Am Coll Cardiol 2008;52:1724-32.

13. Dewey M, Zimmermann E, Laule M et al. Three-vessel coronary artery disease examined with 320-slice computed tomography coronary angiography. Eur Heart J 2008;29:1669.

14. Francone M, Napoli A, Carbone I et al. Noninvasive imaging of the coronary arteries using a 64-row multidetector CT scanner: initial clinical experience and radiation dose concerns. Radiol Med 2007;112:31-46.

15. Achenbach S, Ropers D, Kuettner A et al. Contrast-enhanced coronary artery visualization by dual-source computed tomography-initial experience. Eur J Radiol 2006;57:331-5.

16. Raff GL, Chinnaiyan KM, Share DA et al. Radiation dose from cardiac computed tomography before and after implementation of radiation dose-reduction techniques. JAMA 2009;301:2340-8.

17. Maruyama T, Takada M, Hasuike T et al. Radiation dose reduction and coronary assessability of prospective electrocardiogram-gated computed tomography coronary angiography: comparison with retrospective electrocardiogram-gated helical scan. J Am Coll Cardiol 2008;52:1450-5.

18. Mori S, Endo M, Nishizawa K et al. Comparison of patient doses in 256-slice CT and 16-slice CT scanners. Br J Radiol 2006;79:56-61.

19. Steigner ML, Otero HJ, Cai T et al. Narrowing the phase window width in prospectively ECG-gated single heart beat 320-detector row coronary CT angiography. Int J Cardiovasc Imaging 2009;25:85-90.
20. Husmann L, Valenta I, Gaemperli O et al. Feasibility of low-dose coronary CT angiography: first experience with prospective ECG-gating. Eur Heart J 2008;29:191-7.
21. Herzog BA, Husmann L, Burkhard N et al. Accuracy of low-dose computed tomography coronary angiography using prospective electrocardiogram-triggering: first clinical experience. Eur Heart J 2008;29:3037-42.
22. Deak PD, Langner O, Lell M et al. Effects of adaptive section collimation on patient radiation dose in multisection spiral CT. Radiology 2009;252:140-7.
23. Achenbach S, Marwan M, Schepis T et al. High-pitch spiral acquisition: a new scan mode for coronary CT angiography. J Cardiovasc Comput Tomogr 2009;3:117-21.
24. Einstein AJ, Henzlova MJ, Rajagopalan S. Estimating risk of cancer associated with radiation exposure from 64-slice computed tomography coronary angiography. JAMA 2007;298:317-23.

CHAPTER 12

Performance and Efficacy of
320-Row Computed Tomography
Coronary Angiography in Patients
presenting with Acute Chest Pain –
Results from a Clinical Registry

Joëlla E. van Velzen, Fleur R. de Graaf, Lucia J. Kroft, Abert de Roos, Johan H.C. Reiber, Jeroen J. Bax, J. Wouter Jukema, Joanne D. Schuijf, Martin J. Schalij, Ernst E. van der Wall

ABSTRACT

Background: The purpose of the study was to evaluate the performance of 320-row computed tomography angiography (CTA) in the identification of significant coronary artery disease (CAD) in patients presenting with acute chest pain and to examine the relation to outcome during follow-up.

Methods: A total of 106 patients with acute chest pain underwent CTA to evaluate presence of CAD. Each CTA was classified as: normal, non-significant CAD (<50% luminal narrowing) and significant CAD (≥50% luminal narrowing). CTA results were compared with quantitative coronary angiography. After discharge, the following cardiovascular events were recorded: cardiac death, non-fatal infarction, and unstable angina requiring revascularization.

Results: Among the 106 patients, 23 patients (22%) had a normal CTA, 19 patients (18%) had non-significant CAD on CTA, 59 patients (55%) had significant CAD on CTA and 5 patients (5%) had non-diagnostic image quality. In total, 16 patients (15%) were immediately discharged after normal CTA and 90 patients (85%) underwent invasive coronary angiography. Sensitivity, specificity, and positive and negative predictive values to detect significant CAD on CTA were 100, 87, 93, and 100%, respectively. During mean follow-up of 13.7 months, no cardiovascular events occurred in patients with a normal CTA examination. In patients with non-significant CAD on CTA, no cardiac death or myocardial infarctions occurred and only 1 patient underwent revascularization due to unstable angina.

Conclusion: In patients presenting with acute chest pain, an excellent clinical performance for the non-invasive assessment of significant CAD was demonstrated using CTA. Importantly, normal or non-significant CAD on CTA predicted a low rate of adverse cardiovascular events and favorable outcome during follow-up.

INTRODUCTION

Every year, a substantial number of patients present at the emergency department with acute chest pain complaints.[1] While diagnosis is relatively straightforward in case of typical ECG changes and elevated biomarkers, a substantial number of patients present with both biomarkers and ECG that are either within normal limits or inconclusive. Accordingly, most patients will undergo extensive work-up including invasive coronary angiography to exclude coronary artery disease (CAD) as the cause of their symptoms to avoid inappropriate discharge. However, this approach leads to many unnecessary hospital admissions and is both time-consuming and expensive. Therefore, a non-invasive and rapid examination to establish or exclude CAD as the underlying cause of symptoms could substantially improve the clinical care of patients presenting with acute chest pain.

Several studies have suggested that computed tomography coronary angiography (CTA) may be of value in the diagnostic work-up in patients with acute chest pain in the emergency department.[2-4] Recently, a new generation of scanners has been introduced equipped with 320 detector rows of 0.5 mm wide, yielding a maximum of 16 cm craniocaudal coverage.[5] This design allows three-dimensional volumetric whole-heart imaging in a single gantry rotation. Accordingly, a marked reduction in radiation dose is achieved by the elimination of oversampling or overranging, observed with helical scanning techniques.[6] In addition, the 320-row CTA system eliminates the problem of stair-step artifacts caused by inter-heartbeat variations as well as a reduction in cardiac motion artifacts. Furthermore, the temporal resolution has improved (175 ms using half reconstruction) resulting in superior image quality and accuracy for the detection of CAD.[7][8]

The performance of 320-row CTA in the evaluation of significant CAD in clinical practice in patients presenting with acute chest pain and the relation to outcome has not been previously reported. Therefore, the purpose of the current study was to evaluate the performance of 320-row CTA in the identification of significant CAD in patients presenting with acute chest pain and to examine the relation to outcome during follow-up.

METHODS

The population consisted of patients included as part of an ongoing clinical registry who presented with acute chest pain to the Emergency Department. In all patients, physicians had sufficient clinical suspicion for an ischemic origin of chest pain and admitted these patients to the hospital to rule out presence of significant CAD.[9][10] However, patients presenting with an ST-segment elevation myocardial infarction (STEMI) were excluded and were immediately referred for direct percutaneous coronary intervention (PCI).

According to clinical protocol, patients were referred for CTA imaging for non-invasive evaluation of acute chest pain. Consequently, patients were referred for invasive coronary angiography (ICA) based on clinical presentation and/or imaging results to further evaluate the extent and severity of CAD. Due to the relative novelty of the use of CTA in patients

with acute chest pain, a conservative approach was applied before discharging patients after CTA examination. If CTA examination showed no significant CAD and was of good to reasonable image quality and was in line with clinical presentation and/or biomarkers, patients were subsequently discharged from the hospital. The remaining patients (abnormal CTA, uninterpretable CTA or high clinical suspicion of CAD) were referred for ICA, which served as the standard of reference. In addition, TIMI risk scores were calculated and patients were classified as low, intermediate or high risk.[11]

Exclusion criteria for CTA examination were: (i) (supra) ventricular arrhythmias and/or increased heart rate, (ii) renal failure (glomerular filtration rate <30 mL/min), (iii) known allergy to iodine contrast material, (iv) severe claustrophobia, (v) pregnancy, (vi) previous coronary artery bypass grafting (CABG), (vii) contra-indications for beta-blockers, (viii) clinically unstable presentation and (ix) STEMI.

CTA data acquisition

Prior to CTA examination, beta-blocking medication (metoprolol 50 or 100 mg, single oral dose, 1 hour prior to CTA examination) was administered if the heart rate was ≥65 beats per minute, unless contra-indicated. If heart rate was still ≥65 beats per minute on arrival to the scanner and if no medical contra-indications existed, intravenous metoprolol (2.5-10 mg) was added. In addition, sublingual nitroglycerin (0.4 or 0.8 mg sublingual) was administered 5 minutes prior to start scan. In all patients CTA was performed using a 320-row CTA scanner (Aquilion ONE, Toshiba Medical Systems, Otawara, Japan) with 320 detector rows (each 0.5 mm wide) before ICA. The entire heart was imaged in a single volume, with a maximum of 16 cm cranio-caudal coverage, using prospective ECG triggering. If the heart rate was stable and <60 beats/min the phase window was set at 70-80% of R-R interval, if the heart rate was 60-65 beats/min the phase window was set at 65-85% of R-R interval and if the heart rate was ≥65 beats/min the phase window was set at 30-80% of the R-R interval (using multiple beats). Tube voltage and current were adapted to body mass index (BMI). Tube voltage was 100 kV (BMI <23 kg/m^2), 120 kV (BMI, 23-35 kg/m^2), or 135 kV (BMI ≥35 kg/m^2) and maximal tube current was 400–580 mA (depending on body weight). Contrast material was administered in a triple-phase protocol: first a bolus of 60 to 80 ml, followed by 40 ml of a 50:50 mixture of contrast and saline, followed by saline flush with a flow rate of 5-6 ml/sec (Iomeron 400®). Automatic bolus arrival detection was used to synchronize arrival of the contrast in the left ventricle with a threshold of +180 Hounsfield Units. All images were acquired during an inspiratory breath-hold of approximately 5 seconds. First, a data set was reconstructed in the end-diastolic phase (75% of R-R interval) with a slice thickness of 0.5 mm and a reconstruction interval of 0.25 mm. If motion artifacts were present, multiple phases were reconstructed to obtain maximal diagnostic image quality. Total time for the CTA examination was typically 10 to 15 minutes. Data sets were transferred to a remote workstation (Vitrea FX 1.0, Vital Images, Minnetonka, MN, USA). Radiation dose was quantified with a dose-length product conversion factor of 0.014 mSv/(mGy x cm). When scanning prospectively at 70-80% of R-R interval, estimated mean radiation dose was 3.6 ± 0.9 mSv. When scanning prospectively at

65 - 85% of R-R interval, estimated mean radiation dose was 6.0 ± 1.7 mSv. The estimated mean radiation dose was 12.0 ± 4.5 mSv when scanning prospectively with multiple beats.

CTA image analysis

Assessment of the contrast-enhanced CTA datasets for the presence of significant CAD was performed by 2 experienced investigators. CTA examinations were assessed as rec-ommended by the SCCT guidelines for the interpretation and reporting of CTA.[12] Image quality was scored as good, reasonable, moderate or non-diagnostic.[13] Coronary anatomy was assessed in a standardized manner by dividing the coronary artery tree into 17 seg-ments according to a modified American Heart Association (AHA) classification.[14] Each segment was deemed interpretable or uninterpretable, and evaluated for the presence of ≥50% luminal narrowing on the axial slices with the assistance of multiplanar and curved multiplanar reconstructed images. Subsequently, vessel-based analysis was performed. In the analysis on a vessel basis, the left main was considered part of the left anterior descending coronary artery (LAD) and the intermediate branch was considered part of the left circumflex coronary artery (LCx). Of note, if one segment was uninterpretable, an intention to diagnose strategy was applied. However, if more than one segment in a single vessel was uninterpretable, the vessel was considered to be of non-diagnostic image qual-ity. Finally, a patient-based analysis was performed using a similar approach. Each CTA was classified according to three groups: normal, non-significant CAD (<50% luminal nar-rowing) and significant CAD (≥50% luminal narrowing). If one vessel was uninterpretable, an intention to diagnose strategy was applied. However, if more than one vessel was uninterpretable, the entire scan was considered to be of non-diagnostic image quality.

Invasive coronary angiography

ICA was performed according to standard protocols. Quantitative coronary angiography (QCA) analysis was performed on a segment basis by an observer unaware of CTA findings with the use of validated QCA software (QAngioXA 6.0, CA-CMS, Medis Medical Imaging Sys-tems, Leiden, The Netherlands). Coronary artery segments by QCA were also evaluated using a 17-segment AHA coronary tree model. The tip of the catheter was used for calibration and for each segment examined, the reference diameter and minimum luminal diameter were measured and percent diameter stenosis was reported. Measurements were performed on at least two orthogonal projections and the highest percent diameter stenosis was used for further analysis. Significant CAD was defined as ≥50% luminal narrowing on QCA analysis.

Follow-up

Revascularization procedures (percutaneous coronary intervention (PCI) and/or CABG) during hospitalization were recorded. After discharge, patient follow-up data were gath-ered from the departmental Cardiology Information system by a single observer blinded to the baseline CTA and ICA results using clinical visits or contacted by standardized telephone interviews. The following cardiovascular events were regarded as clinical endpoints: cardiac death, non-fatal myocardial infarction, and unstable angina requiring

revascularization. Cardiac death was defined as death by acute myocardial infarction, ventricular arrhythmias, or refractory heart failure. Non-fatal infarction was defined based on criteria of typical chest pain, elevated cardiac enzyme levels, and typical changes on the ECG.[15] Unstable angina was defined according to the European Society of Cardiology guidelines as acute chest pain with or without the presence of ECG abnormalities, and negative cardiac enzyme levels.[9]

Statistical analysis

First, the performance (sensitivity, specificity, positive and negative predictive values including 95% confidence intervals) of CTA for the detection of significant CAD (defined as luminal narrowing ≥50% on QCA) was calculated on patient, vessel and segment basis. ICA was the standard of reference for detection of significant CAD and a patient, vessel or segment was classified as true positive if significant CAD was identified correctly by CTA. Initially, the performance of 320-row CTA was determined excluding patients, vessels and segments of non-diagnostic image quality. Subsequently, a second analysis was performed in which non-diagnostic patients, vessels and segments were included in the analysis and were considered positive for significant CAD. Clinical events were reported as numbers and percentages according to three groups: normal CTA, non-significant CAD on CTA (<50% luminal narrowing) and significant CAD on CTA (≥50% luminal narrowing). Statistical analysis was performed using SPSS 18.0 software (SPSS Inc., Chicago. Illinois).
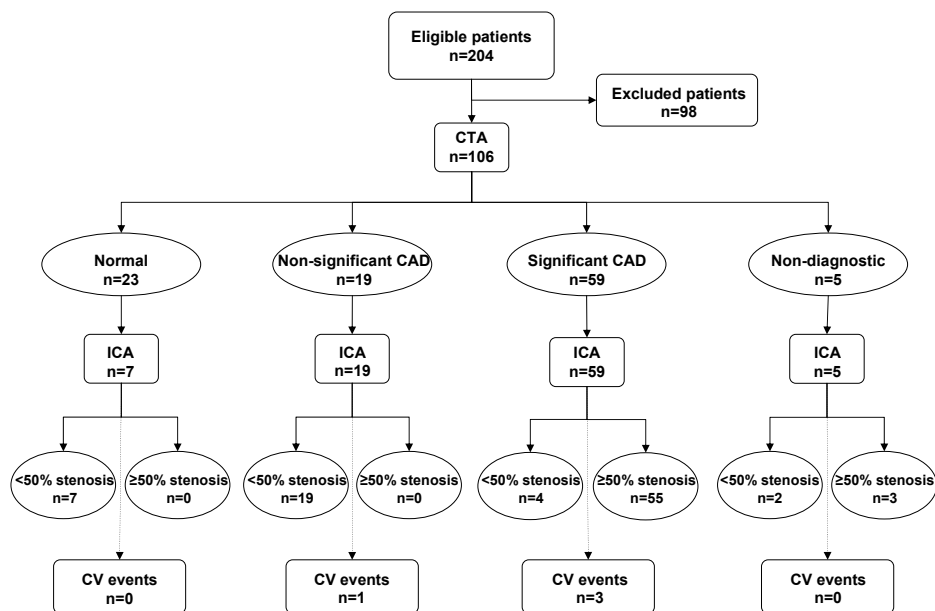
Figure 1. Flow chart of patient inclusion. CTA indicates computed tomography coronary angiography; ICA, invasive coronary angiography; CV events, cardiovascular events.

RESULTS

Patient population

In total, 204 patients with a primary complaint of acute chest pain were found eligible during the inclusion period. Exclusion criteria were present in 98 patients (48%) (clinical instability (n=25), impaired renal function (n=16), previous CABG (n=15), (supra) ventricular arrhythmias and/or increased heart rate (n=9), scanner availability (n=6), contra-indications to beta-blockers (n=3) and other (n=24) (Figure 1). The remaining study population consisted of 106 patients who underwent non-invasive coronary angiography with a 320-row CTA scanner. Baseline patient characteristics are described in Table 1. In summary, mean age was 57 ± 10 years and 71 patients were male (67%). The majority of patients (83%) had a low to intermediate TIMI risk score.

Table 1. Baseline patient characteristics

Number of patients	106
Age	57 ± 10
Male gender	71 (67%)
Cardiovascular risk factors	
Hypertension†	55 (52%)
Hypercholesterolemia‡	41 (39%)
Family history of CAD	54 (51%)
Current smoker	41 (39%)
Diabetes	17 (16%)
Obesity (≥30 kg/m^2)	29 (27%)
Medication at time of referral	
Beta-blockers	50 (47%)
Statins	52 (49%)
Aspirine	52 (49%)
ACE-inhibitors	45 (43%)
Previous myocardial infarction	28 (26%)
Previous PCI	32 (30%)
Mean troponin level (μg/L)	0.05 ±0.16
TIMI score	
Low	36 (34%)
Intermediate	52 (49%)
High	18 (17%)
Average heart rate during CTA	58 ±8

Data are absolute values, percentages or means ± standard deviation.
†Defined as systolic blood pressure ≥140 mm Hg or diastolic blood pressure ≥90 mm Hg or the use of antihypertensive medication.
‡Serum total cholesterol ≥230 mg/dL or serum triglycerides ≥200 mg/dL or treatment with lipid lowering drugs.
Abbreviations: CAD, coronary artery disease; ACE, angiotensin converting enzyme; PCI, percutaneous coronary intervention; TIMI, thrombolysis in myocardial infarction, QCA; quantitative coronary angiography; CTA, computed tomography angiography

CTA

Overall, image quality was good in 50 patients (47%), reasonable in 40 patients (38%) and moderate in 11 patients (10%). Five patients (5%) had a non-diagnostic CTA examination. Furthermore, 23 patients (22%) had a normal CTA 19 patients (18%) had non-significant CAD on CTA, 59 patients (55%) had significant CAD on CTA, and the remaining 5 patients (5%) with non-diagnostic scan quality were considered as significant CAD on CTA. In 16 patients (15%) with a normal CTA examination, clinical presentation and biomarkers were in line with the CTA findings and therefore patients were discharged home (case example illustrated in Figure 2). Nevertheless, the remaining 7 patients with a normal CTA examination had a high clinical suspicion of CAD and they were still referred for ICA. In total, 90 patients (85%) were clinically referred for ICA (case example illustrated in Figure 3).

Patient based analysis

When excluding patients with non-diagnostic scan quality, CTA correctly identified the presence of significant CAD in all 55 patients (100%). Furthermore, CTA correctly excluded significant CAD in 26 of 30 patients (87%). Thus, only 4 patients were overestimated on CTA. Importantly, no patients with significant CAD on ICA were missed by CTA. Accordingly, when excluding non-diagnostic CTA examinations, sensitivity and specificity on a patient's basis were 100% and 87%, respectively. Moreover, when including non-diagnostic CTA examinations (considered as positive for the presence of significant CAD), sensitivity and specificity on a patient basis were 100% and 81%, respectively (Table 2).

Vessel analysis

Out of the 255 vessels (85 patients) evaluated on CTA, 6 vessels (2%) (the right coronary artery (RCA), n=5 and LAD, n=1) were deemed non-diagnostic. Regarding the vessels with diagnostic image quality, 93 of 94 vessels were correctly identified by CTA as significant CAD on ICA. Additionally, 147 of 155 vessels were correctly identified as normal or non-significant CAD by CTA. However, 1 vessel which was deemed as significant CAD on ICA was incorrectly classified as non-significant CAD on CTA. Moreover, CTA overestimated 8 vessels as significant CAD which were classified as non-significant CAD on ICA. Thus, when excluding non-diagnostic vessels from analysis, sensitivity and specificity on a vessel basis were 99% and 95%, respectively. However, when including non-diagnostic vessels, sensitivity and specificity on a vessel basis were 99% and 92%, respectively (Table 2).

Segment analysis

In total, 44 of 1216 segments (4%) were deemed non-diagnostic on CTA examination. Of the 44 segments, 21 segments were located in the RCA, 15 segments were located in the LAD and 8 segments were located in the LCx. Out of the 1172 segments with diagnostic image quality, significant CAD was correctly identified by CTA in 136 of the 149 segments. Moreover, CTA correctly ruled out presence of significant CAD in 989 of 1023 segments. Nevertheless, CTA overestimated 34 lesions that were considered as non-significant CAD on ICA. In addition, 13 lesions were underestimated on CTA which
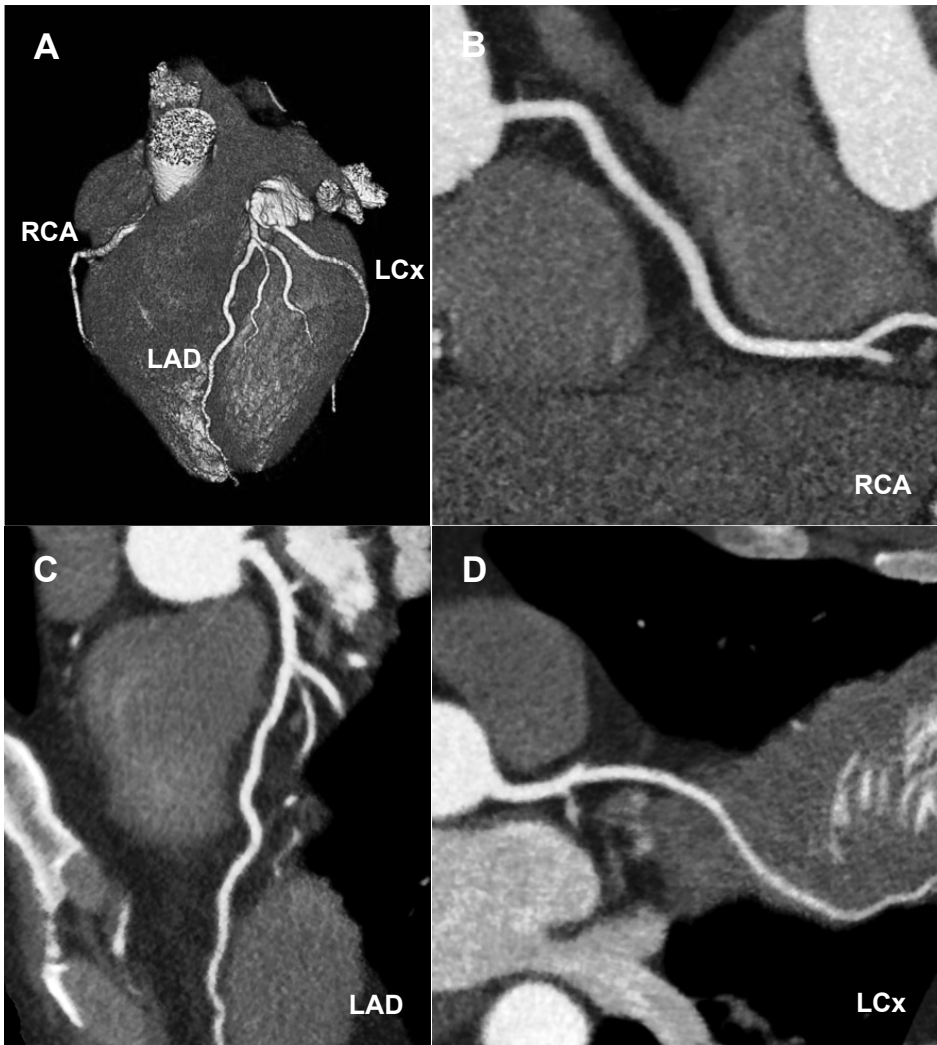
Figure 2. Non-invasive coronary angiography using 320-row computed tomography angiography (CTA) of a 42 year-old male presenting with acute chest pain revealing a normal CTA examination. The patient was subsequently discharged home and no events occurred during follow-up. (A) A three-dimensional volume-rendered reconstruction of the heart, providing an overview of the left anterior descending coronary artery (LAD) and proximal right coronary artery (RCA). (B-D) The curved multiplanar reconstructions of a normal RCA, LAD, and left circumflex coronary artery (LCx), respectively, without significant coronary artery disease.

were deemed as significant CAD on ICA. Accordingly, when excluding non-diagnostic segments, the sensitivity and specificity for the detection of significant CAD on a segment basis were 91% and 97%, respectively. Notably, when including non-diagnostic segments, the sensitivity and specificity for the detection of significant CAD on a segment basis were 91% and 93%, respectively (Table 2).
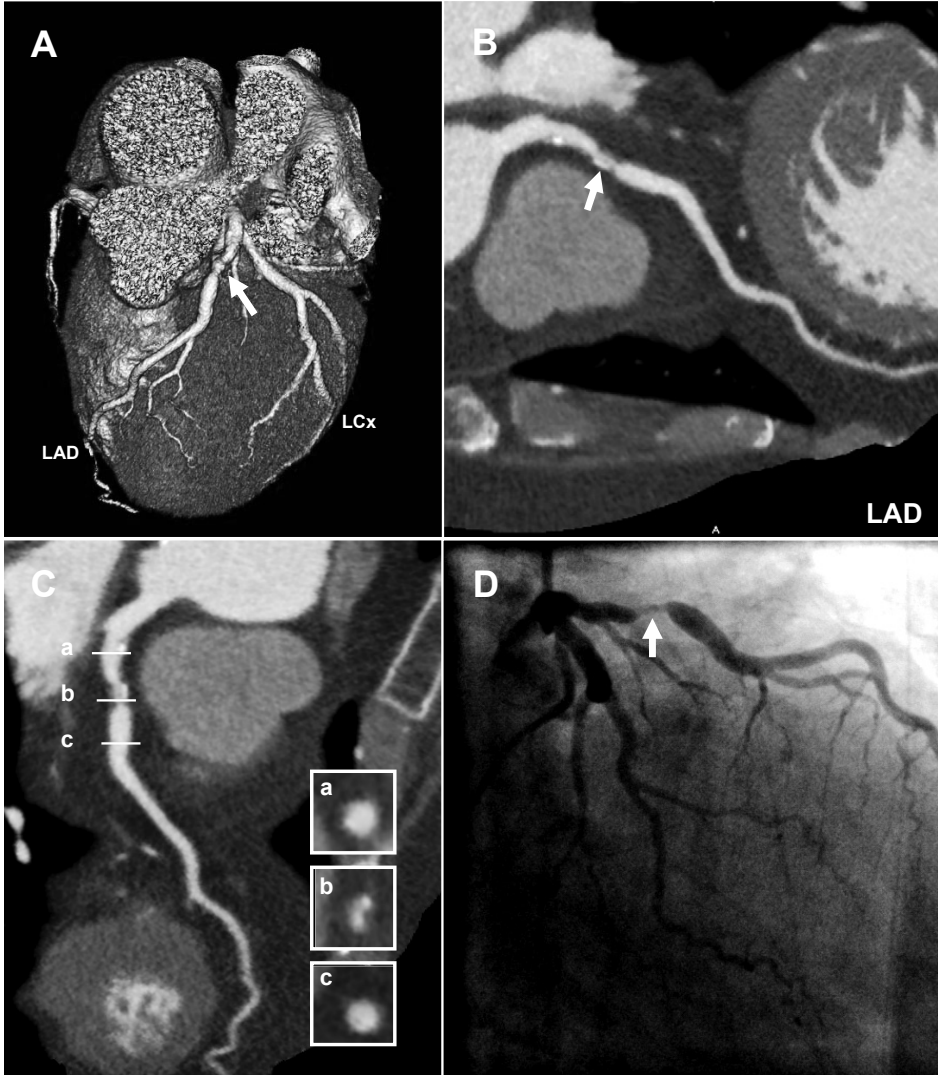
Figure 3. Non-invasive coronary angiography using 320-row computed tomography angiography of a 68 year-old female presenting with acute chest pain revealing a significant lesion in the mid left anterior descending coronary artery (LAD). (A) A three-dimensional volume-rendered reconstruction of the heart, providing an overview of the LAD and left circumflex coronary artery (LCx) revealing signs of luminal narrowing in the mid LAD (arrow). (B, C) Curved multiplanar reconstruction of the LAD demonstrating a significant stenosis in the mid LAD (arrow and b, respectively). (D) Corresponding invasive coronary angiography image confirming the presence of a significant stenosis in the mid LAD (arrow).

Table 2. Diagnostic performance of 320-row computed tomography angiography for detection of significant coronary artery disease in patients presenting with acute chest pain, excluding and including non-diagnostic segments, vessels and patients.

	Segment Analysis	Vessel Analysis	Patient Analysis
Excluding non-diagnostic segments, vessels and patients			
Sensitivity	136/149 (91%, 87 - 96%)	93/94 (99%, 97 - 100%)	55/55 (100%)
Specificity	989/1023 (97%, 96 - 98%)	147/155 (95%, 91 - 98%)	26/30 (87%, 75% - 99%)
PPV	136/170 (80%, 74 - 86%)	93/101 (92%, 87 - 97%)	55/59 (93%, 87 - 99.6%)
NPV	989/1002 (99%, 98 - 99%)	147/148 (99%, 98 - 100%)	26/26 (100%)
Diagnostic Accuracy	1125/1172 (95%, 95 - 97%)	240/249 (96%, 94 - 99%)	81/85 (95%, 91 - 99.7%)
Including non-diagnostic segments, vessels and patients			
Non-diagnostic	44/1216 (4%)	6/255 (2%)	5/90 (6%)
Sensitivity	138/151 (91%, 87 - 96%)	95/96 (99%, 97 - 100%)	58/58 (100%)
Specificity	989/1065 (93%, 91 - 94%)	147/159 (92%, 88 - 97%)	26/32 (81%, 68 - 95%)
PPV	138/214 (64%, 58 - 71%)	95/107 (89%, 83 - 95%)	58/64 (91%, 83 - 98%)
NPV	989/1002 (99%, 98 - 99%)	147/148 (99%, 98 - 100%)	26/26 (100%)
Diagnostic Accuracy	1127/1216 (93%, 91 - 94%)	242/255 (95%, 92 - 98%)	84/90 (93%, 88 - 98%)

Data are absolute values used to calculate percentages. Data in parentheses are percentages with 95% confidence intervals. Patients with scans of non-diagnostic image quality were excluded from vessel and segment analyses.

Abbreviations: NPV, negative predictive value; PPV, positive predictive value.

Revascularization during admission period

In relationship to CTA findings, in the 7 patients with normal CTA, no revascularization was performed. Of the 19 patients with non-significant CAD on CTA examination, PCI was performed in 2 patients (11%), both with angiographically non-significant CAD. One patient underwent PCI with stent placement due to coronary spasm and 1 patient underwent PCI because of angiographically non-significant lesion which was deemed significant on intravascular ultrasound. In the 59 patients with significant CAD on CTA examination, PCI was performed in 42 patients (71%), CABG was performed in 6 patients (10%) and 7 patients (12%) were treated conservatively. Lastly, in 5 patients with non-diagnostic image quality, 3 patients had significant CAD on ICA, PCI was performed in 1 patient (20%), CABG was performed in 1 patient (20%) and 1 patient (20%) was treated conservatively.

Clinical end points during follow-up

The mean follow-up period was 13.7 months (25-75th percentile: 6.5-18.7 months). The overall cardiovascular event rate was low (3.8%), only 4 cardiovascular events occurred in all patients. Of note, 1 patient with non-significant CAD on CTA and normal coronary arteries on ICA died of a non-cardiac cause 12 days after the angiographic procedure as a result of the consequences of severe chronic pulmonary hypertension which developed after previous liver transplantation. Importantly, no cardiovascular events occurred in the 23 patients with a normal CTA examination. In the 19 patients with non-significant CAD

on CTA, no cardiac death or myocardial infarctions occurred and only 1 patient (5.3%) was hospitalized because of unstable angina and underwent revascularization for a borderline lesion in the LAD. Moreover, in the 59 patients with significant CAD on CTA, 1 patient (1.7%) underwent non-fatal myocardial infarction and 2 patients (3.4%) were revascularized because of unstable angina. Lastly, in the 5 patients with a non-diagnostic CTA no cardiovascular events occurred.

DISCUSSION

Several studies have recently shown a high sensitivity and specificity of 320-row CTA for the detection of significant CAD in patients electively referred for ICA.[7 8 16] However, to the best of our knowledge, the clinical performance of the 320-row scanner in patients presenting with acute chest pain has not been previously reported. Therefore, the purpose was to evaluate the performance of 320-row CTA in the identification of significant CAD in patients presenting with acute chest pain and to assess clinical outcome.

In summary, 16 patients were discharged after normal CTA without further invasive examination. In the remaining subset of patients with acute chest pain referred for ICA, an excellent sensitivity and specificity of 100% and 87% for the detection of significant CAD using CTA was demonstrated when excluding scans with non-diagnostic image quality. In addition, a negative predictive value of 100% was observed, indicating that 320-row CTA did not miss any patients with significant CAD. When including CTA scans of non-diagnostic image quality, sensitivity and negative predictive value remained high (100%), but specificity decreased to 81%. In all patients with a normal CTA, no cardiovascular events occurred in the follow-up period. The excellent negative predictive value of 320-row CTA suggests that this technique could be useful in ruling out CAD in patients presenting with acute chest pain. Nevertheless, as demonstrated by the relatively low specificity values, lesion severity is still being overestimated by CTA as compared to ICA.

The present findings seem to be in line with previous studies evaluating the diagnostic accuracy with 64-row CTA for the detection of the presence of coronary stenosis in patients presenting with acute chest pain.[2-4 17 18] Recently, Chow et al assessed the diagnostic accuracy of 64-row CTA in 107 patients with acute chest pain as compared to ICA.[19] The investigators demonstrated a good diagnostic accuracy of 64-row CTA for detection of significant CAD (defined as ≥50% luminal narrowing), reporting sensitivity, specificity, and positive and negative predictive values on a patient basis of 94%, 90%, 89%, and 94%, respectively. Similarly, Meijboom et al also reported a high diagnostic accuracy of 64-row CTA for detecting significant CAD in 104 patients with non-ST elevation myocardial infarction.[20] In line with our findings, the investigators reported an excellent sensitivity and negative predictive value of 100%. However, specificity was also relatively low (75%). These studies suggest that CTA could be an attractive non-invasive modality to exclude CAD in patients presenting with acute chest pain.

Regarding the performance of 320-row CTA, Dewey et al recently assessed the diagnostic accuracy of 320-row CTA in 30 patients with stable chest pain as compared to ICA.[8] Besides significantly reducing radiation dose, the investigators demonstrated a good diagnostic accuracy of 320-row for detection of significant CAD (defined as ≥50% luminal narrowing), reporting sensitivity, specificity, and positive and negative predictive values on a patient basis of 100%, 94%, 100%, and 92%, respectively. Similarly, de Graaf et al demonstrated a high diagnostic accuracy of 320-row CTA for detection of significant CAD in 64 patients referred for ICA.[7] As compared to the older generation 64-row CTA scanners, one of the main advantages of the 320-row CTA system is the improved z-axis coverage of 16 cm that can cover the entire heart in a single gantry rotation. Therefore, 320-row CTA can accurately acquire images of the heart in a single heartbeat, which is substantially faster than the 6-10 seconds needed for 64-row CTA. Accordingly, a decreased amount of contrast is needed and breath hold is reduced to a minimum. Furthermore, due to the volumetric scanning approach, the presence of stair-step artifacts and typical pitch artifacts are eliminated. Lastly, as the entire heart can be imaged in one rotation, there is potential to assess myocardial perfusion as part of the acute chest pain work-up. These advantages of volumetric scanning may substantially optimize image quality and could possibly expand the use of CTA.

The excellent negative predictive value of CTA has made it a particular interesting modality for rapid diagnosis of patients with acute chest pain. Importantly, patients with a normal CTA had an excellent clinical outcome without cardiovascular events during the follow-up period. Therefore, the present findings demonstrate that the strength of CTA is that it can completely and safely rule out presence of CAD. Nevertheless, events still occurred in patients with significant as well as non-significant CAD on CTA, indicating that presence of plaque on CTA may still be considered relevant in this patient population. Notably, in the present study, the overall cardiovascular event rate was low (3.8%). However, in the majority of patients (both low and high risk) underwent subsequent intervention after CTA, including revascularization and initiation of anti-atherosclerotic medical treatment, which may have had a positive effect on outcome.

In line with the present study, several studies have demonstrated that coronary CTA is useful and safe in ruling out CAD and facilitates early and accurate release of patients with acute chest pain.[3][4][18] Rubinshtein and colleagues prospectively studied 58 patients with acute chest pain in the emergency department and evaluated the performance of 64-row coronary CTA for diagnosing or excluding acute coronary syndrome.[4] The investigators evaluated clinical outcomes during a follow-up of 15 months and found that no deaths or myocardial infarctions occurred in the 35 patients discharged from the emergency department with a normal CTA. In a larger cohort, Hollander et al prospectively evaluated 586 low to intermediate risk patients who received 64-row CTA in the emergency department for evaluation of acute chest pain.[18] Interestingly, patients discharged from the emergency department with a negative CTA (n=476, 84%) had a very low event rate of 0.2% (n=1). These studies demonstrate that CTA has a high positive predictive value for diagnosing an acute coronary syndrome, and a normal CTA predicts a favourable outcome and low rate

of major adverse cardiovascular events during follow-up. Furthermore, CTA evaluation in patients with acute chest pain has been shown to significantly reduce time to diagnosis, lower costs and require fewer repeat investigations when compared to standard of care.[2] As a result, the noninvasive assessment of coronary anatomy and presence of significant stenosis with 320-row CTA may impact clinical management in patients presenting with acute chest pain.

Clinical implications

In the current study, patients with acute chest pain and a normal CTA examination had an excellent clinical outcome without cardiovascular events during the follow-up period. Therefore, it seems that patients presenting with acute chest pain and a normal CTA can be safely discharged. Furthermore, although CTA still overestimates lesion severity, most patients with significant CAD on CTA (81%) were subsequently revascularized by means of PCI or CABG. Thus, 320-row CTA was demonstrated to be a relatively safe and useful technique for both excluding and including CAD in patients with acute chest pain. Nevertheless, it is important to realize that the presence of significant CAD on CTA does not necessarily equal myocardial ischemia, unless microcirculatory flow is impeded. Indeed, anatomical assessment of the coronaries is most reassuring when the vessels are normal or have minimal disease. In addition, even though 320-row CTA significantly reduces radiation dose and contrast dose, careful patient selection regarding age, renal function and body mass index are of fundamental importance to optimize use of CTA. Furthermore, heart rate reduction is essential for acquiring diagnostic image quality and is usually more challenging in patients admitted to the emergency department. Currently, use of CTA in symptomatic patients has a class IIa recommendation for patients with an intermediate pre-test likelihood of obstructive disease, suggesting that this technique can be an appropriate alternative for the evaluation of patients with acute chest pain.[21 22]

Limitations

The following limitations of the present study should be considered. First, in the present study a referral bias is present as patients are referred for ICA on the basis of CTA examination findings in combination with clinical presentation and/or other imaging results. Nevertheless, this approach reflects current clinical practice and thus could possibly be valuable in evaluating the use of this new imaging technique. Secondly, no quantitative measurements were performed on segments assessed with 320-row CTA, such as percentage luminal narrowing. Although visual estimation will be sufficient in most segments, more precise grading of luminal narrowing is preferred. However, new developments are ongoing, and dedicated software techniques are being expected. Furthermore, a substantial number of patients with acute chest pain were excluded such as patients with hemodynamic or electrical instability, or ongoing chest pain to prevent further delays of revascularization treatment. Therefore, coronary CTA is not generally applicable to all patients with acute chest pain. In addition, the presence of a significant stenosis on coronary CT does not by definition confirm the presence of ACS or significant flow limitation.

Potentially, a combination of anatomical CTA images with functional information would be preferable. Finally, radiation dose still remains of concern. Nevertheless, with the new 320-row systems as well as prospective triggering, radiation dose may be even lower than estimated radiation dose with conventional ICA.[8 23]

Conclusion

The present study shows that 320-row CTA enables accurate and safe evaluation of significant CAD in patients presenting with acute chest pain. Importantly, a negative CTA predicted a low rate of adverse cardiovascular events and favorable outcome during follow-up. Consequently, the noninvasive assessment of coronary anatomy and presence of significant CAD with 320-row CTA may impact clinical management in patients presenting with acute chest pain.

REFERENCES

1. Pitts SR, Niska RW, Xu J et al. National Hospital Ambulatory Medical Care Survey: 2006 emergency department summary. Natl Health Stat Report 2008;1-38.
2. Goldstein JA, Gallagher MJ, O'Neill WW et al. A randomized controlled trial of multi-slice coronary computed tomography for evaluation of acute chest pain. J Am Coll Cardiol 2007;49: 863-71.
3. Hoffmann U, Bamberg F, Chae CU et al. Coronary computed tomography angiography for early triage of patients with acute chest pain: the ROMICAT (Rule Out Myocardial Infarction using Computer Assisted Tomography) trial. J Am Coll Cardiol 2009;53:1642-50.
4. Rubinshtein R, Halon DA, Gaspar T et al. Usefulness of 64-slice cardiac computed tomographic angiography for diagnosing acute coronary syndromes and predicting clinical outcome in emergency department patients with chest pain of uncertain origin. Circulation 2007;115:1762-8.
5. Rybicki FJ, Otero HJ, Steigner ML et al. Initial evaluation of coronary images from 320-detector row computed tomography. Int J Cardiovasc Imaging 2008;24:535-46.
6. Hausleiter J, Meyer T, Hermann F et al. Estimated radiation dose associated with cardiac CT angiography. JAMA 2009;301:500-7.
7. De Graaf FR, Schuijf JD, Van Velzen JE et al. Diagnostic accuracy of 320-row multidetector computed tomography coronary angiography in the non-invasive evaluation of significant coronary artery disease. Eur Heart J 2010;31:1908-15.
8. Dewey M, Zimmermann E, Deissenrieder F et al. Noninvasive coronary angiography by 320-row computed tomography with lower radiation exposure and maintained diagnostic accuracy: comparison of results with cardiac catheterization in a head-to-head pilot investigation. Circulation 2009;120:867-75.
9. Bassand JP, Hamm CW, Ardissino D et al. Guidelines for the diagnosis and treatment of non-ST-segment elevation acute coronary syndromes. Eur Heart J 2007;28:1598-660.
10. Anderson JL, Adams CD, Antman EM et al. ACC/AHA 2007 guidelines for the management of patients with unstable angina/non-ST-Elevation myocardial infarction: a report of the American College of Cardiology/American Heart Association Task Force on Practice Guidelines (Writing Committee to Revise the 2002 Guidelines for the Management of Patients With Unstable Angina/Non-ST-Elevation Myocardial Infarction) developed in collaboration with the American College of Emergency Physicians, the Society for Cardiovascular Angiography and Interventions, and the Society of Thoracic Surgeons endorsed by the American Association of Cardiovascular and Pulmonary Rehabilitation and the Society for Academic Emergency Medicine. J Am Coll Cardiol 2007;50:e1-e157.
11. Antman EM, Cohen M, Bernink PJ et al. The TIMI risk score for unstable angina/non-ST elevation MI: A method for prognostication and therapeutic decision making. JAMA 2000;284:835-42.
12. Raff GL, Abidov A, Achenbach S et al. SCCT guidelines for the interpretation and reporting of coronary computed tomographic angiography. J Cardiovasc Comput Tomogr 2009;3:122-36.
13. Shuman WP, Branch KR, May JM et al. Prospective versus retrospective ECG gating for 64-detector CT of the coronary arteries: comparison of image quality and patient radiation dose. Radiology 2008;248:431-7.
14. Austen WG, Edwards JE, Frye RL et al. A reporting system on patients evaluated for coronary artery disease. Report of the Ad Hoc Committee for Grading of Coronary Artery Disease, Council on Cardiovascular Surgery, American Heart Association. Circulation 1975;51:5-40.
15. Thygesen K, Alpert JS, White HD. Universal definition of myocardial infarction. Eur Heart J 2007; 28:2525-38.

16. De Graaf FR, Schuijf JD, Van Velzen JE et al. Diagnostic accuracy of 320-row multidetector computed tomography coronary angiography to noninvasively assess in-stent restenosis. Invest Radiol 2010;45:331-40.
17. Hoffmann U, Nagurney JT, Moselewski F et al. Coronary multidetector computed tomography in the assessment of patients with acute chest pain. Circulation 2006;114:2251-60.
18. Hollander JE, Chang AM, Shofer FS et al. One-year outcomes following coronary computerized tomographic angiography for evaluation of emergency department patients with potential acute coronary syndrome. Acad Emerg Med 2009;16:693-8.
19. Chow BJ, Joseph P, Yam Y et al. Usefulness of computed tomographic coronary angiography in patients with acute chest pain with and without high-risk features. Am J Cardiol 2010;106:463-9.
20. Meijboom WB, Mollet NR, van Mieghem CA et al. 64-Slice CT coronary angiography in patients with non-ST elevation acute coronary syndrome. Heart 2007;93:1386-92.
21. Taylor AJ, Cerqueira M, Hodgson JM et al. ACCF/SCCT/ACR/AHA/ASE/ASNC/NASCI/SCAI/SCMR 2010 appropriate use criteria for cardiac computed tomography: a report of the American College of Cardiology Foundation Appropriate Use Criteria Task Force, the Society of Cardiovascular Computed Tomography, the American College of Radiology, the American Heart Association, the American Society of Echocardiography, the American Society of Nuclear Cardiology, the North American Society for Cardiovascular Imaging, the Society for Cardiovascular Angiography and Interventions, and the Society for Cardiovascular Magnetic Resonance. J Am Coll Cardiol 2010;56:1864-94.
22. Wijns W, Kolh P, Danchin N et al. Guidelines on myocardial revascularization: The Task Force on Myocardial Revascularization of the European Society of Cardiology (ESC) and the European Association for Cardio-Thoracic Surgery (EACTS). Eur Heart J 2010;31:2501-55.
23. Herzog BA, Wyss CA, Husmann L et al. First head-to-head comparison of effective radiation dose from low-dose 64-slice CT with prospective ECG-triggering versus invasive coronary angiography. Heart 2009;95:1656-61.

CHAPTER 13

Comparison of the Relation between the Calcium Score and Plaque Characteristics in Patients with Acute Coronary Syndrome versus Patients with Stable Coronary Artery Disease, assessed by CTA and VH IVUS

Joëlla E. van Velzen, Fleur R. de Graaf, J. Wouter Jukema, Greetje J. de Grooth, Gabija Pundziute, Lucia J. Kroft, Albert de Roos, Johan H.C. Reiber, Jeroen J. Bax, Martin J. Schalij, Joanne D. Schuijf, Ernst E. van der Wall

ABSTRACT

Background: A considerable number of patients with an acute coronary syndrome (ACS) who present with a zero or low calcium score (CS) still demonstrate coronary artery disease (CAD) and significant stenosis. The aim of the present study was to evaluate the relationship between the CS and the degree and character of atherosclerosis in patients suspected of ACS versus patients with stable CAD, obtained by computed tomography angiography (CTA) and virtual histology intravascular ultrasound (VH IVUS).

Methods: Overall, 112 patients were studied; 53 with ACS and 59 with stable CAD. CS and CTA was performed and followed by VH IVUS. On CTA, each segment was evaluated for plaque and classified as non-calcified, mixed or calcified. Vulnerable plaque characteristics on VH IVUS were defined by % necrotic core and presence of thin cap fibroatheroma (TCFA).

Results: If CS was zero, patients with ACS had a higher mean number of plaques (5.0 ± 2.0 vs 2.0 ± 1.9, $p<0.05$) and non-calcified plaques (4.6 ± 3.5 vs 1.3 ± 1.9, $p<0.05$) on CTA than stable CAD. In zero CS, VH IVUS demonstrated that patients with ACS had a larger amount of necrotic core area (0.58 ± 0.73 vs 0.22 ± 0.43 mm^2, $p<0.05$) and higher mean number of TCFA (0.6 ± 0.7 vs 0.1 ± 0.3, $p<0.05$) than stable CAD.

Conclusion: Even in the presence of a zero CS, patients with ACS have increased plaque burden as well as increased vulnerability as compared to stable CAD. Accordingly, absence of coronary calcification does not exclude the presence of clinically relevant and potentially vulnerable atherosclerotic plaque burden in patients with ACS.

INTRODUCTION

The prognostic value of the coronary calcium score (CS) has been extensively investigated, and very low rates of cardiac events have been demonstrated in individuals with a zero CS.[1-4] However, preliminary data in patients presenting with acute coronary syndrome (ACS) suggest a larger contribution of non-calcified plaque to the overall plaque burden as compared with patients with stable coronary artery disease (CAD).[5 6] As a consequence, a zero or low CS may significantly underestimate the overall plaque burden in the setting of ACS.[7] However, at present, data on how clinical presentation impacts the relation between CS and coronary plaque characteristics are still scarce. An important advantage of computed tomography angiography (CTA) over the CS is that additional information on stenosis severity and plaque composition can be obtained.[8 9] Invasively, virtual histology intravascular ultrasound (VH IVUS) offers detailed information on coronary plaque characteristics.[10-12] The aim of the present study was to compare the relationship between the CS and plaque characteristics in patients with ACS versus patients with stable CAD, assessed non-invasively by CTA and invasively by VH IVUS.

METHODS

Patients and Study Protocol

The study population consisted of 112 patients without known CAD (defined as previous myocardial infarction, coronary arterial bypass grafting and percutaneous coronary intervention) who were referred for CTA imaging for non-invasive evaluation of chest pain. Subsequently, patients were referred for invasive coronary angiography (ICA) in combination with VH IVUS based on patient's clinical presentation and/or imaging results. Patient data were prospectively collected in the departmental Cardiology Information System (EPD-Vision®, Leiden University Medical Center, Leiden, the Netherlands) and retrospectively analyzed. Patients with diagnostic CTA image quality were selected from an ongoing registry addressing the relative merits of CTA in relation to other imaging modalities. A total of 53 patients were included with suspected ACS, which was defined according to the guidelines of the European Society of Cardiology and the American College of Cardiology/American Heart Association.[13 14] The remaining 59 patients presented to the outpatient clinic with stable chest pain complaints.[15] Contra-indications for CTA were 1) (supra) ventricular arrhythmias, 2) renal insufficiency (glomerular filtration rate <30 ml/min), 3) known allergy to iodine contrast material, 4) severe claustrophobia, 5) pregnancy.

CTA acquisition

The CS and CTA scans were performed using either a 64-row or a 320-row scanner (Aquilion 64 or Aquilion ONE, Toshiba Medical Systems, Otawara, Japan). Beta-blocking medication (metoprolol 50 or 100 mg) was administered if the patient's heart rate was ≥65 beats/minute and no contra-indications existed. A non-contrast enhanced low dose

scan (tube voltage of 120 kV and tube current of 200 mA) was performed to assess the total CS.[16] A total CS of 0 was defined as no calcium, a CS of 1-399 was defined as mild calcium and a CS of ≥400 was defined as severe calcium. A standard scanning protocol was followed for the 64-row as well as for the 320-row contrast enhanced CTA scan, as previously described.[17][18]

CTA analyzation

CTA datasets were evaluated using dedicated software (Vitrea 2.0 or Vitrea FX 1.1 Vital images, Minnetonka, MN, USA) by two experienced readers, blinded to baseline patient characteristics, CS and VH IVUS results. The coronary arteries were divided into 17 segments according to a modified American Heart Association classification.[19] Per segment one coronary plaque (if present) was selected at the site of the most severe luminal narrowing. To describe plaque composition, plaques were further classified as: 1) non-calcified plaque (plaques with lower density compared to contrast-enhanced lumen without any calcification), 2) mixed plaque (non-calcified and calcified elements in single plaque) 3) calcified plaque (plaques with high density compared to contrast-enhanced lumen).

VH IVUS acquisition

The VH IVUS examinations were performed during ICA according to standard protocols. A dedicated IVUS-console (Volcano Corporation, Rancho Cordova, CA, USA) was used for the examination. VH IVUS was performed with a 20 MHz, 2.9 F phased-array IVUS catheter (Eagle Eye, Volcano Corporation, Rancho Cordova, CA, USA). Subsequently, with a speed of 0.5 mm/s, motorized automated IVUS pullback was performed until the IVUS catheter reached the guiding catheter. Images were stored for off-line analysis.

VH IVUS analyzation

VH IVUS analysis was performed by two experienced observers blinded to baseline patient characteristics, CS and CTA results. Offline analysis of the VH IVUS images was performed using dedicated software (pcVH 2.1 and VIAS 3.0, Volcano Corporation, Rancho Cordova, CA, USA). The lumen and the media-adventitia interface were defined by automatic contour detection and on all individual frames manual editing was performed. Analysis was performed on a per plaque basis. Plaque area (mm^2) was defined as plaque area plus media area and was calculated as vessel area minus lumen area. Four plaque components were differentiated into different color-codes (fibrotic tissue displayed in dark green, fibro-fatty in light green, necrotic core in red and dense calcium in white), as validated previously.[20] Vulnerable plaque characteristics on VH IVUS were defined by % of necrotic core and presence of thin cap fibroatheroma (TCFA). A TCFA was defined as a lesion with a plaque burden ≥40%, the presence of confluent necrotic core of >10%, and no evidence of an overlying fibrous cap.[21,22]

Statistical analysis

Statistical analysis was performed using SPSS 16.0 (SPSS, Inc., Chicago, Illinois). The impact on clinical presentation (ACS versus stable CAD) of coronary plaque characteristics (plaque burden and composition) on CTA was explored in all patients and related to the CS score (no, mild or severe). Finally, the impact of clinical presentation on coronary plaque characteristics in relation to the CS score was also evaluated using VH IVUS. Continuous values are expressed as means (±SD). Continuous values were assessed with the Student's t test if normally distributed or with the Mann-Whitney test if not normally distributed. Categorical values are expressed as number (%) and compared between groups with the 2-tailed Chi-square test. A p-value of <0.05 was considered statistically significant.

RESULTS

Patients

Overall, 112 patients were studied of which 53 patients presented with ACS and 59 presented with stable CAD. No differences were observed in the prevalence of risk factors for CAD between the 2 groups (Table 1). In patients with ACS, cardiac troponin levels were

Table 1. Patient characteristics
Patient characteristics of the study population compared between patients with suspected acute coronary syndrome (ACS) and stable coronary artery disease (CAD). Only the calcium score was significantly higher in patients presenting with stable CAD as compared to patients with suspected ACS.

Patient characteristics	Suspected ACS (n=53)	Stable CAD (n=59)	p-value
Age (years)	57±11	58±11	0.69
Male	37 (70%)	35 (59%)	0.25
Obesity (body mass index ≥ 30 kg/m^2)	12 (23%)	8 (14%)	0.24
Hypertension[†]	28 (53%)	36 (61%)	0.38
Hypercholesterolemia[‡]	32 (60%)	29 (49%)	0.23
Positive family history	25 (47%)	29 (49%)	0.83
Smoker	25 (47%)	22 (37%)	0.29
Type 2 diabetes mellitus	9 (17%)	17 (29%)	0.14
Mean calcium score	149±141	530±1258	<0.001
Presence of significant stenosis[§] (≥50% luminal narrowing)	31 (58%)	35 (59%)	0.93

Data are absolute values, percentages or means ± standard deviation.
[†]Defined as systolic blood pressure ≥140 mm Hg or diastolic blood pressure ≥90 mm Hg or the use of antihypertensive medication.
[‡]Serum total cholesterol ≥230 mg/dL or serum triglycerides ≥200 mg/dL or treatment with lipid lowering drugs.
[§]Visually assessed on invasive coronary angiography
Abbreviations: CAD, coronary artery disease; ACS, acute coronary syndrome.

elevated in 11 patients (21%) and in 31 patients (58%) significant CAD was demonstrated on ICA. VH IVUS could be performed in all patients and was obtained in 241 vessels (124 vessels (51%) in ACS and 117 vessels (48%) in stable CAD). Regarding the CS, calcium was absent (CS of 0) in 11 patients (21%) with ACS and 10 patients (17%) with stable CAD. Moreover, mild calcium (CS of 1-399) was observed in 37 patients (70%) with ACS and in 32 patients (54%) with stable CAD. Severe calcium (CS of ≥400) was demonstrated in 5 patients (9%) with ACS and 17 patients (29%) with stable CAD (p=0.04).

CTA findings

In total, 662 coronary plaques were indentified on CTA. Overall, 327 coronary plaques (49% of the total amount of plaques) were observed in patients with ACS whereas 335 coronary plaques (51% of the total amount of plaques) were observed in patients with stable CAD (p=0.14). No difference in total plaque burden on CTA, reflected by the mean number of total plaques per patient, was observed between patients with ACS (6.3±3.1) and stable CAD (5.7±3.7, p=0.30). Subsequently, the mean number of plaques per patient was compared between patients with ACS and stable CAD within the various CS categories (Figure 1). If coronary calcium was absent, significantly more plaques were present in patients with ACS (5.0±3.2) than patients with stable CAD (2.0±1.9, p=0.04). Similarly, if coronary calcium was mild, significantly more plaques were still detected in patients with ACS (6.6±3.0) than patients with stable CAD (5.0±2.9, p=0.02). However, if coronary calcium was severe, no differences were observed.

The differences in plaque composition were evaluated within the various CS categories between patients with ACS and stable CAD. Regarding non-calcified plaques, if coronary calcium was absent, significantly more non-calcified plaques were observed in patients
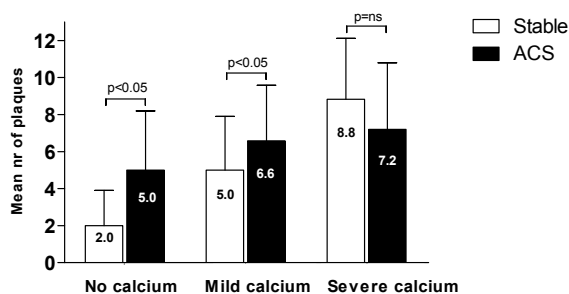
Figure 1. Relation between CS and plaque burden on CTA
Bar graph demonstrating the difference in the mean number of plaques per patient on CTA within different calcium score categories (no, mild and severe calcium) between patients presenting with ACS and stable CAD. As demonstrated, if coronary calcium was absent or mild on CTA, patients with ACS had a significantly higher mean number of plaques than patients with stable CAD. However, in severe calcium, the mean number of plaques on CTA was not different between patients with ACS and stable CAD. ACS, acute coronary syndrome; CAD, coronary artery disease; CTA, computed tomography angiography.

with ACS (4.6±3.5) than patients with stable CAD (1.3±1.9, p=0.03). Similarly, if coronary calcium was mild, significantly more non-calcified plaques were observed in patients with ACS (2.9±2.5) than patients with stable CAD (1.9±2.4, p=0.03). However, with regard to severe coronary calcium, no significant differences were identified in the mean number of non-calcified plaques between patients with ACS (0.8±1.1) and stable CAD (1.5±1.5, p=0.36). Regarding mixed plaques, if coronary calcium was mild, more mixed plaques were observed in patients with ACS than patients with stable CAD (3.0±2.1 vs 1.6±1.9, p=0.002). In contrast, regarding calcified plaques, in patients with mild or severe calcium, calcified lesions were more prominent in patients with stable CAD as compared to patients with ACS for each CS category.

VH IVUS findings

VH IVUS was available in 429 coronary plaques of which 219 plaques were present in patients with ACS (49% of total amount of plaques) and 210 plaques were present in patients with stable CAD (51% of total amount of plaques). No difference in total plaque burden on VH IVUS, reflected by the mean plaque area per patient, was observed between patients with ACS (7.55 ± 3.09 mm^2) and stable CAD (7.68 ± 3.14 mm^2, p=0.66). In addition, the difference in plaque area between patients with ACS and stable CAD within the various CS categories was assessed as presented in Figure 2. Accordingly, if coronary calcium was absent, plaque area (mm^2) was significantly higher in coronary plaques of patients with ACS as compared to patients with stable CAD. However, in case of mild or severe coronary calcium, plaque area (mm^2) was not significantly different between patients with ACS and stable CAD.

Plaque composition on VH IVUS was compared between patients with ACS and stable CAD within the different CS categories as illustrated in Figure 3. Interestingly, if coronary

Figure 2. Relation between CS and plaque burden on VH IVUS
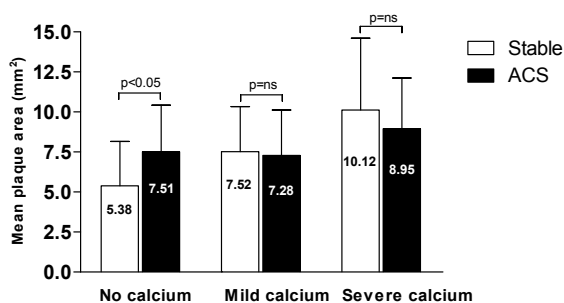Bar graph demonstrating the difference in mean plaque area (mm2) on VH IVUS within different calcium score categories (no, mild and severe calcium) between patients with ACS and stable CAD. As demonstrated, if coronary calcium was absent, patients with ACS had significantly larger mean plaque area on VH IVUS than patients with stable CAD. However, in mild or severe calcium, plaque area was not different between patients with ACS and stable CAD. ACS, acute coronary syndrome; CAD, coronary artery disease; VH IVUS, virtual histology intravascular ultrasound.
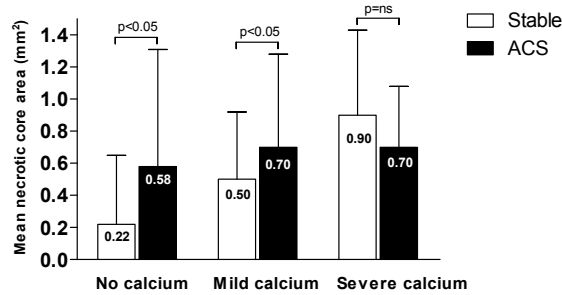
Figure 3. Relation between CS and plaque composition on VH IVUS
Bar graph demonstrating the difference in mean necrotic core area (mm2) on VH IVUS within different calcium score categories (no, mild and severe calcium) between patients with ACS and stable CAD. As demonstrated, if coronary calcium was absent or mild, patients with ACS had significantly larger mean necrotic core area on VH IVUS than patients with stable CAD. However, in the presence of severe calcium, mean necrotic core area was not different between patients with ACS and stable CAD. ACS, acute coronary syndrome; CAD, coronary artery disease; VH IVUS, virtual histology intravascular ultrasound.

calcium was absent, necrotic core area (mm^2) was significantly higher in coronary plaques of patients with ACS than stable CAD. This difference was still preserved when coronary calcium was mild. However, regarding severe coronary calcium, no differences in necrotic core area between coronary plaques of patients with ACS and patients with stable CAD were identified. Regarding the mean number of TCFA within different CS categories, the number of TCFA was significantly higher in patients with ACS in all CS categories as compared to stable CAD, which is demonstrated in Figure 4. An example of a patient with ACS without coronary calcium but with considerable atherosclerosis is provided in Figure 5.
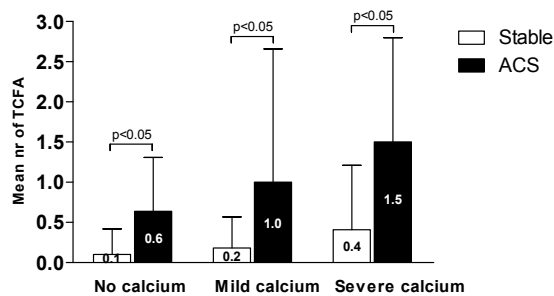
Figure 4. Relation between CS and TCFA on VH IVUS
Bar graph demonstrating the difference in mean number of TCFA on VH IVUS within different calcium score categories (no, mild and severe calcium) between patients with ACS and stable CAD. As demonstrated, patients with ACS had significantly larger number of TCFA on VH IVUS than patients with stable CAD in all calcium score categories. ACS, acute coronary syndrome; CAD, coronary artery disease; TCFA, thin cap fibroatheroma; VH IVUS, virtual histology intravascular ultrasound.
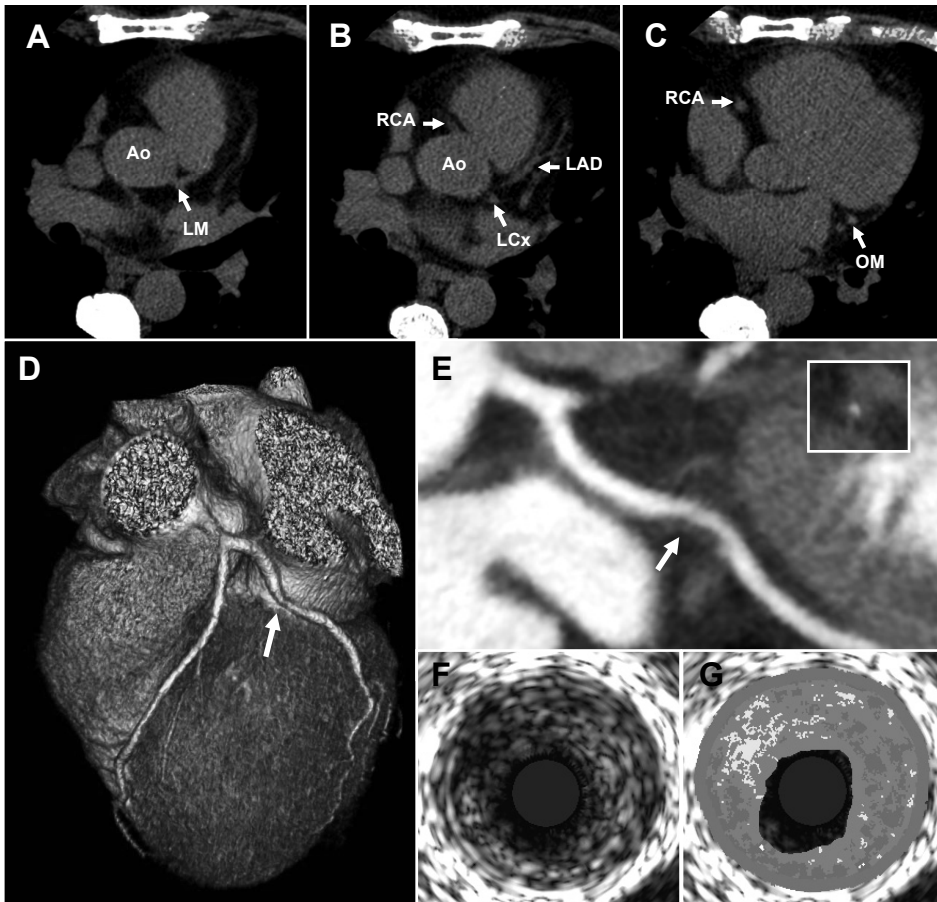
Figure 5. Example of patient with zero CS and extensive atherosclerosis
Example of a patient suspected of an acute coronary syndrome without coronary calcification but with relevant coronary atherosclerosis. The coronary calcium score showed no presence of coronary calcium in the entire coronary artery tree (Panel A, B, C). Additionally, 320-row CTA was performed. The 3D volume reconstruction showed signs of luminal narrowing in the LCx (Panel D, white arrow). On the multiplanar reconstruction of the LCx a substantial non-calcified plaque (white arrow) was demonstrated suggestive of significant luminal narrowing on cross-sectional view (enlargement) (Panel E). Grayscale IVUS confirmed substantial non-calcified plaque burden with significant luminal narrowing and signs of thrombus (Panel F). Virtual histology IVUS showed a large plaque without calcifications and large necrotic core area (red). Ao, aorta; IVUS, intravascular ultrasound; LAD, left anterior descending coronary artery; LCx, left circumflex coronary artery; LM, left main; OM, obtuse marginal; RCA, right coronary artery.

DISCUSSION

The main finding of the present study was that clinical presentation (ACS versus stable CAD) has a strong impact on the relation between the CS and coronary plaque character-istics. Although the mean number of plaques was similar between patients with ACS and stable CAD, when coronary calcium was absent the plaque burden on CTA was significantly larger in patients with ACS than in patients with stable CAD. Invasive VH IVUS findings paralleled non-invasive CTA findings. When coronary calcium was absent, a significantly larger plaque area (mm^2) was observed in patients with ACS as compared to patients with stable CAD. Regarding plaque composition, when coronary calcium was absent or mild, a significantly higher number of both non-calcified and mixed plaques on CTA was observed in patients with ACS as compared to patients with stable CAD. Importantly, as demonstrated invasively with VH IVUS, when coronary calcium was absent, a higher degree of high-risk plaque features (more TCFA and necrotic core) was noted in ACS. Consequently, the present findings indicate that if the CS is zero in patients with ACS, the presence of substantial atherosclerotic plaque burden cannot be reliably excluded, as demonstrated both non-invasively by CTA and invasively by VH IVUS.

Initially, the observation that a zero CS does not exclude substantial plaque burden appears to be in conflict with data from the general population. Indeed, an extensive body of previous published reports exists supporting the value of CS as a marker of plaque burden, and thus indirectly of prognosis.[1-4] [23] Large, multicenter trials have shown that absence of calcium is consistently associated with a low risk of either obstructive stenosis or cardiovascular events. Nonetheless, it should be noted that these data have been based predominantly on asymptomatic, low-risk populations and may not be fully representa-tive of symptomatic patients at higher risk. Several studies have investigated the pres-ence of atherosclerosis or significant stenosis in patients without detectable calcium.[24] [25] Akram et al reported in asymptomatic patients without calcium that the prevalence of significant stenosis was zero.[24] In symptomatic patients, however, the prevalence of sig-nificant stenosis increased to 8%. Moreover, these observations may be more pronounced in patients presenting with unstable symptoms, as suggested by Henneman et al.[7] In patients with ACS, the authors showed that significant luminal narrowing was present in 39% of patients with a zero CS.

It is conceivable that underlying differences in plaque composition in relation to clini-cal presentation may influence the reliability of CS as a marker of plaque burden. Indeed, previous histopathological data have demonstrated that lesions associated with ACS are not often heavily calcified.[26-28] Moreover, several post-mortem series have reported that calcifications develop relatively late in the process of atherosclerosis.[22] [29] In fact, intimal thickening with lipid accumulation is typically the first stage of atherosclerosis. This process is followed by the growth of the lipid core, fibrous cap formation and possibly deposition of small calcifications in the plaque.[22] Interestingly, Burke et al demonstrated in a series of sudden cardiac death patients that plaque ruptures show relatively little calcification; the majority of acute plaque ruptures resulting in sudden death occurred in

areas of only mild calcification.[29] Indeed, calcium is not often demonstrated in the culprit lesions of ruptured plaques but is more often related to stable CAD. It seems that, in contrast to the destabilizing effects of the lipid core, calcium is a more stabilizing force.[30] Similarly, previous studies comparing plaque composition between patients presenting with ACS and stable CAD have also revealed a relatively lower proportion of extensive calcifications. Notably this observation has been reported using both non-invasive and invasive imaging modalities.[26] [31-34] Also, in the present study relative plaque composition on CTA was significantly different in patients with ACS than in patients with stable CAD. More non-calcified and mixed lesions were observed in patients with ACS, whereas patients with stable CAD showed more calcified plaques. The observed difference in plaque composition was shown to strongly influence the relationship between CS and plaque burden and composition. Importantly, as demonstrated invasively for the first time, absence of calcium in patients presenting with ACS does not exclude the potential presence of vulnerable atherosclerotic plaque. Accordingly, the current study provides a valuable link between previous studies in patients with ACS, reporting a lower extent of calcium on the one hand and an increased rate of obstructive CAD in the absence of calcium on the other hand. Moreover, our observations may also indicate that as compared to stable or asymptomatic patients, the negative predictive value of absent or low CS for cardiovascular events may be reduced in patients at higher risk, such as patients with ACS. In this population, more detailed imaging tools may be preferred to establish or exclude the presence of substantial and potentially vulnerable plaque burden.

The following limitations of the present study should be considered. First, the present study only evaluated 112 patients in a single center. Ideally, a larger patient population should be studied, preferably in a multicenter setting. Second, based on the current small size of the study population it was not be possible to draw any firm conclusions if smaller subgroups of the CS were used. Future studies with larger cohorts are necessary to perform analysis with smaller subgroups of the CS. Third, one of the general disadvantages of CTA is the use of ionizing radiation and contrast. Therefore, careful patient selection regarding age, renal function and body mass index are of fundamental importance to optimize use of CTA. Furthermore, image protocols should be carefully selected to prevent unnecessary exposure to radiation. In addition, a referral bias could be present, as in a limited number of cases patients were referred for invasive imaging on the basis of CTA findings. Lastly, correlation with events would be of interest. However, due to the relative novelty of the technology, longer follow-up data have yet to become available.

REFERENCES

1. Detrano R, Guerci AD, Carr JJ et al. Coronary calcium as a predictor of coronary events in four racial or ethnic groups. N Engl J Med 2008;358:1336-45.
2. Greenland P, LaBree L, Azen SP et al. Coronary artery calcium score combined with Framingham score for risk prediction in asymptomatic individuals. JAMA 2004;291:210-5.
3. Raggi P, Callister TQ, Cooil B et al. Identification of patients at increased risk of first unheralded acute myocardial infarction by electron-beam computed tomography. Circulation 2000;101: 850-5.
4. Shaw LJ. Prognostic value of cardiac risk factors and coronary artery calcium screening for all-cause mortality. Radiology 2003;228:826-33.
5. Wu X, Maehara A, Mintz GS et al. Virtual histology intravascular ultrasound analysis of non-culprit attenuated plaques detected by grayscale intravascular ultrasound in patients with acute coronary syndromes. Am J Cardiol 2010;105:48-53.
6. Schuijf JD, Beck T, Burgstahler C et al. Differences in plaque composition and distribution in stable coronary artery disease versus acute coronary syndromes; non-invasive evaluation with multi-slice computed tomography. Acute Card Care 2007;9:48-53.
7. Henneman MM, Schuijf JD, Pundziute G et al. Noninvasive evaluation with multislice computed tomography in suspected acute coronary syndrome: plaque morphology on multislice computed tomography versus coronary calcium score. J Am Coll Cardiol 2008;52:216-22.
8. Choi BJ, Kang DK, Tahk SJ et al. Comparison of 64-slice multidetector computed tomography with spectral analysis of intravascular ultrasound backscatter signals for characterizations of noncalcified coronary arterial plaques. Am J Cardiol 2008;102:988-93.
9. Leber AW, Knez A, Becker A et al. Accuracy of multidetector spiral computed tomography in identifying and differentiating the composition of coronary atherosclerotic plaques: a comparative study with intracoronary ultrasound. J Am Coll Cardiol 2004;43:1241-7.
10. Pundziute G, Schuijf JD, Van Velzen JE et al. Assessment with multi-slice computed tomography and gray-scale and virtual histology intravascular ultrasound of gender-specific differences in extent and composition of coronary atherosclerotic plaques in relation to age. Am J Cardiol 2010;105:480-6.
11. Nasu K, Tsuchikane E, Katoh O et al. Accuracy of in vivo coronary plaque morphology assessment: a validation study of in vivo virtual histology compared with in vitro histopathology. J Am Coll Cardiol 2006;47:2405-12.
12. Hong MK, Mintz GS, Lee CW et al. Comparison of virtual histology to intravascular ultrasound of culprit coronary lesions in acute coronary syndrome and target coronary lesions in stable angina pectoris. Am J Cardiol 2007;100:953-9.
13. Anderson JL, Adams CD, Antman EM et al. ACC/AHA 2007 guidelines for the management of patients with unstable angina/non-ST-Elevation myocardial infarction: a report of the American College of Cardiology/American Heart Association Task Force on Practice Guidelines (Writing Committee to Revise the 2002 Guidelines for the Management of Patients With Unstable Angina/Non-ST-Elevation Myocardial Infarction) developed in collaboration with the American College of Emergency Physicians, the Society for Cardiovascular Angiography and Interventions, and the Society of Thoracic Surgeons endorsed by the American Association of Cardiovascular and Pulmonary Rehabilitation and the Society for Academic Emergency Medicine. J Am Coll Cardiol 2007;50:e1-e157.
14. Bassand JP, Hamm CW, Ardissino D et al. Guidelines for the diagnosis and treatment of non-ST-segment elevation acute coronary syndromes. Eur Heart J 2007;28:1598-660.
15. Fox K, Garcia MA, Ardissino D et al. Guidelines on the management of stable angina pectoris: executive summary: The Task Force on the Management of Stable Angina Pectoris of the European Society of Cardiology. Eur Heart J 2006;27:1341-81.

16. Agatston AS, Janowitz WR, Hildner FJ et al. Quantification of coronary artery calcium using ultrafast computed tomography. J Am Coll Cardiol 1990;15:827-32.

17. van Werkhoven JM, Schuijf JD, Gaemperli O et al. Prognostic value of multislice computed tomography and gated single-photon emission computed tomography in patients with suspected coronary artery disease. J Am Coll Cardiol 2009;53:623-32.

18. De Graaf FR, Schuijf JD, Van Velzen JE et al. Diagnostic accuracy of 320-row multidetector computed tomography coronary angiography in the non-invasive evaluation of significant coronary artery disease. Eur Heart J 2010;31:1908-15.

19. Austen WG, Edwards JE, Frye RL et al. A reporting system on patients evaluated for coronary artery disease. Report of the Ad Hoc Committee for Grading of Coronary Artery Disease, Council on Cardiovascular Surgery, American Heart Association. Circulation 1975;51:5-40.

20. Nasu K, Tsuchikane E, Katoh O et al. Accuracy of in vivo coronary plaque morphology assessment: a validation study of in vivo virtual histology compared with in vitro histopathology. J Am Coll Cardiol 2006;47:2405-12.

21. Carlier SG, Mintz GS, Stone GW. Imaging of atherosclerotic plaque using radiofrequency ultrasound signal processing. J Nucl Cardiol 2006;13:831-40.

22. Virmani R, Kolodgie FD, Burke AP et al. Lessons from sudden coronary death: a comprehensive morphological classification scheme for atherosclerotic lesions. Arterioscler Thromb Vasc Biol 2000;20:1262-75.

23. Fernandez-Friera L, Garcia-Alvarez A, Bagheriannejad-Esfahani F et al. Diagnostic value of coronary artery calcium scoring in low-intermediate risk patients evaluated in the emergency department for acute coronary syndrome. Am J Cardiol 2011;107:17-23.

24. Akram K, O'Donnell RE, King S et al. Influence of symptomatic status on the prevalence of obstructive coronary artery disease in patients with zero calcium score. Atherosclerosis 2009; 203:533-7.

25. Marwan M, Ropers D, Pflederer T et al. Clinical characteristics of patients with obstructive coronary lesions in the absence of coronary calcification: an evaluation by coronary CT angiography. Heart 2009;95:1056-60.

26. Beckman JA, Ganz J, Creager MA et al. Relationship of clinical presentation and calcification of culprit coronary artery stenoses. Arterioscler Thromb Vasc Biol 2001;21:1618-22.

27. Richardson PD, Davies MJ, Born GV. Influence of plaque configuration and stress distribution on fissuring of coronary atherosclerotic plaques. Lancet 1989;2:941-4.

28. Virmani R, Burke AP, Kolodgie FD et al. Pathology of the vulnerable plaque. J Am Coll Cardiol 2006;47:C13-C18.

29. Burke AP, Weber DK, Kolodgie FD et al. Pathophysiology of calcium deposition in coronary arteries. Herz 2001;26:239-44.

30. Huang H, Virmani R, Younis H et al. The impact of calcification on the biomechanical stability of atherosclerotic plaques. Circulation 2001;103:1051-6.

31. Ehara S, Kobayashi Y, Yoshiyama M et al. Spotty calcification typifies the culprit plaque in patients with acute myocardial infarction: an intravascular ultrasound study. Circulation 2004; 110:3424-9.

32. Motoyama S, Kondo T, Sarai M et al. Multislice computed tomographic characteristics of coronary lesions in acute coronary syndromes. J Am Coll Cardiol 2007;50:319-26.

33. Pundziute G, Schuijf JD, Jukema JW et al. Evaluation of plaque characteristics in acute coronary syndromes: non-invasive assessment with multi-slice computed tomography and invasive evaluation with intravascular ultrasound radiofrequency data analysis. Eur Heart J 2008;29: 2373-81.

34. Shemesh J, Stroh CI, Tenenbaum A et al. Comparison of coronary calcium in stable angina pectoris and in first acute myocardial infarction utilizing double helical computerized tomography. Am J Cardiol 1998;81:271-5.

CHAPTER 14

Non-invasive Computed Tomography Coronary Angiography as a Gatekeeper for Invasive Coronary Angiography

Fleur R. de Graaf, Joëlla E. van Velzen, Stephanie M. de Boer, Jaap M. van Werkhoven, Lucia J. Kroft, Albert de Roos, Allard Sieders, Greetje J. de Grooth, J. Wouter Jukema, Joanne D. Schuijf, Jeroen J. Bax, Martin J. Schalij, Ernst E. van der Wall

ABSTRACT

Background: The purpose was to determine the rate of subsequent invasive coronary angiography (ICA) and revascularization in relation to computed tomography coronary angiography (CTA) results. In addition, independent determinants of subsequent ICA and revascularization were evaluated.

Methods: CTA studies were performed using a 64-row (n=413) or 320-row (n=224) multidetector scanner. The presence and severity of CAD were determined on CTA. Following CTA, patients were followed up for one year for the occurrence of ICA and revascularization.

Results: A total of 637 patients (296 male, 56±12 years) were enrolled and 578 CTA investigations were available for analysis. In patients with significant CAD on CTA, subsequent ICA rate was 76%. Among patients with non-significant CAD on CTA, subsequent ICA rate was 20% and among patients with normal CTA results, subsequent ICA rate was 5.7% (p<0.001). Of patients with significant CAD on CTA, revascularization rate was 47%, as compared to a revascularization rate of 0.6% in patients with non-significant CAD on CTA and no revascularizations in patients with a normal CTA results (p<0.001). Significant CAD on CTA and significant three-vessel or left main disease on CTA were identified as the strongest independent predictors of ICA and revascularization.

Conclusion: CTA results are strong and independent determinants of subsequent ICA and revascularization. Consequently, CTA has the potential to serve as a gatekeeper for ICA to identify patients who are most likely to benefit from revascularization and exclude patients who can safely avoid ICA.

INTRODUCTION

Invasive coronary angiography (ICA) is routinely used for the identification of patients with suspected coronary artery disease (CAD). Advantages of ICA are high resolution imaging and the possibility of revascularization by percutaneous coronary intervention (PCI). Due to its invasive nature, ICA is associated with a small risk of complications, radiation exposure and relatively high cost of hospital stay. Additionally, the rate of normal ICA examinations is still quite high and health-care costs associated with the increase in ICA and revascularization rates are substantial. Moreover, a recent multicenter study showed that PCI has no superiority over pharmacological therapy in patients with stable CAD.[1] Accordingly a non-invasive test to select the most suitable patients for ICA and revascularization would be preferable. Most traditional non-invasive cardiac imaging techniques rely on the detection of stress-inducible ischemia.[2] However, with the introduction of computed tomography coronary angiography (CTA), the non-invasive anatomic assessment of CAD with high diagnostic accuracy has become possible. Prior studies have shown that CTA allows reliable patient risk stratification, and normal CTA examinations indicate good prognosis.[3][4] Although CTA cannot replace ICA, this technique could serve as a gatekeeper for ICA in selected patients, and thus avoid unnecessary additional examinations. At the same time concerns have been raised that CTA may trigger unnecessary referral for ICA. Rates of ICA and interventional therapy following CTA have been largely unreported. The purpose of the present study therefore was to determine the rate of subsequent ICA and revascularization in relation to CTA results. Furthermore, independent determinants of subsequent ICA and revascularization were investigated.

METHODS

Patient population

The study group consisted of patients who were referred for CTA as part of a large ongoing registry exploring the prognostic value of CTA.[5] Reasons for referral were typical chest pain, atypical chest pain and non-anginal chest pain, according to the appropriate use criteria for cardiac computed tomography.[6] Exclusion criteria for CTA investigation were: renal insufficiency (glomerular filtration rate < 30 ml/min), (supra)ventricular arrhythmias, known allergy to iodine contrast material, severe claustrophobia, pregnancy and high heart rate in the presence of contra-indications to β-blocker medication.[7] Patients were entered prospectively into the departmental patient information system (EPD-Vision®, Leiden University Medical Center) and retrospectively analysed. Patients with known CAD or congenital cardiac abnormalities were excluded from the study.

CTA data acquisition

CTA studies were performed using a 64-row (n=413) or 320-row (n=224) multidetector scanner (Aquilion 64, and Aquilion ONE, Toshiba Medical Systems, Otawara, Japan) with

64 and 320 simultaneous detector rows, respectively (each 0.5 mm wide), as previously described.[8][9] One hour before the investigation, oral β-blocker medication (metoprolol 50 or 100 mg) was administered to patients with a heart rate ≥ 65 beats/min, unless contra-indicated. The total amount of non-ionic contrast media (Iomeron 400; Bracco, Milan, Italy) injected into the antecubital vein was 60-100 ml (depending on scanner type and body weight) at a flow rate of 5.0 - 6.0 ml/s. In order to synchronize the arrival of the contrast media, bolus arrival was detected using a real-time bolus tracking technique. All images were acquired during a single inspiratory breath-hold of maximally 12 seconds for 64 row-CTA and 5 seconds for 320-row CTA. For 64-row CTA, a helical-scanning technique was used as previously described.[10] In brief, during the examination the ECG was registered simultaneously for retrospective gating of the data. A collimation of 64 x 0.5 mm was used. During 320-row CTA, the ECG was registered simultaneously for prospective triggering of the data. A collimation of 320 x 0.5 mm was used and the entire heart was imaged in a single heart beat, as previously reported.[11]

CTA data analysis

Data were transferred to a remote workstation with dedicated analysis software (for 64-row CTA reconstructions: Vitrea 2; for 320-row CTA reconstructions: Vitrea FX 2.0, Vital Images, Minnetonka, MN, USA). First, calcium score was assessed and an overall Agatston score was registered for each patient. Next, coronary arteries were evaluated as previously described.[8] Presence of CAD was assessed as recommended by the SCCT guidelines for the interpretation and reporting of CTA.[12] Each scan classified as having (1) normal, (2) non-significant CAD (luminal narrowing < 50% in diameter), (3) obstructive CAD (≥ 50% luminal narrowing), as described.[13] In addition, the presence of significant left main disease and significant three-vessel disease was noted. After data evaluation, CTA results were entered in into the departmental Cardiology Information System (EPD-Vision®) without recommendations for further clinical management. Further clinical management was determined at the discretion of the referring cardiologist.

ICA and revascularization

Following CTA, patients were followed up for one year for the occurrence of ICA and revascularization. Patient follow-up information was obtained by one observer, blinded to the baseline CTA results, using data from clinical visits and/or standardized telephone interviews.

Statistical analysis

Statistical analysis was performed using SPSS software (version 16.0, Inc., Chicago, Illinois). Quantitative data were expressed as mean ± standard deviation (SD). Categorical variables were described as numbers and percentages and comparison was performed by chi-square test. Univariate analysis of clinical baseline variables and significant CAD on CTA was performed. For each variable, odds ratio (OR) and 95%-confidence interval (CI) were calculated. Subsequently, multivariate logistic regression analysis for ICA and

revascularization were performed (using backward elimination method with p-value > 0.2 as the criterion for elimination) to determine the independent association with significant CAD on CTA and significant three-vessel or left main disease on CTA, each corrected for clinical baseline variables (age, gender, diabetes, hypercholesterolemia, hypertension, family, smoking and obesity) in a separate model. A p-value < 0.05 was considered statistically significant.

RESULTS

Study population

A total of 637 patients were enrolled in the study population. An overview of the patient characteristics is shown in Table 1. In brief, 47% of patients were male with a mean age of 56 ± 12 years. Reasons for referral were typical chest pain in 21%, atypical chest pain in 46% and non-anginal chest pain in 33%. A total of 27 scans (4.2%) were of non-diagnostic image quality, and excluded from the analysis. The presence of blooming artifacts in patients with a high calcium score ≥400 accounted for 7 uninterpretable scans. Furthermore, 30 patients (3.8%) were lost to follow-up and 2 patients died before follow up was completed. As a result, a total of 578 patients were included in the analysis.

Table 1.

Clinical characteristics (n= 637)	
Age (years)	56 ± 12
Men / women	296 / 341
Diabetes	19%
Hypercholesterolemia*	34%
Hypertension[†]	43%
Family history of CAD)[‡]	46%
Smoking	20%
Obesity[§]	21%
Reason of referral for CTA	
Typical chest pain	21%
Atypical chest pain	46%
Non-anginal chest pain	33%

* Serum total cholesterol ≥ 230 mg/dl and/or serum triglycerides ≥ 200 mg/dl or treatment with lipid lowering drugs, [†] Defined as systolic blood pressure ≥ 140 mm Hg and/or diastolic blood pressure ≥ 90 mm Hg and/or the use of antihypertensive medication, [‡] Defined as presence of coronary artery disease in first degree family members at < 55 years in men and < 65 years in women, [§] Defined as a BMI ≥ 30 kg/m2
Data are absolute values, percentages or means ± standard deviation

CTA results

In a total of 578 patients, CTA results were normal in 212 patients (37%), non-significant CAD was observed in 177 patients (30%) and significant (≥ 50%) CAD was identified in 189 patients (33%). Additionally, significant three-vessel or left main disease on CTA was observed in 34 patients (5.9%), while the presence of significant three-vessel or left main disease could not be determined in 2 patients due to insufficient image quality.

ICA

Subsequent to CTA, ICA was performed in 190 patients (33%). The mean duration between CTA and ICA was 2.6 ± 2.7 months. Of the 189 CTA investigations with significant CAD, subsequent ICA rate was 76% (n=143). Among 177 patients with non-significant CAD on CTA, subsequent ICA rate was 20% (n=35) and among 212 patients with normal CTA results, subsequent ICA rate was 5.7% (n=12; p<0.001). Figure 1 illustrates the relationship between CTA results and subsequent ICA. Moreover, of the 34 patients with significant three-vessel or left main disease on CTA, subsequent ICA rate was 88% (n=30), while ICA rate in 542 patients without significant three-vessel or left main disease on CTA was 29% (n=158, p<0.001).
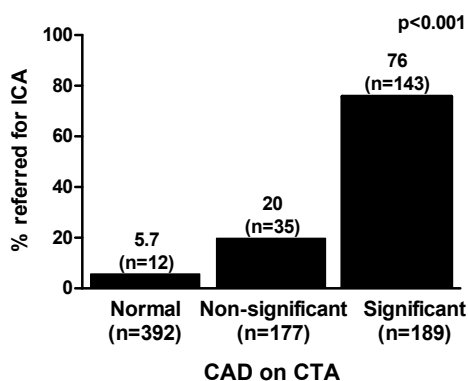
Figure 1. Bar graph illustrating the relationship between degree of CAD on CTA and subsequent referral for ICA.

Univariate regression analysis was performed to identify determinants of subsequent ICA. Table 2 shows that significant CAD on CTA (OR 22.62) as well as significant three-vessel or left main disease on CTA (OR 18.23) were identified as a significant univariate determinant of subsequent ICA. Furthermore, the clinical baseline variables age, gender, hypercholesterolemia, hypertension and smoking were significant univariate determinants of ICA. Subsequently, multivariate logistic regression analysis for ICA was performed to determine the independent association with significant CAD on CTA and significant three-vessel or left main disease on CTA, each corrected for clinical baseline variables in a separate model. Significant CAD on CTA (OR 18.60) and significant three-vessel or left main disease on CTA (OR 15.67) were identified as the strongest independent predictors of ICA. Other determinants of ICA of lesser statistical significance were gender and smoking. Table 2 shows the results of uni- and multivariate regression analysis to identify determinants of subsequent ICA.

Table 2. Independent determinants of subsequent ICA and revascularization

Variable	Univariate		Multivariate	
	OR (95%-CI)	p-value	OR (95%-CI)	p-value
ICA				
Age	1.05 (1.03-1.06)	<0.001	1.02 (0.99-1.04)	0.112
Gender	1.92 (1.35-2.73)	<0.001	1.81 (1.13-2.91)	0.014
Diabetes	1.35 (0.87-2.08)	0.182	-	-
Hypercholesterolemia	2.19 (1.53-3.14)	<0.001	1.42 (0.87-2.30)	0.162
Hypertension	2.09 (1.47-2.98)	<0.001	1.51 (0.93-2.46)	0.098
Family history of CAD	0.83 (0.58-1.17)	0.282	-	-
Smoking	2.70 (1.78-4.09)	<0.001	2.35 (1.33-4.14)	0.003
Obesity	1.08 (0.69-1.67)	0.749	-	-
Significant CAD on CTA[*]	22.62 (14.41-35.51)	<0.001	18.60 (11.46-30.19)	<0.001
Significant three-vessel or left main disease on CTA[*]	18.23 (6.32-52.59)	<0.001	15.67 (4.59-53.43)	<0.001
Revascularization				
Age	1.05 (1.03-1.07)	<0.001	1.02 (0.99-1.06)	0.134
Gender	2.80 (1.73-4.53)	<0.001	2.90 (1.54-5.46)	0.001
Diabetes	2.08 (1.24-3.49)	0.005	2.10 (1.00-4.43)	0.050
Hypercholesterolemia	2.31 (1.46-3.66)	<0.001	1.45 (0.78-2.69)	0.243
Hypertension	1.92 (1.22-3.04)	0.005	-	-
Family history of CAD	0.67 (0.42-1.07)	0.095	-	-
Smoking	3.43 (2.11-5.58)	<0.001	3.24 (1.60-6.57)	0.001
Obesity	1.09 (0.62-1.92)	0.773	-	-
Significant CAD on CTA[*]	338.06 (46.53-2456.30)	<0.001	282.61 (38.21-2090.31)	<0.001
Significant three-vessel or left main disease on CTA[*]	15.62 (7.27-33.54)	<0.001	12.31 (5.52-28.91)	<0.001

[*] Each variable was included in a separate model corrected for clinical baseline variables (age, gender, diabetes, hypercholesterolemia, hypertension, family, smoking and obesity). Results from multivariate analysis for clinical baseline variables shown in the table were derived from the model including significant CAD on CTA.
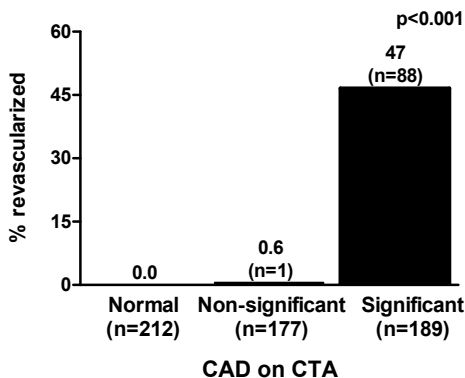
Figure 2. Bar graph illustrating the relationship between degree of CAD on CTA and revascularization.

Revascularization

A total of 89 patients (15%) underwent revascularization, of whom 74 patients underwent PCI and 15 patients coronary artery bypass grafting (CABG). Of the 189 patients with significant CAD on CTA, revascularization rate was 47% (n=88), as compared to a revascularization rate of 0.6% (n=1) in 348 patients with non-significant CAD on CTA. Of note, this patient had a significant lesion in the distal RCA, which was underestimated on CTA. No revascularizations were performed in patients with a normal CTA examination (p<0.001). The frequency of revascularization in relation to CAD on CTA is illustrated in Figure 2.

In 34 patients with significant three-vessel or left main disease on CTA, revascularization rate was 68% (n=23), as compared to 12% (n=64) in 542 patients without significant three-vessel or left main disease on CTA (p<0.001). Table 2 shows that significant CAD on CTA (OR 338.06) as well as significant three-vessel or left main disease on CTA (OR 15.62) were identified as significant determinants of revascularization in univariate analysis. Furthermore, the clinical baseline variables age, gender, hypercholesterolemia, hypertension and smoking were significant univariate determinants of revascularization. Next, multivariate logistic regression analysis for revascularization was performed to determine the independent association of significant CAD on CTA and significant three-vessel or left main disease on CTA, each corrected for clinical baseline variables in a separate model. Multivariate regression analysis identified significant CAD on CTA (OR 282.61) and significant three-vessel or left main disease on CTA (OR 12.31) as the strongest predictors of revascularization. Additional significant determinants were gender and smoking. In Table 2, the results of uni- and multivariate regression analysis to identify determinants of revascularization are shown.

DISCUSSION

The present clinical investigation evaluated the association between CTA results and subsequent rates of ICA and revascularization. The majority of patients with significant CAD on CTA were referred for subsequent ICA (76%), while in patients with normal CTA results a very low rate of referral was demonstrated (5.7%). Additionally, no patients with normal CTA results underwent revascularization. Moreover, significant CAD and significant three-vessel or left main disease on CTA were identified as the strongest independent determinants of subsequent ICA and revascularization.

Previous literature

The use of CTA to reliably exclude significant CAD is supported by extensive literature validating this technique against ICA.[14] Nevertheless, limited information is available regarding the influence of CTA results on clinical decision making and referral for downstream testing such as ICA. Henneman and colleagues previously showed that a substantial proportion of patients with suspected CAD have normal coronaries on CTA examination.[15] As a result, in a substantial percentage of patients with suspected CAD,

significant stenosis may be excluded using CTA. Furthermore, Chow et al. recently studied the clinical impact of CTA on the rate of normal ICA. In a large cohort of 7017 consecutive patients who were referred for ICA before and after implementation of a dedicated CTA program, the implementation of CTA had a positive effect on ICA referral by reducing the frequency of normal ICA from 32% to 27%.[16] The present results expand on these findings, in identifying a strong association between CTA results and referral for ICA. Moreover, the current findings showed a high percentage of normal and non-significant CT results. Considering that normal CTA examinations are associated with a good prognosis,[17] these data imply that, using CTA, a large proportion of patients with chest pain or a high risk profile may be safely excluded from ICA.

Even though significant CAD on CTA was the strongest predictor for revascularization, still a considerable proportion of patients (24%) with significant CTA results were not referred for ICA. Similarly, a small percentage of patients with non-significant and normal CTA results (20% and 5.7%, respectively) were referred for ICA. These findings could be explained by the fact that other clinical information and test results, such as exercise ECG or myocardial perfusion imaging (MPI), may have also influenced referral for ICA. Indeed, clinical presentation and functional information also influence subsequent referral to ICA and revascularization. While no previous studies have investigated ICA rates in relation to CTA results, a prior investigation by Bateman and colleagues showed comparable ICA referral rates in patients who were referred for MPI using single photon emission computed tomography (SPECT).[18] In a group of 4162 patients with a mean follow up of 8.9 months, 60% of patients with high-risk ischemia were referred for ICA, as compared with 9% with mild ischemia and 3.5% of patients without ischemia on SPECT. In this population, 40% of high-risk patients were not referred for invasive imaging, most likely due to the fact that other clinical information and previous study results also influenced patient management. A more recent study by Shaw et al. showed comparable results.[19] In analyzing post-SPECT referral rates, 52% of patients with 3 ischemic perfusion areas underwent ICA. Unfortunately, studies directly comparing CTA and MPI are not available, and future investigations are warranted.

Anatomical and functional imaging prior to ICA

Most traditional non-invasive cardiac imaging techniques rely on the detection of stress-inducible ischemia.[18 20 21] In this setting, perfusion abnormalities or systolic dysfunction serve as surrogate markers for flow-limiting CAD.[22] Although CTA and MPI (the most frequently applied functional imaging technique) provide complementary information,[22] concerns about radiation exposure preclude the use of both CTA and MPI in all patients. With the introduction of CTA, the use of MPI as a gatekeeper for ICA has been challenged.[23] First, CTA has a negative predictive value approaching 100%, making it an excellent modality for the exclusion of CAD in patients with a low-to-intermediate pre-test likelihood. Conversely, MPI enables the identification of perfusion abnormalities, due to which this modality is particularly suitable for ruling in CAD, especially in higher risk patients or

patients with unknown CAD.[24] Thus, individual patient characteristics are important in the choice of non-invasive imaging modality to further guide patient management. Second, while both MPI and CTA are associated with radiation exposure, radiation exposure of CTA has been substantially reduced using novel low-dose algorithms. In daily clinical practice, however, the choice of non-invasive imaging modality prior to ICA may also depend on availability[20] and local expertise. Finally, with the large increase in health-care costs, focus is increasingly shifting to cost-effective use of resources. Preliminary results suggest that costs of CTA as a gatekeeper for ICA may be significantly lower than MPI[25] and therefore more cost-effective. Nevertheless, precise cost-benefit analyses are currently not available and further studies evaluating the relationship between CTA and MPI in selecting patients for ICA are warranted.

Clinical implications

The use of CTA to exclude significant CAD may allow cardiologists to restrict referral for ICA to patients in whom the need for interventional therapy is highly likely.[26] In patients with a normal CTA examination CAD can be safely ruled out and the patient may be reassured. Conversely, patients with significant stenosis on CTA should be referred for further evaluation. Furthermore, patients with recurrent or worsening symptoms as well as patients with left main or three-vessel disease on CTA could be directly referred for ICA. In patients with non-significant stenosis on CTA, however, medical therapy and lifestyle interventions may be appropriate and these patients may be excluded from ICA. Nevertheless, in patients with uncertain results, functional analysis could be performed to further guide referral for ICA. Notably, while CTA may aid risk stratification for the presence of CAD in patients with a low-to-intermediate risk profile, CTA may be less useful in patients with known CAD, in whom the need for ICA and interventional therapy is likely.[6 27 28]

Limitations

Several limitations of the present study merit further consideration. Firstly, CTA is inherently associated with ionizing radiation.[29] Secondly, CTA and ICA do not provide information regarding the functional significance of a lesion. Combined anatomic and perfusion imaging using either a hybrid imaging approach or volumetric CTA in a single examination would be advantageous and research is ongoing.[30] Third, the effect of other clinical information, such as perfusion imaging, may have also influenced referral for ICA. However, studying the effects other tests as well as cost-benefit analysis were beyond the scope of this study. Last, the present investigation did not evaluate clinical outcome. Future studies are needed to evaluate the effect of CTA on clinical outcome and health-care costs.

Conclusion

The present investigation showed that the results of CTA are strong and independent determinants of subsequent ICA as well as revascularization. Consequently, CTA has the potential to serve as a gatekeeper for ICA to identify patients who are most likely to benefit from revascularization and exclude patients who can safely avoid ICA.

REFERENCES

1. Boden WE, O'Rourke RA, Teo KK et al. Optimal medical therapy with or without PCI for stable coronary disease. N Engl J Med 2007;356:1503-16.
2. Hachamovitch R, Hayes SW, Friedman JD et al. Stress myocardial perfusion single-photon emission computed tomography is clinically effective and cost effective in risk stratification of patients with a high likelihood of coronary artery disease (CAD) but no known CAD. J Am Coll Cardiol 2004;43:200-8.
3. Min JK, Shaw LJ, Devereux RB et al. Prognostic value of multidetector coronary computed tomographic angiography for prediction of all-cause mortality. J Am Coll Cardiol 2007;50:1161-70.
4. van Velzen JE, de Graaf FR, Kroft LJ et al. Performance and efficacy of 320-row computed tomography coronary angiography in patients presenting with acute chest pain: results from a clinical registry. Int J Cardiovasc Imaging 2011.
5. van Werkhoven JM, Schuijf JD, Gaemperli O et al. Incremental prognostic value of multi-slice computed tomography coronary angiography over coronary artery calcium scoring in patients with suspected coronary artery disease. Eur Heart J 2009;30:2622-9.
6. Taylor AJ, Cerqueira M, Hodgson JM et al. CCF/SCCT/ACR/AHA/ASE/ASNC/NASCI/SCAI/SCMR 2010 appropriate use criteria for cardiac computed tomography: a report of the American College of Cardiology Foundation Appropriate Use Criteria Task Force, the Society of Cardiovascular Computed Tomography, the American College of Radiology, the American Heart Association, the American Society of Echocardiography, the American Society of Nuclear Cardiology, the North American Society for Cardiovascular Imaging, the Society for Cardiovascular Angiography and Interventions, and the Society for Cardiovascular Magnetic Resonance. J Am Coll Cardiol 2010;56:1864-94.
7. de Graaf FR, Schuijf JD, van Velzen JE et al. Evaluation of contraindications and efficacy of oral Beta blockade before computed tomographic coronary angiography. Am J Cardiol 2010;105: 767-72.
8. de Graaf FR, van Werkhoven JM, van Velzen JE et al. Incremental prognostic value of left ventricular function analysis over non-invasive coronary angiography with multidetector computed tomography. J Nucl Cardiol 2010;17:1034-40.
9. Schuijf JD, Pundziute G, Jukema JW et al. Diagnostic accuracy of 64-slice multislice computed tomography in the noninvasive evaluation of significant coronary artery disease. Am J Cardiol 2006;98:145-8.
10. Schuijf JD, Wijns W, Jukema JW et al. Relationship between noninvasive coronary angiography with multi-slice computed tomography and myocardial perfusion imaging. J Am Coll Cardiol 2006;48:2508-14.
11. de Graaf FR, Schuijf JD, van Velzen JE et al. Diagnostic accuracy of 320-row multidetector computed tomography coronary angiography to noninvasively assess in-stent restenosis. Invest Radiol 2010;45:331-40.
12. Raff GL, Abidov A, Achenbach S et al. SCCT guidelines for the interpretation and reporting of coronary computed tomographic angiography. J Cardiovasc Comput Tomogr 2009;3:122-36.
13. de Graaf FR, Schuijf JD, van Velzen JE et al. Diagnostic accuracy of 320-row multidetector computed tomography coronary angiography in the non-invasive evaluation of significant coronary artery disease. Eur Heart J 2010;31:1908-15.
14. Meijboom WB, Meijs MF, Schuijf JD et al. Diagnostic accuracy of 64-slice computed tomography coronary angiography: a prospective, multicenter, multivendor study. J Am Coll Cardiol 2008;52: 2135-44.

15. Henneman MM, Schuijf JD, van Werkhoven JM et al. Multi-slice computed tomography coronary angiography for ruling out suspected coronary artery disease: what is the prevalence of a normal study in a general clinical population? Eur Heart J 2008;29:2006-13.

16. Chow BJ, Abraham A, Wells GA et al. Diagnostic accuracy and impact of computed tomographic coronary angiography on utilization of invasive coronary angiography. Circ Cardiovasc Imaging 2009;2:16-23.

17. Hulten EA, Carbonaro S, Petrillo SP et al. Prognostic value of cardiac computed tomography angiography: a systematic review and meta-analysis. J Am Coll Cardiol 2011;57:1237-47.

18. Bateman TM, O'Keefe JH, Jr., Dong VM et al. Coronary angiographic rates after stress single-photon emission computed tomographic scintigraphy. J Nucl Cardiol 1995;2:217-23.

19. Shaw LJ, Hachamovitch R, Berman DS et al. The economic consequences of available diagnostic and prognostic strategies for the evaluation of stable angina patients: an observational assessment of the value of precatheterization ischemia. Economics of Noninvasive Diagnosis (END) Multicenter Study Group. J Am Coll Cardiol 1999;33:661-9.

20. Wijns W, De BB, Vanhoenacker PK. What does the clinical cardiologist need from noninvasive cardiac imaging: is it time to adjust practices to meet evolving demands? J Nucl Cardiol 2007; 14:366-70.

21. Nucifora G, Schuijf JD, van Werkhoven JM et al. Relationship between obstructive coronary artery disease and abnormal stress testing in patients with paroxysmal or persistent atrial fibrillation. Int J Cardiovasc Imaging 2010.

22. van Werkhoven JM, Schuijf JD, Gaemperli O et al. Prognostic value of multislice computed tomography and gated single-photon emission computed tomography in patients with suspected coronary artery disease. J Am Coll Cardiol 2009;53:623-32.

23. Priest VL, Scuffham PA, Hachamovitch R et al. Cost-effectiveness of coronary computed tomography and cardiac stress imaging in the emergency department: a decision analytic model comparing diagnostic strategies for chest pain in patients at low risk of acute coronary syndromes. JACC Cardiovasc Imaging 2011;4:549-56.

24. Hoilund-Carlsen PF, Johansen A, Christensen HW et al. Potential impact of myocardial perfusion scintigraphy as gatekeeper for invasive examination and treatment in patients with stable angina pectoris: observational study without post-test referral bias. Eur Heart J 2006;27:29-34.

25. Budoff MJ, Karwasky R, Ahmadi N et al. Cost-effectiveness of multidetector computed tomography compared with myocardial perfusion imaging as gatekeeper to invasive coronary angiography in asymptomatic firefighters with positive treadmill tests. J Cardiovasc Comput Tomogr 2009;3:323-30.

26. Achenbach S, Daniel WG. Cardiac imaging in the patient with chest pain: coronary CT angiography. Heart 2010;96:1241-6.

27. Bluemke DA, Achenbach S, Budoff M et al. Noninvasive coronary artery imaging: magnetic resonance angiography and multidetector computed tomography angiography: a scientific statement from the american heart association committee on cardiovascular imaging and intervention of the council on cardiovascular radiology and intervention, and the councils on clinical cardiology and cardiovascular disease in the young. Circulation 2008;118:586-606.

28. de Graaf FR, Schuijf JD, Scholte AJ et al. Usefulness of hypertriglyceridemic waist phenotype in type 2 diabetes mellitus to predict the presence of coronary artery disease as assessed by computed tomographic coronary angiography. Am J Cardiol 2010;106:1747-53.

29. van der Wall EE, Jukema JW, Schuijf JD et al. 100 kV versus 120 kV: effective reduction in radiation dose? Int J Cardiovasc Imaging 2011;27:587-91.

30. Ko BS, Cameron JD, Meredith IT et al. Computed tomography stress myocardial perfusion imaging in patients considered for revascularization: a comparison with fractional flow reserve. Eur Heart J 2011.

CHAPTER 15

Predictive Value of Multislice Computed Tomography Variables of Atherosclerosis for Ischemia on Stress-Rest Single Photon Emission Computed Tomography (SPECT)

Joëlla E. van Velzen, Joanne D. Schuijf, Jacob M. van Werkhoven, Bernhard A. Herzog, Aju P. Pazhenkottil, Eric Boersma, Fleur R. de Graaf, Arthur J. Scholte, Lucia J. Kroft, Albert de Roos, Marcel P. Stokkel, J. Wouter Jukema, Philipp A. Kaufmann, Ernst E. van der Wall, Jeroen J. Bax

ABSTRACT

Background: Previous studies have shown that the presence of stenosis alone on multislice computed tomography (MSCT) has a limited positive predictive value for the presence of ischemia on myocardial perfusion imaging (MPI). The purpose of this study was to assess which variables of atherosclerosis on MSCT angiography are related to ischemia on MPI.

Methods: Both MSCT and MPI were performed in 514 patients. On MSCT, the calcium score, degree of stenosis (≥50% and ≥70% stenosis), plaque extent and location were determined. Plaque composition was classified as non-calcified, mixed or calcified. Ischemia was defined as a summed difference score ≥2 on a per patient basis.

Results: Ischemia on MPI was observed in 137 patients (27%). On MSCT, on a patient basis, multivariate analysis showed that the degree of stenosis (presence of ≥70% stenosis, OR 3.5), plaque extent and composition (mixed plaques ≥3, OR 1.7 and calcified plaques ≥3, OR 2.0) and location (atherosclerotic disease in left main coronary artery and/ or proximal left anterior descending coronary artery, OR 1.6) were independent predictors for ischemia on MPI. In addition, MSCT variables of atherosclerosis such as plaque extent, composition and location had significant incremental value for the prediction of ischemia over the presence of ≥70% stenosis.

Conclusion: In addition to the degree of stenosis, MSCT variables of atherosclerosis describing plaque extent, composition and location are predictive of the presence of ischemia on MPI.

INTRODUCTION

Over the past decade, multislice computed tomography (MSCT) angiography has emerged as a non-invasive modality for visualization of the coronary arteries. Recently, several studies have addressed the diagnostic accuracy of MSCT as compared to invasive coronary angiography reporting high accuracies for the detection of 50% stenosis.[1] Importantly, the high negative predictive value of 99% indicates that the technique may be particularly useful for ruling out the presence of coronary artery disease (CAD) in patients with lower likelihood of CAD. On the other hand, while MSCT angiography provides insight into the severity and extent of anatomical disease, it is currently unable to evaluate the hemodynamical relevance of CAD. In fact, previous studies have revealed a large discrepancy between the presence of atherosclerosis on MSCT angiography and the presence of ischemia during functional testing.[2-5] These investigations demonstrated that approximately only half of obstructive stenoses (≥50% luminal narrowing) on MSCT were associated with abnormal perfusion, whereas a large proportion of obstructive lesions on MSCT did not result in perfusion abnormalities.

Therefore, identification of anatomical MSCT variables of atherosclerosis that are associated with ischemia on MPI, in addition to the presence of obstructive CAD, may improve selection of further diagnostic and/or therapeutic management. Thus, the purpose of this study was to identify variables of atherosclerosis on MSCT angiography that are related to ischemia on MPI, in addition to the presence of obstructive CAD.

METHODS

Patients and study protocol

The study population consisted of 524 patients who were clinically referred for functional and anatomical imaging because of chest pain or an elevated risk profile as part of an ongoing registry addressing the relative merits of MSCT in relation to other imaging techniques. Patients underwent both myocardial perfusion imaging (MPI) with stress-rest gated single photon emission computed tomography (SPECT) and MSCT within 3 months in two different institutions. Patients were included at the University Hospital in Zurich, Switzerland (n=263) and at the Leiden University Medical Center, Leiden, the Netherlands (n=261). Exclusion criteria were: known CAD (previous myocardial infarction, percutaneous coronary intervention and coronary artery bypass surgery), atrial fibrillation, renal insufficiency (glomerular filtration rate <30 ml/min), known allergy to iodine contrast and pregnancy. The clinical symptoms of included patients were recorded and patients were further classified as having a low, intermediate or high pre-test likelihood of obstructive CAD using the method described by Diamond and Forrester.[6]

Stress-rest gated MPI

Patients were instructed to withhold beta-blocking medication and calcium antagonists 48 hours before examination and caffeine 12 hours before examination. For each center a different gated MPI protocol was used. In Leiden (n=261) a two-day gated stress-rest SPECT protocol was performed using either technetium-99 tetrofosmin (500 MBq) or technetium-99m sestamibi (500 MBq). In patients that were able to exercise, symptom-limited bicycle test was performed and in patients unable to exercise pharmacological stress was performed using adenosine or dobutamine. In Zurich (n=263) a one day gated stress-rest SPECT was performed using adenosine stress and technetium-99m tetrofosmin (300 MBq at peak stress and 900 MBq at rest). The images were acquired on a triple-head SPECT camera (GCA 9300/HG, Toshiba Corp., Tokyo, Japan) or a dual-head detector camera (Millennium VG & Hawkeye, General Electric Medical Systems, Milwaukee, WI, USA; or Vertex Epic ADAC Pegasus, Philips Medical Systems, Eindhoven, the Netherlands). All cameras were equipped with low energy high resolution collimators. A 20% window was used with a 140-keV energy peak of technetium-99m and data were stored in a 64x64 matrix.

Subsequently, stress-rest gated MPI datasets were quantitatively evaluated using previously validated automated software.[7] The data were reconstructed into long- and short-axis perpendicular to the heart axis. A 20-segment model was used in which the myocardial segments were assigned to the different perfusion territories. Each segment was scored by an experienced observer according to the standard scoring scale of 0-4 (normal, mild, moderate, severe reduction or absence of uptake). The total segmental perfusion scores during stress and rest were added to calculate the summed stress score (SSS) and the summed rest score (SRS), respectively. The summed difference score (SDS) was calculated as the sum of difference between the SRS and SSS. Ischemia was defined as a SDS ≥2 and severe ischemia was defined as a SDS ≥8.[8] On a per vessel basis, the presence of ischemia was assessed visually in the corresponding vascular territory. Consequently, ischemia in the anterior and septal wall was allocated to the left anterior descending coronary artery, ischemia in the lateral wall was allocated to the left circumflex coronary artery and ischemia in the inferior wall was allocated to the right coronary artery.[9]

MSCT coronary angiography

Heart rate and blood pressure were evaluated before each scan. If a patient's heart rate was above 65 beats per minute and no contra-indications existed, beta-blocking medica-tion was administered one hour before the examination (50-100 mg metoprolol orally or 5-10 mg metoprolol intravenously).

In the first 41 patients data acquisition was performed using a 16-slice MSCT scanner (Aquilion 16, Toshiba Medical Systems, Otawara, Japan) with a collimation of 16 x 0.5 mm, a gantry rotation time of 400 ms, tube voltage of 120 kV and tube current of 250 to 350 mA. A 64-slice MSCT scanner (Aquilion 64, Toshiba Medical Systems, Otawara, Japan or General Electrics Lightspeed VCT, Milwaukee, WI, USA) was used for the remaining 483 patients with a collimation of 64 x 0.5 mm, a gantry rotation time of 400 ms, tube voltage of 100 to

135 kV and tube current of 250 to 350 mA, depending on body shape. First, a non-contrast enhanced low dose scan prospectively triggered at 75% of the R-R interval was performed before helical scanning. This examination was used for calcium scoring and followed by a triggered helical scan. For the 16-slice MSCT non-ionic contrast (Iomeron 400, Bracco, Milan, Italy) was administered in the ante-cubital vein, with a dose of 130 to 140 ml and a flow-rate of 4 ml/s, followed by a saline flush. For 64-slice MSCT, 80 to 110 ml contrast was

Figure 1. Assessment of variables of atherosclerosis on multislice computed tomography (MSCT) Examples of the classification of different variables of atherosclerosis on MSCT. Panel A: Assessment of the presence of atherosclerosis: curved multiplanar reconstruction (MPR) of right coronary artery (RCA) revealing the absence of atherosclerosis. Panel B: Assessment of the degree of stenosis: MPR showing a lesion resulting in ≥50% stenosis in the mid RCA (arrow). Panel C: Assessment of the extent and composition of atherosclerotic disease: MPR of the left anterior descending coronary artery (LAD) revealing a single mixed plaque (arrow). Panel D: Assessment of location of atherosclerosis: MPR of the LAD demonstrating the presence of an atherosclerotic lesion in the left main coronary artery and proximal LAD (arrow).

administered with a flow rate of 5 ml/s followed by a saline flush. Automatic detection of peak enhancement in the descending aorta was used for timing. Subsequently data sets were reconstructed at the best phase of the R-R interval and transferred to dedicated work stations (Vitrea2, Vital Images, USA, or Advantage, GE Healthcare, USA).

The non-contrast enhanced CT images were used to calculate the calcium score using the Agatston method.[10] MSCT angiographic examinations were evaluated in consensus by 2 experienced readers including an interventional cardiologist blinded to stress-rest SPECT findings. A 17-segment model modified according to the American Heart Association was used and for each segment was determined if atherosclerosis was present using axial and/or orthogonal images and curved multiplanar reconstructions. If atherosclerosis was present, the degree of stenosis was graded as non-obstructive (<50% stenosis), obstructive (≥50% stenosis) and severely obstructive (≥70% stenosis). Additionally, the extent of atherosclerosis was determined by assessing the number of diseased segments. Consequently, plaques were scored according to plaque composition (non-calcified, mixed or calcified). Non-calcified plaques were regarded as plaques having a lower CT attenuation compared to the contrast lumen and no visible calcifications, calcified plaques were plaques with predominantly high CT attenuation and without non-calcified plaque elements and mixed plaques were plaques consisting of both non-calcified and calcified elements. Lastly, the location of disease was classified as being present in left main coronary artery (LM) and/or proximal left anterior descending coronary artery (LAD) or not (example provided in Figure 1).

Statistical analysis

Continuous data were expressed as mean and standard deviation, and categorical data were expressed in numbers and percentages. Binary logistic regression analysis was performed to determine the predictive value of MSCT variables of atherosclerosis for presence of ischemia on MPI on both a patient and vessel basis. First univariate analysis of baseline clinical risk variables (age and gender),[6] calcium score and MSCT variables was performed. To analyze the predictive value of variables of atherosclerosis on MSCT (degree of stenosis, plaque extent, composition and location), optimal binary cutoffs were created for analysis. For each variable, an odds ratio with 95% confidence interval (OR (CI 95%) was calculated.

The current study used 2 generations of MSCT scanners (16-slice and 64-slice), thus to correct for scanner type, scanner type was included in the univariate analysis. In addition, interaction was assessed between scanner type and MSCT variables of atherosclerosis (describing degree of stenosis, plaque extent, composition and location). In this analysis, no interaction was demonstrated between MSCT scanner type and MSCT variables of atherosclerosis (data not shown).

The intention was to build a multivariate model that combines clinical variables and MSCT variables of atherosclerosis for the prediction of ischemia on MPI, in a stepwise fashion. The first model consisted of clinical risk variables only. Consequently, the presence of (severely) obstructive CAD was added, followed by plaque extent and composition (≥3

mixed plaques and ≥3 calcified plaques). Finally, plaque location (atherosclerotic disease in the LM and/or proximal LAD) was added to the model. For each next iterative step, variables may not remain statistically significant. Thus, all variables with a p-value <0.15 were kept in the model in order not to miss clinically relevant predictors of ischemia.

The performance of the final multivariate model for prediction of ischemia on both a patient and vessel basis was studied with respect to discrimination and calibration. Discrimination was quantified by a measure of concordance, the c-index. For binary outcomes the c-index is identical to the area under the receiver operating characteristic (ROC) curve. The c-index lies between 0.5 and 1, and is better if closer to one.[11] Calibration refers to whether the predicted risks agree with the observed risk frequencies. Calibration was measured with the Hosmer-Lemeshow goodness-of-fit test (p>0.10 considered to indicate lack of deviation between the model and observed event rates). Statistical analysis was performed using SPSS software (version 16.0, SPSS inc., Chicago, IL, USA) and SAS software (The SAS system 6.12, Cary, NC, USA: SAS Institute Inc). A p-value <0.05 was considered statistically significant.

Table 1. Baseline patient characteristics

	n (%)
Male	302 (59%)
Age (years)	60 ±11
Obesity (BMI ≥30 kg/m^2)	111 (22%)
Diabetes	155 (30%)
Hypercholesterolemia	209 (41%)
Hypertension	287 (56%)
Positive family history for CAD	191 (37%)
Smoking currently	153 (30%)
Pre-test likelihood	
Low pre-test likelihood	113 (22%)
Intermediate pre-test likelihood	334 (65%)
High pre-test likelihood	67 (13%)
Symptoms patient population	
Typical chest pain	78 (15%)
Atypical chest pain	146 (28%)
Non-anginal chest pain	41 (8%)
Asymptomatic	181 (35%)
Other (dyspnea, tiredness, dizziness ect.)	68 (13%)

BMI, body mass index; CAD, coronary artery diseas

RESULTS

Patient characteristics

In total, 524 patients were enrolled in the present study. In 10 patients (2%) the MSCT data set was not interpretable because of an irregular or elevated heart rate and these patients were excluded from the analysis. Therefore, 514 patients were included in the analysis. Baseline patient characteristics are described in Table 1.

Stress-rest gated MPI results

In 87 patients symptom-limited bicycle test was performed and in the remaining 427 patients pharmacological stress was applied using either adenosine (n=395) or dobuta-mine (n=32). MPI imaging results are presented in Table 2. The mean SSS was 2.8 ±4.5, the mean SRS was 1.5 ±3.0 and the mean SDS was 1.3 ±3.6. Ischemia (SDS ≥2) was observed in 137 patients (27%). Within this group, 16 patients (3%) were shown to have severe ischemia (SDS ≥8).

Table 2. Imaging results of MPI, calcium score and MSCT angiography

	n (%)
MPI	
Normal perfusion (SDS <2)	377 (73%)
Ischemia (SDS ≥2)	137 (27%)
Severe ischemia (SDS ≥8)	16 (3%)
Calcium score	
0	174 (34%)
1-100	140 (27%)
101-400	88 (17%)
>400	112 (22%)
MSCT angiography	
Degree	
Presence of non-obstructive CAD	354 (69%)
Presence of obstructive CAD (≥50%)	157 (31%)
Presence of severely obstructive CAD (≥70%)	83 (16%)
Extent and Composition	
Non-calcified plaques ≥3	39 (8%)
Mixed plaques ≥3	93 (18%)
Calcified plaques ≥3	126 (25%)
Location	
LM and/or proximal LAD diseased	74 (14%)

MPI, myocardial perfusion imaging; SDS, summed difference score; MSCT, multislice computed tomography; CAD, coronary artery disease; LM, left main coronary artery; LAD, left anterior descending coronary artery;

Baseline MSCT results

Average heart rate during MSCT acquisition was 63 ±10 beats per minute. The baseline calcium score and MSCT imaging results are shown in Table 2. The mean calcium score was 324 ±751.

MSCT predictors for ischemia on MPI: patient based analysis

Results of the univariate analysis regarding the predictive value of MSCT variables for ischemia on MPI (patient basis) are listed in Table 3. As demonstrated, scanner type (16-slice or 64-slice) was not related to the presence of ischemia on MPI. To determine the independent predictive value of MSCT variables of atherosclerosis for ischemia on MPI, multivariate models were created including MSCT variables of atherosclerosis corrected for baseline clinical variables and the presence of severely obstructive CAD (Table 4). Interestingly, several MSCT variables of atherosclerosis remained predictive of ischemia on MPI in the multivariate model. Regarding contrast enhanced MSCT coronary angiography, degree of stenosis (presence of ≥50% and ≥70% stenosis), extent and composition

Table 3. Univariate analysis for prediction of ischemia on MPI on patient basis

	OR (CI 95%)	P-value	Reference
Clinical	2.0 (1.4-3.8)	<0.001	
Calcium score			
1-100	0.6 (0.4-0.9)	0.02	Calcium score 0
101-400	1.2 (0.7-2.0)	0.48	Calcium score 0
>400	4.8 (3.1-7.5)	<0.001	Calcium score 0
MSCT angiography			
MSCT scanner type (64-slice)	1.3 (0.7-2.6)	0.46	16-slice MSCT
Degree			
Number of obstructive segments	1.4 (1.3-1.6)	<0.001	
Presence obstructive CAD*	5.4 (3.5-8.3)	<0.001	Absence obstructive CAD
Presence severely obstructive CAD†	6.8 (4.1-11.2)	<0.001	Absence severely obstructive CAD
Extent and Composition			
Number of non-calcified plaques	1.1 (1.0-1.2)	0.15	
Number of mixed plaques	1.3 (1.2-1.4)	<0.001	
Number of calcified plaques	1.3 (1.2-1.4)	<0.001	
Non-calcified plaques ≥3	0.9 (0.4-2.0)	0.86	Non-calcified plaques <3
Mixed plaques ≥3	3.9 (2.5-6.3)	<0.001	Mixed plaques <3
Calcified plaques ≥3	3.3 (2.2-5.1)	<0.001	Calcified plaques <3
Location			
LM and/or proximal LAD diseased	3.4 (2.2-5.3)	<0.001	Absence disease LM and/or proximal LAD

MPI, myocardial perfusion imaging; OR (CI 95%), odds ratio with 95% confidence interval; MSCT, multislice computed tomography; CAD, coronary artery disease; LM, left main coronary artery; LAD, left anterior descending coronary artery; *stenosis ≥50%; †stenosis ≥70%

**Table 4.** Multivariate models for prediction of ischemia on MPI on patient basis

	OR (CI 95%)	P-value	Reference
Model I			
Clinical	2.0 (1.4-3.8)	<0.001	
Model II			
Clinical	1.6 (1.1-2.3)	0.01	
Presence obstructive CAD*	5.0 (3.3-7.7)	<0.0001	Absence obstructive CAD
Model III			
Clinical	1.7 (1.2-2.5)	0.006	
Presence severely obstructive CAD[†]	6.2 (3.7-10.4)	<0.0001	Absence severely obstructive CAD
Model IV			
Clinical	1.6 (1.1-2.3)	0.02	
Presence severely obstructive CAD[†]	3.8 (2.2-6.7)	<0.0001	Absence severely obstructive CAD
Mixed plaques ≥3	2.0 (1.2-3.5)	0.012	Mixed plaques <3
Calcified plaques ≥3	2.3 (1.5-3.7)	<0.0001	Calcified plaques <3
Model V			
Clinical	0.7 (1.1-2.4)	0.008	
Presence severely obstructive CAD[†]	4.2 (2.5-7.3)	<0.0001	Absence severely obstructive CAD
Calcified plaques ≥3	1.9 (1.2-3.1)	0.01	Calcified plaques <3
LM and/or proximal LAD diseased	1.8 (1.1-3.0)	0.03	Absence disease LM and/or proximal LAD
Model VI			
Clinical	1.6 (1.1-2.4)	0.01	
Presence severely obstructive CAD[†]	3.5 (2.0-6.3)	<0.0001	Absence severely obstructive CAD
Mixed plaques ≥3	1.7 (0.9-3.1)	0.053	Mixed plaques <3
Calcified plaques ≥3	2.0 (2.2-3.3)	0.007	Calcified plaques <3
LM and/or proximal LAD diseased	1.6 (0.9-2.7)	0.107	Absence diseaset LM and/or proximal LAD

MPI, myocardial perfusion imaging; OR (CI 95%), odds ratio with 95% confidence interval; CAD, coronary artery disease; LM, left main coronary artery; LAD, left anterior descending coronary artery; *stenosis ≥50%; [†]stenosis ≥70%

(presence of ≥3 mixed plaques and/or ≥3 calcified plaques) and location (atherosclerotic disease in LM and/or proximal LAD) remained independent predictors of ischemia. An example of a patient with all predictors on MSCT is provided in Figure 2.

MSCT predictors for ischemia on MPI: vessel based analysis

Results of the univariate analysis regarding the predictive value of MSCT variables for ischemia on MPI (vessel basis) are listed in Table 5. To determine the independent predictive value of MSCT variables of atherosclerosis for ischemia on MPI on a vessel basis, multivariate models were created including MSCT variables of atherosclerosis which were corrected for baseline clinical risk variables (Table 6). Interestingly, several MSCT variables of atherosclerosis remained predictive of ischemia on MPI in the multivariate model on a vessel basis. Indeed, degree of stenosis (presence of ≥50% and ≥70% stenosis) and extent and composition (presence of ≥2 mixed plaques and/or ≥2 calcified plaques) remained significant independent predictors of ischemia.
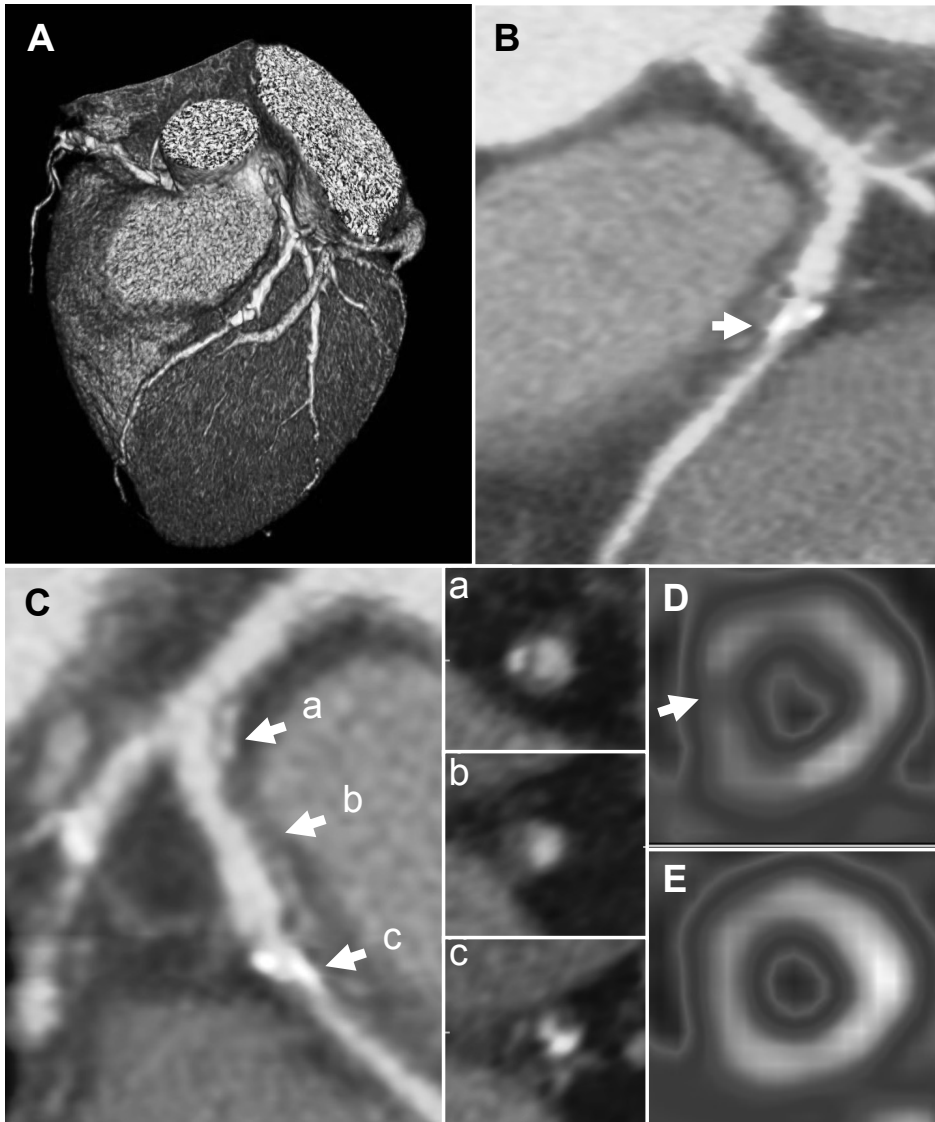
Figure 2. Example of a 72 year-old male patient exhibiting all the significant predictors on multislice computed tomography (MSCT) for prediction of ischemia on myocardial perfusion imaging (MPI)

In panel A, a 3D volume rendered reconstruction is provided, showing the left anterior descending coronary artery (LAD). Panel B: A curved multiplanar reconstruction (MPR) of the LAD is shown demonstrating the presence of obstructive CAD (≥50%) in the proximal segment (arrow). Panel C: Another curved MPR of the LAD is shown in a different view, revealing the presence of multiple diseased segments (cross sectional images a, b and c), the presence of obstructive lesion in the LAD (arrow c) and the presence of mixed plaque (cross sectional images a, b and c). Panel D: Stress single photon emission computed tomography (SPECT) short axis image showing the presence of a perfusion defect, particularly evident in the antero-septal region (arrow). Panel E: Rest SPECT short axis image demonstrating normal perfusion.

Table 5. Univariate analysis for prediction of ischemia on MPI on vessel basis

	OR (CI 95%)	P-value	Reference value
Clinical	1.9 (2.5-1.4)	<0.001	
MSCT angiography			
Degree			
Number of obstructive segments	2.0 (1.7-2.4)	<0.001	
Presence obstructive CAD*	4.0 (3.0-5.3)	<0.001	Absence obstructive CAD
Presence severely obstructive CAD[†]	5.3 (3.6-7.8)	<0.001	Absence severely obstructive CAD
Extent and Composition			
Number of non-calcified plaques	1.2 (1.0-1.4)	0.08	
Number of mixed plaques	1.6 (1.4-1.8)	<0.001	
Number of calcified plaques	1.4 (1.2-1.6)	<0.001	
Non-calcified plaques ≥2	1.0 (0.6-1.9)	0.91	Non-calcified plaques<2
Mixed plaques ≥2	3.0 (2.1-4.2)	<0.001	Mixed plaques <2
Calcified plaques ≥2	2.1 (1.5-2.9)	<0.001	Calcified plaques <2

MPI, myocardial perfusion imaging; OR (CI 95%), odds ratio with 95% confidence interval; MSCT, multislice computed tomography; CAD, coronary artery disease; *stenosis ≥50%, [†]stenosis ≥70%

Table 6. Multivariate models for prediction of ischemia on MPI on vessel basis

	OR (CI 95%)	P-value	Reference
Model I			
Clinical	1.9 (2.5-1.4)	<0.001	
Model II			
Clinical	1.8 (1.4-2.2)	<0.001	
Presence obstructive CAD*	3.8 (2.8-5.0)	<0.001	Absence obstructive CAD
Model III			
Clinical	1.8 (1.5-2.2)	<0.001	
Presence severely obstructive CAD[†]	5.0 (3.3-7.3)	<0.001	Absence severely obstructive CAD
Model IV			
Clinical	1.8 (1.4-2.2)	<0.001	
Presence severely obstructive CAD[†]	3.5 (2.3-5.3)	<0.001	Absence severely obstructive CAD
Mixed plaques ≥2	1.9 (1.3-2.8)	<0.001	Mixed plaques <2
Calcified plaques ≥2	1.8 (1.3-2.5)	<0.001	Calcified plaques <2

MPI, myocardial perfusion imaging; OR (CI 95%), odds ratio with 95% confidence interval; CAD, coronary artery disease, *stenosis ≥50%, [†]stenosis ≥70%

Incremental value of angiographic MSCT variables of atherosclerosis to predict ischemia on MPI

In total, 157 patients (31%) had obstructive CAD and 83 patients (16%) had severely obstructive CAD on MSCT. Regarding these patients, 80 patients (51%) and 52 patients (63%) revealed ischemia on MPI, respectively. Moreover, of the 259 patients with at least

one of the significant predictors on MSCT, only 119 patients (33%) showed ischemia on MPI. Example of a patient demonstrating only one significant predictor and a normal MPI is provided in Figure 3. In addition, of the 22 patients with all of the significant predictors on MSCT (describing degree of stenosis, plaque extent, composition, and location), 18 patients (82%) showed ischemia on MPI.

Finally, the performance of the multivariate models for prediction of ischemia on both a patient (model V in Table 4) and vessel basis (model IV in Table 6) were studied with

Figure 3. Example of a 69 year-old female patient exhibiting an obstructive lesion on multislice computed tomography (MSCT) while myocardial perfusion imaging (MPI) showed normal perfusion A 3D volume rendered reconstruction is provided in panel A, showing the left anterior descending coronary artery (LAD) and left circumflex coronary artery (LCx). Panel B: A curved multiplanar reconstruction (MPR) of the right coronary artery (RCA) is shown demonstrating the presence of non-obstructive non-calcified plaque (arrow). Panel C: A curved MPR of the LAD is shown revealing the presence of a single non-obstructive mixed plaque (arrow). Panel D: A curved MPR of LCx is shown demonstrating the presence of obstructive lesion (however <70%) in the mid LAD (arrow). Panel E: Single photon emission computed tomography (SPECT) short axis image showing normal perfusion in stress and rest (panel F).

respect to discrimination and calibration. Discrimination was quantified by a measure of concordance, the c-index. In this model, plaque extent, composition and location had significant incremental value over clinical risk stratification and the presence of severely obstructive CAD (p<0.05) for the prediction of ischemia on both a patient and vessel basis (Figure 4 and Figure 5, respectively). The performance of the model (calibration) was assessed by the Hosmer-Lemeshow goodness-of-fit test (p>0.10 considered to indicate lack of deviation between the model and observed event rates). As demonstrated in Figure 6, on both a patient and vessel basis, the estimated risk of the models showed good agreement with the observed risk frequencies.
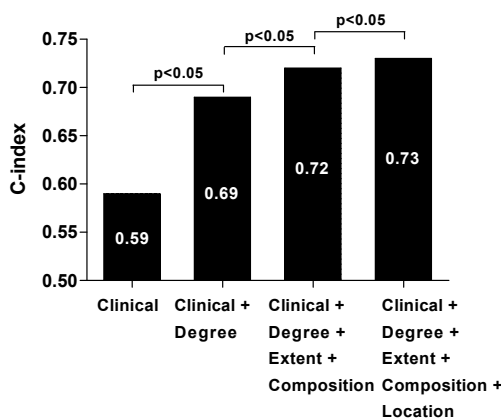
Figure 4. Bars representing the c-index (area under the curve) on the y-axis illustrating the incremental predictive value of angiographic multislice computed tomography (MSCT) variables of atherosclerosis for the prediction of ischemia on myocardial perfusion imaging (MPI) on a patient basis. The addition of the degree of stenosis (presence of ≥70% stenosis) provided incremental predictive information to baseline clinical variables for the prediction of ischemia on MPI on a patient basis. Furthermore the addition of extent and composition of atherosclerosis (≥3 calcified plaques) and location (atherosclerotic disease in the left main coronary artery and/or proximal left anterior descending coronary artery) on MSCT resulted in further incremental predictive value over baseline clinical variables and degree of stenosis on MSCT.

DISCUSSION

The main findings of the present study can be summarized as follows. In a population with predominantly low-to-intermediate pre-test likelihood for CAD, MSCT variables of atherosclerosis such as plaque extent, composition and location were significant predictors of ischemia on MPI, over the presence of obstructive CAD. Moreover, the incremental value of angiographic MSCT variables of atherosclerosis over clinical risk stratification and the presence of severely obstructive CAD was investigated. In this model, plaque extent, composition (presence of ≥3 mixed plaques and/or ≥3 calcified plaques) and location
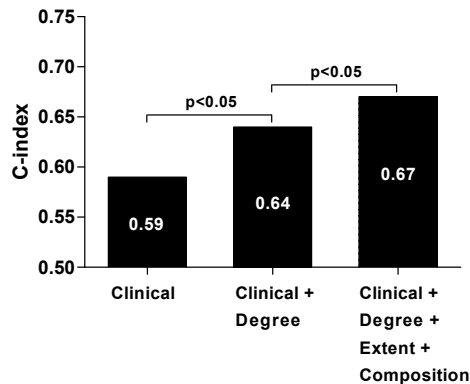
Figure 5. Bars representing the c-index (area under the curve) on the y-axis illustrating the incremental predictive value of angiographic multislice computed tomography (MSCT) variables of atherosclerosis for the prediction of ischemia on myocardial perfusion imaging (MPI) on a vessel basis. The addition of the degree of stenosis (presence of ≥70% stenosis) provided incremental predictive information to baseline clinical variables for prediction of ischemia on MPI on a vessel basis. Furthermore the addition of extent and composition of atherosclerosis (≥2 mixed plaques and ≥2 calcified plaques) on MSCT resulted in further incremental predictive value over baseline clinical variables, and degree of stenosis on MSCT.
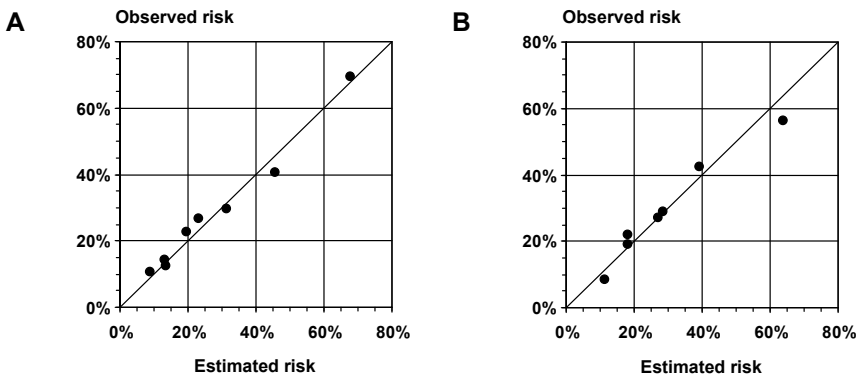
Figure 6. Hosmer-Lemeshow plot of estimated risk for ischemia on multislice computed tomography (MSCT) (x-axis) versus observed risk for ischemia on myocardial perfusion imaging (MPI) (y-axis) by decile of risk, on a patient (A) and vessel (B) basis.
A calibration plot is shown for the prediction of ischemia on MPI (myocardial perfusion imaging) by the multivariate model of atherosclerosis variables on MSCT. Patient basis analysis is shown in panel A, describing model VI in Table 4. Vessel basis analysis is demonstrated in panel B, describing model IV in Table 5. The diagonal line in both plots demonstrates a good fit on both a patient and vessel basis. The Hosmer-Lemeshow goodness-of-fit test statistic was p=0.93 on a patient basis and p=0.11 on a vessel basis.

(atherosclerotic disease in LM and/or proximal LAD) further significantly enhanced prediction of ischemia over clinical risk stratification and the presence of severely obstructive CAD.

Previous investigations assessing the relation between MSCT and MPI demonstrated that normal coronary arteries on MSCT were highly associated with normal perfusion on MPI.[12] Accordingly, patients with normal coronary arteries on MSCT may be reassured and in general do not require further testing. Nevertheless, in a substantial number of patients MSCT will reveal the presence of atherosclerotic disease. However, previous comparisons demonstrated that only half of patients with stenosis of 50% or greater showed abnormal perfusion, resulting in a low positive predictive value of merely 50%.[4 5] Accordingly, with the expanding use of MSCT, clinicians will be increasingly confronted with patients having an obstructive lesion detected on MSCT but without information on the hemodynamic relevance. To determine further management, additional evaluation with functional imaging techniques remains necessary in these patients. However, if the likelihood of ischemia on MPI can be estimated more accurately based on MSCT results, a more appropriate selection of further testing and management can be achieved. Possibly, knowledge of the extent, composition and location of atherosclerotic disease, as can be derived from MSCT, may enhance prediction of the presence of ischemia over the mere assessment of the degree of stenosis.

Extent and composition of atherosclerosis

In addition to the presence of a single stenotic lesion in the coronary arteries, previous studies have reported that diffuse atherosclerosis also contributes to ischemia.[13 14] By measuring coronary flow reserve, de Bruyne et al. demonstrated that diffuse atherosclerotic disease can cause a decline in coronary flow despite the absence of obstructive CAD.[13] These findings suggest that the severity of perfusion abnormalities not only depends on the presence of obstructive disease but is also influenced by the atherosclerotic burden in the coronary artery. The current study is in line with these observations, suggesting that more extensive atherosclerotic plaque burden indicates a higher likelihood for ischemia. Moreover, the present results parallel previous studies comparing MPI with coronary calcium scoring.[15 16] He et al. studied the relationship between the presence of stress-induced ischemia on MPI and coronary artery calcium (CAC) and demonstrated in approximately 4000 asymptomatic patients that CAC was predictive of ischemia on MPI.[16] However, only a minority of patients (22%) with an abnormal CAC had abnormal perfusion on MPI. Similarly, Berman et al. established that the frequency of abnormal perfusion was related to the magnitude of CAC abnormality.[17] However, patients with normal MPI results frequently had extensive atherosclerosis on the basis of CAC criteria, indicating that a normal MPI did not exclude the presence of CAD. Conversely, the presence of CAC did not necessarily result in perfusion abnormalities on MPI. Therefore, although a relation exists between the extent of atherosclerosis and ischemia, the extent alone may not be a strong predictor of ischemia. Importantly, to improve agreement of MSCT and MPI, integration

of the extent of CAD with other variables of atherosclerosis identified on MSCT can refine identification of patients with ischemic MPI.

In the present study, extent of mixed and calcified plaque independently predicted the presence of ischemia on MPI. Indeed, mixed and calcified lesions are thought to typically represent the more advanced stages of atherosclerosis and thus linked with larger plaque volume and a higher extent of ischemia. Additionally, plaque composition on MSCT has previously been linked to abnormal perfusion on SPECT by Lin et al. in 163 patients.[18] The authors demonstrated that the presence of mixed plaques was found to be the strongest independent predictor of abnormal perfusion (OR 1.6, p=0.01). The current and previous studies indicate that an association between extent and composition of atherosclerosis and a higher likelihood of ischemia may exist. Accordingly, plaque extent and composition should be taken into consideration when evaluating and reporting coronary MSCT angiograms. However, the exact underlying mechanisms remain largely unknown and should be further investigated.

Location of atherosclerosis

Location of atherosclerotic disease has been shown to influence myocardial perfusion. In general, the more proximal the location of stenosis, the more severe and extensive the corresponding perfusion abnormality will be. Conversely, the effect of distal lesions on myocardial perfusion will be limited as a smaller amount of myocardium is involved. In the current study, location of atherosclerotic disease in the LM and/or proximal LAD was demonstrated to be a predictor for the presence of ischemia on MPI. Similarly, previous studies have shown that patients with angiographically observed atherosclerotic disease in the LM and/or proximal LAD are at higher risk for events. Califf et al. developed the jeopardy score (an angiographic risk stratification score) which, in addition to severity of disease, incorporated location of atherosclerotic disease to estimate the amount of myocardium at risk.[19] As more proximally located lesions were associated with a higher occurrence of events, the jeopardy score demonstrated to allow improved risk stratification as compared to other angiographic scoring techniques. Interestingly, Lin et al. adapted this scoring technique for MSCT angiography; the MSCT segment-at-risk score.[18] Using this method, individuals with reversible defects could be more accurately identified.

Clinical implications

Recently, MSCT cardiac imaging has been increasingly applied for the evaluation of patients presenting with suspected CAD. The reported high negative predictive values of almost 100% precipitate MSCT as a particularly effective technique for ruling out the presence of obstructive CAD. Accordingly, if patients show normal coronary arteries on MSCT angiography further testing is not required, whereas if atherosclerotic disease has been verified on MSCT, unfortunately no information is provided on the hemodynamical relevance. As a result, the decision which patient requires further functional testing or direct invasive evaluation with potential revascularization currently remains largely dependent on individual interpretation of the coronary arteries on MSCT angiography combined

with pre-test likelihood and clinical judgment. Preferably, more information than merely presence of luminal narrowing is required from this technique. In our study several MSCT variables of atherosclerosis were identified which were associated with a higher likelihood of ischemia. Moreover, integration of all MSCT variables of atherosclerosis significantly improved prediction of the presence of ischemia on MPI. Possibly, these results may allow a more refined and individualized assessment of patients undergoing MSCT angiography and provide the basis for the development of an algorithm to improve identification of patients requiring more aggressive therapy or intervention.

However, it is important to realize that in the current study, MSCT and MPI data were acquired in two different institutions with slightly different image acquisition protocols, which may have influenced our findings.

Conclusion

The results of the current study demonstrate that in addition to the presence of obstructive CAD, anatomical MSCT variables describing plaque extent, composition and location of atherosclerosis are independent predictors for the presence of ischemia on MPI.

REFERENCES

1. Abdulla J, Abildstrom SZ, Gotzsche O et al. 64-multislice detector computed tomography coronary angiography as potential alternative to conventional coronary angiography: a systematic review and meta-analysis. Eur Heart J 2007;28:3042-50.
2. Gaemperli O, Schepis T, Koepfli P et al. Accuracy of 64-slice CT angiography for the detection of functionally relevant coronary stenoses as assessed with myocardial perfusion SPECT. Eur J Nucl Med Mol Imaging 2007;34:1162-71.
3. Gaemperli O, Schepis T, Valenta I et al. Functionally relevant coronary artery disease: comparison of 64-section CT angiography with myocardial perfusion SPECT. Radiology 2008;248: 414-23.
4. Hacker M, Jakobs T, Hack N et al. Sixty-four slice spiral CT angiography does not predict the functional relevance of coronary artery stenoses in patients with stable angina. Eur J Nucl Med Mol Imaging 2007;34:4-10.
5. Schuijf JD, Wijns W, Jukema JW et al. Relationship between noninvasive coronary angiography with multi-slice computed tomography and myocardial perfusion imaging. J Am Coll Cardiol 2006;48:2508-14.
6. Diamond GA, Forrester JS. Analysis of probability as an aid in the clinical diagnosis of coronary-artery disease. N Engl J Med 1979;300:1350-8.
7. Germano G, Kavanagh PB, Waechter P et al. A new algorithm for the quantitation of myocardial perfusion SPECT. I: technical principles and reproducibility. J Nucl Med 2000;41:712-9.
8. Sharir T, Germano G, Kang X et al. Prediction of myocardial infarction versus cardiac death by gated myocardial perfusion SPECT: risk stratification by the amount of stress-induced ischemia and the poststress ejection fraction. J Nucl Med 2001;42:831-7.
9. Cerqueira MD, Weissman NJ, Dilsizian V et al. Standardized myocardial segmentation and nomenclature for tomographic imaging of the heart: a statement for healthcare professionals from the Cardiac Imaging Committee of the Council on Clinical Cardiology of the American Heart Association. Circulation 2002;105:539-42.
10. Agatston AS, Janowitz WR, Hildner FJ et al. Quantification of coronary artery calcium using ultrafast computed tomography. J Am Coll Cardiol 1990;15:827-32.
11. Steyerberg EW, Harrell FE, Jr., Borsboom GJ et al. Internal validation of predictive models: efficiency of some procedures for logistic regression analysis. J Clin Epidemiol 2001;54:774-81.
12. Schuijf JD, Wijns W, Jukema JW et al. A comparative regional analysis of coronary atherosclerosis and calcium score on multislice CT versus myocardial perfusion on SPECT. J Nucl Med 2006; 47:1749-55.
13. De Bruyne B., Hersbach F, Pijls NH et al. Abnormal epicardial coronary resistance in patients with diffuse atherosclerosis but "Normal" coronary angiography. Circulation 2001;104:2401-6.
14. Marcus ML, Harrison DG, White CW et al. Assessing the physiologic significance of coronary obstructions in patients: importance of diffuse undetected atherosclerosis. Prog Cardiovasc Dis 1988;31:39-56.
15. Anand DV, Lim E, Raval U et al. Prevalence of silent myocardial ischemia in asymptomatic individuals with subclinical atherosclerosis detected by electron beam tomography. J Nucl Cardiol 2004;11:450-7.
16. He ZX, Hedrick TD, Pratt CM et al. Severity of coronary artery calcification by electron beam computed tomography predicts silent myocardial ischemia. Circulation 2000;101:244-51.
17. Berman DS, Wong ND, Gransar H et al. Relationship between stress-induced myocardial ischemia and atherosclerosis measured by coronary calcium tomography. J Am Coll Cardiol 2004; 44:923-30.

18. Lin F, Shaw LJ, Berman DS et al. Multidetector computed tomography coronary artery plaque predictors of stress-induced myocardial ischemia by SPECT. Atherosclerosis 2008;197:700-9.
19. Califf RM, Phillips HR, III, Hindman MC et al. Prognostic value of a coronary artery jeopardy score. J Am Coll Cardiol 1985;5:1055-63.

Summary and Conclusion

SUMMARY AND CONCLUSION

Coronary atherosclerosis remains one of the leading causes of morbidity and mortality in the modern western world. It has been established that the majority of acute coronary events (>70%) are caused by plaque rupture followed by thrombus formation. The most common substrate for thrombus formation has been proposed to be the thin cap fibroatheroma; a plaque with a large necrotic core and thin fibrous cap (<65 μm thick) infiltrated by macrophages and lymphocytes. Notably, a considerable number of patients who present with an acute coronary event due to rupture or erosion of an atherosclerotic plaque do not experience any prior symptoms. This observation emphasizes the need to improve the early detection of atherosclerosis. Traditionally, imaging of the coronary arteries has focused on the assessment of the coronary lumen and the presence of severe stenosis by means of invasive coronary angiography. However, invasive coronary angiography only allows the assessment of the lumen and is less suited to evaluate the presence of non-obstructive atherosclerosis, including the presence of (potentially high-risk) plaques. As a result, there is an emerging need for imaging modalities that can identify atherosclerotic lesions with high-risk features indicating increased vulnerability. In this regard, non-invasive techniques may be valuable, as they may identify high-risk patients at a relatively early stage before an adverse events occurs and may provide the opportunity for novel treatment strategies. Accordingly, this thesis focuses on the performance and clinical impact of imaging modalities for the evaluation of atherosclerosis and detection of vulnerable plaques in the coronary arteries.

The general introduction in **Chapter 1** of this thesis provides a description of the rationale to improve early detection of atherosclerosis and vulnerable plaque before the occurrence of an adverse cardiac event. An overview of the currently available invasive and non-invasive modalities for the imaging of coronary atherosclerosis and vulnerable plaque is provided, describing the individual strengths and accuracies of each imaging modality. Lastly, the outline of the current thesis is presented.

Part 1

Part 1 describes the current advances of computed tomography angiography (CTA) in the characterization of coronary atherosclerosis and vulnerable plaque. CTA is a rapidly evolving imaging tool that allows for the non-invasive visualization of coronary atherosclerosis. The temporal and spatial resolution have improved with each new scanner generation, resulting in superior image quality and diagnostic accuracy for the detection of coronary stenosis. CTA is not only able to identify stenosis, but also has the potential to provide information on lesion morphology and plaque composition. Further improvement in plaque characterization, however, is needed before accurate evaluation of plaque composition and subsequent identification of patients at higher risk of events can be achieved.

In **Chapter 2**, the performance of the novel volumetric CTA system regarding plaque characterization was evaluated. This scanner is equipped with 320-detector rows and can potentially improve the ability and reliability of CTA to characterize plaque composition

in the coronary arteries. In this chapter, plaque observations on 320-row CTA were compared to plaque composition on virtual histology intravascular ultrasound (VH IVUS) in 65 patients. On CTA, three plaque types were identified: non-calcified, mixed and calcified. On VH IVUS, plaque composition (% fibrotic, fibro-fatty, necrotic core, dense calcium) and presence of thin cap fibroatheroma (more high risk) were evaluated. Plaque observations on 320-row CTA show good agreement to relative plaque composition on VH IVUS. Moreover, mixed plaques on 320-row CTA parallel the more vulnerable plaque on VH IVUS.

In **Chapter 3**, the relation between plaque composition and degree of stenosis was evaluated by CTA and VH IVUS. In 78 patients CTA was performed (identifying 3 plaque types; non-calcified, calcified, mixed) followed by invasive coronary angiography and VH IVUS. VH IVUS evaluated plaque composition (% fibrotic, fibro-fatty, necrotic core, dense calcium) and plaques were visually classified. For each plaque, degree of stenosis was evaluated by quantitative coronary angiography. Interestingly, plaque types on CTA were equally distributed among significant (≥ 50%) and non-significant stenoses. In addition, VH IVUS observed no differences in % fibrotic, fibro-fatty, dense calcium and necrotic core. Importantly, thin cap fibroatheroma (the more vulnerable plaque) was distributed equally between significant and non-significant stenosis (p=0.18). This study indicates that there is no evident relation between the degree of stenosis and plaque composition or vulnerability.

Chapter 4 assessed the difference in location between site of greatest vulnerability and site of most severe narrowing with invasive VH IVUS. In 92 patients, the site of greatest vulnerability on VH IVUS was defined as the cross-section with the largest necrotic core area per vessel, the maximum necrotic core site and the site of most severe narrowing was defined the minimum lumen area site. The distance from both the maximum necrotic core site and minimum lumen area site to the origin of the coronary artery was evaluated with a dedicated software tool in the longitudinal IVUS view. In addition, the presence of a thin cap fibroatheroma was assessed. Interestingly, there was a substantial difference between the minimum lumen area site and maximum necrotic core site (10.8 ±20.6 mm). Moreover, the maximum necrotic core site was located at the minimum lumen area site in only 7 vessels (5%). In 92 vessels (66%) the maximum necrotic core site was located proximally to the minimum lumen area site and in 40 vessels (29%) distally to the minimum lumen area site. The present findings demonstrate that the site of greatest vulnerability is rarely at the site of most severe narrowing. Moreover, the site of greatest vulnerability is frequently located proximal from the site of most severe narrowing.

In **Chapter 5**, the aim of the study was to systematically investigate the accuracy of CTA for detecting significant stenosis (using conventional coronary angiography as the reference standard) versus detecting the presence of atherosclerosis (using IVUS as reference of standard). CTA correctly ruled out significant stenosis in 53 of 53 (100%) patients. However, 9 patients (19%) were incorrectly diagnosed as having significant lesions on CTA resulting in sensitivity, specificity, positive and negative predictive values of 100%, 85%, 81% and 100%. Interestingly, CTA correctly ruled out the presence of atherosclerosis in 7 patients (100%) and correctly identified the presence of atherosclerosis in 93 patients

(100%). No patients were incorrectly classified, resulting in sensitivity, specificity, positive and negative predictive values of 100%. These findings confirm that the diagnostic performance of CTA is superior in the evaluation of presence or absence of clinically relevant atherosclerosis as compared to the evaluation of significant stenosis.

More accurate lesion assessment may be feasible with CTA as compared to invasive coronary angiography. Accordingly, lesion length assessment was compared between invasive coronary angiography and CTA in patients referred for CTA who underwent subsequent percutaneous coronary intervention in **Chapter 6.** In 89 patients, lesion length was measured from the proximal to the distal shoulder of the plaque on CTA. Quantitative coronary angiography was performed to analyze lesion length. Interestingly, lesion length on CTA was significantly longer than on quantitative coronary angiography (difference 8.8 ±6.7mm, p<0.001). Moreover, lesion length visualized on CTA was also significantly longer than mean stent length (CTA lesion length-stent length was 4.2 ±8.7 mm, p<0.001). The study concludes that CTA provides more accurate lesion length assessment than invasive coronary angiography and may facilitate improved guidance of percutaneous treatment of coronary lesions.

Several previous studies have identified specific plaque characteristics which are frequently observed with CTA in patients presenting with acute coronary syndrome. Among these characteristics, a spotty pattern of calcifications and positive remodeling have been related to the presence of acute coronary syndrome. **Chapter 7** systematically compared calcification patterns in plaques visualized on CTA with vulnerable plaque characteristics on VH IVUS in 108 patients. Interestingly, plaques with small spotty calcifications on CTA were related to more vulnerable plaque characteristics on VH IVUS. **Chapter 8** further addressed this issue by assessing the association between positive remodeling on quantitative CTA and vulnerable plaque characteristics on VH IVUS. On CTA, the remodeling index was determined for each lesion using a novel dedicated quantitative analysis strategy. Notably, the study confirms that lesions with positive remodeling on CTA were associated with a higher percentage necrotic core and a higher prevalence of thin cap fibroatheroma. Accordingly, evaluation of spotty calcifications and remodeling on CTA may be valuable markers for plaque vulnerability.

Part 2

In part 2 of this thesis, the relation between characterization of atherosclerosis on CTA and the effect on clinical management was evaluated in more detail. **Chapter 9** provides an overview regarding the evolving role of coronary CTA (including coronary calcium scoring) in the diagnosis of patients with acute chest pain which constitute a common and important diagnostic challenge. As a result of rapid developments in coronary CTA technology, high diagnostic accuracies for detecting coronary stenosis are obtained. Additionally, CTA is an excellent modality in patients whose symptoms suggest other non-coronary causes of acute chest pain such as aortic aneurysms, aortic dissection, or pulmonary embolism. However, although CT shows great potential in evaluating patients

with acute chest pain, more randomized clinical trials are needed to determine the value of this technique in this challenging patient population.

Chapter 10 addresses effective strategies to reduce radiation dose with CTA. On the one hand, a conservative approach regarding radiation dose may result in a high level of image noise and therefore in non-diagnostic images. On the other hand, higher radiation exposure may put patients at unnecessary risk of radiation damage. Thus, effective strategies to reduce radiation dose, such as prospective triggering, heart rate control, ECG-modulation of the tube current, and use of tube voltage below 100 kV, will need to be applied in the clinical setting.

Chapter 11 evaluated the diagnostic accuracy of the novel 320-row CTA in the evaluation of significant coronary artery stenosis in 64 patients, compared with invasive coronary angiography as the standard of reference. High sensitivity, specificity, and positive and negative predictive values to detect ≥ 50% luminal narrowing on a patient basis of 100%, 88%, 92%, and 100%, respectively, were demonstrated. The study concludes that 320-row CTA allows for accurate non-invasive assessment of significant coronary artery disease (CAD). **Chapter 12** further addressed the diagnostic accuracy of 320-row CTA, specifically in patients presenting with acute chest pain and examined the relation to outcome during follow-up. Among the 106 patients presenting with chest pain, 22% had a normal CTA, 18% had non-significant CAD on CTA and 55% had significant CAD on CTA (5% had uninterpretable CTA). Sensitivity, specificity, and positive and negative predictive values to detect significant CAD on CTA were 100%, 87%, 93%, and 100%, respectively. The study concludes that in patients presenting with acute chest pain, an excellent clinical performance for the non-invasive assessment of significant CAD is demonstrated using 320-row CTA. Importantly, normal or non-significant CAD on CTA predicted a low rate of adverse cardiovascular events and favorable outcome during follow-up.

The aim of **Chapter 13** was to evaluate the relationship between the calcium score and the degree and character of atherosclerosis in patients suspected of acute coronary syndrome versus patients with stable CAD. Overall, 112 patients were studied; 53 with acute coronary syndrome and 59 with stable CAD. CTA and VH IVUS were performed to evaluate plaque characteristics. Interestingly, if the calcium score was zero, patients with acute coronary syndrome had a higher mean number of plaques and non-calcified plaques on CTA than patients with stable CAD. In zero calcium score, VH IVUS demonstrated that patients with acute coronary syndrome had a larger amount of necrotic core area and higher mean number of thin cap fibroatheroma than stable CAD. Thus, even in the presence of a zero calcium score, patients with acute coronary syndrome have increased plaque burden as well as increased vulnerability as compared to stable CAD.

The aim of **Chapter 14** was to determine the relation between CTA findings and the rate of subsequent invasive coronary angiography and revascularization. A total of 1042 CTA investigations were available for analysis. In patients with significant CAD on CTA, subsequent invasive coronary angiography rate was 64%. In patients with non-significant CAD on CTA, subsequent invasive coronary angiography rate was 12% and in patients with normal CTA results, subsequent invasive coronary angiography rate was 3.6% (p<0.001).

Of patients with significant CAD on CTA, revascularization rate was 36%, as compared to a revascularization rate of 0.3% in patients with non-significant CAD on CTA and no revascularizations in patients with a normal CTA results (p<0.001). This chapter concludes that CTA results are strong and independent determinants of subsequent invasive coronary angiography and revascularization.

Previous studies have shown that the presence of stenosis alone on CTA only has a limited value for predicting the presence of ischemia on myocardial perfusion imaging. In the last chapter (**Chapter 15**), different variables of atherosclerosis on CTA were related to ischemia on myocardial perfusion imaging to determine the different predictors of ischemia in 514 patients. On a patient basis, multivariate analysis showed that the degree of stenosis (presence of ≥70% stenosis, OR 3.5), plaque extent and composition (mixed plaques ≥3, OR 1.7 and calcified plaques ≥3, OR 2.0) and location (atherosclerotic disease in left main coronary artery and/or proximal left anterior descending coronary artery, OR 1.6) were independent predictors for ischemia on myocardial perfusion imaging. In addition, CTA variables of atherosclerosis such as plaque extent, composition and location had significant incremental value for the prediction of ischemia over the presence of ≥70% stenosis. Thus, in addition to the degree of stenosis, CTA variables of atherosclerosis describing plaque extent, composition and location are predictive of the presence of ischemia on myocardial perfusion imaging.

Conclusions

During the past few years CTA has rapidly developed into a versatile non-invasive imaging modality. While imaging of the coronary arteries to determine or rule out the presence of stenosis will remain one of the main indications, additional information on plaque severity and composition can be obtained. The improvements in technology (faster gantry rotation times, an increasing number of detectors, volumetric image acquisition) and consequential improvement in image quality have resulted in advances in the characterization of coronary atherosclerosis and vulnerable plaque. Interestingly, the diagnostic performance of CTA was superior in the evaluation of presence or absence of clinically relevant atherosclerosis as compared to the evaluation of significant stenosis. Regarding plaque observations with the novel 320-row CTA scanner, the results showed good agreement to relative plaque composition on invasive VH IVUS. Moreover, mixed plaques on 320-row CTA paralleled the more vulnerable plaque on VH IVUS. In addition, lesions with spotty calcifications and positive remodeling on CTA were associated with a higher percentage necrotic core and a higher prevalence of vulnerable plaques. Accordingly, evaluation of spotty calcifications and remodeling on CTA may be valuable markers for plaque vulnerability.

The relation between characterization of atherosclerosis on CTA and its effect on clinical management was also evaluated. As a result of rapid developments in coronary CTA technology, high diagnostic accuracies of 320-row CTA for detecting coronary stenosis were obtained in patients with stable chest pain complaints as well as in patients presenting with acute chest pain. In addition, although a zero calcium score has important

prognostic value, patients with acute coronary syndrome and zero calcium had increased plaque burden as well as increased vulnerability as compared to patients with stable chest pain. Accordingly, absence of coronary calcification did not exclude the presence of clinically relevant and potentially vulnerable atherosclerotic plaque burden in patients with acute coronary syndrome. Lastly, in addition to the degree of stenosis, CTA variables of atherosclerosis describing plaque extent, composition and location were predictive of the presence of ischemia on myocardial perfusion imaging. Possibly, these results may allow a more refined and individualized assessment of patients undergoing CTA imaging and provide the basis for the development of an algorithm to improve identification of patients requiring more aggressive therapy or intervention.

Nederlandse Samenvatting

NEDERLANDSE SAMENVATTING

Ondanks verbeteringen in behandeltechnieken blijven plotse hartdood en een hartinfarct (door afsluiting van een kransslagader) tot de voornaamste redenen behoren van ziekte en sterfte in de geïndustrialiseerde wereld. Veel patiënten met een hartinfarct hebben nooit eerder klachten gehad zoals pijn op de borst of kortademigheid. Onderzoek heeft laten zien dat niet zo zeer de ernst van de atherosclerotische vernauwing in de kransslagader, maar juist de bestanddelen waaruit de aderverkalking (plaque) bestaat (ofwel het "type plaque") een belangrijke rol speelt in het ontwikkelen van cardiale complicaties, zoals een hartinfarct of zelfs plotse dood. Juist de aanwezigheid van "kwetsbare" plaques geven meer risico op een hartinfarct. Een "kwetsbare" plaque bestaat uit een vetophoping in de binnenbekleding van de vaatwand en onder een dunne kap bevindt zich een kern van vettige stoffen zoals cholesterol met dode cellen. Zonder dat een patiënt ooit eerder klachten heeft gehad kan deze plaque scheuren, wat de vorming van bloedstolsels bevordert, de kransslagader afsluit en een hartinfarct veroorzaakt. Met standaard invasieve coronairangiografie (een onderzoeksmethode waarbij de bloedcirculatie van het hart door middel van röntgenopnamen en contrast in beeld wordt gebracht) kan wel de ernst van de vernauwing zichtbaar worden gemaakt, maar niet de aanwezigheid van de kwetsbare plaques. Hierdoor zijn op dit moment meerdere niet-invasieve en invasieve technieken in ontwikkeling om met hoge nauwkeurigheid de verschillende bestanddelen van atherosclerotische plaques te herkennen. Het bestuderen van het type plaque kan mogelijk een aanknopingspunt zijn voor verbeterde inschatting van een individueel verhoogd risico evenals verbeterde preventie. In dit proefschrift wordt de rol en klinische betekenis van beeldvormende technieken in 1) het eerder herkennen en 2) karakteriseren van atherosclerose en kwetsbare plaques in de kransslagaderen beschreven.

De algemene inleiding in **Hoofdstuk 1** van dit proefschrift geeft een beschrijving van de huidige invasieve en niet-invasieve technieken die beschikbaar zijn voor het beoordelen van plaques in de kransslagaders. Van elke techniek worden de voor- en nadelen beschreven, evenals de huidige nauwkeurigheid, die op basis van de huidige literatuur bekend is. Als laatste wordt de indeling van het huidige proefschrift beschreven.

Deel 1

In het eerste gedeelte van dit proefschrift wordt de onlangs geïntroduceerde niet-invasieve techniek "Computed Tomography Angiography (CTA)" besproken. Op niet-invasieve wijze kan de aanwezigheid van atherosclerotische plaques in de kransslagaders met CTA beoordeeld worden. Met deze techniek is er een onderscheid tussen de verschillende plaque types mogelijk. Een groot voordeel van deze techniek is dat terwijl invasieve beeldvorming beperkt is tot symptomatische patiënten met een hoog risico op ernstige vernauwingen, CTA ook toegepast kan worden in patiënten met een lagere voorafkans op ernstige vernauwingen vanwege het lage risico op complicaties. Op deze manier kan de aanwezigheid van atherosclerose in een vroeger stadium gedetecteerd worden. Echter, op het moment zijn nog weinig gegevens beschikbaar over wat de precieze betekenis is van

de verschillende plaque types die gezien worden met CTA en is er geen systematische vergelijking met de invasieve techniek "Virtual Histology Intravascular Ultrasound (VH IVUS)". VH IVUS is een invasieve techniek die in tegenstelling tot angiografie, een cross-sectionele beeldvorming van de kransslagaders en een uitgebreide beoordeling van de atherosclerotische plaque vanuit binnen uit biedt. Deze techniek gebruikt spectrale analyse van de echografische gegevens (backscatter radiofrequentie signalen) om de samenstelling en de karakteristieken van de plaque te analyseren met een hoge nauwkeurigheid.

In **Hoofdstuk 2** wordt de prestatie van de nieuwe 320-rij CTA scanner geëvalueerd. Deze nieuwe scanner heeft 320 detectoren op een rij en kan mogelijk het vermogen van CTA om plaques te karakteriseren verbeteren. In dit hoofdstuk wordt plaque compositie op 320-rij CTA vergeleken met invasieve VH IVUS. Op CTA beelden werden de volgende plaques geïdentificeerd: niet-gecalcificeerd, gemixed en gecalcificeerd. Met VH IVUS beoordeelden we de verschillende typen atherosclerose en beoordeelden we of er "kwetsbare" plaques aanwezig waren in de kransslagaders. De conclusie van dit hoofdstuk was dat plaque waarnemingen met 320-rij CTA goed overeenkomen met relatieve plaque compositie op VH IVUS. Vooral de plaques die gemixed waren op CTA hadden de gevaarlijke "kwetsbare" plaque kenmerken op VH IVUS.

In **Hoofdstuk 3** wordt de relatie tussen de ernst van de vernauwing en het type plaque beoordeeld door middel van niet-invasieve CTA en invasieve VH IVUS. De ernst van de vernauwing van de kransslagaders werd beoordeeld met behulp van een kwantitatieve software die speciaal hiervoor ontwikkeld is. Een ernstige vernauwing werd geduid als meer dan 50% vernauwing van de kransslagader. In totaal werden 227 plaques (bij 78 patiënten) gevonden waarvan 43 plaques (19%) een ernstige vernauwing hadden. Er werden geen verschillen waargenomen in plaque karakteristieken (zoals "necrotic core" en "dense calcium") op CTA and VH IVUS tussen plaques met een ernstige vernauwing en plaques zonder een ernstige vernauwing. Zelfs de meer gevaarlijke plaques werden even vaak gevonden in plaques met ernstige vernauwing als zonder ernstige vernauwing. Uit deze resultaten kunnen we concluderen dat er geen verschillen in plaque karakteristieken bestaan tussen plaques met ernstige en zonder ernstige vernauwing.

De verschillen in locatie tussen de kwetsbare plaques en plaques met de ernstigste vernauwing worden beoordeeld in **Hoofdstuk 4.** Het idee was dat de meeste plaques niet altijd vanzelfsprekend ter plaatse van de meest kwetsbare plaques gelokaliseerd zijn. Per kransslagader werd de meest kwetsbare plaque gedifinieerd als de locatie met de meeste "necrotic core" en de ernstigste vernauwing werd gedefinieerd als de locatie met het kleinste lumen oppervlakte. In totaal werden 92 patiënten en 139 kransslagaders beoordeeld. Er werd een aanzienlijk verschil gemeten tussen de locatie van de meest kwetsbare plaque en de locatie van de ernstigste vernauwing (10,8 ± 20,6 mm). Daarnaast werd waargenomen dat de kwetsbare plaques vaak proximaal (vooraan) gelokaliseerd zijn in de kransslagaders ten opzichte van de locatie van de ernstigste vernauwing. De resultaten van dit onderzoek wijzen uit dat de locatie van de kwetsbare plaques niet altijd ter plaatse van de locatie van de ernstigste vernauwing is.

Het doel van **Hoofdstuk 5** was om de diagnostische nauwkeurigheid (sensitiviteit en specificiteit) van CTA om significante vernauwingen in de kransslagaders te herkennen , te onderzoeken. Vervolgens werd dit vergeleken met de nauwkeurigheid van CTA om de aanwezigheid van atherosclerose in de kransslagaders aan te tonen. De sensitiviteit is een maat voor de "gevoeligheid" van de test, de specificiteit bepaalt hoe "specifiek" de test is. Voor het aantonen van significante vernauwingen (vergeleken met de standaard coronairangiografie) werd een sensitiviteit gevonden van 100% en een specificiteit van 85%. Voor het aantonen van atherosclerose (vergeleken met intravasculaire echo) werd een sensitiviteit van 100% en specificiteit van 100% gevonden. Deze resultaten bevestigen dat CTA nauwkeuriger is in het beoordelen van klinisch relevante atherosclerose dan het beoordelen van significante vernauwingen.

CTA kan de omvang van de plaque in de kransslagaderwand beter beoordelen dan de standaard coronairangiografie. **Hoofdstuk 6** beschrijft de vergelijking tussen het beoordelen van de lengte van de plaque op CTA met standaard coronair angiografie. De lengte van de plaque werd gemeten bij 89 patiënten met CTA en met standaard invasieve coronairangiografie (met behulp van speciaal ontwikkelde software, genaamd "quantitative coronary angiography"). De lengte van de plaques was aanzienlijk langer op CTA dan op coronairangiografie. Dit duidt erop dat CTA waarschijnlijk een meer accurate meting van de lengte van de plaque geeft en dit mogelijk een betere techniek is om de lengte van de stent te bepalen dan de standaard coronairangiografie. Het is van belang de lengte van de stent goed in te schatten om zo de vernauwing op de beste manier te behandelen en zo complicaties te voorkomen.

Eerdere onderzoeken met CTA hebben bepaalde plaque karakteristieken aangetoond die vaker werden waargenomen in patiënten met acute pijn op de borst, ook wel bekend als een acuut coronair syndroom (ACS), dan bij patiënten met stabiel coronarialijden (stabiele pijn op de borst). Eén van deze plaque karakteristieken was het aanwezig zijn van kleine ronde ("spotty") kalkspatjes en een ander karakteristiek was naar buiten uitzetten van de vaatwand ter hoogte van de plaque ("positive remodeling"). In **Hoofdstuk 7** worden de verschillende soorten kalk in plaques op CTA vergeleken met invasieve VH IVUS bij 108 patiënten. Hier werd aangetoond dat inderdaad de kleine ronde "spotty" kalkspatjes op CTA meer gevaarlijke kenmerken hadden, zoals de aanwezigheid van een "thin cap fibroatheroma" en "necrotic core" op VH IVUS, dan de meer ernstig verkalkte plaques. In **Hoofdstuk 8** wordt aangetoond met speciaal ontwikkelde kwantitatieve sofware dat de plaques met "positive remodeling" op CTA ook meer gevaarlijke kenmerken hadden op VH IVUS. Dus het aantonen van kleine ronde "spotty" kalkspatjes en "positive remodeling" in plaques op CTA kunnen mogelijk aanwijzingen zijn voor aanwezigheid van de meer gevaarlijke "kwetsbare" plaques.

Deel 2

In het tweede deel van dit proefschrift wordt de klinische betekenis van het beoordelen van atherosclerose op CTA verder uitgediept. **Hoofdstuk 9** geeft een overzicht over de toenemende rol van CTA in de diagnostiek bij patiënten met acute pijn op de borst. Gezien

de recente technische ontwikkeling, zoals het vermeerderen van het aantal detectorrijen, heeft CTA een hoge nauwkeurigheid wat betreft het herkennen van ernstige vernauwingen in de kransslagaders. Daarnaast is CTA ook een belangrijk middel om andere levensbedreigende oorzaken van pijn op de borst uit te sluiten zoals een longembolie, dissectie of aneurysma van de aorta. Ondanks dat CTA een steeds grotere rol heeft in het diagnostisch proces van patiënten met acute pijn op de borst, zijn er meer grotere gerandomiseerde studies nodig die de waarde van deze techniek in deze setting kunnen bepalen. **Hoofdstuk 10** bespreekt effectieve strategieën om de stralingbelasting van het CTA onderzoek zo beperkt mogelijk te houden. Het is belangrijk de voordelen van dosis vermindering (schade door straling) af te wegen tegen de nadelen van stralingsvermindering (ruizige beelden en slechtere scan kwaliteit). Effectieve manieren om de stralingsdosis te verminderen kunnen bereikt worden door het aanpassen van de scantechnieken zoals o.a. prospectief scannen, ECG modulatie toepassen, een lage hartslag, lage dosis kV en/of mA.

Hoofdstuk 11 beschrijft de diagnostische nauwkeurigheid van de nieuwe 320-rij CTA scanner voor het herkennen van significante vernauwingen in de kransslagaders bij 64 patiënten vergeleken met standaard coronairangiografie. De resultaten laten zien dat de sensitiviteit, specificiteit, positief voorspellende waarde en negatief voorspellende waarde respectievelijk 100%, 88%, 92% en 100% waren. Deze studie bevestigt dat 320-rij CTA een zeer goede en nauwkeurige niet-invasieve techniek is voor het herkennen van significante vernauwingen in de kransslagaderen. **Hoofdstuk 12** gaat hier nog iets verder op in en beschrijft de nauwkeurigheid van de nieuwe 320-rij CTA scanner specifiek in 106 patiënten die zich presenteren met acute pijn op de borst. Daarnaast werden diezelfde patiënten gemiddeld 13 maanden gevolgd om te kijken of er cardiale gebeurtenissen (cardiale dood, het optreden van een hartinfarct of onstabiele angina pectoris) plaatsvonden na de CTA. Van de 106 patiënten met pijn op de borst, had 22% geen kransslagader afwijkingen, 18% had wel atherosclerose maar geen significante vernauwing en 55% had een significante vernauwing. De sensitiviteit, specificiteit, positief voorspellende waarde en negatief voorspellende waarde voor het hebben van een significante vernauwing waren hoog, namelijk respectievelijk 100%, 87%, 93% en 100%. In alle patiënten met een normale CTA vonden geen cardiale gebeurtenissen plaats gedurende de genoemde periode. Met andere woorden, 320-rij CTA lijkt een nauwkeurig en veilig alternatief voor het beoordelen van vernauwingen in de kransslagaders bij patiënten met acute pijn op de borst.

Eerdere onderzoeken hebben laten zien dat de prognostische waarde van de kalkscore erg goed is en dat er zeer weinig cardiale gebeurtenissen plaatsvinden bij patiënten bij de afwezigheid van kalk (kalkscore van 0), vooral bij patiënten met een laag risico op ernstige vernauwingen of zonder klachten als pijn op de borst. Recentelijk werd echter aangetoond dat in patiënten met acute pijn op de borst, een kalkscore van 0 de aanwezigheid van significante vernauwingen niet uitsluit. **Hoofdstuk 13** beschrijft de relatie tussen de kalkscore en de compositie van atherosclerose in patiënten met acute pijn op de borst (ofwel ACS) vergeleken met patiënten met stabiele pijn op de borst. In totaal werden 112

patiënten bestudeerd waarvan 53 met ACS en 59 met stabiele klachten. Bij een kalkscore van 0 hadden patiënten met ACS meer plaques en met name meer niet-gecalcificeerde plaques op CTA vergeleken met patiënten met stabiele klachten. Op VH IVUS werd bij een kalkscore van 0, meer "necrotic core" en meer kwetsbare plaques gevonden. De conclusie van dit hoofdstuk is dat zelfs bij afwezigheid van kalk op de kalkscan, patiënten met ACS meer plaques en meer kwetsbare plaque kenmerken hebben dan patiënten met stabiele klachten. Oftewel, een kalkscore van 0 bij patiënten met ACS sluit aanzienlijke atherosclerose en aanwezigheid van kwetsbare plaques niet uit.

In **Hoofdstuk 14** wordt de frequentie van verwijzing voor invasieve coronairangiografie en revascularisatie (dotteren, stent plaatsing of omleidingen) na een CTA onderzoek van de kransslagaders in kaart gebracht. In totaal werden 1042 patiënten via CTA scans beoordeeld. Deze patiënten werden gedurende 1 jaar gevolgd. In patiënten met een significante vernauwing op CTA onderging vervolgens 64% invasieve coronairangiografie. In patiënten met niet-significante vernauwing onderging 12% invasieve coronairangiografie. En in patiënten met normale bevindingen onderging 3,6% invasieve coronairangiografie. Vervolgens onderging 36% van de patiënten met een significante vernauwing op de CTA een revascularisatie. In patiënten met een niet-significante vernauwing onderging 0,3% een revascularisatie en bij patiënten met een normale CTA onderging 0% revascularisatie binnen een jaar. Uit de resultaten blijkt dat CTA een sterke en onafhankelijke voorspeller is voor latere verwijzing voor invasieve coronairangiografie en revascularisatie. Bovendien kan CTA als poortwachter fungeren voordat verwijzing naar invasieve coronairangiografie plaatsvindt.

Eerdere onderzoeken hebben laten zien dat het hebben van een significante vernauwing in de kransslagaders op CTA maar in 50% van de gevallen leidt tot zuurstoftekort in de hartspier (ischemie). In het laatste hoofdstuk, **Hoofdstuk 15,** wordt de voorspellende waarde van verschillende variabelen van atherosclerose op CTA voor het hebben van zuurstof tekort op "single photon emission computed tomography (SPECT)" bestudeerd. Deze studie laat inderdaad zien dat de uitgebreidheid, compositie en locatie van de plaques toegevoegde waarde hebben voor het voorspellen van zuurstoftekort in de hartspier op SPECT.

List of Publications

LIST OF PUBLICATIONS

van Velzen JE, de Graaf FR, de Graaf MA, Schuijf JD, Kroft LJ, de Roos A, Reiber JH, Bax JJ, Jukema JW, Boersma E, Schalij MJ, van der Wall EE. Comprehensive assessment of spotty calcifications on computed tomography angiography: Comparison to plaque characteristics on intravascular ultrasound with radiofrequency backscatter analysis. J Nucl Cardiol 2011;18:893-903.

van Velzen JE, de Graaf FR, Jukema JW, de Grooth GJ, Pundziute G, Kroft LJ, de Roos A, Reiber JH, Bax JJ, Schalij MJ, Schuijf JD, van der Wall EE. Comparison of the relation between the calcium score and plaque characteristics in patients with acute coronary syndrome versus patients with stable coronary artery disease, assessed by computed tomography angiography and virtual histology intravascular ultrasound. Am J Cardiol 2011;108:658-64.

van Velzen JE, de Graaf FR, Kroft LJ, de Roos A, Reiber JH, Bax JJ, Jukema JW, Schuijf JD, Schalij MJ, van der Wall EE. Performance and efficacy of 320-row computed tomography coronary angiography in patients presenting with acute chest pain: results from a clinical registry. Int J Cardiovasc Imaging 2011.

van Velzen JE, Schuijf JD, de Graaf FR, Boersma E, Pundziute G, Spano F, Boogers MJ, Schalij MJ, Kroft LJ, de Roos A, Jukema JW, van der Wall EE, Bax JJ. Diagnostic performance of non-invasive multidetector computed tomography coronary angiography to detect coronary artery disease using different endpoints: detection of significant stenosis vs. detection of atherosclerosis. Eur Heart J 2011;32:637-45.

van Velzen JE, Schuijf JD, de Graaf FR, Jukema JW, Roos A, Kroft LJ, Schalij MJ, Reiber JH, van der Wall EE, Bax JJ. Imaging of atherosclerosis: invasive and noninvasive techniques. Hellenic J Cardiol 2009;50:245-63.

van Velzen JE, Schuijf JD, de Graaf FR, Nucifora G, Pundziute G, Jukema JW, Schalij MJ, Kroft LJ, de Roos A, Reiber JH, van der Wall EE, Bax JJ. Plaque type and composition as evaluated non-invasively by MSCT angiography and invasively by VH IVUS in relation to the degree of stenosis. Heart 2009;95:1990-6.

van Velzen JE, Schuijf JD, Kroft LJ, Bax JJ. CT angiography and other applications of CT. The ESC Textbook of Intensive and Acute Cardiac Care. Oxford University Press; 2011. p. 192-204.

van Velzen JE, de Graaf MA, Ciarka A, de Graaf FR, Schalij MJ, Kroft LJ, de Roos A, Jukema JW, Reiber JHC, Schuijf JD, Bax JJ, van der Wall EE. Non-invasive assessment of athero-sclerotic coronary lesion length using multidetector computed tomography angiography: comparison to quantitative coronary angiography. Int J Cardiovasc Imaging. In press.

van Velzen JE, Schuijf JD, van Werkhoven JM, Herzog BA, Pazhenkottil AP, Boersma E, de Graaf FR, Scholte AJ, Kroft LJ, de Roos A, Stokkel MP, Jukema JW, Kaufmann PA, van der Wall EE, Bax JJ. Predictive value of multislice computed tomography variables of athero-sclerosis for ischemia on stress-rest single-photon emission computed tomography. Circ Cardiovasc Imaging 2010;3:718-26.

Boogers MJ, Schuijf JD, Kitslaar PH, van Werkhoven JM, de Graaf FR, Boersma E, **van Velzen JE**, Dijkstra J, Adame IM, Kroft LJ, de Roos A, Schreur JH, Heijenbrok MW, Jukema JW, Reiber JH, Bax JJ. Automated quantification of stenosis severity on 64-slice CT: a comparison with quantitative coronary angiography. JACC Cardiovasc Imaging 2010;3:699-709.

de Graaf FR, Schuijf JD, Delgado V**, van Velzen JE**, Kroft LJ, de Roos A, Jukema JW, van der Wall EE, Bax JJ. Clinical application of CT coronary angiography: state of the art. Heart Lung Circ 2010;19:107-16.

de Graaf FR, Schuijf JD, Scholte AJ, Djaberi R, **van Velzen JE**, Roos CJ, Kroft LJ, de Roos A, van der Wall EE, Wouter JJ, Despres JP, Bax JJ. Usefulness of hypertriglyceridemic waist phenotype in type 2 diabetes mellitus to predict the presence of coronary artery disease as assessed by computed tomographic coronary angiography. Am J Cardiol 2010;106:1747-53.

de Graaf FR, Schuijf JD, **van Velzen JE**, Boogers MJ, Kroft LJ, de Roos A, Reiber JH, Sieders A, Spano F, Jukema JW, Schalij MJ, van der Wall EE, Bax JJ. Diagnostic accuracy of 320-row multidetector computed tomography coronary angiography to noninvasively assess in-stent restenosis. Invest Radiol 2010;45:331-40.

de Graaf FR, Schuijf JD, **van Velzen JE**, Kroft LJ, de Roos A, Reiber JH, Boersma E, Schalij MJ, Spano F, Jukema JW, van der Wall EE, Bax JJ. Diagnostic accuracy of 320-row multidetector computed tomography coronary angiography in the non-invasive evaluation of signifi-cant coronary artery disease. Eur Heart J 2010;31:1908-15.

de Graaf FR, Schuijf JD, **van Velzen JE**, Kroft LJ, de Roos A, Sieders A, Jukema JW, Schalij MJ, van der Wall EE, Bax JJ. Evaluation of contraindications and efficacy of oral Beta block-ade before computed tomographic coronary angiography. Am J Cardiol 2010;105:767-72.

de Graaf FR, Schuijf JD, **van Velzen JE**, Nucifora G, Kroft LJ, de Roos A, Schalij MJ, Jukema JW, van der Wall EE, Bax JJ. Assessment of global left ventricular function and volumes with 320-row multidetector computed tomography: A comparison with 2D-echocardiography. J Nucl Cardiol 2010;17:225-31.

de Graaf FR, **van Velzen JE**, Witkowska AJ, Schuijf JD, van der Bijl N, Kroft LJ, de Roos A, Reiber JH, Bax JJ, de Grooth GJ, Jukema JW, van der Wall EE. Diagnostic performance of 320-slice multidetector computed tomography coronary angiography in patients after coronary artery bypass grafting. Eur Radiol 2011;21:2285-96.

de Graaf FR, van Werkhoven JM, **van Velzen JE**, Antoni ML, Boogers MJ, Kroft LJ, de Roos A, Schalij MJ, Jukema JW, van der Wall EE, Schuijf JD, Bax JJ. Incremental prognostic value of left ventricular function analysis over non-invasive coronary angiography with multidetector computed tomography. J Nucl Cardiol 2010;17:1034-40.

Kroner ES, **van Velzen JE**, Boogers MJ, Siebelink HM, Schalij MJ, Kroft LJ, de Roos A, van der Wall EE, Jukema JW, Reiber JH, Schuijf JD, Bax JJ. Positive remodeling on coronary computed tomography as a marker for plaque vulnerability on virtual histology intravascular ultrasound. Am J Cardiol 2011;107:1725-9.

Pundziute G, Schuijf JD, **van Velzen JE**, Jukema JW, van Werkhoven JM, Nucifora G, van der Kley F, Kroft LJ, de Roos A, Boersma E, Reiber JH, Schalij MJ, van der Wall EE, Bax JJ. Assessment with multi-slice computed tomography and gray-scale and virtual histology intravascular ultrasound of gender-specific differences in extent and composition of coronary atherosclerotic plaques in relation to age. Am J Cardiol 2010;105:480-6.

Schuijf JD, Delgado V, van Werkhoven JM, de Graaf FR, **van Velzen JE**, Boogers MJ, Kroft LJ, de Roos A, Jukema JW, Reiber JH, van der Wall EE, Bax JJ. Novel applications of state-of-the-art multi-slice computed tomography. Int J Cardiovasc Imaging 2009;25:241-54.

Top AP, van DM, **van Velzen JE**, Ince C, Tibboel D. Functional capillary density decreases after the first week of life in term neonates. Neonatology 2011;99:73-7.

van der Wall EE, de Graaf FR, **van Velzen JE**, Jukema JW, Bax JJ, Schuijf JD. 320-row CT: does beat-to-beat motion of the coronary arteries affect image quality? Int J Cardiovasc Imaging 2011.

van der Wall EE, de Graaf FR, **van Velzen JE**, Jukema JW, Bax JJ, Schuijf JD. IVUS detects more coronary calcifications than MSCT; matter of both resolution and cross-sectional assessment? Int J Cardiovasc Imaging 2011;27:1011-4.

van der Wall EE, de Graaf FR, **van Velzen JE**, Jukema JW, Schuijf JD, Bax JJ. Functional analysis by 64-slice CT scanning: prediction of left ventricular dysfunction together with reduction in radiation exposure? Int J Cardiovasc Imaging 2011;27:1089-93.

van der Wall EE, **van Velzen JE**, de Graaf FR, Boogers MM, Schuijf JD, Bax JJ. Increased accuracy in computed tomography coronary angiography; a new body surface area adapted protocol. Int J Cardiovasc Imaging 2010;26:601-4.

van der Wall EE, **van Velzen JE**, de Graaf FR, Jukema JW. Reduction of radiation dose using 80 kV tube voltage: a feasible strategy? Int J Cardiovasc Imaging 2011.

van der Wall EE, **van Velzen JE**, de Graaf FR, Jukema JW, Schuijf JD, Bax JJ. 320-row CT scanning: reduction in tube current parallels reduction in radiation exposure? Int J Cardiovasc Imaging 2010.

Yiu KH, de Graaf FR, Schuijf JD, van Werkhoven JM, **van Velzen JE**, Boogers MJ, Roos CJ, de Bie MK, Pazhenkottil A, Kroft LJ, Boersma E, Herzog B, de Roos A, Kaufmann PA, Bax JJ, Jukema JW. Prognostic value of renal dysfunction for the prediction of outcome versus results of computed tomographic coronary angiography. Am J Cardiol 2011;108:968-72.

Dankwoord

DANKWOORD

Het onderzoek beschreven in dit proefschrift is uitgevoerd op de afdeling cardiologie van het Leids Universitair Medisch Centrum. Graag wil ik iedereen bedanken met wie ik tijdens mijn promotietijd heb samengewerkt en ik wil graag een paar mensen in het bijzonder noemen.

Allereerst wil ik iedereen bedanken die het mogelijk heeft gemaakt om onderzoek te kunnen uitvoeren. Het secretariaat (Cora, Talitha, Marina en Monique) ontzettend bedankt voor jullie inzet en hulp met al mijn vragen en problemen. Ook de verpleegkundigen op de cathkamer, alsook Bea en Els, wil ik bedanken. Jullie hulp met de IVUS acquisitie was onmisbaar, bedankt voor jullie inzet. Ook Fabrizio Spano, Greetje de Grooth en Frank van der Kley enorm bedankt voor jullie geduld en bereidwilligheid bij de IVUS acquisitie. Natuurlijk kan ik de CT laboranten niet vergeten, we hebben veel tijd achter de scanner doorgebracht samen, het waren zeker de leukere uurtjes van mijn promotietijd. Bedankt voor de kopjes thee en alle hulp. Computer boys (Hilke, Tom, Wybo), ontzettend bedankt voor jullie ondersteuning. Enno, zonder jouw steun met software, computers en hard drives was dit boekje niet tot stand gekomen. Natuurlijk wil ik graag alle collega's in de tuin (Hadrian, Carine, Jan, Roxana, Rutger, Roderick, Jan Willem, Louisa, Mihaly, Hans, Sum-Che, Joep, Jeffrey, Sander, Helene, Georgette, Marieke, Victoria en Dominique) bedanken. Verder wil ik Eric Boersma niet vergeten, bedankt voor uw hulp met mijn statistische problemen.

Ellen en Jael, wat hebben we het altijd fijn gehad samen, even koffie drinken, lunchen en soms ook even klagen over alles waar we mee zaten. Jullie hebben mijn promotietijd kleur gegeven, hopelijk kunnen we deze afspraken nog lang voortzetten. Dennis, wat heb jij het soms moeilijk gehad tussen al die vrouwen, maar ik vind je echt een mooi mens, bedankt voor al je advies (en alle koffie!).

Daarnaast wil ik in het bijzonder het CT team bedanken (Gabija, Jaap, Mark, Fleur, Noor, Caroline, Cees, Michiel, Robert en Agnieska), we hebben veel tijd samen doorgebracht achter de scanner, met Prof. Jukema koffie gedronken, scans uitgewerkt, fantastische congressen meegemaakt, elkaar gesteund met praatjes houden, bedankt voor alles (I will never forget Vegas!). Michiel, een speciaal bedankje voor jou, je was een topper als student en volgens mij nu ook een topper als onderzoeker, bedankt voor je inzet.

Joanne, zonder jou was dit boekje nooit zo mooi geworden. Ik weet niet hoe ik het moeten doen zonder jou. Als ik denk aan alle tijd en moeite had die jij in mijn promotie hebt gestoken, ben ik je zó ontzettend dankbaar. Bedankt voor je stimulatie en feedback, je tips en trucs, je positiviteit en geduld. Ik zal het nooit vergeten.

Fleur, mijn maatje, mijn beste collegaatje, mijn vriendin. Hoe had ik het zonder jou kunnen overleven? Wij samen in de imaging kamer, wat een stel! Ik heb jou de afgelopen 3 jaar vaker gezien dan iedereen. Samen op congres, Mrs and Mrs van Velzen, we hebben echt veel van de wereld gezien. Ik zal deze tijd nooit vergeten, ook al zien we elkaar nu niet meer dagelijks, hopelijk blijft onze band net zo sterk. Bedankt dat je mijn paranimf wilt zijn.

Mijn lieve vriendinnen, (Doreen, Nina, Mirjam, Barbara, Laurence, Mandy, Brigitte, Anese, Gwen, Meike, Carlijn en Julie) eindelijk zijn jullie van het gezucht en gesteun over mijn promotie af en is er meer tijd voor leuke dingen. Bedankt voor jullie eindeloze support. Brigitte, ik vind het geweldig hoe jij mijn proefschrift hebt doorgespit op zoek naar foutjes, bedankt dat je mijn paranimf wilt zijn.

Nog een speciaal bedankje voor Merel. Ik vind het super dat je me hebt geholpen met het ontwerpen van de voorkant van dit boekje. Je bent zo creatief. Ik vind het resultaat echt prachtig. Bedankt!

Pap en mam, er zijn geen woorden voor mijn dankbaarheid. Jullie hebben mij altijd gestimuleerd om gelukkig te zijn, het beste uit mezelf te halen en alles gedaan om dit mogelijk te maken. Zonder jullie steun had deze dag nooit bestaan. Ik heb heel veel geluk gehad met ouders als jullie. Hannah en Michelle, mijn lieve zusjes, bedankt voor alle steun de afgelopen jaren en ik weet dat jullie er altijd voor me zijn. Ook opa en oma van Velzen, Nana, tante Jannie, Mathijs, Marianne, Frans, Derek en Isabelle, bedankt voor jullie liefde en steun.

Rolf, mijn lief, mijn dank aan jou is de allergrootste. Zonder jouw geduld, liefde, steun, positivisme, energie en stomme grapjes (of zoals jij het noemt: hele goede humor) had ik hier niet gestaan. Jij bent de belangrijkste (en aller-grappigste) persoon in mijn leven en ik ben daar ontzettend dankbaar voor.

Curriculum Vitae

CURRICULUM VITAE

De auteur van dit proefschrift is geboren op 20 januari 1982 te Fullford, Groot-Brittannië. Op jonge leeftijd verhuisde zij naar Nederland en behaalde in 1999 het eindexamen VWO aan het PENTA college CSG de Angelus Merula te Spijkenisse. Vervolgens startte zij de studie Geneeskunde in het Erasmus Medisch Centrum te Rotterdam. Tijdens de doctoraal fase van haar studie verrichtte zij van 2002 tot 2003 wetenschappelijk onderzoek aan de kinderchirurgische intensive care van het Erasmus MC-Sophia kinderziekenhuis onder leiding van Prof. Dr. D. Tibboel. Tevens reisde zij in 2006 af naar Melbourne, Australië, voor een co-schap op de afdeling Anaesthesie. In augustus 2006 behaalde zij cum laude haar artsenbul. Na haar afstuderen werkte zij eerst als arts op de spoedeisende hulp in het Vlietland ziekenhuis te Vlaardingen alwaar haar interesse voor de cardiologie werd gewekt. Vervolgens heeft zij van 2007 tot 2008 als arts-assistent cardiologie gewerkt in het Amphia ziekenhuis te Breda. In 2008 startte zij haar promotie traject op de afdeling cardiologie in het Leids Universitair Medisch Centrum onder leiding van Prof. Dr. E.E. van der Wall en Prof. Dr. J.J. Bax. De resultaten hiervan staan beschreven in dit proefschrift.

Per 1 juni 2011 is zij begonnen aan de opleiding cardiologie verbonden aan het Leids Universitair Medisch Centrum. Momenteel volgt zij de vooropleiding Interne Geneeskunde in het Sint Franciscus Gasthuis te Rotterdam.